



HAL
open science

Mathematical modelling of problems related to image registration

Solène Ozeré

► **To cite this version:**

Solène Ozeré. Mathematical modelling of problems related to image registration. Analysis of PDEs [math.AP]. INSA de Rouen, 2015. English. NNT : 2015ISAM0010 . tel-01270213

HAL Id: tel-01270213

<https://theses.hal.science/tel-01270213>

Submitted on 5 Feb 2016

HAL is a multi-disciplinary open access archive for the deposit and dissemination of scientific research documents, whether they are published or not. The documents may come from teaching and research institutions in France or abroad, or from public or private research centers.

L'archive ouverte pluridisciplinaire **HAL**, est destinée au dépôt et à la diffusion de documents scientifiques de niveau recherche, publiés ou non, émanant des établissements d'enseignement et de recherche français ou étrangers, des laboratoires publics ou privés.

THESE

*présentée à
l'Institut National des Sciences Appliquées de Rouen
en vue de l'obtention du grade de
Docteur en Mathématiques Appliquées*

par Solène OZERÉ

MODÉLISATION MATHÉMATIQUE DE PROBLÈMES RELATIFS AU RECALAGE D'IMAGES

Devant le jury composé de

Après avis de :

*Mme Stéphanie ALLASSONNIERE, Professeur, Ecole Polytechnique
M. Simon MASNOU, Professeur, Université de Lyon 1
Mme Carola SCHÖNLIEB, Professeur, University of Cambridge*

*Rapporteur
Rapporteur
Rapporteur*

Devant la commission d'examen formée des rapporteurs et de :

*M. Christian GOUT, Professeur, INSA Rouen
Mlle Carole LE GUYADER, Professeur, INSA Rouen
M. Olivier LEY, Professeur, INSA Rennes
Mme Caroline PETITJEAN, Maître de Conférences, Université de Rouen
M. Gabriel PEYRÉ, Directeur de Recherche CNRS, Université Paris-Dauphine*

*Directeur de thèse
Co-directrice de thèse
Examineur
Examineur
Président du jury*

6 novembre 2015



À mon grand-père.

REMERCIEMENTS

Au terme de ces trois années de thèse, je souhaiterais remercier toutes les personnes qui m'ont aidées, qui ont cru en moi, et qui m'ont permis d'arriver au bout de cette thèse.

En premier lieu, j'adresse un immense merci à mes directeurs de thèse Christian Gout et Carole Le Guyader. Merci de m'avoir fait confiance et de m'avoir donné l'opportunité de réaliser cette thèse avec eux, ce fut un plaisir de travailler sous leur direction. Je remercie Christian pour son soutien, ses conseils, sa gentillesse, la confiance qu'il m'a accordée et sa bonne humeur. Je remercie Carole pour sa disponibilité, sa patience, nos nombreuses discussions et ses précieux conseils. J'ai beaucoup appris grâce à elle, de par sa grande culture scientifique, sa rigueur mathématique mais aussi ses qualités humaines. J'espère avoir été digne de la confiance qu'ils m'ont accordée et que ce travail est finalement à la hauteur de leurs espérances.

Je remercie très sincèrement Madame Stéphanie Allassonnière, Monsieur Simon Masnou et Madame Carola Schönlieb qui ont accepté d'être rapporteurs de cette thèse. Je les remercie pour l'intérêt qu'ils ont porté à ce travail et pour l'honneur qu'ils m'ont fait en participant au jury.

Je remercie également Monsieur Olivier Ley, Madame Caroline Petitjean et Monsieur Gabriel Peyré pour l'honneur qu'ils m'ont fait de participer au jury de thèse.

Je remercie également Monsieur Hervé Le Dret pour les réponses et l'aide qu'il nous a apportées au cours de ce travail.

Je tiens également à remercier l'ensemble des membres du Laboratoire de Mathématiques de l'INSA. Merci à Brigitte Diarra pour sa gentillesse et son efficacité, à Nicolas Forcadel à la fois pour son humour et pour son aide. Je remercie tout particulièrement les doctorants, Florentina Nicolau et Zacharie Alès pour leur gentillesse et leurs conseils et d'avoir partagé avec moi le bureau, pour l'une, et les groupes de TD pour l'autre. Merci à Théophile Chaumont-Frelet pour sa bonne humeur, nos fous rires, et sa présence ponctuelle dans le bureau ! Merci à Wilfredo Salazar sans qui ces deux dernières années n'auraient pas été aussi agréables. Merci d'avoir partagé toutes ces pauses-café et tous ces repas avec moi, merci de m'avoir écoutée et conseillée.

Je voudrais également remercier le département du premier cycle de l'INSA qui m'a accueillie dans le cadre de ma mission enseignement, en particulier Jean-Marc Cabanial et Carole Le Guyader pour la confiance qu'ils m'ont accordée. Ce fut une expérience très intéressante et enrichissante.

Je voudrais maintenant remercier d'autres personnes qui m'ont aidée, peut-être sans le savoir, ma famille. Merci à mes parents pour leur soutien inconditionnel et leurs encouragements. Merci également à mon frère et mon père pour leurs avis et leur aide en matière de graphismes et d'esthétique pour mon manuscrit !

Enfin, merci à celui qui m'a aidée plus qu'il ne le réalise sans doute, Sébastien. Merci d'une part pour m'avoir aidée grâce à tes talents d'informaticien, à déboguer mes codes et améliorer ma façon de procéder. Mais surtout, merci d'avoir toujours été là, de m'avoir encouragée, de m'avoir fait voir le bon côté des choses quand il le fallait. Merci de tout ce que tu m'apportes.

Contents

1	Introduction générale	1
1.1	Traitement d'images et cadre mathématique	1
1.2	Le recalage d'images	2
1.2.1	Interpolation et approximation des images	4
1.2.2	La mesure de similarité	6
1.2.3	Le modèle de déformation	10
1.2.4	La préservation de la topologie	12
1.3	Contribution	13
1.3.1	Préservation de la topologie du champ de déformation associé au recalage d'images	13
1.3.2	Modèle conjoint de segmentation et recalage fondé sur la variation totale pondérée et l'élasticité non linéaire	16
1.3.3	Modèle conjoint de segmentation et recalage non local	17
1.4	Organisation de la thèse	18
2	Mathematical preliminaries	25
2.1	L^p Spaces	25
2.2	Sobolev spaces	28
2.3	Functions of bounded variation	33
2.4	Direct methods in the calculus of variations	34
2.4.1	Quasiconvexity, Polyconvexity and Rank one convexity	35
2.5	Tridimensional elasticity	36
3	Topology preservation	41
3.1	Correction of the deformation	46
3.2	Deformation reconstruction	49
3.2.1	Functional to be minimized	50
3.2.2	Characterization of the solution	55
3.2.3	Lagrange multipliers	56
3.2.4	Theoretical convergence result	57
3.2.5	Discretization	62
3.3	Numerical experiments	66
3.3.1	First example : a slice of the brain	67
3.3.2	Second example : brain mapping	70
3.3.3	Third example: the disks	71

4	Joint segmentation/registration model by shape alignment	77
4.1	Mathematical Modelling	79
4.1.1	General mathematical background	79
4.1.2	Depiction of the original model	80
4.1.3	Mathematical obstacle and derivation of a relaxed problem	83
4.1.4	Theoretical results	84
4.2	Numerical method of resolution	90
4.2.1	Description and Analysis of the Proposed Numerical Method	90
4.2.2	Numerical Scheme	96
4.3	Numerical experiments	99
4.3.1	Regridding technique, choice of the parameters and registration accuracy	99
4.3.2	Letter C	101
4.3.3	Noisy triangle	103
4.3.4	Mouse brain gene expression data	104
4.3.5	Slices of the brain	109
4.3.6	MRI images of cardiac cycle	110
4.3.7	Comparisons with prior related works	113
5	Nonlocal Joint Segmentation Registration Model	121
5.1	Mathematical Modelling	122
5.2	Theoretical results	125
5.2.1	Existence of minimizers and relaxation theorem	125
5.2.2	Well-definedness of $\tilde{\Phi}$	126
5.3	Numerical Method of Resolution	132
5.4	Discretization and Implementation	136
5.4.1	Introduction of an AOS scheme for the evolution problem	136
5.4.2	Thomas algorithm	140
5.4.3	Euler-Lagrange equations for functional \bar{I}_γ	141
5.5	Numerical results	141
5.5.1	Letter C	142
5.5.2	Triangle	143
5.5.3	Mouse brain gene expression	144
5.5.4	Slices of brain	145
6	Nonlinear elasticity and geometric constraints	151
6.1	Mathematical modelling	152
6.1.1	Preliminaries	152
6.1.2	Depiction of the model	153
6.1.3	Mathematical obstacle and relaxed problem	155
6.1.4	Theoretical results	163
6.1.5	Relaxation theorem	168
6.2	A convergence result	168
6.3	Discretization and Implementation	171
6.3.1	Augmented Lagrangian	171
6.3.2	Implementation details	174
6.4	Numerical experiments	175

7	Registration based on Gradient Comparison	183
7.1	Mathematical modelling	185
7.2	Existence minimizers for the initial problem	186
7.3	Introduction of an auxiliary variable	188
7.3.1	Existence of minimizers for the decoupled problem	190
7.4	Approximation method of the total variation of $T \circ \varphi$	193
7.4.1	Existence of minimizers for the Problem with approximation of the total variation	194
7.4.2	Study of $\lim_{n \rightarrow \infty} \bar{\varphi}_n$ and Γ -convergence	196
7.4.3	Euler-Lagrange equation	205
7.5	Implementation details	206
7.5.1	Experiments on a restoration problem	207
7.6	Implementation of the registration problem	214
7.6.1	Scheme for the auxiliary variable method	214
7.6.2	Scheme for the approximation method	214
7.6.3	Numerical results	215

1.1 Traitement d'images et cadre mathématique

L'imagerie est un domaine qui ne cesse de se développer et dont les applications sont nombreuses, telles

- la photographie, avec l'argentique depuis les années 1800 et la photographie numérique,
- l'imagerie médicale depuis le premier échographe en 1960, puis l'échographie numérique dans les années 1990,
- la biométrie, avec la reconnaissance d'empreintes depuis les années 1970,
- l'imagerie satellitaire, avec les premiers satellites numériques en 1976,

pour n'en citer que quelques unes. Afin d'aborder l'ensemble des problèmes rencontrés, l'utilisation des mathématiques se révèle précieuse depuis la fin des années 90 (pour le formalisme mathématique relatif aux modèles d'imagerie, on pourra se référer à [3], [4] et [20]). En effet, une image de taille $N \times M$, c'est-à-dire contenant $N \times M$ pixels, est modélisée comme une fonction u :

$$u : \{1, \dots, N\} \times \{1, \dots, M\} \mapsto \{0, \dots, 255\}.$$

Une image numérique est donc un tableau où chaque entité correspond à un pixel et contient une valeur comprise entre 0 et 255 : c'est son intensité lumineuse ou niveau de gris.



Figure 1.1: Exemple d'une image en niveaux de gris. Issue de <http://images.math.cnrs.fr/Le-traitement-numerique-des-images.html> (rédigé par Gabriel Peyré)

Grâce à cette fonction u on peut, par exemple, en déduire les contours des objets dans l'image en calculant les gradients discrets, c'est-à-dire les différences de deux pixels consécutifs.

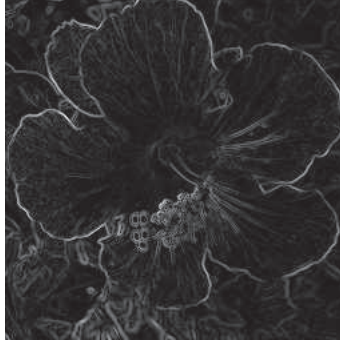


Figure 1.2: Exemple de carte des contours. Issue de <http://images.math.cnrs.fr/Letraitements-numerique-des-images.html> (rédigé par Gabriel Peyré)

Parmi les tâches fréquemment rencontrées en traitement d'images, on compte:

- la détection de contours et la segmentation qui consiste à partitionner l'image en un ensemble de régions d'intérêt ([44], [19], [17], [77], [46]),
- la restauration et le débruitage qui consistent à réduire le bruit ou le flou dus par exemple au système d'acquisition de l'image ([61], [18] [15], [39], [21] [59]),
- l'inpainting qui consiste à reconstruire une zone endommagée de l'image à partir des données présentes ([5], [7], [10], [11], [65]),
- la compression d'images ([49], [8]),
- le recalage qui consiste à trouver une déformation optimale de sorte que l'image template déformée s'aligne sur une image de référence.

1.2 Le recalage d'images

Le recalage d'images ([53], [54], [14]) est une tâche fondamentale rencontrée dans un grand éventail d'applications comme l'imagerie médicale, le suivi de forme, la comparaison de données, etc. Étant données deux images appelées *Template* et *Reference* (définies sur un domaine ouvert borné Ω - en général un rectangle), le recalage consiste à déterminer une transformation difféomorphique optimale telle que l'image *Template* déformée s'aligne sur l'image *Reference*.

Pour les images de même modalité, le but du recalage est de corrélérer les caractéristiques géométriques et les niveaux d'intensité de l'image *Template* déformée et l'image *Reference*. Quand les images ont été obtenues via des mécanismes différents et ont des modalités différentes, le recalage a pour but de corrélérer les deux images en préservant la modalité de l'image *Template*.

Dans [66], Sotiras *et al.* fournissent un aperçu des différentes méthodes de recalage existantes. D'après les auteurs, un algorithme de recalage d'images se compose de trois principaux éléments :

1. **un modèle de déformation**, c'est-à-dire la signification physique que l'on donne à la déformation recherchée,
2. **une fonction objectif**, c'est-à-dire un critère dit de fidélité ou d'attache aux données que l'on vise à minimiser,
3. et **une méthode d'optimisation**, c'est-à-dire la méthode numérique mise en œuvre pour résoudre le problème de minimisation.

Les modèles de déformations (ou transformations) sont organisés en trois classes:

1. les transformations géométriques dérivant d'un modèle **physique**,
2. les transformations géométriques dérivant de la **théorie de l'interpolation**,
3. les transformations géométriques fondées sur des **connaissances a priori**.

D'après [53], les modèles physiques peuvent eux-mêmes être séparés en cinq catégories : les modèles élastiques ([13], [31], [60], [78]), les modèles fluides ([22]), les modèles de diffusion ([36]), le recalage par courbure ([38]) et les flots de difféomorphismes ([9]).

Ensuite, parmi les plus importantes familles de stratégies d'interpolation, on peut citer : les fonctions de base radiales ([80]), les splines élastiques ([32]), les déformations de forme libre ([62]), les fonctions de base du traitement du signal ([2]) et les modèles affines par morceaux. Ces modèles sont assez riches pour décrire les transformations, en ayant peu de degrés de liberté.

La troisième catégorie de modèle de déformation permet d'introduire des connaissances par rapport à la déformation grâce à des transformations géométriques contraintes statistiquement ou grâce à des modèles biomécaniques/biophysiques (modèle de croissance de tumeur ou modèle biomécanique de la poitrine par exemple) ([28]).

La deuxième composante d'une méthode de recalage d'images est la fonction objectif ou critère d'attache aux données. Il existe de nombreux types de critères de fidélité qui peuvent être repartis en trois catégories :

1. les méthodes **géométriques** : elles consistent à apparier des primitives géométriques de l'image, par exemple des points d'intérêt ([24]),
2. les méthodes **iconiques** : elles concernent les méthodes fondées sur la comparaison des intensités ([34]), des attributs ([64]), les approches fondées sur la théorie de l'information ([75]),
3. les méthodes **hybrides**, qui combinent les méthodes géométriques et iconiques ([42], [67]).

Finalement, la dernière composante est la méthode d'optimisation :

1. la méthode **continues** : descente de gradient ([9]), gradient conjugué ([52]), méthode de Quasi-Newton ([74]), descente de gradient stochastique ([75]) ... C'est le problème continu qui est discrétisé.

2. les méthodes **discrètes** : méthodes fondées sur la théorie des graphes ([68]), belief propagation, méthodes de programmation linéaire,
3. les algorithmes **gloutons** et **évolutionnistes**.

Dans [54], Modersitzki fournit également un aperçu des méthodes de recalage paramétriques et non paramétriques (incluant les méthodes géométriques avec appariement de points d'intérêt, les méthodes iconiques avec la dissimilarité fondée sur la norme L^2 par exemple, les modèles d'élasticité linéaire, la diffusion linéaire, les modèles fluides, ...).

Dans le cas des méthodes paramétriques, un ensemble de caractéristiques de l'image *Template* est défini et le but est de trouver une déformation appariant ces caractéristiques avec leur homologue dans l'image *Reference*. De plus, l'ensemble des transformations admissibles est restreint à une certaine classe d'applications (applications polynomiales, splines, etc...) en exprimant la transformation à l'aide de fonctions de base.

Dans le cas des méthodes non paramétriques (notre cadre), la transformation n'est pas restreinte à un ensemble paramétrisable et le problème est formulé en termes de minimisation de fonctionnelle (avec le champ de déformation inconnu φ) comprenant un critère de mesure de distance et un régularisateur portant sur le champ de déformation afin que le problème soit bien posé. Le plus souvent, des arguments physiques motivent la construction du régularisateur. Des régularisateurs classiques comme ceux fondés sur la théorie de l'élasticité linéaire ne sont pas adaptés à des problèmes impliquant de grandes déformations (notre cas d'étude) puisqu'ils supposent de petites déformations et la validité de la loi de Hooke. Cette loi de comportement énoncée par Robert Hooke en les termes latins "ut tensio sic vis" traduit la relation de proportionnalité entre la force exercée sur un solide et l'allongement qui en résulte.

Dans la suite, les problématiques relatives à la mise en œuvre pratique des méthodes de recalage sont examinées, la question de l'interpolation des images (en effet, si φ désigne la déformation recherchée, il nous faut évaluer $T \circ \varphi$), la conception du critère d'attache aux données (les critères classiques et les critères plus évolués fondés sur des modèles combinés de segmentation et recalage) et la construction de régularisateur portant sur la déformation.

1.2.1 Interpolation et approximation des images

Au cours de l'algorithme mis en œuvre dans le cadre du recalage, il faut calculer l'image déformée $T \circ \varphi$. Un point $y \in \Omega$ fixé de l'image *Template* déformée (de coordonnées entières en pratique) est lié au point $x = \varphi(y)$ (de coordonnées non nécessairement entières) et l'intensité lumineuse de l'image déformée en y , $\tilde{T} = T \circ \varphi(y)$ est donnée par : $T \circ \varphi(y) = T(x)$. Le point x n'étant pas nécessairement situé à un nœud de la grille discrète, il est alors nécessaire de mettre en œuvre une méthode d'interpolation (on pourra se référer à [40] pour plus de détails sur les cadres eulérien et lagrangien).

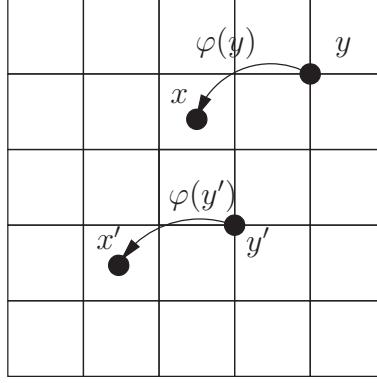


Figure 1.3: Déformation considérée dans le cadre eulérien.

Les valeurs aux positions entières de la grille seront calculées à partir de la version continue de l'image. Parmi les nombreuses méthodes d'interpolation existantes, les plus utilisées en recalage d'images médicales sont l'interpolation linéaire et l'interpolation par splines et par B-splines cubiques [54]. On pourra se référer à Lehmann *et al.* [48] pour un état de l'art et une comparaison des méthodes d'interpolation et d'approximation. Pour l'implémentation de nos différentes méthodes, nous utilisons une approximation de l'image par B-splines cubiques. Comme décrit dans [54], commençons par introduire ce modèle en dimension un. Le problème d'interpolation peut s'écrire comme un problème de minimisation de fonctionnelle sous contraintes. On cherche à réécrire les données dans une base de fonctions splines. On vise en particulier à minimiser la norme L^2 de la dérivée seconde de la fonction interpolante afin que celle-ci oscille le moins possible. Pour des points $x_i \in \Omega$ donnés, on vise à ce que la fonction f satisfasse les conditions d'interpolation $f(x_i) = data(i)$, $\forall i \in \{1, \dots, N\}$, où $data(i)$ correspond aux valeurs connues que l'on souhaite interpoler. En dimension 1, le problème de minimisation considéré est alors le suivant :

$$\min_{c_k} \left\{ \int (f''(x))^2 \mid f(x) = \sum_{k=1}^N c_k b(x-k), f(x_i) = data(i), \forall i \in \{1, \dots, N\} \right\}, \quad (1.1)$$

où b est une spline de base. Comme dans [54], on choisit de prendre :

$$b = \begin{cases} (x+2)^3 & -2 \leq x < -1, \\ -x^3 - 2(x+1)^3 + 6(x+1) & -1 \leq x < 0, \\ x^3 + 2(x-1)^3 - 6(x-1) & 0 \leq x < 1, \\ (2-x)^3 & 1 \leq x < 2 \\ 0 & \text{sinon.} \end{cases}$$

En pratique, les données à interpoler peuvent être bruitées, dans ce cas une stricte interpolation des données n'est pas pertinente. Une solution intermédiaire consiste à remplacer le problème (1.1) par un problème dit relaxé en introduisant un paramètre θ qui pondère le terme d'attache aux données et la régularisation. Fixer θ à 0 conduit à la définition du problème pur d'interpolation, tandis qu'une valeur de θ élevée induit une solution plus régulière. Soit à considérer

$$\min_{c_k} \left\{ \|f - data\|_{\mathbb{R}^N}^2 + \theta \int_{\Omega} (f'')^2 \mid f(x) = \sum_{k=1}^N c_k b(x - k) \right\} \quad (1.2)$$

où $\|f - data\|_{\mathbb{R}^N}^2 = \sum_{i=1}^N (f(x_i) - data(i))^2$.

La résolution de ce problème conduit à résoudre un système linéaire que l'on peut écrire sous la forme suivante :

$$(B^T B + \theta M)c = B^T data$$

avec $B = (b_k(x_i) = b(x_i - k))_{\substack{1 \leq i \leq N \\ 1 \leq k \leq N}}$, $c = (c_k)_{1 \leq k \leq N}$ et $M_{jk} = \int_{\Omega} (b_j)''(b_k)'' dx$.

Une approche plus générale consiste à remplacer M par une matrice arbitraire symétrique semi-définie positive W . Le choix $W = M$ est théoriquement bien justifié puisque l'optimisation est réalisée dans l'espace de splines. Cependant, d'autres régularisations sont possibles : $W = I$ appelée régularisation de Tychonoff ou $W = D^T D$ appelée régularisation de Ty-

chonoff-Phillips avec $D = \begin{pmatrix} -1 & 1 & & \\ & \ddots & \ddots & \\ & & & -1 & 1 \end{pmatrix} \in \mathbb{R}^{N-1, N}$.

Pour des images en dimension deux, l'interpolation bicubique est utilisée et l'extension au cas bidimensionnel est immédiat. La formulation matricielle du problème permet de simplifier les écritures. Pour d'avantage de détails, on renvoie le lecteur à l'ouvrage [54], Chapitre 3, section 3.6.1.

1.2.2 La mesure de similarité

Comparaison des intensités

La norme L^2 (ou SSD pour Sum of Squared Distance) correspond à la somme des erreurs au carré pixel par pixel. On la calcule grâce à la formule suivante :

$$\mathcal{D}^{SSD}(R, T \circ \varphi) = \frac{1}{2} \|R - T \circ \varphi\|_{L^2(\Omega)}^2 = \frac{1}{2} \int_{\Omega} (R(x) - T \circ \varphi(x))^2 dx,$$

où R correspond à l'image *Reference* et $T \circ \varphi$ correspond à l'image *Template* déformée.

Ce critère est le critère le plus utilisé pour recaler des images de même modalité bien qu'il soit assez sensible aux valeurs aberrantes.

Coefficient de corrélation linéaire

Il est parfois nécessaire de remettre à l'échelle les valeurs des images considérées, par exemple dans le cas où elles ont été obtenues par des instruments de mesure différents. Cette remise à l'échelle se fait au moyen d'une relation affine entre les intensités des deux images. Pour évaluer l'existence de cette relation affine entre deux images, on utilise le coefficient de corrélation linéaire :

$$\sigma^2(R, T \circ \varphi) = \frac{\text{cov}(R, T \circ \varphi)}{\text{var}(R)\text{var}(T \circ \varphi)},$$

où var et cov représentent respectivement la variance et la covariance des intensités. Si le coefficient de corrélation est nul, cela signifie qu'il n'existe pas de relation affine entre les deux

images et donc que les deux images sont des réalisations aléatoires non corrélées. Le but est alors de déterminer φ maximisant ce terme.

Information mutuelle

L'information mutuelle est un critère qui provient de la théorie de l'information et qui s'applique couramment au recalage multi-modal (dans le cas où les images sont de modalités différentes) depuis 1995 (Wells [75], Collignon [29]).

Ce critère est utilisé pour le recalage multi-modal puisqu'il ne nécessite aucune connaissance a priori sur les intensités et il ne suppose pas de relation affine entre les images. L'idée est de maximiser l'information mutuelle des images par rapport à la transformation.

Definition 1.2.1

Soit $q \in \mathbb{N}$ et ρ une densité sur \mathbb{R}^q , ie, $\rho : \mathbb{R}^q \rightarrow \mathbb{R}, \rho(x) \geq 0, \int_{\mathbb{R}^q} \rho(x) dx = 1$.

L'entropie (différentielle) de la densité est définie par

$$H(\rho) = -\mathbb{E}_\rho[\log \rho] = - \int_{\mathbb{R}^q} \rho \log \rho dx$$

L'entropie se mesure donc à partir de l'histogramme des niveaux de gris. Si l'image est la réalisation d'une variable aléatoire ne privilégiant aucune valeur de pixel alors l'histogramme de l'amplitude sera relativement plat et l'entropie maximale.

L'information mutuelle est alors définie par :

$$\text{MI}(R, T) = H(\rho_R) + H(\rho_T) - H(\rho_{R,T})$$

où ρ_R, ρ_T et $\rho_{R,T}$ représentent les densités des niveaux de gris de R, T et la densité conjointe des niveaux de gris. L'information mutuelle correspond alors à la réduction d'entropie apportée par leur apparitions communes.

En imagerie médicale, l'information mutuelle est un critère particulièrement adapté aux images n'ayant pas les mêmes modalités. Cependant, cette mesure possède certains inconvénients : elle est coûteuse en temps de calcul, elle est non convexe et possède un nombre important de minima locaux. Sa complexité en termes de coût de calcul vient du fait que l'information mutuelle nécessite d'évaluer les probabilités conjointes pour chaque niveau de gris sur l'ensemble de l'image. Mais malgré ces limites, elle reste très utilisée pour le recalage multi-modal.

Champ de gradients

Il est aussi possible de comparer les champs de gradients des deux images. C'est ce qui a été fait par Haber et Modersitzki ([41]) et par Droske et Rumpf ([35]). Dans [41], Haber *et al.* utilisent les champs de gradients pour comparer deux images, en s'appuyant sur l'idée que deux images sont similaires si les changements d'intensité ont lieu à la même position. Pour cela, ils appairent les champs de gradients normalisés des deux images.

Le champ de gradients normalisés est défini comme suit :

$$n_\varepsilon(I, x) = \frac{\nabla I(x)}{\sqrt{\nabla I(x)^T \nabla I(x) + \varepsilon^2}},$$

avec ε une constante strictement positive. La mesure de similarité entre les deux images est alors évaluée comme suit :

$$\mathcal{D}^c(T, R) = \frac{1}{2} \int_{\Omega} \|n_{\varepsilon}(R, x) \times n_{\varepsilon}(T \circ \varphi, x)\|^2 dx,$$

où \times représente le produit vectoriel.

Lignes de niveau

Dans [35], Droske et Rumpf proposent un critère fondé sur la notion de morphologie mathématique ([63]). La morphologie mathématique d'une image est définie comme la collection des courbes de niveau :

$$M[I] = \left\{ \mathcal{M}_c^I \mid c \in \mathbb{R} \right\}, \quad \mathcal{M}_c^I = \left\{ x \in \Omega \mid I(x) = c \right\}.$$

On peut définir de manière équivalente le vecteur normal à une courbe de niveau quelconque :

$$N_I : \Omega \longrightarrow \mathbb{R}^d; x \longmapsto \frac{\nabla I}{\|\nabla I\|}.$$

On cherche alors une déformation telle que $M[T \circ \varphi] = M[R]$. Cette mesure a l'avantage d'être invariante par une reparamétrisation des niveaux de gris, ce qui la rend adaptée au recalage multi-modal.

Modèles conjoints de segmentation et de recalage

Le recalage d'images peut également être réalisé simultanément avec la segmentation. Yezzi *et al.* [79] proposent une approche variationnelle conjointe de segmentation et de recalage. Les deux images *Template* et *Reference* sont supposées contenir un objet commun visualisé avant et après avoir été soumis à une déformation que l'on cherche à apparier et à segmenter. L'objectif est de définir une courbe fermée \mathcal{C} capturant les bords de l'objet dans l'image *Reference* et une courbe $\hat{\mathcal{C}}$ capturant son homologue dans l'image *Template*, telles que $\hat{\mathcal{C}} = g(\mathcal{C})$, où g est un élément d'un groupe de dimension finie par exemple l'ensemble des déformations rigides. Il y a alors deux inconnues : la courbe \mathcal{C} et la déformation g .

Les auteurs formulent le problème comme la minimisation d'une fonctionnelle d'énergie dont la construction est fondée sur le modèle des contours actifs sans bord de Chan et Vese [19] :

$$\begin{aligned} E(g, \mathcal{C}) &= E_1(\mathcal{C}) + E_2(g(\mathcal{C})) \\ &= \int_{\mathcal{C}_{in}} (R - u)^2 dx + \int_{\mathcal{C}_{out}} (R - v)^2 dx + \int_{\hat{\mathcal{C}}_{in}} (T - \hat{u})^2 dx + \int_{\hat{\mathcal{C}}_{out}} (T - \hat{v})^2 dx, \\ &= \int_{\mathcal{C}_{in}} f_{in} dx + \int_{\mathcal{C}_{out}} f_{out} dx + \int_{\hat{\mathcal{C}}_{in}} \hat{f}_{in} dx + \int_{\hat{\mathcal{C}}_{out}} \hat{f}_{out} dx, \end{aligned}$$

avec \mathcal{C}_{in} et \mathcal{C}_{out} les régions à l'intérieur et à l'extérieur de \mathcal{C} , u et v la moyenne des valeurs de R dans \mathcal{C}_{in} et \mathcal{C}_{out} , $\hat{\mathcal{C}}_{in}$ et $\hat{\mathcal{C}}_{out}$ les régions à l'intérieur et à l'extérieur de $\hat{\mathcal{C}}$, et \hat{u} et \hat{v} la moyenne des valeurs de T dans $\hat{\mathcal{C}}_{in}$ et $\hat{\mathcal{C}}_{out}$.

Comme $\hat{\mathcal{C}} = g(\mathcal{C})$, on peut réécrire la fonctionnelle de la façon suivante, en exprimant les intégrales seulement sur l'ouvert Ω sur lequel est défini l'image *Reference* R :

$$E(g, \mathcal{C}) = \int_{\mathcal{C}_{in}} (f_{in}(x) + \hat{f}_{in}(g(x)) |g'(x)|) dx + \int_{\mathcal{C}_{out}} (f_{out}(x) + \hat{f}_{out}(g(x)) |g'(x)|) dx.$$

Ce modèle a été étendu aux déformations non rigides dans [70], [73] et [76].

Dans [71], [72], Vemuri *et al.* proposent un modèle d'équations aux dérivées partielles pour réaliser conjointement la segmentation et le recalage. Dans la première EDP, les level sets de l'image source évoluent selon leur normale avec une vitesse définie comme la différence entre l'image cible et l'image source déformée. La deuxième EDP permet de retrouver explicitement le champ de vecteurs déplacement. Le modèle est fondé sur la minimisation de la fonctionnelle suivante inspirée du modèle de segmentation proposé par Chan et Vese dans [19] et intégrant un a priori de forme :

$$\begin{aligned} E(\phi, u^+, u^-, \mu, \mathcal{R}, \mathcal{T}) = & \alpha \int_{\Omega} |u^+ - I|^2 H(\phi) dx + \alpha \int_{\Omega} |u^- - I|^2 (1 - H(\phi)) dx \\ & + \beta \int_{\Omega} |\nabla u^+|^2 H(\phi) dx + \beta \int_{\Omega} |\nabla u^-|^2 (1 - H(\phi)) dx \\ & + \int_{\Omega} d^2(\mu \mathcal{R}x + \mathcal{T}) \delta(\phi) |\nabla \phi| dx, \end{aligned}$$

où I est l'image à segmenter, ϕ la fonction level set inconnue, d la fonction distance à un a priori de forme, μ un paramètre d'échelle, \mathcal{R} et \mathcal{T} une matrice de rotation et un vecteur de translation.

Dans [50], Lord *et al.* traitent le problème de quantification de la différence de deux formes. Leur travail s'inscrit dans le contexte de l'analyse de forme de l'hippocampe et est motivé par le fait que la classification de maladies est facilitée par la comparaison d'asymétries. Pour effectuer ces analyses comparatives, les auteurs proposent une méthode traitant simultanément le processus de segmentation et de recalage en introduisant deux inconnues : le champ de déformation et la courbe réalisant la segmentation. La segmentation est guidée par la déformation, et le critère d'attache aux données, contrairement aux méthodes classiques de recalage, s'appuie sur la comparaison des structures métriques des deux surfaces et plus précisément sur la minimisation de la déviation par rapport à une isométrie. Le critère d'attache aux données est basé sur la comparaison des structures métriques des surfaces, plus précisément sur leur première forme fondamentale (FFF) et sur une contrainte d'homogénéité de type Chan-Vese.

Dans [47], Le Guyader et Vese proposent un modèle de recalage et de segmentation simultanés. Les auteurs proposent de joindre le modèle des contours actifs sans bord de Chan et Vese [19] à un recalage d'images dont le terme de régularisation est fondé sur la théorie de l'élasticité non linéaire. Les formes à apparier sont assimilées à des matériaux homogènes, isotropes, hyperélastiques de type Ciarlet-Geymonat. Le problème est formulé comme la minimisation d'une fonctionnelle composée d'un terme lié à la segmentation et d'un second terme lié au modèle de déformation :

$$\begin{aligned} E(c_1, c_2, u) = & E_d(c_1, c_2, u) + E_{reg}(u), \\ = & \nu_1 \int_{\Omega} |R(x) - c_1|^2 H(\Phi_0(x - u(x))) dx \\ & + \nu_2 \int_{\Omega} |R(x) - c_2|^2 (1 - H(\Phi_0(x - u(x)))) dx + E_{reg}(u), \end{aligned}$$

où Φ_0 est une level set fixée dont le niveau zéro est une courbe segmentant l'image *Template* T , c_1 et c_2 sont respectivement la moyenne des niveaux de gris à l'intérieur et à l'extérieur de la courbe, $u = \varphi - \text{Id}$ est le vecteur déplacement.

1.2.3 Le modèle de déformation

Le modèle de déformation ou régularisateur est généralement motivé par des arguments physiques et définit l'espace fonctionnel dans lequel évolue la déformation φ .

Modèle élastique linéaire

Le modèle élastique a été introduit par Broit [13], puis développé par Bajcsy [6]. Les images sont appréhendées comme les observations d'un même corps élastique, l'une avant et l'autre après avoir été soumis à une déformation. Le terme de régularisation est le potentiel élastique linéaire du déplacement u :

$$\mathcal{P}(u) = \int_{\Omega} \frac{\mu}{4} \sum_{j,k=1}^d (\partial_{x_j} u_k + \partial_{x_k} u_j)^2 + \frac{\lambda}{2} (\text{div } u)^2 dx,$$

où μ et λ sont les constantes de Lamé. L'utilisation de l'élasticité linéaire présente deux inconvénients : la topologie n'est pas nécessairement préservée, et le modèle est restreint au cas de petites déformations.

Modèle fluide

Dans [22], Christensen *et al.* proposent un modèle fluide visqueux sous forme non variationnelle. Les objets à apparier sont assimilés à des fluides évoluant selon les équations de Navier-Stokes. Si le modèle élastique est caractérisé par une régularisation spatiale du déplacement, le modèle fluide, lui, est caractérisé par une régularisation de la vitesse :

$$\mu \Delta v + (\lambda + \mu) \text{div } v + F = 0,$$

avec $v = \partial_t u$ et F , la mesure de similarité choisie. Avec le temps, $u = \varphi - \text{Id}$ devient stationnaire et de larges déformations sont théoriquement possibles.

Modèle de diffusion

Dans [69], Thirion *et al.* proposent d'assimiler le recalage non rigide à un modèle de diffusion qui est un cas particulier des méthodes de flot optique utilisées en traitement d'images pour évaluer le mouvement. Il introduit de nouvelles entités appelées démons qui sont en fait des effecteurs poussant localement l'image. Les contours des objets présents dans l'image sont appréhendés comme des membranes semi-perméables pouvant se mouvoir sous l'action de démons. Cet algorithme montre des résultats très satisfaisants avec des temps de calcul réduits et il permet d'avoir de larges déformations. Cependant, le comportement de cet algorithme n'est pas encore bien compris (voir [58] et [37] pour plus de détails). Dans [37], Fischer et Modersitzki introduisent un nouveau modèle de diffusion dans lequel le régularisateur s'écrit :

$$\mathcal{S}[u] = \frac{1}{2} \sum_{l=1}^d \int_{\Omega} \|\nabla u_l\|^2 dx.$$

Dans cette méthode aussi, les transformations sont restreintes à de petites déformations, mais le modèle peut être combiné avec l'idée précédente de fluide pour générer de plus larges déformations.

Modèle par courbure

Dans [38], Fischer et Modersitzki introduisent un modèle de recalage fondé sur la courbure. Le régularisateur est défini par :

$$\mathcal{S}[u] = \frac{1}{2} \sum_{l=1}^d \int_{\Omega} (\Delta u_l)^2 dx,$$

$(\Delta u_l)^2$ pouvant être appréhendé comme une approximation de la courbure. Ainsi l'idée du régularisateur est de minimiser la courbure des composantes de la déformation.

Encore une fois, les transformations sont restreintes à de petites déformations, et ce modèle peut être combiné avec l'idée précédente de fluide pour générer de plus larges déformations.

Modèles élastiques non linéaires

Afin d'obtenir de larges déformations, l'utilisation de l'élasticité non linéaire se révèle nécessaire (voir [27] et [26] pour plus de détails). En effet, la théorie de l'élasticité linéaire n'est pas adaptée à des problèmes impliquant de grandes déformations puisque cette théorie suppose de petites déformations et la validité de la loi de Hooke. On peut remarquer que le caoutchouc, les tissus biologiques, les élastomères sont fréquemment modélisés par des matériaux hyperélastiques. En élasticité, on introduit souvent le tenseur de déformation de Green-Saint Venant :

$$E(u) = \frac{1}{2}(\nabla u + \nabla u^T) + \frac{1}{2}\nabla u^T \nabla u,$$

qui constitue une mesure de la déviation de la déformation associée $\varphi = \text{Id} + u$ par rapport à une déformation rigide. La partie linéaire du tenseur de Green-Saint Venant :

$$e(u) = \frac{1}{2}(\nabla u + \nabla u^T),$$

est ce que l'on appelle le tenseur de déformation linéarisé que l'on retrouve dans le cadre de la théorie de l'élasticité linéaire.

Dans le cadre du recalage d'images fondé sur des principes d'élasticité non linéaire, Droske et Rumpf [35] traitent le problème du recalage non rigide d'images multi-modales. Le critère de similarité inclut les dérivées du premier ordre de la déformation et est complété par une régularisation élastique non linéaire basée sur une densité d'énergie polyconvexe. Dans [47], Le Guyader et Vese introduisent un modèle couplé de segmentation et recalage dans lequel les objets à apparier sont assimilés à des matériaux de type Ciarlet-Geymonat. On peut également mentionner [51] et [9] pour une méthode variationnelle de recalage dans le cas de grandes déformations (Large Deformation Diffeomorphic Metric Mapping - LDDMM), ainsi que [60] qui présente également une méthode utilisant une régularisation élastique non linéaire.

Plus récemment, dans [16], les auteurs construisent une densité d'énergie hyperélastique pénalisant les variations de longueur et d'aire, et ajoutent une pénalisation sur le jacobien de la déformation de telle sorte que l'énergie tende vers l'infini quand le jacobien tend vers zéro.

1.2.4 La préservation de la topologie

Il est également possible d'ajouter certaines contraintes sur la déformation recherchée. Une des plus importantes propriétés qu'un algorithme de recalage doit satisfaire est la préservation de la topologie ou de l'orientation. La préservation de la topologie est équivalente à l'inversibilité du champ de déformation. Le jacobien de la déformation contient l'information concernant les propriétés locales du champ de déformation. En effet, si le jacobien de la déformation devient négatif alors la déformation perd son caractère injectif et cela traduit physiquement une interpénétration de la matière.

Afin d'éviter des singularités dans le champ de déformation, Christensen *et al.* [22] proposent de contrôler les valeurs du jacobien au fur et à mesure de l'algorithme. Lorsque sa valeur est inférieure à un seuil prédéfini, une image déformée intermédiaire est créée et l'algorithme de recalage est réinitialisé.

Une autre façon de préserver la topologie est d'inclure des contraintes, c'est-à-dire d'ajouter dans la fonction objectif un terme contrôlant le jacobien. Dans [23], Christensen and Johnson ajoutent un terme à la fonction objectif qui pénalise les petites et les grandes valeurs du jacobien.

1.3 Contribution

Cette thèse se divise en trois parties dont les résultats ont été exposés dans les articles [56], [57] et [55].

Dans [56], on s'intéresse à la construction d'une méthode de correction du champ de déformation associé à un algorithme de recalage d'images afin que celui-ci préserve la topologie ou l'orientation.

La violation de cette contrainte de préservation de la topologie se manifeste, numériquement, par la présence de chevauchements ou de plis sur la grille de déformation (cf Figure 3.1 page 42). La méthode se compose de deux étapes : la première consiste à détecter et corriger les zones où le jacobien discret est négatif. La deuxième consiste à reconstruire la déformation à partir des valeurs de ses gradients discrets. Le problème est formulé comme la minimisation d'une fonctionnelle sous contraintes de type interpolation de Lagrange.

Dans [57], on introduit un modèle conjoint de segmentation et de recalage fondé sur l'élasticité non linéaire. On construit une mesure de similarité basée sur la variation totale pondérée et un régularisateur faisant intervenir la densité d'énergie d'un matériau de Saint Venant-Kirchhoff. Le fait d'ajouter le terme de variation totale pondérée permet d'aligner les bords des objets même si les modalités sont différentes.

Dans [55], on construit également un modèle conjoint de segmentation et de recalage. Dans cette partie, les objets à apparier sont modélisés par des fonctions level sets et évoluent de façon à minimiser une fonctionnelle contenant un régularisateur fondé sur l'élasticité non linéaire et un critère de similarité basé sur des résultats intermédiaires de segmentation.

Dans ce qui suit, on donne un résumé de chacune de ces contributions qui seront développées respectivement dans les chapitres 3, 4 et 5.

1.3.1 Préservation de la topologie du champ de déformation associé au recalage d'images

Cette méthode visant à obtenir un champ de déformation préservant la topologie se divise en deux étapes : la première consiste à localiser les chevauchements de la grille de déformation et à appliquer un paramètre de correction aux jacobiens discrets de la déformation. La deuxième étape consiste à reconstruire la déformation à partir des gradients discrets corrigés.

Correction du jacobien

La première étape est fondée sur cette proposition de Karaçali et Davatzikos :

Proposition 1.3.1 (De Karaçali et Davatzikos [43])

Soit \mathcal{C} la classe de déformations $h = (f, g)$ définies sur un rectangle discret $\Omega = [0, 1, \dots, M_1] \times [0, 1, \dots, N_1] \subset \mathbb{N}^2$ pour lesquelles $J_{ff}, J_{fb}, J_{bf}, J_{bb}$ sont positifs pour tout $(x, y) \in \Omega$.

Soit $h = (f, g)$ une déformation appartenant à \mathcal{C} . Alors son équivalent continu déterminé par l'interpolation de h sur le domaine $\Omega_C = [0, M_1] \times [0, N_1] \subset \mathbb{R}^2$ en utilisant l'interpolant Φ donné par $\Phi(x, y) = \Psi(x)\Psi(y)$ avec

$$\Psi : \begin{cases} 1 + t \text{ si } -1 \leq t \leq 0 \\ 1 - t \text{ si } 0 \leq t \leq 1 \\ 0 \text{ sinon} \end{cases}$$

préserve la topologie avec le schéma backward et forward de différences finies $f_x^b, f_x^f, f_y^b, f_y^f$

pour approximer les dérivées partielles de f (de même pour g) et :

$$\begin{cases} J_{ff} = f_x^f(p_1)g_y^f(p_1) - f_y^f(p_1)g_x^f(p_1) \\ J_{bf} = f_x^b(p_2)g_y^f(p_2) - f_y^f(p_2)g_x^b(p_2) \\ J_{fb} = f_x^f(p_3)g_y^b(p_3) - f_y^b(p_3)g_x^f(p_3) \\ J_{bb} = f_x^b(p_4)g_y^b(p_4) - f_y^b(p_4)g_x^b(p_4). \end{cases}$$

On rappelle :

$$\begin{cases} f_x^f(x, y) = f(x + 1, y) - f(x, y) \\ f_x^b(x, y) = f(x, y) - f(x - 1, y) \\ f_y^f(x, y) = f(x, y + 1) - f(x, y) \\ f_y^b(x, y) = f(x, y) - f(x, y - 1). \end{cases}$$

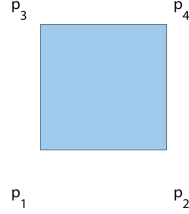


Figure 1.4: Disposition des points sur un carré de référence $[0, 1] \times [0, 1]$. Ces points coïncident avec les centres de gravité des pixels.

L'idée résultant de cette proposition est donc de pondérer au niveau discret et en chaque point de la grille, les gradients du champ de déplacement par un paramètre $\alpha \in]0, 1[$ afin de satisfaire les conditions de positivité des jacobiens discrets. La construction de l'algorithme est motivée par l'observation suivante. Dans le domaine continu, si l'on décompose une déformation $h = (f, g)$ en $h = \text{Id} + u$ avec $u = (u_1, u_2)$ le champ de vecteurs déplacement, on peut calculer le jacobien $J(x, y)$ en tout point (x, y) du domaine. Si maintenant on considère le champ de déformation associé

$$h_\alpha : (x, y) \longrightarrow (\text{Id} + \alpha u)(x, y) = (f_\alpha(x, y), g_\alpha(x, y)) = (x + \alpha u_1(x, y), y + \alpha u_2(x, y)),$$

on peut de façon analogue calculer le jacobien $J_\alpha(x, y)$ en chaque point (x, y) du domaine :

$$J_\alpha(x, y) = \left(1 + \alpha \frac{\partial u_1}{\partial x}(x, y)\right) \left(1 + \alpha \frac{\partial u_2}{\partial y}(x, y)\right) - \alpha^2 \frac{\partial u_2}{\partial x}(x, y) \frac{\partial u_1}{\partial y}(x, y).$$

Il revêt les propriétés suivantes : $J_\alpha(x, y)$ est un polynôme de degré 2 en α , $\lim_{\alpha \rightarrow 0} J_\alpha(x, y) = 1$ et $\lim_{\alpha \rightarrow 1} J_\alpha(x, y) = J(x, y)$.

Si on suppose que $J(x, y) < 0$, alors en utilisant le théorème des valeurs intermédiaires, il existe $\alpha^* \in]0, 1[$ tel que $J_{\alpha^*}(x, y) = \varepsilon \in [0, 1]$. L'idée est donc de confiner les valeurs du jacobien à un intervalle positif en corrigeant les gradients du champ de vecteur déplacement (c'est-à-dire, en les affectant d'un poids positif compris entre 0 et 1).

Grâce à ce paramètre α , on peut calculer les matrices jacobienues corrigées (quand cela est nécessaire) en chaque point de la grille discrète. Le résultat de cette première étape de l'algorithme est donc l'ensemble discret des matrices jacobienues éventuellement corrigées notées $\{\omega_i\}$ dans la suite.

Reconstruction de la déformation

Pour la seconde étape, on suppose que l'on a identifié (manuellement pour le moment) \mathcal{N} sous-espaces connexes non vides Ω_i de Ω , $i \in \{1, \dots, \mathcal{N}\}$ sur lesquels la préservation de l'orientation n'est pas satisfaite. Nous introduisons ensuite notre modèle mathématique de reconstruction, valide pour chaque sous-domaine Ω_i , $i \in \{1, \dots, \mathcal{N}\}$. Une approche D^m -spline est retenue (voir [1] pour plus de détails).

Soient $A = \{a_i\}_{i=1, \dots, N}$ un ensemble de N points de $\overline{\Omega_\nu}$ contenant un sous-ensemble P_1 -unisolvant. Dans notre cas, l'ensemble A contient les coordonnées des pixels de l'image inclus dans $\overline{\Omega_\nu}$.

Soient $\{\omega_i\}_{i=1, \dots, N}$ l'ensemble des N matrices jacobienues de la déformation données aux points $\{a_i\}_{i=1, \dots, N}$. Cet ensemble contient les gradients corrigés de la déformation obtenus à l'étape de correction de l'algorithme.

Enfin, soient $\{b_i\}_{i=1, \dots, l}$ l points de $\overline{\Omega_\nu}$ où les gradients sont restés inchangés. En pratique, ces points appartiennent à la frontière du domaine Ω_ν , $\partial\Omega_\nu$. On fixe des contraintes d'interpolation de Lagrange en ces points. Cela signifie que si h représente la déformation non altérée et v la déformation inconnue du problème de minimisation, on doit avoir

$$\forall i \in \{1, \dots, l\}, v(b_i) = h(b_i).$$

Soit K l'ensemble défini par $K = \{v \in H^3(\Omega_\nu, \mathbb{R}^2), \beta(v) = \eta\}$, avec β l'application :

$$\beta : \begin{cases} H^3(\Omega_\nu, \mathbb{R}^2) \rightarrow \mathbb{R}^{2l} \\ v \mapsto \beta(v) = (v(b_1), \dots, v(b_l))^T \end{cases}$$

et $\eta = (h(b_1), \dots, h(b_l))^T$.

On définit également :

$$\rho : \begin{cases} H^2(\Omega_\nu, \mathbb{R}^{2 \times 2}) \rightarrow (\mathbb{R}^{2 \times 2})^N \\ v \mapsto \rho(v) = (v(a_1), v(a_2), \dots, v(a_N))^T \end{cases} \quad (1.3)$$

Le problème, formulé au moyen de la fonctionnelle \mathcal{J}_ϵ ($|\cdot|_{3, \Omega_\nu, \mathbb{R}^2}$ désignant la semi-norme sur $H^3(\Omega_\nu, \mathbb{R}^2)$),

$$\mathcal{J}_\epsilon : \begin{cases} H^3(\Omega_\nu, \mathbb{R}^2) \rightarrow \mathbb{R} \\ v \mapsto \langle \rho(Dv) - w \rangle_N^2 + \epsilon |v|_{3, \Omega_\nu, \mathbb{R}^2}^2, \end{cases}$$

est défini par :

$$\begin{cases} \text{Trouver } \sigma_\epsilon \in K \text{ telle que} \\ \forall v \in K, \mathcal{J}_\epsilon(\sigma_\epsilon) \leq \mathcal{J}_\epsilon(v). \end{cases} \quad (1.4)$$

On peut également définir un problème équivalent au moyen des multiplicateurs de Lagrange. Si σ_ϵ est l'unique solution du problème (1.4), on démontre que σ_ϵ est aussi la solution du

problème suivant avec multiplicateurs de Lagrange :

$$\begin{cases} \text{Trouver } (\sigma_\epsilon, \lambda) \in K \times \mathbb{R}^{2l}, \\ \forall v \in \mathbf{H}^3(\Omega_\nu, \mathbb{R}^2), \mathbf{a}(\sigma_\epsilon, v) - L(v) + \langle \lambda, \beta(v) \rangle_{2l} = 0, \end{cases} \quad (1.5)$$

avec \mathbf{a} la forme bilinéaire symétrique définie par :

$$\mathbf{a} : \begin{cases} \mathbf{H}^3(\Omega_\nu, \mathbb{R}^2) \times \mathbf{H}^3(\Omega_\nu, \mathbb{R}^2) \rightarrow \mathbb{R} \\ (u, v) \mapsto \langle \rho(Du), \rho(Dv) \rangle_N + \epsilon (u, v)_{3, \Omega_\nu, \mathbb{R}^2}, \end{cases}$$

et L la forme linéaire définie par :

$$L : \begin{cases} \mathbf{H}^3(\Omega_\nu, \mathbb{R}^2) \rightarrow \mathbb{R} \\ v \mapsto \langle \rho(Dv), \omega \rangle_N \end{cases} .$$

Il faut ensuite discrétiser le problème (1.5). Pour ce faire, nous utilisons la théorie des éléments finis (voir [1] et [25]).

1.3.2 Modèle conjoint de segmentation et recalage fondé sur la variation totale pondérée et l'élasticité non linéaire

Dans cette méthode, le modèle de déformation choisi est un modèle élastique non linéaire. Plus particulièrement, les objets à apparier sont assimilés à des matériaux de type Saint Venant-Kirchhoff. On introduit également un terme d'attache aux données fondé sur la variation totale pondérée afin d'apparier les bords des objets contenus dans les images.

On note $\varphi : \bar{\Omega} \rightarrow \mathbb{R}^2$ la déformation recherchée, et T et R les images *Template* et *Reference*.

La densité d'énergie d'un matériau de type Saint Venant-Kirchhoff est définie par :

$$W_{SVK}(F) = \widehat{W}(E) = \frac{\lambda}{2} (\text{tr } E)^2 + \mu \text{tr } E^2.$$

Pour s'assurer que le jacobien de la déformation ne présente pas de trop grandes expansions ou contractions, on ajoute à cette densité le terme $\mu (\det F - 1)^2$ contrôlant que le jacobien reste proche de 1.

Le terme de régularisation de notre fonctionnelle s'écrit donc :

$$W(F) = W_{SVK}(F) + \mu (\det F - 1)^2.$$

De même, le critère de similarité s'écrit :

$$W_{fid}(\varphi) = \text{var}_g T \circ \varphi + \frac{\nu}{2} \int_{\Omega} (T \circ \varphi - R)^2 dx, \quad (1.6)$$

avec

$$\text{var}_g(u) = \sup \left\{ \int_{\Omega} u \text{div}(\varphi) dx : |\varphi| \leq g \text{ partout, } \varphi \in \text{Lip}_0(\Omega, \mathbb{R}^2) \right\} < \infty, \quad (1.7)$$

g est une fonction *edge detector* et $\text{Lip}_0(\Omega, \mathbb{R}^2)$ est l'espace des fonctions lipschitziennes à support compact. Le problème de minimisation (P) s'écrit :

$$\inf_{\varphi \in \text{Id} + W_0^{1,4}(\Omega, \mathbb{R}^2)} \left\{ I(\varphi) = \text{var}_g T \circ \varphi + \int_{\Omega} f(x, \varphi(x), \nabla \varphi(x)) dx \right. \quad (\text{P}) \\ \left. = \text{var}_g T \circ \varphi + \int_{\Omega} \left[\frac{\nu}{2} (T(\varphi) - R)^2 + W(\nabla \varphi(x)) \right] dx \right\}.$$

Cependant f n'est pas quasiconvexe (voir [30] Chapitre 9 pour plus de détails sur cette notion) ce qui pose un problème de nature théorique puisqu'on ne peut établir la semi-continuité inférieure faible de la fonctionnelle et subséquemment l'existence de minimiseurs. Pour pallier ce problème, nous avons défini un problème relaxé associé au problème initial en remplaçant f par son enveloppe quasiconvexe.

Cette enveloppe quasiconvexe Qf de f est définie par $Qf(x, \varphi, \xi) = \frac{\nu}{2} (T(\varphi) - R)^2 + QW(\xi)$

$$\text{avec } QW(\xi) = \begin{cases} W(\xi) & \text{si } \|\xi\|^2 \geq 2 \frac{\lambda + \mu}{\lambda + 2\mu}, \\ \Psi(\det \xi) & \text{si } \|\xi\|^2 < 2 \frac{\lambda + \mu}{\lambda + 2\mu}, \end{cases}$$

et Ψ , l'application convexe telle que $\Psi : t \mapsto -\frac{\mu}{2} t^2 + \mu (t - 1)^2 + \frac{\mu(\lambda + \mu)}{2(\lambda + 2\mu)}$.

Le problème relaxé (QP) introduit est alors défini par :

$$\inf \left\{ \bar{I}(\varphi) = \text{var}_g T \circ \varphi + \int_{\Omega} Qf(x, \varphi(x), \nabla \varphi(x)) dx \right\}, \quad (\text{QP})$$

avec $\varphi \in \text{Id} + W_0^{1,4}(\Omega, \mathbb{R}^2)$.

On peut, entre autres, établir un résultat d'existence de minimiseurs de ce problème relaxé, et avec une hypothèse de convergence L^1 supplémentaire, on peut montrer que les solutions du problème relaxé sont des solutions dites généralisées du problème initial.

1.3.3 Modèle conjoint de segmentation et recalage non local

Dans ce chapitre, on utilise le même modèle de déformation que dans le chapitre précédent, à savoir un modèle élastique non linéaire. En ce qui concerne le terme d'attache aux données, sa construction est liée à une équation d'évolution issue d'un problème de segmentation sous contraintes topologiques. Plus précisément, on définit Φ_0 une fonction level set dont le niveau zéro représente le bord des objets contenus dans l'image *Template*.

On se propose d'étudier le problème de minimisation suivant :

$$\inf \left\{ \bar{I}(\varphi) = \int_{\Omega} f(x, \varphi(x), \nabla \varphi(x)) dx : \varphi \in \text{Id} + W_0^{1,4}(\Omega, \mathbb{R}^2) \right\}, \quad (1.8)$$

avec $f(x, \varphi, \xi) = \frac{\nu}{2} \|\Phi_0 \circ \varphi - \tilde{\Phi}(\cdot, T)\|^2 + QW(\xi)$, où $\tilde{\Phi}$ est une solution de l'équation d'évolution provenant du modèle de segmentation préservant la topologie de Le Guyader et Vese ([46])

$$\begin{cases} \frac{\partial \tilde{\Phi}}{\partial t} = |\nabla \tilde{\Phi}| \left[\operatorname{div} \left(\tilde{g}(|\nabla R|) \frac{\nabla \tilde{\Phi}}{|\nabla \tilde{\Phi}|} \right) \right] + 4 \frac{\mu'}{d^2} \bar{H}(\tilde{\Phi}(x) + l) \bar{H}(l - \tilde{\Phi}(x)) \\ \int_{\Omega} \left[\langle x - y, \nabla \tilde{\Phi}(y) \rangle e^{-\|x-y\|_2^2/d^2} \bar{H}(\tilde{\Phi}(y) + l) \bar{H}(l - \tilde{\Phi}(y)) \right] dy, \\ \tilde{\Phi}(x, 0) = \Phi_0(x), \\ \frac{\partial \tilde{\Phi}}{\partial \vec{\nu}} = 0, \quad \text{on } \partial\Omega. \end{cases} \quad (\text{E})$$

La fonction \tilde{g} est une fonction *edge detector* classique.

On peut établir un résultat d'existence de solutions pour ce problème de minimisation.

On étudie ensuite le caractère bien posé de $\tilde{\Phi}$. Pour cela, le cadre de la théorie des solutions de viscosité est un cadre approprié du fait de la non linéarité due au terme de courbure pondérée et de la singularité en $\nabla \tilde{\Phi} = 0$.

1.4 Organisation de la thèse

Dans le chapitre 2, nous présentons les outils mathématiques nécessaires à l'introduction et à l'étude des modèles proposés. Ces rappels concernent les espaces fonctionnels de Lebesgue et de Sobolev, les fonctions à variation bornée, l'analyse convexe, ainsi que la théorie de l'élasticité en suivant principalement [12], [30], [33] et [45].

Dans le chapitre 3, nous présentons la méthode de correction de champ de déformation préservant la topologie développée dans [56].

Dans le chapitre 4, nous étudions un modèle conjoint de segmentation et recalage fondé sur la variation totale pondérée et sur l'élasticité non linéaire suivant [57].

Dans le chapitre 5, nous introduisons un modèle conjoint de segmentation et recalage non local avec une régularisation élastique non linéaire comme présenté dans [55].

Les chapitres 6 et 7 constituent des pistes de recherche qui n'ont été que partiellement abouties à ce jour et qui feront l'objet d'études ultérieures. Le chapitre 6 présente l'ajout de contraintes géométriques au critère de similarité L^2 classique. Dans le chapitre 7, nous avons tenté de construire un critère de similarité basé sur la comparaison des gradients normalisés des images en nous inspirant du modèle d'inpainting introduit par Ballester *et al.* [7].

- [1] R. ARCANGÉLI, M. C. LÓPEZ DE SILANES, AND J. J. TORRENS, *Multidimensional minimizing splines. Theory and applications*, Grenoble Sciences, Kluwer Academic Publishers, Boston, MA, 2004.
- [2] J. ASHBURNER AND K. J. FRISTON, *Nonlinear spatial normalization using basis functions*, *Human brain mapping*, 7 (1999), pp. 254–266.
- [3] G. AUBERT AND P. KORNPORST, *Mathematical problems in image processing, volume 147 of applied mathematical sciences*, 2002.
- [4] ———, *Mathematical problems in image processing: partial differential equations and the calculus of variations*, vol. 147, Springer Science & Business Media, 2006.
- [5] J.-F. AUJOL, S. LADJAL, AND S. MASNOU, *Exemplar-based inpainting from a variational point of view*, *SIAM Journal on Mathematical Analysis*, 42 (2010), pp. 1246–1285.
- [6] R. BAJCSY AND S. KOVAČIČ, *Multiresolution elastic matching*, *Computer Vision, Graphics, and Image Processing*, 46 (1989), pp. 1–21.
- [7] C. BALLESTER, M. BERTALMIO, V. CASELLES, G. SAPIRO, AND J. VERDERA, *Filling-in by joint interpolation of vector fields and gray levels*, *Image Processing, IEEE Transactions on*, 10 (2001), pp. 1200–1211.
- [8] M. F. BARNSLEY AND L. P. HURD, *Fractal image compression*, AK Peters, Ltd., 1993.
- [9] M. BEG, M. MILLER, A. TROUVÉ, AND L. YOUNES, *Computing Large Deformation Metric Mappings via Geodesic Flows of Diffeomorphisms*, *International Journal of Computer Vision*, 61 (2005), pp. 139–157.
- [10] M. BERTALMIO, A. L. BERTOZZI, AND G. SAPIRO, *Navier-stokes, fluid dynamics, and image and video inpainting*, in *Computer Vision and Pattern Recognition, 2001. CVPR 2001. Proceedings of the 2001 IEEE Computer Society Conference on*, vol. 1, IEEE, 2001, pp. I–355.
- [11] M. BERTALMIO, L. VESE, G. SAPIRO, AND S. OSHER, *Simultaneous structure and texture image inpainting*, *Image Processing, IEEE Transactions on*, 12 (2003), pp. 882–889.

- [12] H. BREZIS, *Analyse fonctionnelle. Théorie et Applications*, Dunod, Paris, 2005.
- [13] C. BROIT, *Optimal Registration of Deformed Images*, PhD thesis, Computer and Information Science, University of Pennsylvania, 1981.
- [14] L. G. BROWN, *A survey of image registration techniques*, ACM computing surveys (CSUR), 24 (1992), pp. 325–376.
- [15] A. BUADES, B. COLL, AND J.-M. MOREL, *A review of image denoising algorithms, with a new one*, Multiscale Modeling & Simulation, 4 (2005), pp. 490–530.
- [16] M. BURGER, J. MODERSITZKI, AND L. RUTHOTTO, *A hyperelastic regularization energy for image registration*, SIAM Journal on Scientific Computing, 35 (2013), pp. B132–B148.
- [17] V. CASELLES, R. KIMMEL, AND G. SAPIRO, *Geodesic active contours*, International journal of computer vision, 22 (1997), pp. 61–79.
- [18] A. CHAMBOLLE AND P.-L. LIONS, *Image recovery via total variation minimization and related problems*, Numerische Mathematik, 76 (1997), pp. 167–188.
- [19] T. CHAN AND L. VESE, *An active contour model without edges*, Lecture Notes in Computer Science, 1682 (1999), pp. 141–151.
- [20] T. F. CHAN AND J. J. SHEN, *Image processing and analysis: variational, PDE, wavelet, and stochastic methods*, Siam, 2005.
- [21] T. F. CHAN AND C.-K. WONG, *Total variation blind deconvolution*, Image Processing, IEEE Transactions on, 7 (1998), pp. 370–375.
- [22] G. CHRISTENSEN, R. RABBITT, AND M. MILLER, *Deformable Templates Using Large Deformation Kinematics*, IEEE Trans. Image Process., 5 (1996), pp. 1435–1447.
- [23] G. E. CHRISTENSEN AND H. J. JOHNSON, *Consistent image registration*, Medical Imaging, IEEE Transactions on, 20 (2001), pp. 568–582.
- [24] H. CHUI AND A. RANGARAJAN, *A new point matching algorithm for non-rigid registration*, Computer Vision and Image Understanding, 89 (2003), pp. 114–141.
- [25] P. CIARLET, *The Finite Element Method for Elliptic Problems*, North Holland, Amsterdam, The Netherlands, 1978.
- [26] ———, *Elasticité Tridimensionnelle*, Masson, 1985.
- [27] ———, *Mathematical Elasticity, Volume I: Three-dimensional elasticity*, Amsterdam etc., North-Holland, 1988.
- [28] O. CLATZ, M. SERMESANT, P.-Y. BONDIAU, H. DELINGETTE, S. K. WARFIELD, G. MALANDAIN, AND N. AYACHE, *Realistic simulation of the 3-D growth of brain tumors in MR images coupling diffusion with biomechanical deformation*, Medical Imaging, IEEE Transactions on, 24 (2005), pp. 1334–1346.
- [29] A. COLLIGNON, F. MAES, D. DELAERE, D. VANDERMEULEN, P. SUETENS, AND G. MARCHAL, *Automated multi-modality Image Registration based on information theory*, 3 (1995).

- [30] B. DACOROGNA, *Direct Methods in the Calculus of Variations, Second Edition*, Springer, 2008.
- [31] C. DAVATZIKOS, *Spatial transformation and registration of brain images using elastically deformable models*, Computer Vision and Image Understanding, 66 (1997), pp. 207–222.
- [32] M. H. DAVIS, A. KHOTANZAD, D. P. FLAMIG, AND S. E. HARMS, *A physics-based coordinate transformation for 3-D image matching*, Medical Imaging, IEEE Transactions on, 16 (1997), pp. 317–328.
- [33] F. DEMENGEL AND G. DEMENGEL, *Functional Spaces for the Theory of Elliptic Partial Differential Equations*, Springer, 2012.
- [34] R. DERFOUL AND C. LE GUYADER, *A relaxed problem of registration based on the Saint Venant-Kirchhoff material stored energy for the mapping of mouse brain gene expression data to a neuroanatomical mouse atlas*, SIAM Journal on Imaging Sciences, 7 (2014), pp. 2175–2195.
- [35] M. DROSKE AND M. RUMPF, *A Variational Approach to Non-Rigid Morphological Registration*, SIAM J. Appl. Math., 64 (2004), pp. 668–687.
- [36] B. FISCHER AND J. MODERSITZKI, *Fast diffusion registration*, AMS Contemporary Mathematics, Inverse Problems, Image Analysis, and Medical Imaging, 313 (2002), pp. 11–129.
- [37] ———, *Fast diffusion registration*, AMS Contemporary Mathematics, Inverse Problems, Image Analysis, and Medical Imaging, 313 (2002), pp. 117–129.
- [38] ———, *Curvature based image registration*, J. Math. Imaging Vis., 18 (2003), pp. 81–85.
- [39] G. GILBOA AND S. OSHER, *Nonlocal operators with applications to image processing*, Multiscale Modeling & Simulation, 7 (2008), pp. 1005–1028.
- [40] E. HABER, S. HELDMANN, AND J. MODERSITZKI, *A computational framework for image-based constrained registration*, Linear Algebra and its Applications, 431 (2009), pp. 459–470. Special Issue in honor of Henk van der Vorst.
- [41] E. HABER AND J. MODERSITZKI, *Intensity gradient based registration and fusion of multi-modal images*, in Medical Image Computing and Computer-Assisted Intervention—MICCAI 2006, Springer, 2006, pp. 726–733.
- [42] P. HELLIER AND C. BARILLOT, *Coupling dense and landmark-based approaches for nonrigid registration*, Medical Imaging, IEEE Transactions on, 22 (2003), pp. 217–227.
- [43] B. KARAÇALI AND C. DAVATZIKOS, *Estimating topology preserving and smooth displacement fields*, IEEE Trans. Med. Imag., 23 (2004), pp. 868–880.
- [44] M. KASS, A. WITKIN, AND D. TERZOPOULOS, *Snakes: Active contour models*, International journal of computer vision, 1 (1988), pp. 321–331.
- [45] H. LE DRET, *Notes de Cours de DEA. Méthodes mathématiques en élasticité é*, (2003–2004).

- [46] C. LE GUYADER AND L. VESE, *Self-repelling snakes for topology-preserving segmentation models*, Image Processing, IEEE Transactions on, 17 (2008), pp. 767–779.
- [47] C. LE GUYADER AND L. VESE, *A combined segmentation and registration framework with a nonlinear elasticity smoother*, Computer Vision and Image Understanding, 115 (2011), pp. 1689–1709.
- [48] T. M. LEHMANN, C. GÖNNER, AND K. SPITZER, *Survey: Interpolation methods in medical image processing*, Medical Imaging, IEEE Transactions on, 18 (1999), pp. 1049–1075.
- [49] A. S. LEWIS AND G. KNOWLES, *Image compression using the 2-d wavelet transform*, Image Processing, IEEE Transactions on, 1 (1992), pp. 244–250.
- [50] N. LORD, J. HO, B. VEMURI, AND S. EISENSCHENK, *Simultaneous registration and parcellation of bilateral hippocampal surface pairs for local asymmetry quantification*, IEEE Trans Med Imaging., 26 (2007), pp. 471–478.
- [51] M. MILLER, A. TROUVÉ, AND L. YOUNES, *On the metrics and Euler-Lagrange equations of computational anatomy*, Annual Review of Biomedical Engineering, 4 (2002), pp. 375–405.
- [52] M. I. MILLER AND L. YOUNES, *Group actions, homeomorphisms, and matching: A general framework*, International Journal of Computer Vision, 41 (2001), pp. 61–84.
- [53] J. MODERSITZKI, *Numerical Methods for Image Registration*, Oxford University Press, 2004.
- [54] ———, *FAIR: Flexible Algorithms for Image Registration*, Society for Industrial and Applied Mathematics (SIAM), 2009.
- [55] S. OZERÉ AND C. LE GUYADER, *Nonlocal joint segmentation registration model*, in Scale Space and Variational Methods in Computer Vision, Springer, 2015, pp. 348–359.
- [56] S. OZERÉ AND C. LE GUYADER, *Topology preservation for image-registration-related deformation fields*, Communications in Mathematical Sciences, 13 (2015), pp. 1135–1161.
- [57] S. OZERÉ AND C. LE GUYADER, *Joint segmentation/registration model by shape alignment via weighted total variation minimization and nonlinear elasticity*, accepted for publication in SIIMS, (July 2015).
- [58] X. PENNEC, P. CACHIER, AND N. AYACHE, *Understanding the “demon’s algorithm”: 3d non-rigid registration by gradient descent*, in Medical Image Computing and Computer-Assisted Intervention—MICCAI’99, Springer, 1999, pp. 597–605.
- [59] G. PEYRÉ, *Image processing with nonlocal spectral bases*, Multiscale Modeling & Simulation, 7 (2008), pp. 703–730.
- [60] R. RABBITT, J. WEISS, G. CHRISTENSEN, AND M. MILLER, *Mapping of Hyperelastic Deformable Templates Using the Finite Element Method*, in Proceedings SPIE, vol. 2573, SPIE, 1995, pp. 252–265.

- [61] L. I. RUDIN, S. OSHER, AND E. FATEMI, *Nonlinear total variation based noise removal algorithms*, *Physica D: Nonlinear Phenomena*, 60 (1992), pp. 259–268.
- [62] T. SEDERBERG AND S. PARRY, *Free-form Deformation of Solid Geometric Models*, *SIGGRAPH Comput. Graph.*, 20 (1986), pp. 151–160.
- [63] J. SERRA, *Image analysis and mathematical morphology*, Academic Press, Inc., 1983.
- [64] D. SHEN AND C. DAVATZIKOS, *HAMMER: hierarchical attribute matching mechanism for elastic registration*, *Medical Imaging, IEEE Transactions on*, 21 (2002), pp. 1421–1439.
- [65] J. SHEN, S. H. KANG, AND T. F. CHAN, *Euler’s elastica and curvature-based inpainting*, *SIAM Journal on Applied Mathematics*, 63 (2003), pp. 564–592.
- [66] A. SOTIRAS, C. DAVATZIKOS, AND N. PARAGIOS, *Deformable medical image registration: A survey*, *Medical Imaging, IEEE Transactions on*, 32 (2013), pp. 1153–1190.
- [67] A. SOTIRAS, Y. OU, B. GLOCKER, C. DAVATZIKOS, AND N. PARAGIOS, *Simultaneous geometric-iconic registration*, in *Medical Image Computing and Computer-Assisted Intervention–MICCAI 2010*, Springer, 2010, pp. 676–683.
- [68] T. W. TANG AND A. C. CHUNG, *Non-rigid image registration using graph-cuts*, in *Medical Image Computing and Computer-Assisted Intervention–MICCAI 2007*, Springer, 2007, pp. 916–924.
- [69] J.-P. THIRION, *Image matching as a diffusion process: an analogy with Maxwell’s demons*, *Medical Image Analysis*, 2 (1998), pp. 243 – 260.
- [70] G. UNAL AND G. SLABAUGH, *Coupled PDEs for non-rigid registration and segmentation*, in *Computer Vision and Pattern Recognition, 2005. CVPR 2005. IEEE Computer Society Conference on*, vol. 1, 2005, pp. 168–175.
- [71] B. VEMURI AND Y. CHEN, *Joint Image Registration and Segmentation*, in *Geometric Level Set Methods in Imaging, Vision, and Graphics*, Springer New York, 2003, pp. 251–269.
- [72] B. VEMURI, J. YE, Y. CHEN, AND C. LEONARD, *Image registration via level-set motion: Applications to atlas-based segmentation*, *Medical Image Analysis*, 7 (2003), pp. 1 – 20.
- [73] F. WANG AND B. VEMURI, *Simultaneous Registration and Segmentation of Anatomical Structures from Brain MRI*, in *Medical Image Computing and Computer-Assisted Intervention – MICCAI 2005*, J. Duncan and G. Gerig, eds., vol. 3749 of *Lecture Notes in Computer Science*, Springer Berlin Heidelberg, 2005, pp. 17–25.
- [74] F. WANG, B. C. VEMURI, A. RANGARAJAN, AND S. J. EISENSCHENK, *Simultaneous nonrigid registration of multiple point sets and atlas construction*, *Pattern Analysis and Machine Intelligence, IEEE Transactions on*, 30 (2008), pp. 2011–2022.
- [75] W. M. WELLS, P. VIOLA, H. ATSUMI, S. NAKAJIMA, AND R. KIKINIS, *Multi-modal volume registration by maximization of mutual information*, *Medical image analysis*, 1 (1996), pp. 35–51.

- [76] C. XIAOHUA, M. BRADY, AND D. RUECKERT, *Simultaneous Segmentation and Registration for Medical Image*, in Medical Image Computing and Computer-Assisted Intervention – MICCAI 2004, C. Barillot, D. Haynor, and P. Hellier, eds., vol. 3216 of Lecture Notes in Computer Science, Springer Berlin Heidelberg, 2004, pp. 663–670.
- [77] C. XU AND J. L. PRINCE, *Snakes, shapes, and gradient vector flow*, Image Processing, IEEE Transactions on, 7 (1998), pp. 359–369.
- [78] I. YANOVSKY, C. LE GUYADER, A. LEOW, A. TOGA, P. THOMPSON, AND L. VESE, *Unbiased volumetric registration via nonlinear elastic regularization*, in 2nd MICCAI Workshop on Mathematical Foundations of Computational Anatomy, 2008.
- [79] A. YEZZI, L. ZOLLEI, AND T. KAPUR, *A variational framework for joint segmentation and registration*, in Mathematical Methods in Biomedical Image Analysis, IEEE-MMBIA, 2001, pp. 44–51.
- [80] L. ZAGORCHEV AND A. GOSHTASBY, *A comparative study of transformation functions for nonrigid image registration*, Image Processing, IEEE Transactions on, 15 (2006), pp. 529–538.

In this chapter, we provide definitions and theorems that are needed to introduce our problems and prove the existence of solutions. First, we make a brief reminder about functional spaces, in particular Sobolev spaces and the space of bounded variation functions. Next, we summarize some relevant facts in the theory of calculus of variations. At last, we give a brief exposition of elasticity and hyperelasticity theory.

2.1 L^p Spaces

In a first time, we introduce L^p space. Definitions and theorems of this section are extracted from [3].

In the sequel, we denote by Ω an open set of \mathbb{R}^N endowed with the Lebesgue measure dx .

Definition 2.1.1 (L^p Space)

Let $p \in \mathbb{R}$ with $1 \leq p < \infty$. We set

$$L^p(\Omega) = \{f : \Omega \rightarrow \mathbb{R}, f \text{ measurable and } |f|^p \in L^1(\Omega)\}.$$

We denote by

$$\|f\|_{L^p(\Omega)} = \left(\int_{\Omega} |f(x)|^p dx \right)^{1/p}.$$

Definition 2.1.2 (L^∞ Space)

We set

$$L^\infty(\Omega) = \{f : \Omega \rightarrow \mathbb{R}, f \text{ measurable and } \exists \text{ a constant } C \text{ such that } |f(x)| \leq C \text{ a.e. on } \Omega\}.$$

We denote by

$$\|f\|_{L^\infty(\Omega)} = \inf \{C, |f(x)| \leq C \text{ a.e. on } \Omega\}.$$

Theorem 2.1.3

$L^p(\Omega)$ is a vector space and $\|\cdot\|_{L^p(\Omega)}$ is a norm for all $1 \leq p \leq \infty$.

We start with important integration results.

Theorem 2.1.4 (Monotone Convergence Theorem of Beppo-Levi)

Let (f_n) be an increasing sequence of functions in $L^1(\Omega)$ such that $\sup_n \int_{\Omega} f_n < \infty$. Then $f_n(x)$ converges a.e. on Ω to a finite limit denoted by $f(x)$. Moreover, $f \in L^1(\Omega)$ and $\|f_n - f\|_{L^1(\Omega)} \rightarrow 0$.

Theorem 2.1.5 (Lebesgue Dominated Convergence Theorem)

Let (f_n) be a sequence of functions in $L^1(\Omega)$. We assume that

1. $f_n(x) \rightarrow f(x)$ a.e. on Ω ,
 2. there exists a function $g \in L^1(\Omega)$ such that for every n , $|f_n(x)| \leq g(x)$ a.e. on Ω .
- Then $f \in L^1(\Omega)$ and $\|f_n - f\|_{L^1(\Omega)} \rightarrow 0$.

Lemma 2.1.6 (Fatou Lemma)

Let (f_n) be a sequence of functions in $L^1(\Omega)$ such that

1. for every n , $f_n(x) \geq 0$ a.e. on Ω ,
2. $\sup_n \int_{\Omega} f_n < \infty$.

For every $x \in \Omega$ we set $f(x) = \liminf_{n \rightarrow +\infty} f_n(x)$. Then $f \in L^1(\Omega)$ and

$$\int_{\Omega} f \leq \liminf_{n \rightarrow +\infty} \int_{\Omega} f_n.$$

Theorem 2.1.7 (Hölder inequality)

Let $f \in L^p(\Omega)$ and $g \in L^q(\Omega)$ with $1 \leq p \leq \infty$ and q be the conjugate exponent of p , i.e., $\frac{1}{p} + \frac{1}{q} = 1$.

Then $fg \in L^1(\Omega)$ and

$$\int_{\Omega} |fg| \leq \|f\|_{L^p(\Omega)} \|g\|_{L^q(\Omega)}.$$

Theorem 2.1.8 (Generalized Hölder inequality)

Let $1 \leq r \leq \infty$ and $1 \leq p_j \leq \infty$ with $\sum_{j=1}^n \frac{1}{p_j} = \frac{1}{r} \leq 1$. Let $f_j \in L^{p_j}(\Omega)$ for $j = 1 \dots n$.

Then $\prod_{j=1}^n f_j \in L^r(\Omega)$ and

$$\left\| \prod_{j=1}^n f_j \right\|_{L^r(\Omega)} \leq \prod_{j=1}^n \|f_j\|_{L^{p_j}(\Omega)}.$$

Theorem 2.1.9 (Young inequality)

Assume that $1 < p < \infty$ and q is the conjugate exponent of p , then

$$ab \leq \frac{1}{p}a^p + \frac{1}{q}b^q, \quad \forall a \geq 0, \forall b \geq 0.$$

Theorem 2.1.10 (Young inequality with ε)

Assume that $1 < p < \infty$ and q is the conjugate exponent of p , then

$$ab \leq \varepsilon a^p + C(\varepsilon)b^q, \quad \text{for } C(\varepsilon) = (\varepsilon p)^{-q/p} q^{-1}.$$

Theorem 2.1.11

Let (f_n) be a sequence of L^p and $f \in L^p$, such that $\|f_n - f\|_{L^p} \rightarrow 0$. Then there exists a subsequence (f_{n_k}) such that

1. $f_{n_k}(x) \rightarrow f(x)$ a.e. on Ω
2. $|f_{n_k}(x)| \leq h(x) \forall k$ and a.e. on Ω , with $h \in L^p$.

Theorem 2.1.12 (Fisher-Riesz)

L^p is a Banach space for $1 \leq p \leq \infty$.

Theorem 2.1.13

L^p is a reflexive space for $1 < p < \infty$.

Theorem 2.1.14

L^p is a separable space for $1 \leq p < \infty$.

Theorem 2.1.15 (Compactness properties)

- (i) Let X be a reflexive Banach space and let $C > 0$ be a positive real constant. Let also (u_n) be a sequence of X such that $\|u_n\|_X \leq C$. Then there exists $\bar{u} \in X$ and a subsequence (u_{n_k}) of (u_n) such that $u_{n_k} \xrightarrow{X} \bar{u}$ when $k \rightarrow +\infty$.
- (ii) Let X be a separable Banach space and let $C > 0$ be a positive real constant. Let also (l_n) be a sequence of X' such that $\|l_n\|_{X'} \leq C$. Then there exists $\bar{l} \in X'$ and a subsequence (l_{n_k}) of (l_n) such that $l_{n_k} \xrightarrow[X]{*} \bar{l}$ when $k \rightarrow +\infty$.

2.2 Sobolev spaces**Definition 2.2.1**

The Sobolev space $W^{1,p}(\Omega)$ is defined by

$$W^{1,p}(\Omega) = \left\{ u \in L^p(\Omega) \left| \begin{array}{l} \exists g_1, \dots, g_N \in L^p(\Omega) \text{ such that} \\ \int_{\Omega} u \frac{\partial \varphi}{\partial x_i} = - \int_{\Omega} g_i \varphi, \forall \varphi \in \mathcal{C}_c^\infty(\Omega), \forall i = 1, 2, \dots, N \end{array} \right. \right\}.$$

We set

$$H^1(\Omega) = W^{1,2}(\Omega).$$

For $u \in W^{1,p}(\Omega)$, we denote by

$$\frac{\partial u}{\partial x_i} = g_i \text{ and } \nabla u = \left(\frac{\partial u}{\partial x_1}, \frac{\partial u}{\partial x_2}, \dots, \frac{\partial u}{\partial x_N} \right).$$

The space $W^{1,p}(\Omega)$ is equipped with the norm

$$\|u\|_{W^{1,p}(\Omega)} = \|u\|_{L^p(\Omega)} + \sum_{i=1}^N \left\| \frac{\partial u}{\partial x_i} \right\|_{L^p(\Omega)},$$

or sometimes with the equivalent norm $\left(\|u\|_{L^p(\Omega)}^p + \sum_{i=1}^N \left\| \frac{\partial u}{\partial x_i} \right\|_{L^p(\Omega)}^p \right)^{1/p}$ (if $1 \leq p < \infty$).

In particular, $H^1(\Omega)$ is equipped with the inner product

$$(u, v)_{H^1(\Omega)} = (u, v)_{L^2(\Omega)} + \sum_{i=1}^N \left(\frac{\partial u}{\partial x_i}, \frac{\partial v}{\partial x_i} \right)_{L^2(\Omega)}$$

and the associated norm $\|u\|_{H^1(\Omega)} = \left(\|u\|_{L^2(\Omega)}^2 + \sum_{i=1}^N \left\| \frac{\partial u}{\partial x_i} \right\|_{L^2(\Omega)}^2 \right)^{1/2}$ is equivalent to the norm of $W^{1,2}(\Omega)$.

Unless mentioned otherwise, $W^{1,p}$ will denote $W^{1,p}(\Omega)$.

Proposition 2.2.1

The space $W^{1,p}$ is a Banach space for $1 \leq p \leq \infty$.

It is a reflexive space for $1 < p < \infty$ and a separable space for $1 \leq p < \infty$.

The space H^1 is a separable Hilbert space, that is a vector space endowed with an inner product (u, v) complete for the induced norm $(u, u)^{1/2}$.

Definition 2.2.2

(i) $\mathcal{C}^0(\Omega) = \mathcal{C}(\Omega)$ is the set of continuous functions $u : \Omega \rightarrow \mathbb{R}$.

(ii) $\mathcal{C}^0(\bar{\Omega}) = \mathcal{C}(\bar{\Omega})$ is the set of continuous functions $u : \Omega \rightarrow \mathbb{R}$, which can be continuously extended to $\bar{\Omega}$. The norm over $\mathcal{C}(\bar{\Omega})$ is given by

$$\|u\|_{\mathcal{C}^0} = \sup_{x \in \bar{\Omega}} |u(x)|.$$

(iii) The *support* of a function $u : \Omega \rightarrow \mathbb{R}$ is defined as

$$\text{supp } u := \overline{\{x \in \Omega : u(x) \neq 0\}}.$$

(iv) $\mathcal{C}_c(\Omega) = \{u \in \mathcal{C}(\Omega) : \text{supp } u \subset \Omega \text{ is compact}\}$.

(iv) For all $k \in \mathbb{N}$, we denote by $\mathcal{C}^k(\Omega)$ the space of continuous functions whose all partial derivatives up to order order k are continuous.

(vi) $\mathcal{C}^k(\bar{\Omega})$ is the set of $\mathcal{C}^k(\Omega)$ functions whose derivatives up to order k can be extended continuously to $\bar{\Omega}$. It is equipped with the following norm

$$\|u\|_{\mathcal{C}^k} = \max_{0 \leq \alpha \leq k} \sup_{x \in \bar{\Omega}} |D^\alpha u(x)|.$$

Theorem 2.2.3

Assume that $1 \leq p < \infty$.

(i) (**Product Rule**) If $u, v \in W^{1,p}(\Omega) \cap L^\infty(\Omega)$, then $uv \in W^{1,p}(\Omega) \cap L^\infty(\Omega)$ and

$$\frac{\partial(uv)}{\partial x_i} = \frac{\partial u}{\partial x_i} v + u \frac{\partial v}{\partial x_i}, \quad i = 1, 2, \dots, N.$$

(ii) (**Chain Rule**) Let $G \in \mathcal{C}^1(\mathbb{R})$ such that $G(0) = 0$ and $|G'(s)| \leq M \forall s \in \mathbb{R}$. Let $u \in W^{1,p}(\Omega)$, then

$$G \circ u \in W^{1,p}(\Omega) \quad \text{and} \quad \frac{\partial}{\partial x_i} (G \circ u) = (G' \circ u) \frac{\partial u}{\partial x_i}.$$

Theorem 2.2.4 (Trace Theorem)

Assume that Ω is bounded and of class \mathcal{C}^1 , and $1 \leq p < \infty$. There exists a bounded linear operator $T : W^{1,p}(\Omega) \rightarrow L^p(\partial\Omega)$ such that $Tu = u$ on $\partial\Omega$ for all $u \in W^{1,p}(\Omega) \cap \mathcal{C}(\bar{\Omega})$. Furthermore, for all $\phi \in \mathcal{C}_c^\infty(\mathbb{R}^N, \mathbb{R}^N)$ and $u \in W^{1,p}(\Omega)$,

$$\int_{\Omega} u \operatorname{div} \phi \, dx = - \int_{\Omega} \nabla u \cdot \phi \, dx + \int_{\partial\Omega} (\phi \cdot \nu) Tu \, d\mathcal{H}^{N-1},$$

ν denoting the unit outer normal to $\partial\Omega$.

Theorem 2.2.5 (Generalized Poincaré inequality, [6])

Let Ω be a Lipschitz bounded domain in \mathbb{R}^N . Let $p \in [1, \infty)$ and let \mathcal{N} be a continuous seminorm on $W^{1,p}(\Omega)$, that is, a norm on the constant functions. Then there exists a constant $C > 0$ that depends only on Ω, N, p , such that

$$\|u\|_{W^{1,p}(\Omega)} \leq C \left(\left(\int_{\Omega} |\nabla u|^p \, dx \right)^{1/p} + \mathcal{N}(u) \right).$$

We apply this result to $\mathcal{N}(u) = \int_{\partial\Omega} |u(x)| \, dx$.

Theorem 2.2.6 (Friedrichs)

Let $u \in W^{1,p}(\Omega)$ with $1 \leq p < \infty$. Then there exists a sequence (u_n) of $\mathcal{C}_c^\infty(\mathbb{R}^N)$ such that

1. $u_n|_{\Omega} \rightarrow u$ in $L^p(\Omega)$
2. $\nabla u_n|_{\omega} \rightarrow \nabla u|_{\omega}$ in $L^p(\omega)^N$ for all $\omega \subset\subset \Omega$

(the notation $\omega \subset\subset \Omega$ means that ω is an open such that $\bar{\omega} \subset \Omega$ and $\bar{\omega}$ is a compact set).

Theorem 2.2.7 (Density)

We assume Ω to be of class \mathcal{C}^1 . Let $u \in W^{1,p}(\Omega)$ with $1 \leq p < \infty$. Then there exists a sequence $(u_n) \in \mathcal{C}_c^\infty(\mathbb{R}^N)$ such that $u_n|_{\Omega} \rightarrow u$ in $W^{1,p}(\Omega)$. In other words, the restrictions to Ω of the functions of $\mathcal{C}_c^\infty(\mathbb{R}^N)$ are dense in $W^{1,p}(\Omega)$.

Theorem 2.2.8

We assume Ω to be of class C^1 , with $\partial\Omega$ bounded (or $\Omega = \mathbb{R}_+^N$). Then there exists a linear extension operator

$$P : W^{1,p}(\Omega) \longrightarrow W^{1,p}(\mathbb{R}^N),$$

such that $\forall u \in W^{1,p}(\Omega)$

- (i) $Pu|_{\Omega} = u$,
- (ii) $\|Pu\|_{L^p(\mathbb{R}^N)} \leq C\|u\|_{L^p(\Omega)}$,
- (iii) $\|Pu\|_{W^{1,p}(\mathbb{R}^N)} \leq C\|u\|_{W^{1,p}(\Omega)}$,

where C depends only on Ω .

Theorem 2.2.9 (Sobolev, Gagliardo, Nirenberg)

Let $1 \leq p < N$, then

$$W^{1,p}(\mathbb{R}^N) \subset L^{p^*}(\mathbb{R}^N) \text{ where } p^* \text{ is given by } \frac{1}{p^*} = \frac{1}{p} - \frac{1}{N}, \quad (2.1)$$

and there exists a constant $C = C(p, N)$ such that

$$\|u\|_{L^{p^*}} \leq C\|\nabla u\|_{L^p} \quad \forall u \in W^{1,p}(\mathbb{R}^N).$$

Corollary 2.2.2

Let $1 \leq p < N$. Then

$$W^{1,p}(\mathbb{R}^N) \subset L^q(\mathbb{R}^N) \quad \forall q \in [p, p^*]$$

with continuous embedding.

Corollary 2.2.3

In the case of $p = N$, we have

$$W^{1,N}(\mathbb{R}^N) \subset L^q(\mathbb{R}^N) \quad \forall q \in [N, +\infty[$$

with continuous embedding.

Theorem 2.2.10 (Morrey)

Let $p > N$, then

$$W^{1,p}(\mathbb{R}^N) \subset L^\infty(\mathbb{R}^N)$$

with continuous embedding.

Moreover, for all $u \in W^{1,p}(\mathbb{R}^N)$, we have

$$|u(x) - u(y)| \leq C|x - y|^\alpha \|\nabla u\|_{L^p} \text{ a.e. } x, y \in \mathbb{R}^N$$

with $\alpha = 1 - \frac{N}{p}$ and C is a constant (depending only on p and N).

Corollary 2.2.4

Let $m \geq 1$ be an integer and $1 \leq p < \infty$. We have
 if $\frac{1}{p} - \frac{m}{N} > 0$, then $W^{m,p}(\mathbb{R}^N) \subset L^q(\mathbb{R}^N)$ where $\frac{1}{q} = \frac{1}{p} - \frac{m}{N}$,
 if $\frac{1}{p} - \frac{m}{N} = 0$, then $W^{m,p}(\mathbb{R}^N) \subset L^q(\mathbb{R}^N)$ where $\forall q \in [p, \infty[$,
 if $\frac{1}{p} - \frac{m}{N} < 0$, then $W^{m,p}(\mathbb{R}^N) \subset L^\infty(\mathbb{R}^N)$,
 with continuous embeddings.

Moreover, if $m - \frac{N}{p} > 0$ is not an integer, we set

$$k = \left[m - \frac{N}{p} \right] \text{ and } \theta = m - \frac{N}{p} - k \text{ (} 0 < \theta < 1 \text{)}.$$

We have, for all $u \in W^{1,p}(\mathbb{R}^N)$,

$$\|D^\alpha u\|_{L^\infty} \leq C \|u\|_{W^{m,p}} \quad \forall \alpha \text{ with } |\alpha| \leq k$$

and

$$|D^\alpha u(x) - d^\alpha u(y)| \leq C \|u\|_{W^{m,p}} |x - y|^\theta \text{ ae. } x, y \in \mathbb{R}^N, \forall \alpha, |\alpha| = k.$$

In particular, $W^{m,p}(\mathbb{R}^N) \subset C^k(\mathbb{R}^N)$.

In what follows, we assume that Ω is an open space of class C^1 , with bounded boundary $\partial\Omega$, or $\Omega = \mathbb{R}_+^N$.

Corollary 2.2.5

Let $1 \leq p \leq \infty$. We have

- if $1 \leq p < N$, then $W^{1,p}(\Omega) \subset L^{p^*}(\mathbb{R}^N)$ where $\frac{1}{p^*} = \frac{1}{p} - \frac{1}{N}$,
- if $p = N$, then $W^{1,p}(\Omega) \subset L^q(\mathbb{R}^N)$ where $\forall q \in [p, \infty[$,
- if $p > N$, then $W^{1,p}(\Omega) \subset L^\infty(\Omega)$,

with continuous embeddings.

Moreover, if $p > N$ we have for all $u \in W^{1,p}(\Omega)$

$$|u(x) - u(y)| \leq C \|u\|_{W^{1,p}} |x - y|^\alpha \text{ ae. } x, y \in \Omega,$$

with $\alpha = 1 - \frac{N}{p}$ and C depends only on Ω, p , and N .

In particular, $W^{1,p}(\Omega) \subset C(\bar{\Omega})$.

Corollary 2.2.6

The conclusion of Corollary 2.2.4 remains true if we replace \mathbb{R}^N by Ω .

Theorem 2.2.11 (Rellich-Kondrachev)

Assume that Ω is an open bounded space of class \mathcal{C}^1 . We have

- if $p < N$, then $W^{1,p}(\Omega) \subset L^q(\Omega)$, $\forall q \in [1, p^*[$ where $\frac{1}{p^*} = \frac{1}{p} - \frac{1}{N}$,
- if $p = N$, then $W^{1,p}(\Omega) \subset L^q(\Omega)$, $\forall q \in [1, +\infty[$,
- if $p > N$, then $W^{1,p}(\Omega) \subset \mathcal{C}(\bar{\Omega})$,

with compact embeddings.

2.3 Functions of bounded variation

As stressed in [1], the discontinuities in the images are significant and important features. However, classical Sobolev spaces are not suitable spaces to take into account this phenomenon. When u is discontinuous, the gradient of u has to be understood as a measure and the space $BV(\Omega)$ of functions of *bounded variation* is well adapted to this purpose. Definitions and theorems of this section are extracted from [6] and [7].

Definition 2.3.1 ($BV(\Omega)$ space)

We define $u \in BV(\Omega)$ as the set of u in $L^1(\Omega)$ such that

$$\|Du\|(\Omega) = |u|_{BV(\Omega)} := \sup \left\{ \int_{\Omega} u \operatorname{div} \phi \, dx, \phi \in \mathcal{C}_c^1(\Omega, \mathbb{R}^N), |\phi(x)| \leq 1 \right\} < \infty.$$

$\|Du\|(\Omega)$ is called the total variation of u in Ω .

Definition 2.3.2 (Weak-* convergence in $BV(\Omega)$)

Let $u \in BV(\Omega)$, $(u_n)_{n \in \mathbb{N}} \subseteq BV(\Omega)$. We say that the sequence (u_n) converges weakly-* to u in $BV(\Omega)$ if (u_n) converges to u in $L^1(\Omega)$ and (Du_n) converges to Du weakly-* in $\mathcal{M}(\Omega)$ (space of Radon measures), i.e.,

$$\lim_{n \rightarrow +\infty} \|u_n - u\|_{L^1(\Omega)} = 0 \quad \text{and} \quad \lim_{n \rightarrow +\infty} \int_{\Omega} v Du_n = \int_{\Omega} v Du, \quad \forall v \in \mathcal{C}_c(\Omega, \mathbb{R}^2).$$

Theorem 2.3.3 (Lower Semicontinuity of Total Variation)

Suppose $u_n \in BV(\Omega)$ ($n = 1, 2, \dots$) and $u_n \rightarrow u$ in $L^1(\Omega)$. Then

$$\|Du\|(\Omega) \leq \liminf_{n \rightarrow +\infty} \|Du_n\|(\Omega).$$

Theorem 2.3.4 (Compactness)

Let $\Omega \subset \mathbb{R}^N$ be an open bounded set, with Lipschitz boundary $\partial\Omega$. Assume $\{u_n\}_{n=1}^\infty$ is a sequence in $BV(\Omega)$ satisfying

$$\sup_n \|u_n\|_{BV(\Omega)} < \infty.$$

Then there exists a subsequence $\{u_{n_j}\}_{j=1}^\infty$ and a function $u \in BV(\Omega)$ such that

$$u_{n_j} \xrightarrow{j \rightarrow +\infty} u \text{ in } L^1(\Omega).$$

Theorem 2.3.5 (Embedding Theorem)

Let $\Omega \subset \mathbb{R}^N$ be an open and bounded set, with a Lipschitz boundary $\partial\Omega$.

Then the embedding $BV(\Omega) \rightarrow L^{N/(N-1)}(\Omega)$ is continuous and $BV(\Omega) \rightarrow L^p(\Omega)$ is compact for all $1 \leq p < \frac{N}{N-1}$.

2.4 Direct methods in the calculus of variations

This section is based on the book of B. Dacorogna [5].

The calculus of variation is the set of the methods designed to find extrema of functionals of the form:

$$I(u) = \int_{\Omega} f(x, u(x), \nabla u(x)) dx$$

where

- $\Omega \subset \mathbb{R}^N$, $N \geq 1$, is an open bounded set and a point in Ω is denoted by $x = (x_1, x_2, \dots, x_N)$;
- $u : \Omega \rightarrow \mathbb{R}^M$, $M \geq 1$, and hence

$$\nabla u = \left(\frac{\partial u^j}{\partial x_i} \right)_{\substack{1 \leq j \leq M \\ 1 \leq i \leq N}} \in \mathbb{R}^{M \times N};$$

- $f : \Omega \times \mathbb{R}^M \times \mathbb{R}^{M \times N} \rightarrow \mathbb{R}$, $f = f(x, u, \xi)$, is a given function.

Associated with the functional I is the minimization problem

$$m := \inf\{I(u) : u \in X\}, \tag{P}$$

meaning that we wish to find $\bar{u} \in X$ such that

$$m = I(\bar{u}) \leq I(u) \text{ for every } u \in X.$$

Here, X is the space of admissible functions, in most parts, it is the Sobolev space $u_0 + W_0^{1,p}(\Omega, \mathbb{R}^M)$, where u_0 is a given function. We say that the problem under consideration is *scalar* if $M = 1$ or $N = 1$; otherwise we speak of the *vectorial* case.

As reminded in [1], proving the existence of a solution is usually achieved by the following steps, which constitute the direct method of the calculus of variations:

1. One constructs a *minimizing sequence* $u_n \in X$, i.e., a sequence satisfying

$$\lim_{n \rightarrow +\infty} I(u_n) = \inf_{u \in X} I(u).$$

2. One obtains a uniform bound on $\|u_n\|_X$ by deriving a *coercivity inequality*. Indeed, if I is *coercive*, meaning that $\lim_{\|u\|_X \rightarrow +\infty} I(u) = +\infty$, this uniform bound is straightforwardly extracted. (Arguing by contradiction, let us assume that $\forall C > 0, \exists n \in \mathbb{N}, \|u_n\|_X > C$.

We prove, by construction that there exists a subsequence (u_{n_k}) of (u_n) such that $\lim_{k \rightarrow +\infty} I(u_{n_k}) = +\infty$ owing to the coercivity of I , which contradicts the fact that

$$\lim_{k \rightarrow +\infty} I(u_{n_k}) = \inf_{u \in X} I(u).$$

If I is *reflexive*, then by Theorem 2.1.15, one can thus find $\bar{u} \in X$ and a subsequence (u_{n_k}) of (u_n) such that $u_{n_k} \xrightarrow{X} \bar{u}$ when $k \rightarrow +\infty$.

3. To prove that \bar{x} is a minimizer of F it suffices to have the inequality

$$I(\bar{u}) \leq \liminf_{k \rightarrow +\infty} I(u_{n_k}).$$

The latter property is called *weak lower semi-continuity*.

Definition 2.4.1 (Sequential weak lower semi-continuity)

Let $p \geq 1$ and Ω, u, f be as above. We say that I is sequentially weakly lower semi-continuous in $W^{1,p}(\Omega)$ if for every sequence $u_n \xrightarrow{W^{1,p}(\Omega)} \bar{u}$, then

$$I(\bar{u}) \leq \liminf_{n \rightarrow +\infty} I(u_n).$$

If $p = \infty$, we say that I is sequentially weak-* lower semi-continuous in $W^{1,\infty}(\Omega)$ if the same inequality holds for every sequence $u_n \xrightarrow{W^{1,\infty}(\Omega)}^* \bar{u}$.

2.4.1 Quasiconvexity, Polyconvexity and Rank one convexity

We turn our attention to the vectorial case. The convexity of $\xi \rightarrow f(x, u, \xi)$ plays a central role in the scalar case ($M = 1$ or $N = 1$). In the vectorial case, it is still a sufficient condition to ensure weak lower semi-continuity of I , however, it is not a necessary one. Such a condition is the so-called *quasiconvexity* introduced by Morrey.

$$f \text{ quasiconvex} \Leftrightarrow I \text{ weakly lower semi-continuous.}$$

But the quasiconvexity is difficult to characterize, therefore one is led to introduce a slightly weaker condition, known as *rank one convexity*. We also introduce a stronger condition, called *polyconvexity*.

Definition 2.4.2 (Rank one convex function, [5])

A function $f : \mathbb{R}^{M \times N} \rightarrow \mathbb{R} \cup \{+\infty\}$ is said to be *rank one convex* if

$$f(\lambda\xi + (1 - \lambda)\eta) \leq \lambda f(\xi) + (1 - \lambda)f(\eta)$$

for every $\lambda \in [0, 1], \xi, \eta \in \mathbb{R}^{M \times N}$ with $\text{rank}(\xi - \eta) \leq 1$.

Definition 2.4.3 (Quasiconvex function, [5])

A Borel measurable and locally bounded function $f : \mathbb{R}^{M \times N} \rightarrow \mathbb{R}$ is said to be *quasiconvex* if

$$f(\xi) \leq \frac{1}{\text{meas}D} \int_D f(\xi + \nabla\varphi(x)) dx$$

for every open bounded set $D \subset \mathbb{R}^N$, for every $\xi \in \mathbb{R}^{M \times N}$ and for every $\varphi \in W_0^{1,\infty}(D, \mathbb{R}^M)$.

Definition 2.4.4 (Polyconvex function, [5])

A function $f : \mathbb{R}^{M \times N} \rightarrow \mathbb{R} \cup \{+\infty\}$ is said to be *polyconvex* if there exists $F : \mathbb{R}^{\tau(N,M)} \rightarrow \mathbb{R} \cup \{+\infty\}$ convex such that

$$f(\xi) = F(T(\xi)),$$

where $T : \mathbb{R}^{M \times N} \rightarrow \mathbb{R}^{\tau(N,M)}$ is such that

$$T(\xi) := (\xi, \text{adj}_2 \xi, \dots, \text{adj}_{N \wedge M} \xi).$$

We recall that $\text{adj}_s \xi$ stands for the matrix of all $s \times s$ minors of $\xi \in \mathbb{R}^{M \times N}$, $2 \leq s \leq N \wedge M = \min(N, M)$ and

$$\tau(N, M) = \sum_{s=1}^{N \wedge M} \sigma(s), \quad \text{where } \sigma(s) := \binom{M}{s} \binom{N}{s} = \frac{M!N!}{(s!)^2(M-s)!(N-s)!}.$$

In the case $N = M = 2$, $T(\xi) = (\xi, \det \xi)$.

Proposition 2.4.1

Let $f : \mathbb{R}^{M \times N} \rightarrow \mathbb{R}$. Then

$$f \text{ convex} \implies f \text{ polyconvex} \implies f \text{ quasiconvex} \implies f \text{ rank one convex}.$$

Definition 2.4.5 (Quasiconvex Envelope)

The quasiconvex envelope of f denoted by Qf is the quasiconvex function:

$$Qf = \sup_g \{g \leq f, g \text{ quasiconvex}\}.$$

2.5 Tridimensional elasticity

In this section, we recall some definitions of the theory of tri-dimensional elasticity extracted from [8] and [4].

Let Ω be an open bounded connected space of \mathbb{R}^3 . We consider that the points $x \in \bar{\Omega}$ represent the points of a material. Ω is said to be the reference configuration of the material. The map $\varphi : \bar{\Omega} \rightarrow \mathbb{R}^3$ is a deformation. We also introduce the displacement $u = \varphi - \text{Id}$. The matrix $(\nabla\varphi)_{ij} = \partial_j\varphi_i$ is called the gradient of the deformation.

Remark 2.5.1

The preservation of the orientation corresponds to the condition

$$\det \varphi(x) > 0, \quad x \in \Omega.$$

Definition 2.5.1

- (i) The deformation tensor or right Cauchy-Green tensor associated with the deformation φ is defined by:

$$C = \nabla \varphi^T \nabla \varphi.$$

It can be interpreted as a quantifier of the square of local change in distances due to deformation.

- (ii) The Green-Saint Venant tensor is defined by:

$$E = \frac{1}{2}(C - I) = \frac{1}{2}(\nabla u + \nabla u^T) + \frac{1}{2}\nabla u^T \nabla u.$$

It is a measure of the deviation between φ and a rigid deformation.

Definition 2.5.2

A deformation φ is said to be rigid if it can be written

$$\varphi(x) = a + Qx,$$

where $a \in \mathbb{R}^3$ and $Q \in SO(3)$ are respectively a given vector and a rotation matrix.

Definition 2.5.3

Let $T^\varphi : \varphi(\Omega) \rightarrow M_3$ be a tensor field on the deformed configuration $\varphi(\Omega)$. We define its Piola transform by

$$T(x) = [T^\varphi \circ \varphi(x)] \operatorname{cof} \nabla \varphi(x).$$

Definition 2.5.4

An application $t^\varphi : \overline{\varphi(\Omega)} \times S^2 \rightarrow \mathbb{R}^3$ is called the *Cauchy strain vector* (where S^2 is the unit sphere of \mathbb{R}^3).

Theorem 2.5.5 (Cauchy's theorem)

Assume that the applied body force density $f^\varphi : \overline{\varphi(\Omega)} \rightarrow \mathbb{R}^3$ is continuous and that the Cauchy stress vector field

$$t^\varphi : (y, n) \in \overline{\varphi(\Omega)} \times S^2 \longrightarrow t^\varphi(y, n) \in \mathbb{R}^3$$

is \mathcal{C}^1 with respect to y and continuous with respect to n . The Cauchy's axiome implies that there exists a continuously differentiable tensor field $T^\varphi : \overline{\varphi(\Omega)} \rightarrow M_3$ such that

$$\forall y, n, \quad t^\varphi(y, n) = T^\varphi(y)n,$$

and such that

$$T^\varphi(y) = T^\varphi(y)^T.$$

Moreover, T^φ is of class \mathcal{C}^1 and satisfies

$$-\operatorname{div}_y T^\varphi = f^\varphi.$$

The tensor T^φ is called the Cauchy stress tensor.

Definition 2.5.6

The behavior law of a material is defined by:

$$\hat{T} : \Omega \times \{\text{deformations}\} \longrightarrow S_3,$$

where S_3 is the space of 3×3 symmetric matrices, such that for every deformation φ and every point $x \in \Omega$, we have:

$$T^\varphi(y) = \hat{T}(x, \varphi) \quad \text{for } y = \varphi(x).$$

Definition 2.5.7

- (i) A material is said to be *elastic* if its behavior law can be written:

$$\hat{T} : \bar{\Omega} \times M_3^+ \longrightarrow S_3$$

with

$$T^\varphi(y) = \hat{T}(x, \nabla\varphi(x)).$$

In other words, a material is said to be *elastic* if its behavior law depends only on the gradient of the deformation.

- (ii) A material is said to be *isotropic* if it has the same mechanical properties in every direction.
- (iii) A material is said to be *homogeneous* if its behavior law does not depend on x .

- [1] G. AUBERT AND P. KORNPBST, *Mathematical problems in image processing: partial differential equations and the calculus of variations*, vol. 147, Springer Science & Business Media, 2006.
- [2] S. BENZONI-GAVAGE, *Méthodes directes en calcul des variations, quasiconvexité*, Journal de maths des élèves, 1 (1995), pp. 121–128.
- [3] H. BRÉZIS, *Analyse Fonctionnelle, Théorie et Applications. 1999*, Dunod, Paris, 1999.
- [4] P. G. CIARLET, *Elasticité tridimensionnelle*, vol. 1, Masson, 1986.
- [5] B. DACOROGNA, *Direct methods in the calculus of variations*, vol. 78, Springer, 2007.
- [6] F. DEMENGEL, G. DEMENGEL, AND R. ERNÉ, *Functional spaces for the theory of elliptic partial differential equations*, Springer, 2012.
- [7] L. C. EVANS AND R. F. GARIEPY, *Measure theory and fine properties of functions*, vol. 5, CRC press, 1991.
- [8] H. LE DRET, *Notes de Cours de DEA. Méthodes mathématiques en élasticité*, (2003-2004).

CHAPTER 3

TOPOLOGY PRESERVATION FOR IMAGE-REGISTRATION-RELATED DEFORMATION FIELDS

In this chapter, we address the issue of designing a theoretically well-motivated and computationally efficient method ensuring topology preservation on image-registration-related deformation fields. The model is motivated by a mathematical characterization of topology preservation for a deformation field mapping two subsets of \mathbb{Z}^2 , namely, positivity of the four approximations to the Jacobian determinant of the deformation on a square patch. The first step of the proposed algorithm thus consists in correcting the gradient vector field of the deformation (that does not comply with the topology preservation criteria) at the discrete level in order to fulfill this positivity condition. Once this step is achieved, it thus remains to reconstruct the deformation field, given its full set of discrete gradient vectors. A functional minimization problem under Lagrange interpolation constraints is introduced and its well-posedness is studied.

The remainder of the chapter is organized as follows. In section 3.1, the first step of the method is recalled. Section 3.2 is dedicated to the modelling of the reconstruction step. Theoretical results are established such that the result of existence/uniqueness of the solution of the involved minimization problem, the characterization of the solution, a result of convergence as well as the discretization of the problem. Section 3.3 is devoted to numerical simulations demonstrating the ability of the model to handle large deformations and the interest of having decomposed the problem into independent smaller ones from a computational viewpoint.

Introduction

Given two images called Template and Reference, image registration consists in determining an optimal diffeomorphic transformation φ such that the deformed Template image is aligned with the Reference. This technique is encountered in a wide range of fields, such as medical imaging, when comparing data to a common Reference frame, when fusing images that have not necessarily been acquired through similar sensors, or when tracking shapes. For images of the same modality, the goal of registration is to correlate the geometrical features and the

intensity level distribution of the Reference and those of the Template. For images produced by different mechanisms and possessing distinct modalities, the goal of registration is to correlate the images while maintaining the modality of the Template. For an extensive overview of existing parametric and non-parametric registration methods, we refer the reader to the work by Modersitzki [28] and [29].

Generally, a physical interpretation is given to the problem of registration: the shapes to be matched are considered to be the observations of a body subjected to deformations. The deformation must thus remain physically and mechanically meaningful, and reflect material properties: self-penetration of the matter (indicating that the transformation is not injective, which is not physically consistent) should be prohibited. Mathematically, topology preservation (or orientation preservation) for a deformation field mapping two subdomains of \mathbb{Z}^2 can be expressed by the following equivalent statements (see [25] for further details): positivity of the four approximations to the Jacobian determinant of the deformation on a square patch, corresponding angles of the deformed configuration between 0 and π , or positivity of the signed areas of triangles defined on the deformed configuration. When any of these characterizations is violated, the convexity of the deformed region is infringed, signifying that the images of the corner points of a square patch cross over the diagonal connecting their neighbors. Visually, the deformation field exhibits overlaps (see Fig. 3.1 for such an example). This currently occurs when dealing with problems involving large magnitude deformations.

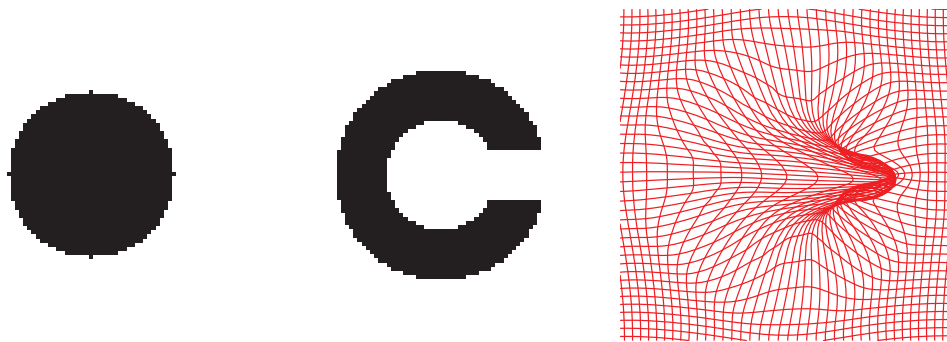


Figure 3.1: Academic example: Registration of a black disk to the letter C without topology-preserving conditions. From left to right: Template image, Reference image and deformation field. The deformation map clearly exhibits overlaps.

The necessity of preserving topology arises in brain mapping for instance. It is well-known that the cortical surface has a spherical topology (*i.e.*, is homeomorphic to the sphere or equivalently, the cortical surface has genus zero), so throughout the registration process, this feature must be preserved. This medical illustration, among others, constitutes a motivation for our work. We refer the reader to [23] and [24] for further discussion about this anatomical property. Generally speaking, as soon as the shapes to be correlated are homeomorphic, the preservation of orientation must be ensured.

Thus, the aim of this chapter is to design a theoretically well-motivated and computationally efficient method taking as input the deformation field that does not comply with the topology preservation criteria, and giving as output, a corrected version of this deformation, as faithful as possible to the original one.

Prior related works addressed this question of maintaining topology. In variational frame-

works, the main idea is to control the Jacobian determinant of the deformation, proper measure for the local volume transformation under the considered deformation. We would like to mention the work by Ashburner *et al.* (see [7], [5] and [6]) and the work by Musse *et al.* (see [30]). In [30], the deformation map is modeled as a hierarchical displacement field decomposed on a multiresolution B-splines basis. Topology preservation is enforced by controlling the Jacobian of the transformation. The problem amounts to solving a constrained optimization problem: the residual energy between the target and the deformed source image is minimized under constraints on the Jacobian. This paper is then extended to the 3D case by Noblet *et al.* (see [32]). The main difference with the proposed approach is that, in our case, the set of feasible transformations is not restricted to a certain class of mappings.

In [14] (work dedicated to registration under nonlinear elasticity principles), Droske and Rumpf address the issue of non-rigid registration of multi-modal image data. A suitable deformation is determined *via* the minimization of a morphological matching functional which locally measures the defect of the normal fields of the set of level lines of the Template image and the deformed Reference image. The matching criterion includes first order derivatives of the deformation and is complemented by a nonlinear elastic regularization of the form $\int_{\Omega} W(D\Phi, \text{Cof } D\Phi, \det D\Phi) dx$, where $W : \mathbb{R}^{3 \times 3} \times \mathbb{R}^{3 \times 3} \times \mathbb{R} \rightarrow \mathbb{R}$ is supposed to be convex, $D\Phi$ is the Jacobian matrix of the deformation Φ , $\text{Cof } D\Phi$, the cofactor matrix of $D\Phi$ and $\det D\Phi$, the Jacobian determinant.

In [27], Le Guyader and Vese introduce a non-parametric combined segmentation/registration model in which the shapes to be matched are viewed as Ciarlet-Geymonat materials. The stored energy function of such a material is built so that it becomes infinite when the Jacobian determinant of the deformation tends to 0^+ . In [21], Haber and Modersitzki address the issue of non-parametric image registration under volume-preserving constraints. They propose to restrict the set of feasible mappings by adding a volume-preserving constraint which forces the Jacobian of the deformation to be equal to 1. In [22], the authors pursue in the same direction: they propose to keep the Jacobian determinant bounded, which leads to an inequality-constrained minimization problem.

An information-theoretic-based approach is proposed in [34] to generate diffeomorphic mappings and to monitor the statistical distribution of the Jacobian determinant. The authors propose to quantify the magnitude of the deformation by means of the Kullback-Leibler distance between the probability density function associated with the deformation and the identity mapping.

Although theoretically well-motivated, the above mentioned models are hard to handle numerically, requiring for instance, the use of optimization techniques such as logarithmic barrier methods or special discretization schemes (see [33] or [29]). This observation led us to disconnect the registration problem from the topology-preserving question.

An alternative to the straight penalization of the Jacobian of the deformation was proposed by Christensen and collaborators. In [11], they introduce a viscous fluid registration model in which objects are viewed as fluids evolving in accordance with the fluid dynamics Navier-Stokes equations. This model is complemented by a regriding technique ensuring positivity of the Jacobian determinant. The method consists in monitoring the values of the Jacobian determinant of the deformation. If the values drop below a defined threshold, the process is reinitialized taking as initialization the last computed deformed Template. However, for problems involving large deformations, numerous regriding steps might be required, which is memory-consuming since one needs to store the last computed deformation field before each

reinitialization. Numerically, the resulting deformation field (computed as the composite of intermediate deformations) may not fulfill the topology-preserving conditions, even if the intermediate ones do.

In this chapter, we propose a theoretically well-motivated algorithm that falls within the framework of a previous work by Le Guyader ([26]). In this preliminary work, the authors, inspired by [25], design a two-step-algorithm enforcing topology preservation, independently of the registration technique used. The algorithm is thus independent of the selected registration model. It can be applied at intermediate steps of the registration process or at the end.

The first step consists in correcting the gradient vector field of the deformation (that does not comply with the topology preservation criteria) at the discrete level in order to fulfill a set of conditions ensuring topology preservation in the continuous domain after bilinear interpolation (see also [25]). Basically, it consists in balancing the gradient vectors of the displacement field u (related to the deformation field φ by the relation $\varphi = \text{Id} + u$) by a parameter α belonging to $]0, 1[$. The proposed algorithm provides a unique optimal parameter α at each node of the grid. Once the correction stage is achieved, it remains to reconstruct the deformation field, given its full set of discrete gradient vectors. The problem is phrased as a regularized least-squares problem but as is, one would fail to get the uniqueness of the solution (the solutions would be defined up to a constant). It is thus complemented by a constraint on the mean of the deformation field, thus ensuring uniqueness of the solution. The algorithm is shown to be efficient and has demonstrated its ability to handle large deformations. Also, it has been compared with Christensen *et al.*'s regriding technique on complex slices of brain data in the case of brain mapping to a disk. In many cases, the proposed algorithm outperforms the regriding technique. Nevertheless, some criticisms can be raised:

- First of all, the computations are carried out on the whole image domain, even though the regions exhibiting overlaps are generally very few and localized on the image domain, which leads to superfluous calculations and strays us from real-time computation requirements. In practice, the deformation components are recomputed over the whole domain, altering somewhat the physics of the problem.
- Besides, the constraint that complements the approximation problem (being about the mean of the deformation) is rather artificial and cannot be physically interpreted. It is global and may not render well the complexity of variations of the deformation components.

We thus propose in this chapter to decompose the original reconstruction problem into independent problems of smaller dimensions, yielding a natural parallelization of the computations. We localize the regions exhibiting overlaps, and formulate for each domain a functional minimization problem equipped with interpolation constraints on the boundary, reproducing more accurately the physics of the problem. The algorithm acts locally (the deformation is left unaltered where the topology-preserving criterion is fulfilled) and the obtained result thus remains more consistent with the physics of the problem (due also to the Lagrange interpolation constraints stemming from the unaltered deformation field). One could object that when applied at the end of the process, the obtained deformation field is no longer a solution of the optimization process. This is indeed true, but as previously mentioned, the proposed algorithm acts locally and the minimization problems are constrained with Lagrange interpolation constraints stemming from the unaltered deformation. Besides, the proposed

algorithm is applied when the registration process produces a deformation field that is itself mechanically and physically meaningless (a minimization problem in registration can be well-posed with the guarantee of existence of minimizers -for instance in the nonlinear elasticity framework-, but may numerically generate overlaps). It thus makes sense to correct the obtained deformation field. At last, the algorithm acts on the magnitude of the displacement vectors, not on their direction.

One could also claim that registration models involving controls on the Jacobian determinant are more relevant than the proposed modelling. We answer first, that for many of those methods, no theoretical result of existence of minimizers is provided (or theoretical results are given but the theoretical model is not the one that is implemented in practice). It thus means that the numerical scheme, at best, makes the energy decrease to the infimum, but the optimization problem does not necessarily admit a minimizer. Besides, some numerical artifices are often used. For instance, for the fluid registration model by Christensen *et al.*, a detailed algorithm is provided in [28]. In the main loop, the displacement vector field is up-

dated in the following way: $\vec{U}^{(k+1)} = \vec{U}^{(k)} + \delta t^{(k)} \delta \vec{U}^{(k)}$ with
$$\begin{cases} \delta u_{\max}^{(k)} = \|\delta \vec{U}^{(k)}\|_V, \\ \delta t^{(k)} = \min \left(1, \text{tol}_u / \delta u_{\max}^{(k)} \right). \end{cases}$$

It means that this procedure has the same effect as the method we propose: the direction of the obtained displacement vector field is preserved while the magnitude can be modified. This strategy of rescaling is further discussed p. 183 of [28] for variational non parametric registration methods.

The implementation of such methods (without heavy numerical artifices) does not guarantee either that the obtained deformation field is topology-preserving and fails to correctly align the shapes when the deformations are too large. That is why we took the side of decoupling the registration process from the topology-preserving question. When applied at intermediate steps of the registration process, the corrected deformation field can be interpreted as a new initial condition of the problem. At last, one could also argue that decomposing the original problem into smaller dimension independent ones may destroy the global coupling. For the reasons stated above, we believe that this decoupling does not affect the result. In particular, the proposed results are qualitatively comparable to those presented in [26], when no decomposition into subproblems is considered.

The novelty of the chapter thus rests upon:

- the decomposition of the original problem into independent problems of smaller dimensions, enabling us to reduce significantly the computational time (up to a factor 80 for some critical applications),
- the proof of the existence/uniqueness of the solution of the introduced functional minimization problem on each subdomain,
- a theoretical result of convergence when the size of the data to approximate increases to infinity, ensuring the well-posedness of the problem,
- a result of convergence of the method in the discrete setting,
- a precise depiction of the discretization of the problem: generic finite element, basis functions, properties of the systems to be solved, and in particular a result of nonsingularity of the symmetric indefinite matrix involved in the linear systems.

3.1 Correction of the deformation

The first step consists in applying the same procedure as the one adopted by Le Guyader *et al.* in [26] (inspired by prior related work [25] but slightly different). For the sake of completeness, we remind the reader about this correction stage.

Let Ω be a connected bounded open subset of \mathbb{R}^2 representing the reference configuration, with Lipschitz boundary $\partial\Omega$.

Let $h : \begin{cases} \overline{\Omega} \rightarrow \mathbb{R}^2 \\ (x, y) \mapsto h(x, y) = (f(x, y), g(x, y)) \end{cases}^T$ be the deformation of the reference configuration.

A deformation is a smooth mapping that is orientation-preserving and injective except possibly on $\partial\Omega$. We denote by u the displacement field associated with h , *i.e.*, $h = \text{Id} + u$.

The deformation gradient is $\nabla h : \overline{\Omega} \rightarrow M_2(\mathbb{R})$ defined by $\nabla h = I_2 + \nabla u$ with $M_2(\mathbb{R})$ the set of 2×2 real square matrices.

The correction algorithm is based on the following proposition that provides a set of conditions to be fulfilled in the discrete setting to ensure topology preservation in the continuous domain. More precisely, Proposition 3.1.1 relates conditions of positivity of some discrete Jacobians to a property of topology-preservation in the continuous domain after bilinear interpolation. This approach seems relevant since we work in practice with digital images: the centers of gravity of the pixels coincide with the nodes of the discrete domain.

Proposition 3.1.1 (From Karaçali and Davatzikos in [25])

Let \mathcal{C} be the class of deformation fields $\mathbf{h} = (\mathbf{f}, \mathbf{g})$ defined over a discrete rectangle $\Omega = [0, 1, \dots, M] \times [0, 1, \dots, N] \subset \mathbb{N}^2$ for which J_{ff} , J_{fb} , J_{bf} , J_{bb} are positive for all $(x, y) \in \Omega$.

Let $\mathbf{h} = (\mathbf{f}, \mathbf{g})$ be a deformation field belonging to \mathcal{C} . Then its continuous counterpart determined by the interpolation of \mathbf{h} over the domain $\Omega_C = [0, M] \times [0, N] \subset \mathbb{R}^2$ using the interpolant Φ given by $\Phi(x, y) = \Psi(x)\Psi(y)$ with

$$\Psi(t) = \begin{cases} 1 + t & \text{if } -1 \leq t < 0 \\ 1 - t & \text{if } 0 \leq t < 1 \\ 0 & \text{otherwise} \end{cases}$$

preserves topology, with the backward and forward finite difference schemes \mathbf{f}_x^b , \mathbf{f}_x^f , \mathbf{f}_y^b , \mathbf{f}_y^f to approximate the partial derivatives of \mathbf{f} (similarly for \mathbf{g}) and

$$\begin{cases} J_{ff} = \mathbf{f}_x^f(p_1)\mathbf{g}_y^f(p_1) - \mathbf{f}_y^f(p_1)\mathbf{g}_x^f(p_1) \\ J_{bf} = \mathbf{f}_x^b(p_2)\mathbf{g}_y^f(p_2) - \mathbf{f}_y^f(p_2)\mathbf{g}_x^b(p_2) \\ J_{fb} = \mathbf{f}_x^f(p_3)\mathbf{g}_y^b(p_3) - \mathbf{f}_y^b(p_3)\mathbf{g}_x^f(p_3) \\ J_{bb} = \mathbf{f}_x^b(p_4)\mathbf{g}_y^b(p_4) - \mathbf{f}_y^b(p_4)\mathbf{g}_x^b(p_4). \end{cases}$$

We recall (similarly for \mathbf{g}) that:

$$\begin{cases} \mathbf{f}_x^f(x, y) = \mathbf{f}(x + 1, y) - \mathbf{f}(x, y) \\ \mathbf{f}_x^b(x, y) = \mathbf{f}(x, y) - \mathbf{f}(x - 1, y) \\ \mathbf{f}_y^f(x, y) = \mathbf{f}(x, y + 1) - \mathbf{f}(x, y) \\ \mathbf{f}_y^b(x, y) = \mathbf{f}(x, y) - \mathbf{f}(x, y - 1). \end{cases}$$

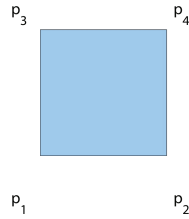


Figure 3.2: Layout of the points on a reference square $[0, 1] \times [0, 1]$. This representation is given as an example: only the order of the points p_1, p_2, p_3 and p_4 matters for the definition of the discrete Jacobians. These points coincide with the centers of gravity of the pixels. In the sequel, these will be denoted by a_i .

Remark 3.1.2

It is shown in [25] that if a deformation field is continuous and globally one-to-one, it preserves topology. This is from this angle that the issue of topology preservation is addressed here. By construction, the continuous counterpart of \mathbf{h} denoted by \mathbf{h}_c is continuous. The one-to-one property is conditional to the local behavior of \mathbf{h}_c : if the continuous deformation field \mathbf{h}_c is one-to-one over all square patches that partition the continuous domain defined by the discrete grid, then \mathbf{h}_c is globally one-to-one. If we go back to Proposition 3.1.1, it involves discrete Jacobians, that is, differences. The continuity of the function is thus sufficient to ensure that the mathematical writing is correct. More precisely, inside a given square (for the purpose of illustration $[0, 1] \times [0, 1]$ and $p_1 = (0, 0)$, $p_2 = (1, 0)$, $p_3 = (0, 1)$ and $p_4 = (1, 1)$), the components of $\mathbf{h}_c = (f_c, g_c)$ are differentiable (as polynomials) and more precisely, with the notations of Proposition 3.1.1,

$$\begin{aligned} \frac{\partial f_c}{\partial x}(x, y) &= (f(1, 0) - f(0, 0))(1 - y) + (f(1, 1) - f(0, 1))y, \\ \frac{\partial g_c}{\partial x}(x, y) &= (g(1, 0) - g(0, 0))(1 - y) + (g(1, 1) - g(0, 1))y, \\ \frac{\partial f_c}{\partial y}(x, y) &= (f(1, 1) - f(1, 0))x + (f(0, 1) - f(0, 0))(1 - x), \\ \frac{\partial g_c}{\partial y}(x, y) &= (g(1, 1) - g(1, 0))x + (g(0, 1) - g(0, 0))(1 - x), \end{aligned}$$

and after intermediate computations, the Jacobian determinant $J = J(x, y)$ is given by:

$$J(x, y) = J_{bf} x(1 - y) + J_{ff} (1 - x)(1 - y) + J_{bb} xy + J_{fb} (1 - x)y,$$

that is, a convex combination of the 4 positive discrete Jacobians. It means that the Jacobian determinant J is positive everywhere inside the square patch. Continuity of the bilinear interpolant provides continuity of \mathbf{h}_c over the square and \mathbf{h}_c is locally one-to-one over all such squares and globally one-to-one over the domain.

The general idea resulting from Proposition 3.1.1 is to balance, at the discrete level and at each node of the grid, the gradients of the displacement vectors by a parameter $\alpha \in]0, 1[$, in order to comply with the above conditions of positivity of the discrete Jacobians. The

construction of the algorithm is motivated by the following observation. In the continuous domain, if we decompose the deformation field $h = (f, g)$ into $h = \text{Id} + u$ with $u = (u_1, u_2)$ the displacement vector field, we can compute the Jacobian $J(x, y)$ at any point (x, y) .

If now we focus on the related deformation field $h_\alpha : (x, y) \mapsto (\text{Id} + \alpha u)(x, y) = (f_\alpha(x, y), g_\alpha(x, y)) = (x + \alpha u_1(x, y), y + \alpha u_2(x, y))$, we can similarly calculate the Jacobian $J_\alpha(x, y)$ at any point (x, y) by:

$$J_\alpha(x, y) = \left(1 + \alpha \frac{\partial u_1}{\partial x}(x, y)\right) \left(1 + \alpha \frac{\partial u_2}{\partial y}(x, y)\right) - \alpha^2 \frac{\partial u_2}{\partial x}(x, y) \frac{\partial u_1}{\partial y}(x, y).$$

It exhibits the following properties:

- $J_\alpha(x, y)$ is a polynomial of order 2 in α ,
- $\lim_{\alpha \rightarrow 0} J_\alpha(x, y) = 1$,
- $\lim_{\alpha \rightarrow 1} J_\alpha(x, y) = J(x, y)$.

If we suppose that $J(x, y) < 0$ then, according to the intermediate value theorem, there exists $\alpha^* \in]0, 1[$ such that $J_{\alpha^*}(x, y) = \varepsilon \in [0, 1]$. The idea is thus to confine the Jacobian values to a positive interval by correcting the gradients of the displacement vector field.

Strictly, we should consider the deformation field defined by

$h_\alpha : (x, y) \mapsto (x + \alpha(x, y)u_1(x, y), y + \alpha(x, y)u_2(x, y))$ in the continuous domain.

But the aim is to adapt the previous idea to the discrete setting. At each node of the grid, a correction parameter is computed and applied not to the displacement vector field itself, but to the gradients of the displacement vector field. Note that applying the correction stage at the level of the displacement vector field itself would not guarantee that the discrete Jacobians obtained fulfill the conditions of Proposition 3.1.1.

We adapt the previous idea to the discrete setting: the algorithm produces a unique optimal correction parameter α at each node. If $J(x, y) < 0$, there are four possible shapes for $J_\alpha(x, y)$:

1. $J_\alpha(x, y)$ reaches its minimum over $]0, 1]$ (cf. Fig. 3.3, solid line),
2. $J_\alpha(x, y)$ reaches its minimum over $]1, +\infty]$ (cf. Fig. 3.3, dotted line),
3. $J_\alpha(x, y)$ reaches its maximum over $[0, 1[$ (cf. Fig. 3.3, dashed line),
4. $J_\alpha(x, y)$ reaches its maximum over $] - \infty, 0[$ (cf. Fig. 3.3, dash-dotted line).

Consequently, if $\alpha^* \in]0, 1[$ is such that $J_{\alpha^*}(x, y) = 0$, then for $0 < \alpha < \alpha^*$, $J_\alpha(x, y) > 0$.

For instance, suppose that for a given node, the four Jacobians are negative (in practice, this is the most spread case). Then we compute four correction parameters α_{ff}^* , α_{fb}^* , α_{bf}^* and α_{bb}^* associated to each combination. It suffices to take the minimum of these four values to guarantee that the four Jacobians are positive.

Now suppose that three Jacobians are negative, for instance, J_{ff} , J_{bf} and J_{fb} . Then we compute α_{ff}^* , α_{fb}^* and α_{bf}^* , and we set $\alpha_{int} = \min(\alpha_{ff}^*, \alpha_{fb}^*, \alpha_{bf}^*)$.

The second-degree polynomial in α , J_{bb}^α is computed for α_{int} .

If $J_{bb}^{\alpha_{int}}(x, y) > 0$, then $\alpha^* = \alpha_{int}$, otherwise we take $\alpha^* = \min(\text{roots}(J_{bb}^\alpha(x, y)))$.

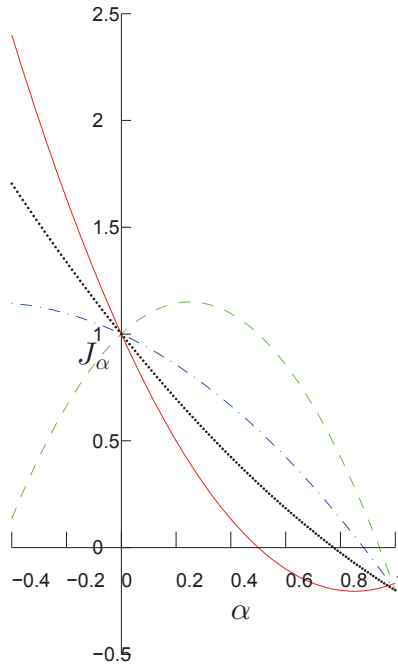


Figure 3.3: The four possible representations of the Jacobian.

And so on for the other cases.

The algorithm thus provides a unique optimal correction parameter per grid node (when necessary) and the approximated gradients of the displacement vector field are corrected in compliance with the obtained correction parameters.

Thanks to this parameter α , we can compute the corrected (when necessary) Jacobian matrix at the considered grid node: the output of the first step is then this discrete set of corrected (when necessary) Jacobian matrices denoted by $\{\omega_i\}$ in the sequel.

3.2 Deformation reconstruction

The issue to be addressed now lies in the reconstruction of the deformation field, given its discrete set of gradients, with the fewest computations possible (real-time computations should be expected).

Unlike our previous model on this topic, formulated as a functional minimization problem on the whole domain Ω (-meaning in particular that the computations were made even on regions of the deformation map complying with the orientation-preserving requirement), we propose to concentrate the computational effort on the subdomains of the deformation grid exhibiting overlaps and to set Lagrange interpolation conditions on the boundary of the subdomains, reproducing more faithfully the physics of the problem. This allows to apply the reconstruction process on each region independently and to reduce significantly the compu-

tational cost. In the sequel, we assume that we have identified (manually for the moment) \mathcal{N} nonempty connected bounded open subsets Ω_i of Ω with Lipschitz boundary, $i \in \{1, \dots, \mathcal{N}\}$ on which orientation preservation is violated. $\forall i \in \{1, \dots, \mathcal{N}\}$, $\Omega_i \subset \Omega$ and $\Omega_i \cap \Omega_j = \emptyset$ for $i \neq j$. We then introduce our mathematical model of reconstruction, valid for each subdomain Ω_i , $i \in \{1, \dots, \mathcal{N}\}$. A D^m -spline approach is retained (cf. [2]). Generally speaking, the D^m -splines over an open subset of \mathbb{R}^n are multidimensional minimizing splines, *i.e.*, functions defined on Ω subjected to interpolation or smoothing conditions and that minimize an energy functional involving derivatives of order m . This choice of methodology is guided by the authors' experience in the field of approximation. This technique proves to be very satisfactory both in terms of theory (convergence results validate the approach) and applications: it provides accurate results. Here again we refer the reader to [2] for more details. Of course, other strategies could have been considered.

3.2.1 Functional to be minimized

We remind the reader that $\forall i \in \{1, \dots, \mathcal{N}\}$, Ω_i is a nonempty connected bounded open subset of $\Omega \subset \mathbb{R}^2$ with Lipschitz boundary. Let ν be an integer such that $\nu \in \{1, \dots, \mathcal{N}\}$. Inspired by the D^m -spline approach, we introduce a regularized least-squares problem defined on a space of vector-valued functions, in order to fit the discrete set of corrected gradient vectors of the deformation and to satisfy Lagrange interpolation constraints. More precisely, the problem is phrased as a constrained functional minimization problem on a convex subspace of the Hilbert space $H^3(\Omega_\nu, \mathbb{R}^2)$ so that the Sobolev's embedding $H^3(\Omega_\nu, \mathbb{R}^2) \hookrightarrow C^1(\overline{\Omega_\nu}, \mathbb{R}^2)$ holds (it means that the inclusion of $H^3(\Omega_\nu, \mathbb{R}^2)$ into $C^1(\overline{\Omega_\nu}, \mathbb{R}^2)$ is continuous, that is to say : $H^3(\Omega_\nu, \mathbb{R}^2) \subset C^1(\overline{\Omega_\nu}, \mathbb{R}^2)$ and there exists $C > 0$, depending only on Ω_ν , such that $\forall u \in H^3(\Omega_\nu, \mathbb{R}^2)$, $\|u\|_{C^1(\overline{\Omega_\nu}, \mathbb{R}^2)} \leq C \|u\|_{H^3(\Omega_\nu, \mathbb{R}^2)}$, see [1] or [8]). It guarantees, in particular, that the pointwise fitting term dealing with the derivatives of the unknown is well-defined. We thus rebuild a smoother-than-required deformation field (by smoother, we mean more regular) but retain only the values of the deformation components obtained at the grid nodes (centers of gravity of the pixels). Before depicting our model, we introduce some fundamental mathematical notions that will be useful to state the functional minimization problem.

For any $\gamma = (\gamma_1, \gamma_2) \in \mathbb{N}^2$, we write $|\gamma| = \gamma_1 + \gamma_2$ and $\partial^\gamma = \frac{\partial^{|\gamma|}}{\partial x_1^{\gamma_1} \partial x_2^{\gamma_2}}$. We recall the standard inner product and the induced norm on $H^3(\Omega_\nu, \mathbb{R}^2)$:

$$((u, v))_{H^3(\Omega_\nu, \mathbb{R}^2)} = \sum_{|\gamma| \leq 3} \int_{\Omega_\nu} \langle \partial^\gamma u, \partial^\gamma v \rangle_2 dx_1 dx_2 \text{ and } \|v\|_{H^3(\Omega_\nu, \mathbb{R}^2)}^2 = ((v, v))_{H^3(\Omega_\nu, \mathbb{R}^2)},$$

and the semi-inner product and the semi-norm:

$$(u, v)_{3, \Omega_\nu, \mathbb{R}^2} = \sum_{|\gamma|=3} \int_{\Omega_\nu} \langle \partial^\gamma u, \partial^\gamma v \rangle_2 dx_1 dx_2 \text{ and } |v|_{3, \Omega_\nu, \mathbb{R}^2}^2 = (v, v)_{3, \Omega_\nu, \mathbb{R}^2},$$

where $\langle \cdot, \cdot \rangle_2$ denotes the Euclidean scalar product in \mathbb{R}^2 . For the sake of clarity, we recall the general definition of a P -unisolvant set.

Definition 3.2.1 (see [2])

For any $l \in \mathbb{N}$, we denote by P_l the space of polynomial functions defined over \mathbb{R}^n of degree $\leq l$ with respect to the set of variables, and for any $l \in \mathbb{N}$ and for any nonempty connected open subset Ω in \mathbb{R}^n , by $P_l(\Omega)$ the space of restrictions to Ω of the functions in P_l . A set $A = \{a_1, \dots, a_N\}$ of N points of \mathbb{R}^n is P_l -unisolvent if $\forall \{\alpha_1, \dots, \alpha_N\} \subset \mathbb{R}$, $\exists! \Psi \in P_l$, $\forall i \in \{1, \dots, N\}$, $\Psi(a_i) = \alpha_i$. In particular, $\exists! \Psi \in P_l$, $\forall i \in \{1, \dots, N\}$, $\Psi(a_i) = 0$ ($\Psi \equiv 0$). It is clear that a necessary condition for the set A to be P_l -unisolvent is that $N = \dim P_l$.

Let $A = \{a_i\}_{i=1, \dots, N}$ be a set of N points of $\overline{\Omega_\nu}$ containing a P_1 -unisolvent subset (As the set A contains a P_1 -unisolvent subset, we can only infer that $N \geq \dim P_1$). In our application, the set A is made of the coordinates of the image pixels included in $\overline{\Omega_\nu}$.

Let also $\{\omega_i\}_{i=1, \dots, N}$ be the set of N Jacobian matrices of the deformation given at $\{a_i\}_{i=1, \dots, N}$. This set is made of the corrected gradient vectors of the deformation obtained at the correction step of the algorithm. At last, let $\{b_i\}_{i=1, \dots, l}$ be l points of $\overline{\Omega_\nu}$ where the discrete gradient vectors of the deformation have been unaltered (so the deformation is unchanged). In all our applications, these points will belong to the boundary $\partial\Omega_\nu$ of Ω_ν . We set Lagrange interpolation constraints at these points (see Fig. 3.4). It means that if h denotes the unaltered deformation and v denotes the unknown deformation of the minimization problem, we must have:

$$\forall i \in \{1, \dots, l\}, v(b_i) = h(b_i).$$

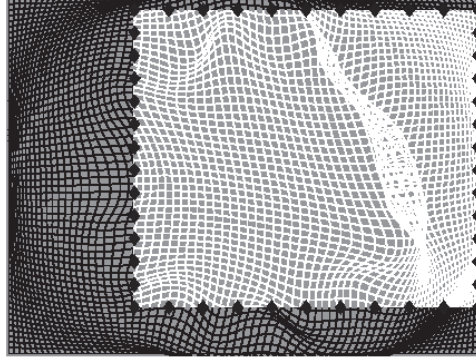


Figure 3.4: Example of a subdomain (white zone) $\Omega_1 \subset \Omega$ on the boundary of which, interpolation conditions are prescribed (black dots representing the b_i , $i \in \{1, \dots, l\}$).

Let K be the set defined by $K = \{v \in \mathbf{H}^3(\Omega_\nu, \mathbb{R}^2), \beta(v) = \eta\}$, with β the mapping:

$$\beta : \begin{cases} \mathbf{H}^3(\Omega_\nu, \mathbb{R}^2) \rightarrow \mathbb{R}^{2l} \\ v \mapsto \beta(v) = (v(b_1), \dots, v(b_l))^T \end{cases}$$

and $\eta = (h(b_1), \dots, h(b_l))^T$. The convex set K is closed as the reciprocal image of a closed set by a continuous mapping (see [8]). The approximation problem can be stated as follows: given the set of N Jacobian matrices defined at $\{a_i\}_{i=1, \dots, N}$, search for v sufficiently smooth such that $\forall i \in \{1, \dots, N\}$, the Jacobian matrix Dv evaluated at a_i is close to w_i and such that $\forall i \in \{1, \dots, l\}$, $v(b_i) = h(b_i)$. In this purpose, we need the following additional notations. We denote by ρ the operator defined by:

$$\rho : \begin{cases} H^2(\Omega_\nu, \mathbb{R}^{2 \times 2}) \rightarrow (\mathbb{R}^{2 \times 2})^N \\ v \mapsto \rho(v) = (v(a_1), v(a_2), \dots, v(a_N))^T \end{cases} \quad (3.1)$$

The problem is then cast as an optimization one by means of functional \mathcal{J}_ϵ defined by:

$$\mathcal{J}_\epsilon : \begin{cases} H^3(\Omega_\nu, \mathbb{R}^2) \rightarrow \mathbb{R} \\ v \mapsto \langle \rho(Dv) - w \rangle_N^2 + \epsilon |v|_{3, \Omega_\nu, \mathbb{R}^2}^2, \end{cases}$$

with $\epsilon > 0$ a tuning parameter and with $w = (w_1, w_2, \dots, w_N)^T \in (\mathbb{R}^{2 \times 2})^N$. The operator $\langle \cdot, \cdot \rangle_N$ is defined as follows: $\forall \xi \in (\mathbb{R}^{2 \times 2})^N, \forall \eta \in (\mathbb{R}^{2 \times 2})^N, \langle \xi, \eta \rangle_N = \sum_{i=1}^N \sum_{j=1}^4 \xi_{ij} \eta_{ij}$ and $\langle \xi \rangle_N = \langle \xi, \xi \rangle_N^{\frac{1}{2}}$. The first term of functional \mathcal{J}_ϵ ensures closeness to the data while the second component is a regularizing component. We consider the following minimization problem :

$$\begin{cases} \text{Search for } \sigma_\epsilon \in K \text{ such that} \\ \forall v \in K, \mathcal{J}_\epsilon(\sigma_\epsilon) \leq \mathcal{J}_\epsilon(v). \end{cases} \quad (3.2)$$

We can notice that minimizing \mathcal{J}_ϵ with respect to v is equivalent to minimizing:

$$\langle \rho(Dv) \rangle_N^2 - 2 \langle \rho(Dv), \omega \rangle_N + \epsilon |v|_{3, \Omega_\nu, \mathbb{R}^2}^2.$$

From now on, we thus denote by \mathcal{J}_ϵ the new functional:

$$\mathcal{J}_\epsilon : \begin{cases} H^3(\Omega_\nu, \mathbb{R}^2) \rightarrow \mathbb{R} \\ v \mapsto \langle \rho(Dv) \rangle_N^2 - 2 \langle \rho(Dv), \omega \rangle_N + \epsilon |v|_{3, \Omega_\nu, \mathbb{R}^2}^2. \end{cases}$$

Our goal being to prove the existence/uniqueness of the solution of the introduced functional minimization problem, we rephrase functional \mathcal{J}_ϵ in terms of the bilinear form \mathbf{a} and the linear form L defined hereafter. Let \mathbf{a} be the symmetric bilinear form such that:

$$\mathbf{a} : \begin{cases} H^3(\Omega_\nu, \mathbb{R}^2) \times H^3(\Omega_\nu, \mathbb{R}^2) \rightarrow \mathbb{R} \\ (u, v) \mapsto \langle \rho(Du), \rho(Dv) \rangle_N + \epsilon (u, v)_{3, \Omega_\nu, \mathbb{R}^2}. \end{cases}$$

Let also L be the linear form defined by:

$$L : \begin{cases} H^3(\Omega_\nu, \mathbb{R}^2) \rightarrow \mathbb{R} \\ v \mapsto \langle \rho(Dv), \omega \rangle_N \end{cases}.$$

The minimization problem thus becomes:

$$\begin{cases} \text{Search for } \sigma_\epsilon \in K \text{ such that} \\ \forall v \in K, \mathbf{a}(\sigma_\epsilon, \sigma_\epsilon) - 2L(\sigma_\epsilon) \leq \mathbf{a}(v, v) - 2L(v). \end{cases} \quad (3.3)$$

The mappings \mathbf{a} and L are continuous, but the trouble is that the bilinear form \mathbf{a} is not $\mathbf{H}^3(\Omega_\nu, \mathbb{R}^2)$ -elliptic, which prevents us from applying Stampacchia's theorem ([8]) straightforwardly. To circumvent this issue, we introduce an artificial term in the minimization problem formulation as follows:

$$\begin{cases} \text{Search for } \sigma_\epsilon \in K \text{ such that} \\ \forall v \in K, \mathbf{a}(\sigma_\epsilon, \sigma_\epsilon) - 2L(\sigma_\epsilon) + \|\beta(\sigma_\epsilon)\|_{2l}^2 \leq \mathbf{a}(v, v) - 2L(v) + \|\beta(v)\|_{2l}^2. \end{cases} \quad (3.4)$$

This new phrasing involves the bilinear form denoted by $\hat{\mathbf{a}}$ defined by

$$\hat{\mathbf{a}} : \begin{cases} \mathbf{H}^3(\Omega_\nu, \mathbb{R}^2) \times \mathbf{H}^3(\Omega_\nu, \mathbb{R}^2) \rightarrow \mathbb{R} \\ (u, v) \mapsto \mathbf{a}(u, v) + \langle \beta(u), \beta(v) \rangle_{2l} \end{cases}$$

and the following propositions hold.

Proposition 3.2.1

The mapping $\|\hat{\cdot}\|$ defined on $\mathbf{H}^3(\Omega_\nu, \mathbb{R}^2)$ by

$$\|\hat{\cdot}\| : \begin{cases} \mathbf{H}^3(\Omega_\nu, \mathbb{R}^2) \rightarrow \mathbb{R} \\ v \mapsto \sqrt{\hat{\mathbf{a}}(v, v)} \end{cases}$$

is a Hilbertian norm.

Proof: The proof is based on the argument of connectedness of Ω_ν and the property of P_1 -unisolvence of the set A .

- It is obvious that $\|\lambda \hat{v}\| = |\lambda| \|\hat{v}\|$, $\forall \lambda \in \mathbb{R}$ according to the definition of $\hat{\mathbf{a}}$.
- The triangle inequality is also obvious as a result of the definition of $\hat{\mathbf{a}}$ and the inner product.
- Let us prove that $\|\hat{v}\| = 0 \Rightarrow v \equiv 0$.
Let $v \in \mathbf{H}^3(\Omega_\nu, \mathbb{R}^2)$ be such that $\|\hat{v}\| = 0$.

It implies that:

- ✓ $|v|_{3, \Omega_\nu, \mathbb{R}^2} = 0$ and as Ω_ν is connected, it yields $v \in P_2(\Omega_\nu, \mathbb{R}^2)$.
- ✓ Also, $\langle \rho(Dv) \rangle_N = 0$. As $v \in P_2(\Omega_\nu, \mathbb{R}^2)$, it follows that $Dv \in P_1(\Omega_\nu, \mathbb{R}^{2 \times 2})$ and from the unisolvence property we conclude that $Dv = 0_{\mathbb{R}^{2 \times 2}}$. The mapping v can thus be written as $v = \begin{pmatrix} c_1 \\ c_2 \end{pmatrix}$ where c_1 and c_2 are constants.
- ✓ At last, $\langle \beta(v) \rangle_{\mathbb{R}^{2l}}^2 = 0 \Leftrightarrow \beta(v) = 0_{\mathbb{R}^{2l}}$ and so $c_1 = c_2 = 0$.

It yields $v \equiv 0$. ■

Proposition 3.2.2

The norm $\|\hat{\cdot}\|$ is equivalent to the norm $\|\cdot\|_{\mathbf{H}^3(\Omega_\nu, \mathbb{R}^2)}$ on $\mathbf{H}^3(\Omega_\nu, \mathbb{R}^2)$.

Proof: The proof is based on a theorem of equivalence of norms by Nečas (Theorem 7.1., [31]) and on the continuity of the bilinear form $\widehat{\mathbf{a}}$ on $\mathbf{H}^3(\Omega_\nu, \mathbb{R}^2) \times \mathbf{H}^3(\Omega_\nu, \mathbb{R}^2)$.

Theorem 3.2.2 (Nečas [31, Theorem 7.1])

Let $\Omega \in \mathfrak{N}^{(0)}$ (with a continuous boundary), f_i functionals satisfying

$$\sum_{i=1}^l |f_i v|^p = 0 \Leftrightarrow v \equiv 0.$$

Let $p \geq 1$, and $k \geq 1$ an integer. We have the inequality:

$$c_1 \|u\|_{W^{k,p}(\Omega)} \leq \left[\sum_{|\alpha|=k} \|D^\alpha u\|_{L^p(\Omega)}^p + \sum_{i=1}^l |f_i u|^p \right]^{\frac{1}{p}} \leq c_2 \|u\|_{W^{k,p}(\Omega)}.$$

The continuity of the bilinear form $\widehat{\mathbf{a}}$ results from the continuity of \mathbf{a} and the following inequality: $\forall (u, v) \in \mathbf{H}^3(\Omega_\nu, \mathbb{R}^2) \times \mathbf{H}^3(\Omega_\nu, \mathbb{R}^2)$,

$$|\langle \beta(u), \beta(v) \rangle_{\mathbb{R}^{2l}}| \leq |\beta(u)|_{\mathbb{R}^{2l}} |\beta(v)|_{\mathbb{R}^{2l}} \quad (\text{Cauchy-Schwarz inequality})$$

$$\text{with } |\beta(u)|_{\mathbb{R}^{2l}} = \sqrt{\sum_{i=1}^l \langle u(b_i) \rangle_2^2}.$$

$$\text{But } \langle u(b_i) \rangle_2 \leq \|u\|_{C^0(\overline{\Omega_\nu, \mathbb{R}^2})} \text{ with } \|u\|_{C^0(\overline{\Omega_\nu, \mathbb{R}^2})} = \sup_{x \in \overline{\Omega_\nu}} \langle u(x) \rangle_2$$

and using the Sobolev's embedding theorem, we have: $\langle u(b_i) \rangle_2 \leq C \|u\|_{\mathbf{H}^3(\Omega_\nu, \mathbb{R}^2)}$.

Therefore, $|\beta(u)|_{\mathbb{R}^{2l}} \leq \sqrt{l} C \|u\|_{\mathbf{H}^3(\Omega_\nu, \mathbb{R}^2)}$ and

$$|\langle \beta(u), \beta(v) \rangle_{\mathbb{R}^{2l}}| \leq l C^2 \|u\|_{\mathbf{H}^3(\Omega_\nu, \mathbb{R}^2)} \|v\|_{\mathbf{H}^3(\Omega_\nu, \mathbb{R}^2)}.$$

The bilinear form $\widehat{\mathbf{a}}$ being continuous on $\mathbf{H}^3(\Omega_\nu, \mathbb{R}^2) \times \mathbf{H}^3(\Omega_\nu, \mathbb{R}^2)$, there exists a constant $c > 0$ such that $\forall v \in \mathbf{H}^3(\Omega_\nu, \mathbb{R}^2)$:

$$\widehat{\mathbf{a}}(v, v) = \|\widehat{v}\|^2 \leq c \|v\|_{\mathbf{H}^3(\Omega_\nu, \mathbb{R}^2)}^2.$$

For the second part of the inequality, we use Nečas' theorem with $k = 3$ and $p = 2$. We

take $f_1 : v \mapsto \frac{1}{\sqrt{\epsilon}} \rho(Dv)$ and $f_2 : v \mapsto \frac{1}{\sqrt{\epsilon}} \beta(v)$. $\forall v \in P_2(\Omega_\nu, \mathbb{R}^2)$, $\sum_{i=1}^2 |f_i v|^2 = 0 \Leftrightarrow v \equiv 0$

from the unisolvence property of the set A . From Nečas' theorem, we then get that there exists a constant $c_1 > 0$ such that:

$$c_1^2 \|v\|_{\mathbf{H}^3(\Omega_\nu, \mathbb{R}^2)}^2 \leq |v|_{3, \Omega_\nu, \mathbb{R}^2}^2 + \frac{1}{\epsilon} \langle \rho(Dv) \rangle_N^2 + \frac{1}{\epsilon} \|\beta(v)\|_{\mathbb{R}^{2l}}^2$$

$$\Leftrightarrow \epsilon c_1^2 \|v\|_{\mathbf{H}^3(\Omega_\nu, \mathbb{R}^2)}^2 \leq \epsilon |v|_{3, \Omega_\nu, \mathbb{R}^2}^2 + \langle \rho(Dv) \rangle_N^2 + \|\beta(v)\|_{\mathbb{R}^{2l}}^2$$

$$\Leftrightarrow \|v\|_{\mathbf{H}^3(\Omega_\nu, \mathbb{R}^2)}^2 \leq \frac{1}{\epsilon c_1^2} \|\widehat{v}\|^2$$

■

It results in the following theorem.

Theorem 3.2.3

Problem (3.2) admits a unique solution $\sigma_\epsilon \in K$. This solution is characterized by the variational inequality: $\forall v \in K, \widehat{\mathbf{a}}(\sigma_\epsilon, v - \sigma_\epsilon) \geq L(v - \sigma_\epsilon)$.

Proof: The proof is based on Stampacchia's theorem ([8]). ■

3.2.2 Characterization of the solution

Let K_0 be the vector subspace of $\mathbf{H}^3(\Omega_\nu, \mathbb{R}^2)$ defined by

$$K_0 = \{v \in \mathbf{H}^3(\Omega_\nu, \mathbb{R}^2) \mid \beta(v) = 0_{\mathbb{R}^{2l}}\}.$$

Let S be the set defined by

$$S = \{u \in \mathbf{H}^3(\Omega_\nu, \mathbb{R}^2) \mid \forall v \in K_0, \mathbf{a}(u, v) = L(v)\}.$$

Then the following proposition holds.

Proposition 3.2.4

The unique solution σ_ϵ of problem (3.2) is characterized by:

$$\{\sigma_\epsilon\} = K \cap S.$$

This is mainly an abstract result that will be useful to prove Theorem 3.2.3.

Proof: First, let us prove that $\{\sigma_\epsilon\} \subset K \cap S$.

From Stampacchia's theorem, we have $\forall v \in K$:

$$\widehat{\mathbf{a}}(\sigma_\epsilon, v - \sigma_\epsilon) \geq L(v - \sigma_\epsilon).$$

But $v - \sigma_\epsilon \in K_0$ so $\widehat{\mathbf{a}}(\sigma_\epsilon, v - \sigma_\epsilon) = \mathbf{a}(\sigma_\epsilon, v - \sigma_\epsilon) \geq L(v - \sigma_\epsilon)$.

Moreover, $-(v - \sigma_\epsilon) \in K_0$ since K_0 is a vector space, so $\forall v \in K$:

$$\widehat{\mathbf{a}}(\sigma_\epsilon, -(v - \sigma_\epsilon)) \geq L(-(v - \sigma_\epsilon)) \iff \widehat{\mathbf{a}}(\sigma_\epsilon, v - \sigma_\epsilon) \leq L(v - \sigma_\epsilon).$$

By gathering the two above results, it yields $\widehat{\mathbf{a}}(\sigma_\epsilon, v - \sigma_\epsilon) = L(v - \sigma_\epsilon)$, which means that $\forall v_0 \in K_0, \mathbf{a}(\sigma_\epsilon, v_0) = L(v_0)$.

Therefore $\sigma_\epsilon \in K \cap S$.

Now, let us prove that $K \cap S \subset \{\sigma_\epsilon\}$.

Let $w \in K \cap S$. So $w \in K$ and $\forall v_0 \in K_0, \mathbf{a}(w, v_0) = L(v_0)$.

$\forall v \in K, v - w \in K_0$ so:

$$\widehat{\mathbf{a}}(w, v - w) = \mathbf{a}(w, v - w) = L(v - w) \geq L(v - w).$$

Therefore, w is a solution of Problem (3.2) and by uniqueness of the solution, $w = \sigma_\epsilon$.

It yields $K \cap S \subset \{\sigma_\epsilon\}$. ■

3.2.3 Lagrange multipliers

We now introduce Lagrange multipliers, which enables us to define the variational formulation of problem (3.2) on the whole space $H^3(\Omega_\nu, \mathbb{R}^2)$ and to obtain a variational equality (efficiently tractable in the context of the Finite Element Method) instead of a variational inequality. Let K_0^\perp be the orthogonal complement of K_0 in $H^3(\Omega_\nu, \mathbb{R}^2)$ for the scalar product $\widehat{\mathbf{a}}(\cdot, \cdot)$:

$$K_0^\perp = \{u \in H^3(\Omega_\nu, \mathbb{R}^2) \mid \widehat{\mathbf{a}}(u, v) = 0, \forall v \in K_0\}.$$

The space $H^3(\Omega_\nu, \mathbb{R}^2)$ can be written as the direct sum $H^3(\Omega_\nu, \mathbb{R}^2) = K_0^\perp \oplus K_0$. Let us denote by $\beta_{|K_0^\perp}$ the restriction of β to K_0^\perp . Then $\beta_{|K_0^\perp}$ is a topological isomorphism (in particular, it is obvious that $\ker \beta_{|K_0^\perp} = K_0 \cap K_0^\perp = \{0\}$). Moreover, $\beta_{|K_0^\perp}$ is onto since K is non-empty). The main theorem is stated as follows.

Theorem 3.2.3

If σ_ϵ is the unique solution of problem (3.2), then σ_ϵ is also the solution of the following problem with Lagrange multipliers:

$$\begin{cases} \text{Search for } (\sigma_\epsilon, \lambda) \in K \times \mathbb{R}^{2l}, \\ \forall v \in H^3(\Omega_\nu, \mathbb{R}^2), \mathbf{a}(\sigma_\epsilon, v) - L(v) + \langle \lambda, \beta(v) \rangle_{2l} = 0. \end{cases} \quad (3.5)$$

Proof: Assume that $(u, \lambda) \in K \times \mathbb{R}^{2l}$ is a solution of problem (3.5). Then $\forall v \in K_0$, we have:

$$\mathbf{a}(u, v) - L(v) = 0,$$

since $\beta(v) = 0_{\mathbb{R}^{2l}}$. Thus $u \in K \cap S$ and from Proposition 3.2.4, $u = \sigma_\epsilon$.

Conversely, from Proposition 3.2.4, $\{\sigma_\epsilon\} = K \cap S$ so $\forall v_0 \in K_0$, $\mathbf{a}(\sigma_\epsilon, v_0) = L(v_0)$.

Let us consider the linear form defined $\forall w \in K_0^\perp$ by:

$$\mathcal{L} : \begin{cases} K_0^\perp \rightarrow \mathbb{R} \\ w \mapsto -\mathbf{a}(\sigma_\epsilon, w) + L(w). \end{cases}$$

We remind the reader that, denoting by E and F two normed vector spaces and by A a continuous linear mapping from E to F , the adjoint operator $A^t : F' \rightarrow E'$ is defined by:

$$\forall v \in E, \forall w \in F', \langle A^t w, v \rangle_{EE} = \langle w, Av \rangle_{F'F},$$

$\langle \cdot, \cdot \rangle_{G'G}$ denoting the dual pairing.

The mapping $\beta_{|K_0^\perp} : K_0^\perp \rightarrow \mathbb{R}^{2l}$ is a topological isomorphism and consequently so is the mapping $\beta_{|K_0^\perp}^t : \mathbb{R}^{2l} \rightarrow (K_0^\perp)'$.

As $\mathcal{L} \in (K_0^\perp)'$, there exists a unique $\lambda \in \mathbb{R}^{2l}$ such that $\beta_{|K_0^\perp}^t(\lambda) = \mathcal{L}$. It means that:

$$\begin{aligned} \mathcal{L}(w) &= -\mathbf{a}(\sigma_\epsilon, w) + L(w) = \langle \beta_{|K_0^\perp}^t(\lambda), w \rangle_{(K_0^\perp)'K_0^\perp}, \\ &\iff \mathbf{a}(\sigma_\epsilon, w) - L(w) + \langle \beta_{|K_0^\perp}^t(\lambda), w \rangle_{(K_0^\perp)'K_0^\perp} = 0, \\ &\iff \mathbf{a}(\sigma_\epsilon, w) - L(w) + \langle \lambda, \beta_{|K_0^\perp}(w) \rangle_{(\mathbb{R}^{2l})'\mathbb{R}^{2l}} = 0. \end{aligned}$$

Let $v \in \mathbf{H}^3(\Omega_\nu, \mathbb{R}^2)$. Since $\mathbf{H}^3(\Omega_\nu, \mathbb{R}^2) = K_0^\perp \oplus K_0$, $\exists!(v_0, w) \in K_0^\perp \times K_0$, $v = v_0 + w$. From the last equality, it yields $\exists!\lambda \in \mathbb{R}^{2l}$, such that $\forall v \in \mathbf{H}^3(\Omega_\nu, \mathbb{R}^2)$:

$$\begin{aligned} \mathbf{a}(\sigma_\epsilon, v) - L(v) - \mathbf{a}(\sigma_\epsilon, v_0) + L(v_0) + \langle \lambda, \beta(w) \rangle_{(\mathbb{R}^{2l})' \mathbb{R}^{2l}} &= 0, \\ \iff \mathbf{a}(\sigma_\epsilon, v) - L(v) + \langle \lambda, \beta(w) \rangle_{(\mathbb{R}^{2l})' \mathbb{R}^{2l}} &= 0, \end{aligned}$$

since $v_0 \in K_0$, and $\mathbf{a}(\sigma_\epsilon, v_0) = L(v_0)$ from Proposition 3.2.4.

To conclude, $\beta(w) = \beta(v - v_0) = \beta(v)$ since $\beta(v_0) = 0_{\mathbb{R}^{2l}}$.

Finally,

$$\exists!\lambda \in \mathbb{R}^{2l}, \forall v \in \mathbf{H}^3(\Omega_\nu, \mathbb{R}^2), \mathbf{a}(\sigma_\epsilon, v) - L(v) + \langle \lambda, \beta(v) \rangle_{(\mathbb{R}^{2l})' \mathbb{R}^{2l}} = 0 \quad \blacksquare$$

3.2.4 Theoretical convergence result

We now provide a theoretical convergence result that is an abstract result highlighting the well-posedness of the modelling.

Let D be a subset of $]0, +\infty[$ admitting 0 as accumulation point (this implies that $0 \in \overline{D}$). For each $d \in D$, let A^d be a set of $N = N(d)$ distinct points of $\overline{\Omega_\nu}$ containing a P_1 -unisolvent subset (we cannot say much on N except that $N \geq \dim P_1$ and as d tends to 0 , $N(d)$ increases to $+\infty$).

We suppose that

$$\sup_{x \in \Omega_\nu} \delta(x, A^d) = d, \quad (3.6)$$

where δ is the Euclidean distance in \mathbb{R}^2 . Let us observe that the left-hand side of (3.6) is just the Hausdorff distance between A^d and $\overline{\Omega_\nu}$. Consequently, it implies that D is bounded and that this distance tends to 0 as d does. Thus d is the radius of the largest sphere included in Ω_ν that contains no point from A^d (Hausdorff distance). Let us remark the ambiguity in the meaning of d defined first as an index and next, independently, in (3.6). This situation is analogous to that found in the Finite Element theory (see [2] and [12]).

We point out that the hypotheses $0 \in \overline{D}$ and (3.6) imply the weaker condition

$$\lim_{d \rightarrow 0} \sup_{x \in \Omega_\nu} \delta(x, A^d) = 0. \quad (3.7)$$

For all $d \in D$, we denote by ρ^d the mapping defined by:

$$\rho^d : \begin{cases} \mathbf{H}^2(\Omega_\nu, \mathbb{R}^{2 \times 2}) \rightarrow (\mathbb{R}^{2 \times 2})^{N(d)} \\ v \mapsto \rho^d(v) = ((v(a))_{a \in A^d})^T \end{cases} .$$

Then we introduce the norm $\|\widehat{\cdot}\|_d$ equivalent to the norm $\|\cdot\|_{\mathbf{H}^3(\Omega_\nu, \mathbb{R}^2)}$ on $\mathbf{H}^3(\Omega_\nu, \mathbb{R}^2)$ defined by: $\forall v \in \mathbf{H}^3(\Omega_\nu, \mathbb{R}^2)$,

$$\|\widehat{v}\|_d = \left[\langle \rho^d(Dv) \rangle_{N(d)}^2 + \epsilon |v|_{3, \Omega_\nu, \mathbb{R}^2}^2 + \|\beta(v)\|_{2l}^2 \right]^{\frac{1}{2}} .$$

(It is possible to check that $\|\widehat{\cdot}\|_d$ is a norm by applying similar arguments to those in Proposition 3.2.1). The following lemma holds and allows to state Theorem 3.2.5.

Lemma 3.2.4

Suppose that (3.7) holds. Let $A_0 = \{b_{01}, \dots, b_{0\aleph}\}$ be a fixed P_1 -unisolvent subset of $\overline{\Omega_\nu}$ (in this case $\aleph = \dim P_1$).

$$\forall j = 1, \dots, \aleph, \quad \exists (a_{0j}^d)_{d \in D}, (\forall d \in D, a_{0j}^d \in A^d) \quad \text{and} \quad (b_{0j} = \lim_{d \rightarrow 0} a_{0j}^d). \quad (3.8)$$

For all $d \in D$, let A_0^d be the set $\{a_{01}^d, \dots, a_{0\aleph}^d\}$ and $\|\cdot\|_{A_0^d}$ be the mapping defined by: $\forall v \in H^3(\Omega_\nu, \mathbb{R}^2)$,

$$\|v\|_{A_0^d} = \left[\sum_{j=1}^{\aleph} \langle Dv(a_{0j}^d) \rangle_4^2 + \epsilon |v|_{3, \Omega_\nu, \mathbb{R}^2}^2 + \|\beta(v)\|_{2l}^2 \right]^{\frac{1}{2}},$$

(where $\langle \xi, \eta \rangle_4 = \sum_{j=1}^4 \xi_j \eta_j$, with $\xi, \eta \in \mathbb{R}^{2 \times 2}$).

Then, there exists $\mu > 0$ such that for all $d \leq \mu$, the set A_0^d is P_1 -unisolvent and $\|\cdot\|_{A_0^d}$ is a norm on $H^3(\Omega_\nu, \mathbb{R}^2)$ uniformly equivalent on $D \cap]0, \mu]$ to the norm $\|\cdot\|_{H^3(\Omega_\nu, \mathbb{R}^2)}$.

Proof: According to the Sobolev embedding:

$$\exists C_1 > 0, \forall d \in D, \forall v \in H^3(\Omega_\nu, \mathbb{R}^2), \|v\|_{A_0^d} \leq C_1 \|v\|_{H^3(\Omega_\nu, \mathbb{R}^2)}$$

Constant C_1 does not depend on d , it only depends on \aleph, l and ϵ .

Now, it suffices to find a constant $C_2 > 0$ independent of d such that $\|v\|_{H^3(\Omega_\nu, \mathbb{R}^2)} \leq C_2 \|v\|_{A_0^d}$.

For $v \in H^3(\Omega_\nu, \mathbb{R}^2)$,

$$\begin{aligned} \frac{1}{2} \sum_{j=1}^{\aleph} \langle Dv(b_{0j}) \rangle_4^2 &= \frac{1}{2} \sum_{j=1}^{\aleph} \langle Dv(b_{0j}) - Dv(a_{0j}^d) + Dv(a_{0j}^d) \rangle_4^2 \\ &\leq \sum_{j=1}^{\aleph} \langle Dv(b_{0j}) - Dv(a_{0j}^d) \rangle_4^2 + \sum_{j=1}^{\aleph} \langle Dv(a_{0j}^d) \rangle_4^2. \end{aligned} \quad (3.9)$$

Also, the Hölder inclusion gives:

$$\exists \lambda \in]0, 1], H^3(\Omega_\nu, \mathbb{R}^2) \circlearrowleft C^{1, \lambda}(\overline{\Omega_\nu}, \mathbb{R}^2).$$

Thus $v \in C^{1, \lambda}(\overline{\Omega_\nu}, \mathbb{R}^2)$ and $\exists C > 0, \forall j = 1, \dots, \aleph, \forall d \in D$,

$$\langle Dv(b_{0j}) - Dv(a_{0j}^d) \rangle_4^2 \leq \|v\|_{C^{1, \lambda}(\overline{\Omega_\nu}, \mathbb{R}^2)}^2 \langle b_{0j} - a_{0j}^d \rangle_2^{2\lambda} \leq C^2 \|v\|_{H^3(\Omega_\nu, \mathbb{R}^2)}^2 \langle b_{0j} - a_{0j}^d \rangle_2^{2\lambda}. \quad (3.10)$$

Moreover, by (3.8), it comes: $\forall j = 1, \dots, \aleph$,

$$\forall \gamma_j > 0, \exists \mu_{\gamma_j}, \forall d \in D, \left(d \leq \mu_{\gamma_j} \Rightarrow \langle a_{0j}^d - b_{0j} \rangle_2 \leq \gamma_j \right).$$

Then

$$\forall \gamma_j > 0, \exists \mu_{\gamma_j}, \forall d \in D, \left(d \leq \mu_{\gamma_j} \Rightarrow \langle Dv(b_{0j}) - Dv(a_{0j}^d) \rangle_4^2 \leq C^2 \gamma_j^{2\lambda} \|v\|_{\mathbf{H}^3(\Omega_\nu, \mathbb{R}^2)}^2 \right).$$

Let $\gamma > 0$ and taking $\gamma_j = \gamma, \forall j = 1, \dots, \aleph$ and $\mu = \min(\mu_{\gamma_1}, \dots, \mu_{\gamma_\aleph})$ then

$$\forall d \in D, \left(d \leq \mu \Rightarrow \sum_{j=1}^{\aleph} \langle Dv(b_{0j}) - Dv(a_{0j}^d) \rangle_4^2 \leq C^2 \aleph \gamma^{2\lambda} \|v\|_{\mathbf{H}^3(\Omega_\nu, \mathbb{R}^2)}^2 \right).$$

Finally,

$$\begin{aligned} & \forall \gamma > 0, \exists \mu > 0, \forall d \in D, \forall v \in \mathbf{H}^3(\Omega_\nu, \mathbb{R}^2), \\ & \left(d \leq \mu \Rightarrow \sum_{j=1}^{\aleph} \langle Dv(b_{0j}) - Dv(a_{0j}^d) \rangle_4^2 \leq C^2 \gamma^{2\lambda} \aleph \|v\|_{\mathbf{H}^3(\Omega_\nu, \mathbb{R}^2)}^2 \right) \end{aligned}$$

Using (3.9), we obtain:

$$\begin{aligned} & \forall \gamma > 0, \exists \mu > 0, \forall d \in D, \forall v \in \mathbf{H}^3(\Omega_\nu, \mathbb{R}^2), \\ & \left(d \leq \mu \Rightarrow \frac{1}{2} \sum_{j=1}^{\aleph} \langle Dv(b_{0j}) \rangle_4^2 + \epsilon |v|_{3, \Omega_\nu, \mathbb{R}^2}^2 + \|\beta(v)\|_{\mathbb{R}^{2l}}^2 \leq \|v\|_{A_0^d}^2 + C^2 \gamma^{2\lambda} \aleph \|v\|_{\mathbf{H}^3(\Omega_\nu, \mathbb{R}^2)}^2 \right), \\ & \left(d \leq \mu \Rightarrow \frac{1}{2} \sum_{j=1}^{\aleph} \langle Dv(b_{0j}) \rangle_4^2 + \epsilon |v|_{3, \Omega_\nu, \mathbb{R}^2}^2 + \|\beta(v)\|_{\mathbb{R}^{2l}}^2 - C^2 \gamma^{2\lambda} \aleph \|v\|_{\mathbf{H}^3(\Omega_\nu, \mathbb{R}^2)}^2 \leq \|v\|_{A_0^d}^2 \right). \end{aligned}$$

The map $v \in \mathbf{H}^3(\Omega_\nu, \mathbb{R}^2) \mapsto \left[\frac{1}{2} \sum_{j=1}^{\aleph} \langle Dv(b_{0j}) \rangle_4^2 + \epsilon |v|_{3, \Omega_\nu, \mathbb{R}^2}^2 + \|\beta(v)\|_{\mathbb{R}^{2l}}^2 \right]^{\frac{1}{2}}$ is an equivalent norm on $\mathbf{H}^3(\Omega_\nu, \mathbb{R}^2)$ to the norm $\|\cdot\|_{\mathbf{H}^3(\Omega_\nu, \mathbb{R}^2)}$, then:

$$\forall \gamma > 0, \exists \mu > 0, \forall d \in D, \forall v \in \mathbf{H}^3(\Omega_\nu, \mathbb{R}^2), \left(d \leq \mu \Rightarrow (C'^2 - C^2 \gamma^{2\lambda} \aleph) \|v\|_{\mathbf{H}^3(\Omega_\nu, \mathbb{R}^2)}^2 \leq \|v\|_{A_0^d}^2 \right).$$

It suffices to choose a right γ to obtain the equivalence of norms. We notice that $\|\cdot\|_{A_0^d}$ is clearly a semi-norm. Thanks to the double inequality obtained, this is a norm on $\mathbf{H}^3(\Omega_\nu, \mathbb{R}^2)$ since $\|v\|_{A_0^d} = 0 \Rightarrow v = 0$. \blacksquare

Theorem 3.2.5

Suppose that there exists a function $\widehat{f} \in K$ such that for all $d \in D$: $\rho^d(D\widehat{f}) = \omega$, and $\epsilon = \epsilon(d) \in]0, \epsilon_0], \epsilon_0 > 0$.

For all $d \in D$, we denote by u_ϵ^d the unique solution of problem (3.2), then under the above assumptions we have:

$$\lim_{d \rightarrow 0} \|u_\epsilon^d - \widehat{f}\|_{\mathbf{H}^3(\Omega_\nu, \mathbb{R}^2)} = 0.$$

Proof: The proof is divided into four steps.

First step

We start by proving that the sequence $(u_\epsilon^d)_{\substack{d \in D \cap]0, \mu] \\ \epsilon \in]0, \epsilon_0]}}$ is bounded in $H^3(\Omega_\nu, \mathbb{R}^2)$ independently of d . By taking $v = \widehat{f}$ in problem (3.2), we obtain :

$$\langle \rho (Du_\epsilon^d - D\widehat{f}) \rangle_{N(d)}^2 + \epsilon |u_\epsilon^d|_{3, \Omega_\nu, \mathbb{R}^2}^2 + \|\beta(u_\epsilon^d)\|_{\mathbb{R}^{2l}}^2 \leq \epsilon |\widehat{f}|_{3, \Omega_\nu, \mathbb{R}^2}^2 + \|\beta(\widehat{f})\|_{\mathbb{R}^{2l}}^2.$$

We deduce that:

$$\begin{cases} |u_\epsilon^d|_{3, \Omega_\nu, \mathbb{R}^2} \leq |\widehat{f}|_{3, \Omega_\nu, \mathbb{R}^2}, \\ \langle \rho (Du_\epsilon^d - D\widehat{f}) \rangle_{N(d)}^2 \leq \epsilon_0 |\widehat{f}|_{3, \Omega_\nu, \mathbb{R}^2}^2. \end{cases}$$

As $A_0^d \subset A^d$ then:

$$\sum_{a \in A_0^d} \langle Du_\epsilon^d(a) - D\widehat{f}(a) \rangle_4^2 \leq \sum_{a \in A^d} \langle Du_\epsilon^d(a) - D\widehat{f}(a) \rangle_4^2 = \langle \rho^d (Du_\epsilon^d - D\widehat{f}) \rangle_{N(d)}^2 \leq \epsilon_0 |\widehat{f}|_{3, \Omega_\nu, \mathbb{R}^2}^2.$$

Moreover,

$$\begin{aligned} \sum_{a \in A_0^d} \langle Du_\epsilon^d(a) \rangle_4^2 &= \sum_{a \in A_0^d} \langle Du_\epsilon^d(a) - D\widehat{f}(a) + D\widehat{f}(a) \rangle_4^2 \\ &\leq \sum_{a \in A_0^d} \langle Du_\epsilon^d(a) - D\widehat{f}(a) \rangle_4^2 + \sum_{a \in A_0^d} \langle D\widehat{f}(a) \rangle_4^2 \\ &\leq \epsilon_0 |\widehat{f}|_{3, \Omega_\nu, \mathbb{R}^2}^2 + 2\aleph \| \widehat{f} \|_{C^1(\overline{\Omega_\nu, \mathbb{R}^2})}^2, \end{aligned}$$

and using the equivalence of norm given in Lemma 3.2.4, we establish that:

$$\exists \tilde{\nu} > 0, \forall d \in D, \forall \epsilon \in]0, \epsilon_0], \left(d \leq \mu \Rightarrow \|u_\epsilon^d\|_{H^3(\Omega_\nu, \mathbb{R}^2)} \leq \tilde{\nu} \right).$$

The sequence $(u_\epsilon^d)_{\substack{d \in D \cap]0, \mu] \\ \epsilon \in]0, \epsilon_0]}}$ is bounded in $H^3(\Omega_\nu, \mathbb{R}^2)$, so one can extract a subsequence $(u_{\epsilon_l}^{d_l})_{l \in \mathbb{N}}$ with $\lim_{l \rightarrow \infty} d_l = 0$ (since 0 is an accumulation point of D) and $\epsilon_l \in]0, \epsilon_0], \forall l \in \mathbb{N}$ (-we assume that $\epsilon = \epsilon(d)$ -) that weakly converges to an element of $H^3(\Omega_\nu, \mathbb{R}^2)$ denoted by f^* .

Second step

In this step, we argue by contradiction and prove that $Df^* = D\widehat{f}$ using compactness arguments (Sobolev's embeddings in Hölder's spaces and Rellich-Kondrachov's theorem, see [8]). Finally, the Lagrange interpolation constraints give us that $f^* = \widehat{f}$.

We start by proving that $D\widehat{f} = Df^*$.

We argue by contradiction. We assume that $D\widehat{f} \neq Df^*$, then there exists an open set ω non empty included in Ω and a positive number α such that:

$$\forall x \in \omega, \langle D\widehat{f}(x) - Df^*(x) \rangle_4 > \alpha.$$

Let $\xi = 1 + E \left[\frac{\epsilon_0 |\widehat{f}|_{3, \Omega_\nu, \mathbb{R}^2}}{\alpha^2} \right]$ where $E[\cdot]$ represents the integer part.

Let $B_0 = \{p_{01}, \dots, p_{0\xi}\}$ a subset of ξ points of ω , we have:

$$\forall i = 1, \dots, \xi, \exists (p_{0i}^d)_{d \in D}, \left(\forall d \in D, p_{0i}^d \in A^d \right) \text{ and } \left(p_{0i} = \lim_{d \rightarrow 0} p_{0i}^d \right)$$

For all $d \in D$, let B_0^d be the set $\{p_{01}^d, \dots, p_{0\xi}^d\}$.

As previously shown and knowing that $B_0^d \subset A^d$, we have

$$\sum_{i=1}^{\xi} \langle Du_\epsilon^{d_i}(p_{0i}^{d_i}) - D\widehat{f}(p_{0i}^{d_i}) \rangle_4^2 \leq \epsilon_0 |\widehat{f}|_{3, \Omega_\nu, \mathbb{R}^2}^2. \quad (3.11)$$

Moreover, $\forall i = 1, \dots, \xi$,

$$\begin{aligned} \langle Du_\epsilon^{d_i}(p_{0i}^{d_i}) - Df^*(p_{0i}) \rangle_4 &= \langle Du_\epsilon^{d_i}(p_{0i}^{d_i}) - Du_\epsilon^{d_i}(p_{0i}) + Du_\epsilon^{d_i}(p_{0i}) - Df^*(p_{0i}) \rangle_4 \\ &\leq \langle Du_\epsilon^{d_i}(p_{0i}^{d_i}) - Du_\epsilon^{d_i}(p_{0i}) \rangle_4 + \langle Du_\epsilon^{d_i}(p_{0i}) - Df^*(p_{0i}) \rangle_4. \end{aligned}$$

As $\exists \lambda \in]0, 1]$, $H^3(\Omega_\nu, \mathbb{R}^2) \circ C^{1, \lambda}(\overline{\Omega_\nu}, \mathbb{R}^2)$, there exists a constant C_3 such that:

$$\left(\|u_{\epsilon_l}^{d_l}\|_{C^{1, \lambda}(\overline{\Omega_\nu}, \mathbb{R}^2)} \leq C_3 \|u_{\epsilon_l}^{d_l}\|_{H^3(\Omega_\nu, \mathbb{R}^2)} \right).$$

Consequently,

$$\langle Du_{\epsilon_l}^{d_l}(p_{0i}^{d_l}) - Du_{\epsilon_l}^{d_l}(p_{0i}) \rangle_4 \leq C_3 \langle p_{0i}^{d_l} - p_{0i} \rangle_2^\lambda.$$

But $\lim_{l \rightarrow \infty} d_l = 0$ and $p_{0i} = \lim_{l \rightarrow \infty} p_{0i}^{d_l}$, we deduce that:

$$\lim_{l \rightarrow \infty} \langle Du_{\epsilon_l}^{d_l}(p_{0i}^{d_l}) - Du_{\epsilon_l}^{d_l}(p_{0i}) \rangle_4 = 0.$$

By Rellich-Kondrachov theorem, $H^3(\Omega_\nu, \mathbb{R}^2) \stackrel{c}{\subset} C^1(\overline{\Omega_\nu}, \mathbb{R}^2)$, then $\lim_{l \rightarrow \infty} \langle Du_{\epsilon_l}^{d_l}(p_{0i}) - Df^*(p_{0i}) \rangle_4 = 0$. Therefore $\lim_{l \rightarrow \infty} \langle Du_{\epsilon_l}^{d_l}(p_{0i}^{d_l}) - Df^*(p_{0i}) \rangle_4 = 0$.
So

$$\lim_{l \rightarrow \infty} Du_{\epsilon_l}^{d_l}(p_{0i}^{d_l}) = Df^*(p_{0i}).$$

Letting $l \rightarrow \infty$ in equation (3.11), yields to:

$$\sum_{i=1}^{\xi} \langle Df^*(p_{0i}) - D\widehat{f}(p_{0i}) \rangle_4^2 \leq \epsilon_0 |\widehat{f}|_{3, \Omega_\nu, \mathbb{R}^2}^2$$

and then,

$$\xi \alpha^2 \leq \epsilon_0 |\widehat{f}|_{3, \Omega_\nu, \mathbb{R}^2}^2$$

This inequality is in contradiction with the choice of ξ . Thus $Df^* = D\widehat{f}$.
To conclude, $\forall i \in \{1, \dots, l\}$, $f^*(b_i) = \widehat{f}(b_i) = \eta_i$ hence $f^* = \widehat{f}$.

Third step

The aim is to prove that $(u_{\epsilon_l}^{d_l})_{l \in \mathbb{N}}$ strongly converges to \widehat{f} in $H^3(\Omega_\nu, \mathbb{R}^2)$.

Thanks to Rellich-Kondrachov's compact embedding theorem, we obtain that $(u_{\epsilon_l}^{d_l})_{l \in \mathbb{N}}$ strongly converges to \widehat{f} in $H^2(\Omega_\nu, \mathbb{R}^2)$. Since

$$\|u_{\epsilon_l}^{d_l} - \widehat{f}\|_{H^3(\Omega_\nu, \mathbb{R}^2)}^2 = \|u_{\epsilon_l}^{d_l} - \widehat{f}\|_{H^2(\Omega_\nu, \mathbb{R}^2)}^2 + |u_{\epsilon_l}^{d_l} - \widehat{f}|_{3, \Omega_\nu, \mathbb{R}^2}^2,$$

we just need to prove that $\lim_{l \rightarrow \infty} |u_{\epsilon_l}^{d_l} - \widehat{f}|_{3, \Omega_\nu, \mathbb{R}^2} = 0$. We have:

$$|u_{\epsilon_l}^{d_l} - \widehat{f}|_{3, \Omega_\nu, \mathbb{R}^2}^2 = |u_{\epsilon_l}^{d_l}|_{3, \Omega_\nu, \mathbb{R}^2}^2 + |\widehat{f}|_{3, \Omega_\nu, \mathbb{R}^2}^2 - 2(u_{\epsilon_l}^{d_l}, \widehat{f})_{3, \Omega_\nu, \mathbb{R}^2}.$$

But $|u_{\epsilon_l}^{d_l}|_{3, \Omega_\nu, \mathbb{R}^2} \leq |\widehat{f}|_{3, \Omega_\nu, \mathbb{R}^2}$, so

$$|u_{\epsilon_l}^{d_l} - \widehat{f}|_{3, \Omega_\nu, \mathbb{R}^2}^2 \leq 2|\widehat{f}|_{3, \Omega_\nu, \mathbb{R}^2}^2 - 2(u_{\epsilon_l}^{d_l}, \widehat{f})_{3, \Omega_\nu, \mathbb{R}^2}.$$

Moreover, $u_{\epsilon_l}^{d_l} \xrightarrow{H^3(\Omega_\nu, \mathbb{R}^2)} \widehat{f}$, consequently

$\forall \varphi \in L^2(\Omega_\nu, \mathbb{R}^2)$, $(\partial^\alpha u_{\epsilon_l}^{d_l}, \varphi)_{L^2(\Omega_\nu, \mathbb{R}^2)} \xrightarrow{l \rightarrow +\infty} (\partial^\alpha \widehat{f}, \varphi)_{L^2(\Omega_\nu, \mathbb{R}^2)}$, $\forall \alpha \in \mathbb{N}$, $|\alpha| = 3$. Taking

$\varphi = \partial^\alpha \widehat{f}$ with $|\alpha| = 3$, yields to:

$(\partial^\alpha u_{\epsilon_l}^{d_l}, \partial^\alpha \widehat{f})_{L^2(\Omega_\nu, \mathbb{R}^2)} \xrightarrow{l \rightarrow +\infty} \|\partial^\alpha \widehat{f}\|_{L^2(\Omega_\nu, \mathbb{R}^2)}^2$ and $(u_{\epsilon_l}^{d_l}, \widehat{f})_{3, \Omega_\nu, \mathbb{R}^2} \xrightarrow{l \rightarrow +\infty} |\widehat{f}|_{3, \Omega_\nu, \mathbb{R}^2}$ when l

tends to $+\infty$.

It follows from the previous inequality that $\lim_{l \rightarrow \infty} \|u_{\epsilon_l}^{d_l} - \widehat{f}\|_{H^3(\Omega_\nu, \mathbb{R}^2)} = 0$.

Fourth Step

Assume that $\|u_{\epsilon}^d - \widehat{f}\|_{H^3(\Omega_\nu, \mathbb{R}^2)}$ does not tend to 0 when d tends to 0.

It means that there exist a real number $\alpha > 0$ and two sequences $(d_k)_{k \in \mathbb{N}}$ and $(\epsilon_k)_{k \in \mathbb{N}}$ such that $d_k \xrightarrow{k \rightarrow +\infty} 0$ and $\epsilon_k = \epsilon(d_k)$, and $\forall k \in \mathbb{N}$,

$$\|u_{\epsilon_k}^{d_k} - \widehat{f}\|_{H^3(\Omega_\nu, \mathbb{R}^2)} > \alpha. \quad (3.12)$$

Following the same steps as previously done, there exists a subsequence of $(u_{\epsilon_k}^{d_k})_{k \in \mathbb{N}}$ that strongly converges to \widehat{f} in $H^3(\Omega_\nu, \mathbb{R}^2)$, which is in contradiction with (3.12). \blacksquare

3.2.5 Discretization

We now discretize the variational problem (3.5). To do so, we will use classical notations used in the Finite Element theory (similar to those in [2] and [12]). Let \mathcal{H} be an open bounded subset of $]0, +\infty[$ admitting 0 as accumulation point. Let us recall that the elements of class $C^{k'}$ can be used for the computation of discrete D^m -splines (in our case $m = 3$) with $m \leq k' + 1$ (where k' is an integer). Consequently, $(k', m) = (2, 3)$ is a satisfactory combination. We also recall that for all $n \in \mathbb{N}$ and for all subset E of \mathbb{R}^2 , $Q_l(E)$ denotes the space of the restrictions to E of the polynomial functions over \mathbb{R}^2 of degree $\leq l$ with respect to each variable. $\forall h \in \mathcal{H}$, let $(V_h)^2$ be the subspace of $H^3(\Omega_\nu, \mathbb{R}^2)$ of finite dimension with $(V_h)^2 \subset C^1(\overline{\Omega_\nu}, \mathbb{R}^2)$. The reference finite element is the Bogner-Fox-Schmit \mathcal{C}^2 rectangle (cf. [12]). It is defined as the following triplet (K, P_K, Σ_K) :

- Let $b_{00} = (b_{00}^1, b_{00}^2) \in \mathbb{R}^2$, $h_1, h_2 > 0$. $K \subset \Omega_\nu$ is the rectangle with vertices $b_\gamma = b_{00} + \gamma_1 h_1 \vec{e}_1 + \gamma_2 h_2 \vec{e}_2$ with $\gamma = (\gamma_1, \gamma_2) \in \mathbb{N}^2$ such that $0 \leq \gamma_1 \leq 1$ and $0 \leq \gamma_2 \leq 1$, and (\vec{e}_1, \vec{e}_2) the canonical basis of \mathbb{R}^2 .
- $P_K = Q_5(K)$.
- The set of linear mappings Σ_K is defined by: $\Sigma_K = \{v \mapsto \partial^\alpha v(b_\gamma) \mid |\alpha|_\infty \leq 2\}$, where, if $\alpha = (\alpha_1, \alpha_2)$, $|\alpha|_\infty = \max(\alpha_1, \alpha_2)$.

The number of degrees of freedom of the Bogner-Fox-Schmit rectangle of class \mathcal{C}^2 is thus equal to 36.

The basis functions are defined by $p_\alpha^\gamma(x_1, x_2) = h_1^{\alpha_1} h_2^{\alpha_2} q_{\alpha_1}^{\gamma_1} \left(\frac{x_1 - b_{00}^1}{h_1} \right) q_{\alpha_2}^{\gamma_2} \left(\frac{x_2 - b_{00}^2}{h_2} \right)$ with:

$$\begin{aligned} q_0^0(t) &= (1-t)^3(6t^2 + 3t + 1), & q_1^0(t) &= t(1-t)^3(3t + 1), & q_2^0(t) &= \frac{1}{2}t^2(1-t)^3 \\ q_0^1(t) &= t^3(6t^2 - 15t + 10), & q_1^1(t) &= t^3(1-t)(3t - 4), & q_2^1(t) &= \frac{1}{2}t^3(t-1)^2. \end{aligned}$$

We can prove that problem (3.5) is decoupled with respect to each component. Let $(v_q)_{q=1,2}$ be the components of $v \in \mathbb{H}^3(\Omega_\nu, \mathbb{R}^2)$, $((\omega_q^i)^T)_{q=1,2}$ the q^{th} row of ω_i , $\forall i \in \{1, \dots, N\}$, and $\lambda = (\lambda^q)_{q=1,2}$ with $\lambda^q \in \mathbb{R}^l$.

Problem (3.5) can therefore be stated as:

$$\left\{ \begin{array}{l} \text{Search for } (\sigma_\epsilon = (\sigma_\epsilon^q)_{q=1,2}, \lambda = (\lambda^q)_{q=1,2}) \in \mathbb{H}^3(\Omega_\nu, \mathbb{R}^2) \times \mathbb{R}^{2l} \text{ such that} \\ \sigma_\epsilon \in K, \\ \forall v = (v^q)_{q=1,2} \in \mathbb{H}^3(\Omega_\nu, \mathbb{R}^2), \\ \forall q \in \{1, 2\}, \\ \sum_{i=1}^N \langle \nabla \sigma_\epsilon^q(a_i), \nabla v^q(a_i) \rangle_2 + \epsilon (\sigma_\epsilon^q, v^q)_{3, \Omega_\nu, \mathbb{R}} + \sum_{i=1}^l \lambda_i^q v^q(b_i) = \sum_{i=1}^N \langle \nabla v^q(a_i), \omega_q^i \rangle_2. \end{array} \right. \quad (3.13)$$

We solve (3.13) in V_h for $q = 1, 2$. Let M_h be the dimension of V_h and $\{P_j^h\}_{j=1, \dots, M_h}$ be basis functions (for the sake of clarity, from now on, we use this notation for the basis functions). We denote by $(\sigma_\epsilon^{h,q})_{q=1,2}$ the approximate solution of (3.13) in $(V_h)^2$; $\sigma_\epsilon^{h,q}$ is decomposed into the basis $\{P_j^h\}_{j=1, \dots, M_h}$ as follows:

$$\left\{ \begin{array}{l} \forall q = 1, 2, \\ \exists (\alpha_j^q)_{j=1, \dots, M_h} \in \mathbb{R} \text{ such that} \\ \sigma_\epsilon^{h,q} = \sum_{j=1}^{M_h} \alpha_j^q P_j^h. \end{array} \right. \quad (3.14)$$

For $q = 1, 2$, taking successively $v^q = P_k^h$, $k = 1, \dots, M_h$ in (3.13), the studied problem becomes:

$$\left\{ \begin{array}{l} \text{Search for } \alpha^q \in \mathbb{R}^{M_h} \text{ such that} \\ \sum_{i=1}^{M_h} \alpha_i^q P_i^h(b_j) = \eta_j^q, \quad \forall j \in \{1, \dots, l\}, \\ \forall k = 1, \dots, M_h, \\ \sum_{i=1}^N \sum_{j=1}^{M_h} \alpha_j^q \langle \nabla P_j^h(a_i), \nabla P_k^h(a_i) \rangle_2 + \epsilon \sum_{j=1}^{M_h} \alpha_j^q (P_j^h, P_k^h)_{3, \Omega_\nu, \mathbb{R}} - \sum_{i=1}^N \langle \nabla P_k^h(a_i), \omega_q^i \rangle_2 \\ + \sum_{i=1}^l \lambda_i^q P_k^h(b_i) = 0. \end{array} \right. \quad (3.15)$$

The numerical problem amounts to solving two decoupled sparse linear systems of dimension $(M_h + l) \times (M_h + l)$ which can be written by means of matrices A^h , B^h and R^h ,

$$A^h = \left(\frac{\partial P_j^h}{\partial x_1}(a_i) \right)_{\substack{1 \leq i \leq N, \\ 1 \leq j \leq M_h}}, \quad B^h = \left(\frac{\partial P_j^h}{\partial x_2}(a_i) \right)_{\substack{1 \leq i \leq N, \\ 1 \leq j \leq M_h}} \in (\mathcal{M}_{N \times M_h}(\mathbb{R}))^2,$$

$$R^h = \left((P_j^h, P_i^h)_{3, \Omega_\nu, \mathbb{R}} \right)_{1 \leq i \leq M_h, 1 \leq j \leq M_h} \in \mathcal{M}_{M_h \times M_h}(\mathbb{R}).$$

Both systems are written in the following way:

$$\left\{ \begin{array}{l} ((A^h)^T A^h + (B^h)^T B^h + \epsilon R) \alpha^q + (P^h)^T \lambda^q = \xi_q, \\ \text{with } P^h \alpha^q = \eta^q, \quad \forall q \in \{1, 2\}, \end{array} \right. \quad (3.16)$$

where $P^h = \left(P_j^h(b_i) \right)_{\substack{1 \leq i \leq l, \\ 1 \leq j \leq M_h}} \in \mathcal{M}_{l \times M_h}(\mathbb{R})$ and $\xi_q = \left(\sum_{i=1}^N \langle \nabla P_k^h(a_i), \omega_q^i \rangle_2 \right)_{1 \leq k \leq M_h}$. We group the unknown α^q and λ^q in a single unknown vector, and we write the system as a matrix equation of the form:

$$\kappa^h \left\{ \begin{array}{c} \begin{array}{cc} & M_h & l \\ M_h & \left((A^h)^T A^h + (B^h)^T B^h + \epsilon R \right) & (P^h)^T \\ l & P^h & 0 \end{array} \begin{pmatrix} \alpha^q \\ \lambda^q \end{pmatrix} = \begin{pmatrix} \xi^q \\ \eta^q \end{pmatrix} \end{array} \right.$$

Remark 3.2.5

A result of convergence analogous to the one in Theorem 3.2.5 can be obtained in the discrete setting.

Remark 3.2.6

The matrix κ^h of the system is symmetric indefinite.

Remark 3.2.7

In practice, the interpolation conditions are set on the boundary nodes of the finite element mesh. In this case, we have the following result:

Proposition 3.2.8

Matrix κ^h is nonsingular.

Proof: For the sake of clarity, we denote by C^h the matrix $C^h = (A^h)^T A^h + (B^h)^T B^h + \epsilon R$. The proof is based on Lemma 16.1 of [33] that states that if Z is a basis for the null space of P^h and if the reduced Hessian $Z^T C^h Z$ is positive definite and $(P^h)^T$ has full rank, then κ^h is nonsingular.

As the interpolation conditions are set on the boundary of the finite element mesh, the columns of $(P^h)^T$ are made of l independent vectors of the canonical basis of \mathbb{R}^{M_h} , so $(P^h)^T$ has full rank. More precisely, if the column of index p of $(P^h)^T$ denoted by $(P^h)_p^T$ is related to node $q(p)$ of the finite element mesh, one has: $(P^h)_{j,p}^T = \begin{cases} 1 & \text{if } j = 9(q-1) + 1, \\ 0 & \text{otherwise} \end{cases}, j \in \{1, \dots, M_h\}$.

The columns (Z_1, \dots, Z_{M_h-l}) of Z are thus made of the $M_h - l$ (independent) vectors of the canonical basis of \mathbb{R}^{M_h} orthogonal to the columns of $(P^h)^T$.

The matrix C^h is semi-positive definite. Indeed, $\forall \alpha \in \mathbb{R}^{M_h}, \alpha^T C^h \alpha = a(v^h, v^h) \geq 0$ with $v^h = \sum_{j=1}^{M_h} \alpha_j P_j^h$. From what was previously done, the quantity $a(v^h, v^h)$ vanishes when v^h is a constant c_1 , which corresponds to $\alpha = (\alpha_j)_{j=1}^{M_h}$ such that $\alpha_j = \begin{cases} c_1 & \text{if } j = 1 + 9s, s \in \{0, \dots, \frac{M_h}{9} - 1\}, \\ 0 & \text{otherwise} \end{cases}$.

In particular, the vector $\xi \in \mathbb{R}^{M_h}$ defined by $\xi_j = \begin{cases} 1 & \text{if } j = 1 + 9s, s \in \{0, \dots, \frac{M_h}{9} - 1\}, \\ 0 & \text{otherwise} \end{cases}$ is not spanned by (Z_1, \dots, Z_{M_h-l}) .

Let us now take $X \in \mathbb{R}^{M_h-l} \setminus \{0_{\mathbb{R}^{M_h-l}}\}$. It is clear that $ZX \notin \text{span}(\xi)$ so $X^T Z^T C^h Z X > 0$, which achieves the proof. \blacksquare

A large variety of methods can be found in the literature to solve the considered linear systems: null-space methods ([17], [3]), direct solvers ([9]), the classical Uzawa algorithm ([4]), the inexact Uzawa algorithm ([16]), splitting schemes ([15]), augmented Lagrangian approach ([18]). In our application, we use the diagonal pivoting method due to Bunch and Parlett ([9]) which computes a permutation P such that $PAP^T = LDL^T$ - when solving a linear system whose symmetric definite matrix is A , where D is a direct sum of 1 by 1 and 2 by 2 pivot blocks and L is unit lower triangular (see also [19]). P is chosen so that the entries in the unit lower triangular L satisfy $|l_{ij}| \leq 1$. This factorization involves $\frac{n^3}{3}$ flops and once computed can be used to solve $Ax = b$ with $\mathcal{O}(n^2)$ work.

Remark 3.2.9

Extension of the algorithm to the 3D case

The main brake to the straight extension of the model to 3D is the phase of identification of subdomains (in practice small cubes) where the computations need to be done. (In 2D, visual inspection suffices to determine these regions). The semi-automation of this process, based on segmentation techniques, is a project in progress. The idea is to work with the 3D images of the discrete Jacobians and to partition the images into two smooth regions: a region for which the discrete Jacobians are greater than a defined threshold and a region for which they are lower (region that thus needs to be processed). This binary partition of the data can be performed using a Chan-Vese like ([10]) segmentation criterion in a level set framework. This step is done for each discrete Jacobian. The regions to be processed are thus localized and are embedded in cubes. The derivation of the topology-preserving conditions in the 3D case is quite analogous to the 2D case. We impose that the 8 corner Jacobians are positive (see [25] for justifications). The Jacobian $J_\alpha(x, y, z)$ is now a polynomial of degree 3 in α but the method, as in the 2D case, amounts to studying the roots of polynomials, here of degree 3. The theoretical results in the reconstruction stage hold in three dimensions. The numerical problem consists in solving three decoupled sparse linear systems of dimension $(M_h + l) \times (M_h + l)$ but this time there are 3^3 basis functions per node so $M_h = \dim V_h = 3^3 \times \text{number of mesh nodes}$. The basis functions are still obtained by tensor product from the 1D case and the system matrix structure is the same, except that the block (1,1) is of the form $(A^h)^T A^h + (B^h)^T B^h + (C^h)^T C^h + \epsilon R$, with $C_h = \left(\frac{\partial P_j^h}{\partial x_3}(a_i) \right)_{\substack{1 \leq i \leq N, \\ 1 \leq j \leq M_h}}$. The optimization computational tools are the same as the ones in Section 3.3. Some very preliminary experiments have been made on cubes of size $36 \times 36 \times 36$ and the computational time decreases to 23 seconds.

3.3 Numerical experiments

In the sequel, we provide numerical simulations. Classically, in the D^m -spline setting, parameter ϵ balancing the semi-norm is set to 10^{-6} . (There also exist methods for an automatic choice of ϵ mainly based on statistical considerations as the generalized cross-validation and the generalized maximum likelihood methods (see [13] and [20])). From our experience, we have realized that it suffices to fix the value ϵ in a neighborhood of 10^{-6} to produce satisfactory results. Besides, the method proves to be not too sensitive to the choice of this parameter. That is why we did not resort to the generalized cross-validation method to set parameter ϵ . Owing to the fact that the proposed algorithm calls basic linear algebra functions such that transposing matrices, summing matrices, multiplying matrices or solving linear systems, it appeared relevant to use LAPACK and Basic Linear Algebra Subprogram routines (official websites: <http://www.netlib.org/blas/> and <http://www.netlib.org/lapack/>). BLAS is a corpus of routines that provides standard building blocks for performing basic vector and matrix operations. LAPACK (designed at the outset to exploit BLAS routines) provides routines for solving systems of linear equations among others. For each subdomain Ω_ν , $\nu \in \{1, \dots, \mathcal{N}\}$, we obtain two disconnected linear systems to be solved with the same matrix. Our resorting to BLAS/LAPACK thus seems apposite. We particularly focused on the *dsysv* function provided by the software package LAPACK which computes the solution of a real

system of linear equations $AX = B$ (where A is an N -by- N symmetric matrix and X and B are N -by- $NRHS$ matrices) using the diagonal pivoting method. Also, we capitalized on the *dgemm* routine to perform matrix-matrix operations. The computations on each subdomain Ω_ν being independent, the use of OpenMP appeared relevant. The OpenMP Application Program Interface supports multi-platform shared-memory programming in C/C++ and Fortran on all architectures (see the official website <http://openmp.org/wp/>). In the sequel, the `OMP_NUM_THREADS` environment variable sets the number of threads that the program uses. The `MKL_NUM_THREAD` environment variable enables to MKL threading inside the threading of the application. For our configuration, the maximal number of threads is equal to 12.

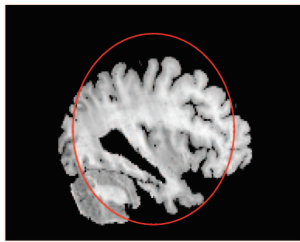
Experiment	Number of regions exhibiting overlaps	OMP_NUM_THREADS	MKL_NUM_THREADS	Computation time	Depleting factor
Slice of the brain 1. Size 120×190	2 regions: Size 30×30 & Size 80×40	2	6	0.63 s	80
Slice of the brain 2. Size 61×81	2 regions: Size 53×61 & Size 21×61	2	6	0.66 s	4
Disks. Size 100×100	2 regions: Size 50×50 & Size 50×50	2	6	0.52 s	6.9

Table 3.1: Summary of the various parameters involved in the experiments.

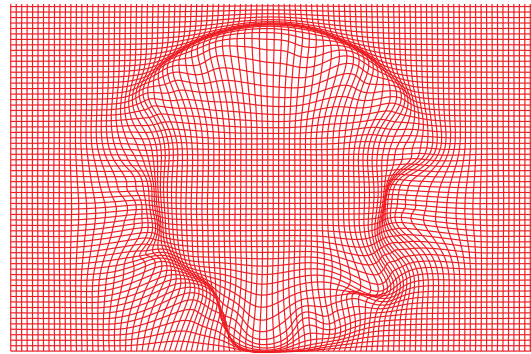
3.3.1 First example : a slice of the brain

In the first application, the goal is to map a disk to a slice of the brain (courtesy of the Laboratory of Neuro-Imaging, School of Medicine, University of California) defined on the same image domain (size 120×190), while preserving topology (see Fig. 3.5 (a)). In this example, we only aim to align the shapes, *i.e.* the contour of the slice of brain with the boundary of the disk (whatever the genus of the shapes is).

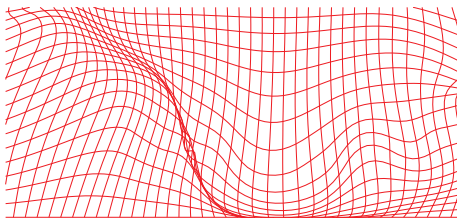
When applying the combined segmentation/registration model developed in [27] without re-gridding steps, we obtain a deformation field exhibiting two regions with overlaps as depicted in Fig. 3.5 (b)–(d). If we merely apply the method developed in [26] (which consists in applying the correction/reconstruction algorithm on the whole image domain with global condition on the deformation component means), the execution time reaches 50.9 seconds. By applying our proposed method, the computational time drops to 0.63 second, which means a depletion by a factor 80. We display the obtained topology-preserving deformation fields together with the values of the discrete Jacobians in Fig. 3.6.



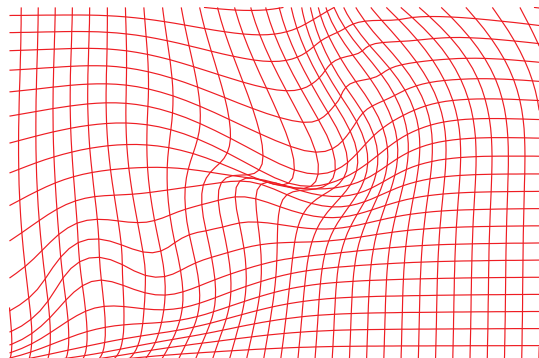
(a) Reference image and boundary (in red) of the disk constituting the Template image.



(b) Obtained global deformation field when topology preservation is not enforced.

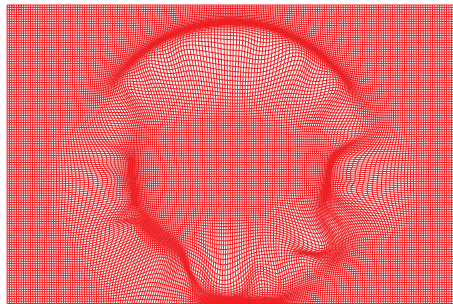


(c) Zoom on the first region exhibiting overlaps.

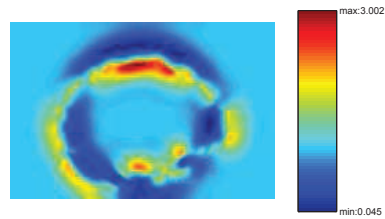


(d) Zoom on the second region exhibiting overlaps.

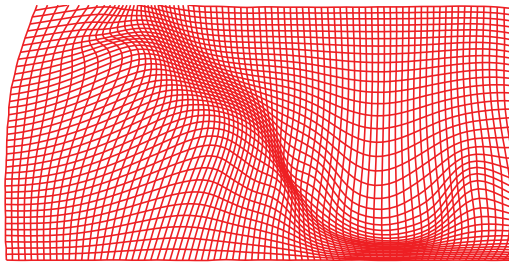
Figure 3.5: Example of the slice of the brain: obtained uncorrected deformation field.



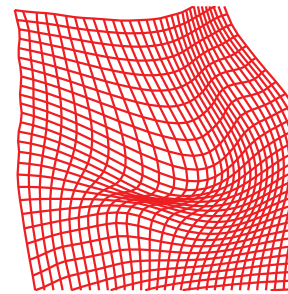
(a) Global obtained deformation field.



(b) Jacobian determinant of the obtained deformation field.



(c) Zoom on the corrected first region:
 $\min(J_{ff}) = 0.20$, $\min(J_{fb}) = 0.21$,
 $\min(J_{bf}) = 0.17$ and $\min(J_{bb}) = 0.19$.



(d) Zoom on the corrected second region:
 $\min(J_{ff}) = 0.13$,
 $\min(J_{fb}) = 0.19$,
 $\min(J_{bf}) = 0.21$ and
 $\min(J_{bb}) = 0.23$.

Figure 3.6: Example of the slice of the brain: obtained orientation-preserving deformation field.

3.3.2 Second example : brain mapping

A second example still dedicated to brain mapping (courtesy of the Laboratory of Neuro-Imaging, School of Medicine, University of California) is given in Fig. 3.7, demonstrating the ability of the method to handle high-magnitude deformations. The goal is to register a disk to the outer boundary of the brain, both defined on the same image domain of size 61×81 , while maintaining topology. When applying the combined segmentation/registration model developed in [27] without regriding steps, we obtain a deformation field exhibiting two regions with overlaps as depicted in Fig. 3.7.

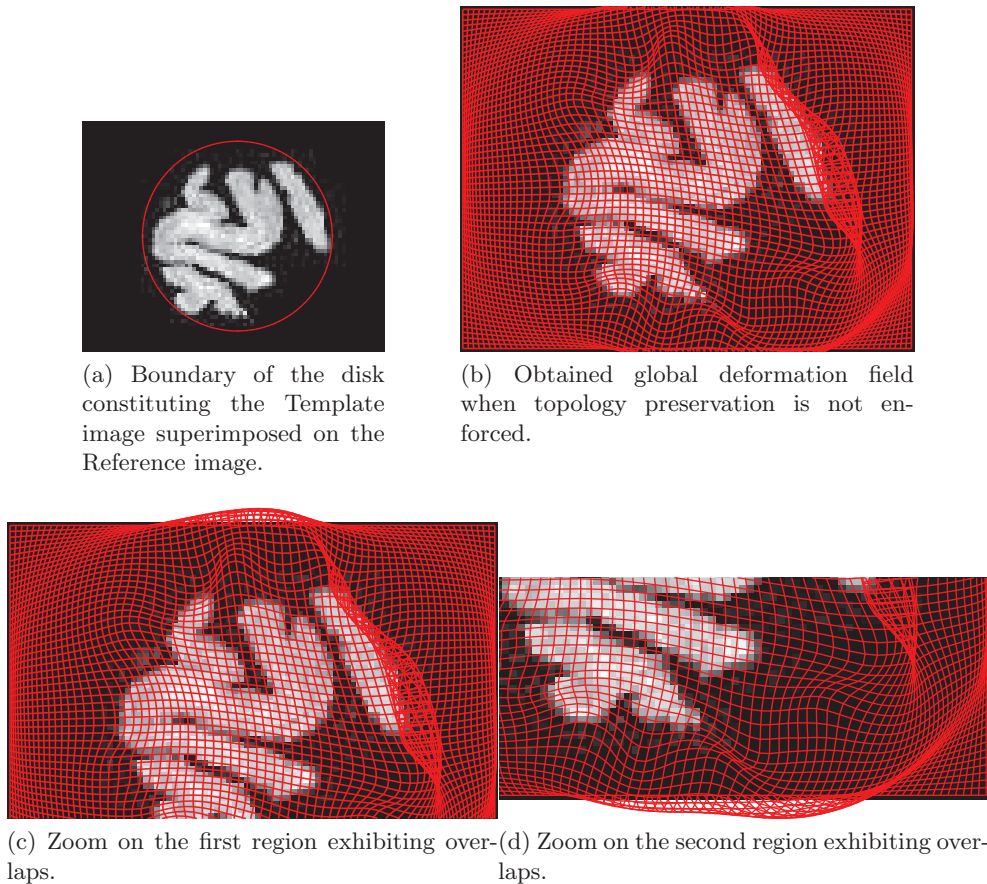


Figure 3.7: Example of the slice of the brain with large deformations: obtained uncorrected deformation field.

Applying the algorithm developed in [26] on the whole image domain yields a computational time of 2.62 seconds. By comparison, when the proposed algorithm is applied simultaneously on the two regions depicted in Fig. 3.7(c) and Fig. 3.7(d) (respectively of size 53×61 and 21×61), the computational time drops to 0.66 second, which means a depletion by a factor 4. We display the obtained topology-preserving deformation field together with the values of the discrete Jacobians in Fig. 3.8. With Christensen *et al.*'s regriding technique ([11]) (in the spirit of our methodology, we compared what was comparable, namely the topology-preserving

method: we applied Christensen *et al.*'s regriding technique within the registration model [26]), 3 regriding steps were necessary: the transformation was considered as admissible if the Jacobian exceeded 0.075. Unfortunately, at the end of the process, the minimum of the Jacobian of the transformation is equal to -0.5288 and overlaps are still visible on the grid (see Fig. 3.8) (d).

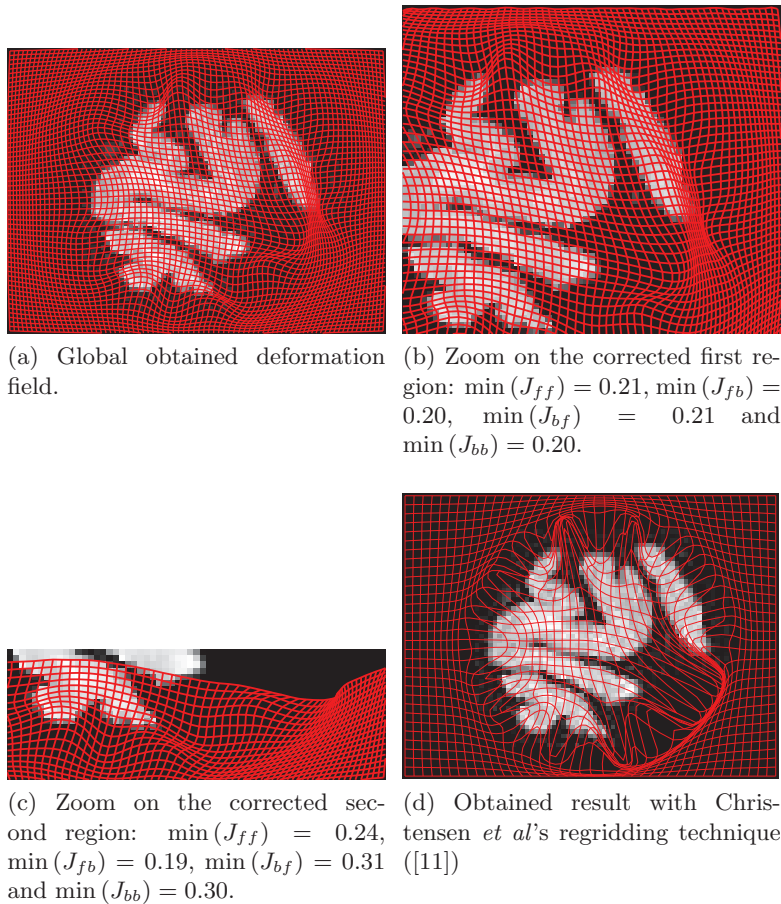
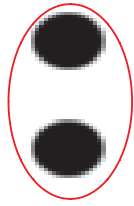


Figure 3.8: Example of the slice of the brain with large deformations: obtained orientation-preserving deformation field.

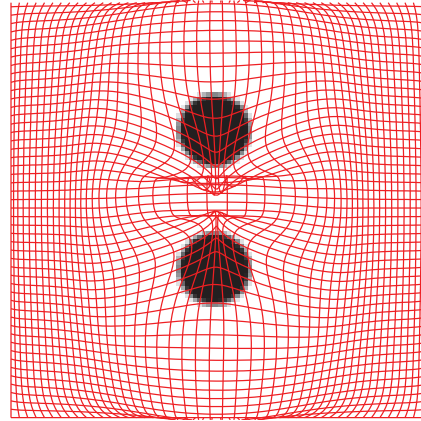
3.3.3 Third example: the disks

Another application involving large deformations is provided in Fig. 3.9 and is similar to an application given in [27] in the case of topology-preserving segmentation. The synthetic Reference image represents two disks. The Template image, which is defined on the same image domain (100×100), is made of a black ellipse such that when superimposed on the Reference image its boundary encloses the two disks (see Fig. 3.9 (a)). The application of the combined segmentation-registration process alone yields to two regions exhibiting overlaps (Fig. 3.9(b)): the upper part of the image including the upper disk (size 50×50) and the lower part of the image containing the lower disk (size 50×50). We thus propose to apply

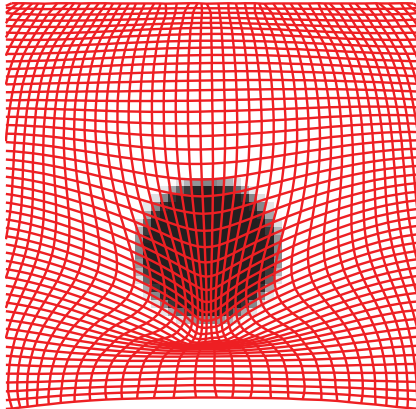
our proposed algorithm on each region independently. The computational time drops to 0.52 second, which means a depletion by a factor 6.9 in comparison to the computational time inherent to the application of the method [26] on the whole domain. We display the obtained topology-preserving deformation fields together with the values of the discrete Jacobians in Fig. 3.9 (c) and Fig. 3.9 (d).



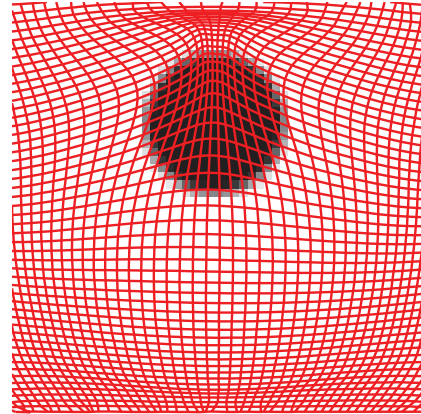
(a) Reference image and boundary of the ellipse constituting the Template image superimposed.



(b) Obtained global deformation field when topology preservation is not enforced.



(c) Corrected first region: $\min(J_{ff}) = 0.06$, $\min(J_{fb}) = 0.08$, $\min(J_{bf}) = 0.09$ and $\min(J_{bb}) = 0.11$.



(d) Corrected second region: $\min(J_{ff}) = 0.33$, $\min(J_{fb}) = 0.31$, $\min(J_{bf}) = 0.35$ and $\min(J_{bb}) = 0.29$.

Figure 3.9: Example of the disks.

- [1] R. A. ADAMS, *Sobolev Spaces*, Academic, Boston, MA, 1975.
- [2] R. ARCANGÉLI, M. C. LÓPEZ DE SILANES, AND J. J. TORRENS, *Multidimensional minimizing splines. Theory and applications*, Grenoble Sciences, Kluwer Academic Publishers, Boston, MA, 2004.
- [3] M. ARIOLI AND L. BALDINI, *A backward error analysis of a null space algorithm in sparse quadratic programming*, SIAM J. Matrix Anal. Appl., 23 (2001), pp. 425–442.
- [4] K. ARROW, L. HURWICZ, AND H. UZAWA, *Studies in Nonlinear Programming*, Stanford University Press, Stanford, 1958.
- [5] J. ASHBURNER, J. L. R. ANDERSSON, AND K. J. FRISTON, *High-dimensional image registration using symmetric priors*, Neuroimage, 9 (1999), pp. 619–628.
- [6] J. ASHBURNER AND K. J. FRISTON, *Voxel-based morphometry: the methods*, Neuroimage, 11 (2000), pp. 805–821.
- [7] J. ASHBURNER, P. NEELIN, D. L. COLLINS, A. EVANS, AND K. J. FRISTON, *Incorporating prior knowledge into image registration*, Neuroimage, 6 (1997), pp. 344–352.
- [8] H. BREZIS, *Analyse fonctionnelle. Théorie et Applications*, Dunod, Paris, 2005.
- [9] J. R. BUNCH AND B. N. PARLETT, *Direct methods for solving symmetric indefinite systems of linear equations*, SIAM J. Numer. Anal., 8 (1971), pp. 639–655.
- [10] T. CHAN AND L. VESE, *Active Contours Without Edges*, IEEE Trans. Image Process., 10 (2001), pp. 266–277.
- [11] G. E. CHRISTENSEN, R. D. RABITT, AND M. I. MILLER, *Deformable templates using large deformation kinematics*, IEEE Trans. Imag. Process., 10 (1996), pp. 1435–1447.
- [12] P. G. CIARLET, *The Finite Element Method for Elliptic Problems*, North Holland, Amsterdam, The Netherlands, 1978.
- [13] P. CRAVEN AND G. WAHBA, *Smoothing noisy data with spline functions*, Numer. Math., 31 (1979), pp. 377–403.

- [14] M. DROSKE AND M. RUMPF, *A Variational Approach to Non-Rigid Morphological Registration*, SIAM J. Appl. Math., 64 (2004), pp. 668–687.
- [15] N. DYN AND W. E. FERGUSON, *The numerical solution of equality-constrained quadratic programming problems*, Math. Comp., 41 (1983), pp. 165–170.
- [16] H. C. ELMAN AND G. H. GOLUB, *Inexact and preconditioned Uzawa algorithms for saddle point problems*, SIAM J. Numer. Anal., 31 (1994), pp. 1645–1661.
- [17] R. FLETCHER AND T. JOHNSON, *On the Stability of Null-Space Methods for KKT Systems*, tech. rep., University of Dundee, Department of Mathematics and Computer Science, Dundee, UK, 1995.
- [18] G. H. GOLUB AND C. GREIF, *On solving block-structured indefinite linear systems*, SIAM J. Sci. Comput., 24 (2003), pp. 2076–2092.
- [19] G. H. GOLUB AND C. F. VAN LOAN, *Matrix Computations*, 4th edition, Johns Hopkins University Press, Baltimore, 2013.
- [20] C. GU AND G. WAHBA, *Minimizing GCV/GML scores with multiple smoothing parameters via the newton method*, SIAM J. Sci. Stat. Comp., 12 (1991), pp. 383–398.
- [21] E. HABER AND J. MODERSITZKI, *Numerical methods for volume preserving image registration*, Inverse Probl., 20 (2004), pp. 1621–1638.
- [22] ———, *Image registration method with guaranteed displacement regularity*, Int. J. Comput. Vision, 71 (2007), pp. 361–372.
- [23] X. HAN, C. XU, U. BRAGA-NETO, AND J. L. PRINCE, *Topology correction in brain cortex segmentation using a multiscale, graph-based algorithm*, IEEE Trans. Med. Imag., 21 (2002), pp. 109–121.
- [24] ———, *A topology preserving geometric deformable model and its application in brain cortical surface reconstruction*, in Geometric Level Set Methods in Imaging, Vis., Graph., Stanley Osher and Nikos Paragios, Eds., New York: Springer-Verlag, 2003.
- [25] B. KARAÇALI AND C. DAVATZIKOS, *Estimating topology preserving and smooth displacement fields*, IEEE Trans. Med. Imag., 23 (2004), pp. 868–880.
- [26] C. LE GUYADER, D. APPRATO, AND C. GOUT, *On the construction of topology-preserving deformation fields*, IEEE Transactions on Image Processing, 21 (2012), pp. 1587–1599.
- [27] C. LE GUYADER AND L. VESE, *A combined segmentation and registration framework with a nonlinear elasticity smoother*, Computer Vision and Image Understanding, 115 (2011), pp. 1689–1709.
- [28] J. MODERSITZKI, *Numerical Methods for Image Registration*, Oxford University Press, 2004.
- [29] ———, *FAIR: Flexible Algorithms for Image Registration*, Society for Industrial and Applied Mathematics (SIAM), 2009.

- [30] O. MUSSE, F. HEITZ, AND J.-P. ARMSPACH, *Topology preserving deformable image matching using constrained hierarchical parametric models*, IEEE Trans. Image Process., 10 (2001), pp. 1081–1093.
- [31] J. NEČAS, *Les méthodes directes en théorie des équations elliptiques*, Masson, Paris, 1967.
- [32] V. NOBLET, C. HEINRICH, F. HEITZ, AND J.-P. ARMSPACH, *3-D deformable image registration: a topology preservation scheme based on hierarchical deformation models and interval analysis optimization*, IEEE Trans. Image Process., 14 (2005), pp. 553–566.
- [33] J. NOCEDAL AND S. J. WRIGHT, *Numerical Optimization*, Springer, New York, 1999.
- [34] I. YANOVSKY, P. M. THOMPSON, S. OSHER, AND A. D. LEOW, *Topology preserving log-unbiased nonlinear image registration: Theory and implementation*, in Proc. IEEE Conf. Comput. Vis. Pattern Recognit., 2007, pp. 1–8.

CHAPTER 4

JOINT SEGMENTATION/REGISTRATION MODEL BY SHAPE ALIGNMENT VIA WEIGHTED TOTAL VARIATION MINIMIZATION AND NONLINEAR ELASTICITY

This work falls within the scope of joint segmentation-registration using nonlinear elasticity principles. We introduce a variational model combining a measure of dissimilarity based on weighted total variation and a regularizer based on the stored energy function of a Saint Venant-Kirchhoff material. Adding a weighted total variation based criterion enables us to align the edges of the objects even if the modalities are different.

We derive a relaxed problem associated to the initial one for which we are able to provide a result of existence of minimizers. A description and analysis of a numerical method of resolution based on a decoupling principle is then provided including a theoretical result of Γ -convergence. Applications on academic and biological images are provided.

Introduction

In [40], Sotiras *et al.* provide an overview of the different existing registration methods. According to the authors, an image registration algorithm consists of three main components:

1. a deformation model,
 - geometric transformations derived from physical models,
 - geometric transformations derived from interpolation theory,
 - and knowledge-based geometric transformations,
2. an objective function,
 - geometric methods: the criterion takes into account landmark information ([14]),
 - iconic methods: it concerns intensity-based methods ([19]), attribute-based methods ([39]), information-theoretic approaches ([44]),
 - and hybrid methods.
3. and an optimization method,

- continuous methods: gradient descent ([3]), conjugate gradient ([31]), Quasi-Newton ([43]), stochastic gradient descent methods ([44])...
- discrete methods: graph-based ([41]), belief propagation, linear programming methods,
- greedy approaches and evolutionary algorithms.

Our method falls within the scope of geometric transformations derived from physical models in particular from nonlinear elasticity based regularization and the iconic methods since we introduce an intensity-based criterion as well as a shape-based criterion. The chosen optimization method is incorporated within the framework of the continuous model since we use a gradient descent method.

The scope of the proposed work is first to devise a theoretically well-motivated registration model in a variational formulation, authorizing large and smooth deformations. In addition, to handle a large class of images, we propose defining a geometric dissimilarity measure based on shape comparisons. This work follows on from that of Derfoul and Le Guyader in [19] in which basic similarity measures are incorporated and a Saint Venant-Kirchhoff like stored energy function is considered. It enriches [19] by treating simultaneously the question of segmentation and registration, by involving new mathematical tools and by broadening the class of considered images. The mathematical treatment proposed in this work introduces the weighted total variation, entailing substantial modifications in the mathematical proofs and in the design of the algorithm. In [19], theoretical results such as the explicit expression of the quasiconvex envelop of this modified Saint Venant-Kirchhoff stored energy function are established as well as a Γ -convergence result.

Thus in addition to devising a theoretically well-motivated registration model, we also design an original dissimilarity measure based on segmentation principles (more precisely, on the weighted total variation stemming from Bresson et al.'s unified active contour model ([6])), unlike classical measures such as intensity-based measures or mutual-information-based techniques. Registration is thus jointly performed with segmentation, which means that the algorithm produces both a smooth mapping between the two shapes, and the segmentation of the object contained in the Reference image. Prior related works (different from the proposed approach) suggest to jointly treat segmentation and registration: [45] in which a curve evolution approach is retained, formulated in a level set framework, [42] in which the authors propose a coupled PDE model to perform both segmentation and registration by evolving the level sets of the source image, [27] in which the model combines a matching criterion founded on the active contours without edges ([11]) and a nonlinear elasticity-based regularizer, [29], model based on metric structure comparisons, or more recently [23].

To summarize, the novelty of the proposed work rests upon:

- (i) an original modelling based on the stored energy function of a Saint Venant-Kirchhoff material (isotropic, homogeneous, hyperelastic material) and on the weighted total variation. Note that rubber, filled elastomers, biological tissues are often modeled within the hyperelastic material, which motivates our modelling,
- (ii) the introduction of a relaxed problem for which we can provide theoretical results,
- (iii) the introduction of an original numerical method of resolution based on the dual formulation of the weighted total variation and on a decoupling principle with a result of Γ -convergence.

4.1 Mathematical Modelling

4.1.1 General mathematical background

Let us denote by

- Ω a connected bounded open subset of \mathbb{R}^2 with boundary $\partial\Omega$ of class \mathcal{C}^1 ,
- $R : \bar{\Omega} \rightarrow \mathbb{R}$, the Reference image,
- $T : \bar{\Omega} \rightarrow \mathbb{R}$, the Template image assumed to be compactly supported and Lipschitz continuous (we denote by k_T the Lipschitz constant),
- $\varphi : \bar{\Omega} \rightarrow \mathbb{R}^2$ the sought deformation with prescribed values on the boundary: $\varphi = \text{Id}$ on $\partial\Omega$.

There are forward and backward transformations: the former is done in the Lagrangian framework where a forward transformation ψ is sought and grid points x with intensity values $T(x)$ are moved and arrive at non-grid points $y = \psi(x)$ with intensity values $T(x) = T(\psi^{-1}(y))$. In the Eulerian framework (considered here), we find a backward transformation $\varphi = \psi^{-1}$ such that grid points y in the deformed image originate from non-grid points $x = \varphi(y) = \psi^{-1}(y)$ and are assigned intensity values $T(\varphi(y)) = T(\psi^{-1}(y)) = T(x)$. We thus compare a point $(y, R(y))$ with $(y, T(\psi^{-1}(y)) = T(\varphi(y)))$. We refer the reader to [24] in which both frameworks are clearly stated.

For theoretical and numerical purposes, we assume that T is compactly supported on Ω to ensure that $T \circ \varphi$ is always defined and we assume that T is Lipschitz continuous. It can thus be considered as an element of $W^{1,\infty}(\mathbb{R}^2, \mathbb{R})$. Also, R is supposed to be smooth enough. The expression smooth enough is a convenient way of saying that in a given definition, the smoothness of the involved variables or data is such that all arguments make sense.

We recall that, in the general case, if U is an open subset of \mathbb{R}^N , for $1 \leq p \leq +\infty$, the Sobolev space denoted by $W^{1,p}(U)$ consists of the functions in $L^p(U)$ whose partial derivatives up to order 1, in the sense of distributions, can be identified with functions in $L^p(U)$. In the considered case, $N = 2$, $U = \mathbb{R}^2$ and $p = \infty$ so that one has the following Sobolev embedding theorem (see [18, Theorem 2.31]):

$$0 < \lambda \leq 1 \Rightarrow W^{1,\infty}(\mathbb{R}^2) := W^{1,\infty}(\mathbb{R}^2, \mathbb{R}) \circlearrowleft \mathcal{C}_b^{0,\lambda}(\mathbb{R}^2),$$

with $\mathcal{C}_b^{0,\lambda}(\mathbb{R}^2)$ the functional space that consists of functions in

$$\mathcal{C}_b^0(\mathbb{R}^2) = \{u \in \mathcal{C}^0(\mathbb{R}^2) \mid \exists K, \|u\|_\infty \leq K\}$$

such that

$$\exists C_\lambda, \forall x, y \in \mathbb{R}^2, |u(x) - u(y)| \leq C_\lambda |x - y|^\lambda.$$

Let $\varphi : \bar{\Omega} \rightarrow \mathbb{R}^2$ be the sought transformation. (Of course, in practice, the sought transformation φ should be with values in $\bar{\Omega}$ but from a mathematical point of view, if we work with such spaces of functions we loose the structure of vector space). A deformation is a smooth enough mapping that is orientation-preserving and injective, except possibly on $\partial\Omega$. As stressed by Ciarlet ([16, p. 26]), the reason a deformation may loose its injectivity on

the boundary of Ω is that self-contact must be allowed. We also denote by u the associated displacement such that $\varphi = \text{Id} + u$. The deformation gradient is $\nabla\varphi = I + \nabla u : \bar{\Omega} \rightarrow M_2(\mathbb{R})$, the set $M_2(\mathbb{R})$ being the set of all real square matrices of order 2 identified to \mathbb{R}^4 . Thus the idea is to find a smooth deformation field φ such that the deformed Template matches the Reference.

4.1.2 Depiction of the original model

The model is phrased as a functional minimization problem whose unknown is φ . It combines a regularizer on the deformation field and a distance measure criterion. To allow large deformations, we introduce a nonlinear-elasticity-based smoother (see [16], [15] for further details), the theory of linear elasticity being unsuitable in this case since assuming small strains and the validity of Hooke's law. We propose viewing the shapes to be warped as isotropic, homogeneous, hyperelastic materials and more precisely as Saint Venant-Kirchhoff materials. Note that rubber, filled elastomers, biological tissues are often modeled within the hyperelastic framework, which motivates our modelling.

For the sake of completeness, we would like to refer the reader to previous works related to registration based on nonlinear elasticity principles. In [21], Droske and Rumpf address the issue of non-rigid registration of multi-modal image data. The matching criterion includes first order derivatives of the deformation and is complemented by a nonlinear elastic regularization based on a polyconvex stored energy function, which is different from our proposed approach. We also mention the combined segmentation/registration model introduced by Le Guyader and Vese ([27]) in which the shapes to be matched are viewed as Ciarlet-Geymonat materials, the works [3] and [30] for a variational registration method for large deformations (Large Deformation Diffeomorphic Metric Mapping - LDDMM), and refer to [36] for a much related work that also uses nonlinear elasticity regularization but implemented by the finite element method.

In [7], the authors design an hyperelastic regularizer. More precisely, they build an hyperelastic stored energy function penalizing variations of lengths and areas, and add a penalty term on the Jacobian determinant such that the energy tends to infinity as $\det \nabla\varphi$ tends to 0 and such that shrinkage and growth have the same price. The numerical implementation is based on a discretize-then-optimize strategy and the authors use a generalized Gauss-Newton scheme to compute a numerical minimizer. In our case, we add a penalty term to the Saint Venant-Kirchhoff stored energy function but we have chosen to force the Jacobian to remain close to 1.

Before depicting the mathematical material, we review some fundamental concepts and notations (see [16] for further details). We recall that the right Cauchy-Green strain tensor is defined by

$$C = \nabla\varphi^T \nabla\varphi = F^T F \in \mathcal{S}^2$$

with $\mathcal{S}^2 = \{A \in M_2(\mathbb{R}), A = A^T\}$, set of all real symmetric matrices of order 2. Physically, the right Cauchy-Green tensor can be interpreted as a quantifier of the square of local change in distances due to deformation. The Green- Saint Venant strain tensor is defined by

$$E = \frac{1}{2} (\nabla u + \nabla u^T + \nabla u^T \nabla u).$$

Associated with a given deformation φ , it is a measure of the deviation between φ and a rigid deformation. We also need the following notations: $A : B = \text{tr} A^T B$ the matrix inner product

and $\|A\| = \sqrt{A : A}$, the related matrix norm (Frobenius norm). The stored energy function of an isotropic, homogeneous, hyperelastic material, if the reference configuration is a natural state, is of the form:

$$W(F) = \widehat{W}(E) = \frac{\lambda}{2} (\operatorname{tr} E)^2 + \mu \operatorname{tr} E^2 + o(\|E\|^2), \quad F^T F = I + 2E, \quad (4.1)$$

with I the identity matrix. The stored energy function of a Saint Venant-Kirchhoff material is the simplest one that agrees with expansion (4.1). It is defined by

$$W_{SVK}(F) = \widehat{W}(E) = \frac{\lambda}{2} (\operatorname{tr} E)^2 + \mu \operatorname{tr} E^2.$$

To ensure that the distribution of the deformation Jacobian determinants does not exhibit contractions or expansions that are too large, we complement the stored energy function $W_{SVK}(F)$ by the term $\mu (\det F - 1)^2$ controlling that the Jacobian determinant remains close to 1. The weighting of the determinant component by parameter μ is justified in the proof of Proposition 4.1.3. Therefore, the regularization can be written as:

$$W(F) = W_{SVK}(F) + \mu (\det F - 1)^2.$$

The regularizer on the deformation φ is complemented by a dissimilarity measure based on the unified active contour model developed by Bresson *et al.* ([6] - designed to overcome the limitation of local minima and to deal with global minimum-) and more precisely, on the unification of the Rudin-Osher-Fatemi model for image restoration ([38]) and the active contour model ([8]).

To this purpose, let $g : \mathbb{R}^+ \rightarrow \mathbb{R}^+$ be an edge detector function satisfying

- $g(0) = 1$,
- g strictly decreasing,
- and $\lim_{r \rightarrow +\infty} g(r) = 0$.

We apply the edge detector function to the norm of the Reference image gradient: $g(|\nabla R|)$ with $|\nabla R| : \Omega \rightarrow \mathbb{R}^+$. From now on, for the sake of conciseness, we set $g := g(|\nabla R|)$ so that $g : \Omega \rightarrow \mathbb{R}^+$, and for theoretical purposes, we assume that $\exists c > 0$ such that $0 < c < g$ and that g is Lipschitz continuous. We then use the generalization of the notion of function of bounded variation to the setting of BV -spaces associated with a Muckenhoupt's weight function depicted in [2]. We follow Baldi's arguments and notations to define the weighted BV -space related to weight g . As noticed by Baldi, the following definition coincides with the BV functions defined in [4].

For a general weight w , some hypotheses are required. More precisely, Ω_0 being a neighborhood of Ω , the positive weight $w \in L^1_{loc}(\Omega_0)$ is assumed to belong to the global Muckenhoupt's $A_1 = A_1(\Omega)$ class of weight functions, i.e., w satisfies the condition:

$$C w(x) \geq \frac{1}{|B(x, r)|} \int_{B(x, r)} w(y) dy \quad \text{a.e.} \quad (4.2)$$

in any ball $B(x, r) \subset \Omega_0$. Now, denoting by A_1^* the class of weight $w \in A_1$, w lower semi-continuous (lsc) and that satisfy condition (4.2) pointwise, the definition of the weighted BV -space related to weight w is given by:

Definition 4.1.1 ([2, Definition 2])

Let w be a weight function in the class A_1^* . We denote by $BV(\Omega, w)$ the set of functions $u \in L^1(\Omega, w)$ (set of functions that are integrable with respect to the measure $w(x) dx$) such that:

$$\sup \left\{ \int_{\Omega} u \operatorname{div}(\varphi) dx : |\varphi| \leq w \text{ everywhere, } \varphi \in \operatorname{Lip}_0(\Omega, \mathbb{R}^2) \right\} < \infty, \quad (4.3)$$

with $\operatorname{Lip}_0(\Omega, \mathbb{R}^2)$ the space of Lipschitz continuous functions with compact support. We denote by $\operatorname{var}_w u$ the quantity (4.3).

Due to the properties of function g (it is obviously L^1 , continuous and it suffices to set $C = \frac{1}{c}$ to satisfy (4.2) pointwise) that enable us to define the weighted BV -space, $BV(\Omega, g)$, and equipped with the above notations, we propose introducing as dissimilarity measure the following functional:

$$W_{fid}(\varphi) = \operatorname{var}_g T \circ \varphi + \frac{\nu}{2} \int_{\Omega} (T \circ \varphi - R)^2 dx. \quad (4.4)$$

(We justify in the sequel that the function $T \circ \varphi$ belongs to $BV(\Omega, g)$).

Adding the term $\operatorname{var}_g T \circ \varphi$ enables us to consider a larger class of images and to compare shapes (alignment of level curves) rather than intensities. We recall that if v is a characteristic function, 1_{Ω_c} , of a closed set $\Omega_c \subset \Omega$ with \mathcal{C} the boundary of Ω_c ,

$$\operatorname{var}_g(v = 1_{\Omega_c}) = \int_{\mathcal{C}} g ds.$$

The term $\int_{\mathcal{C}} g ds$ is a new definition of the curve length with a metric that depends on the Reference image content. We thus aim to locate the curve \mathcal{C} where g is close to zero, that is, on the boundary of the shape contained in the Reference image. In the end, the global minimization problem (P) is stated by:

$$\begin{aligned} \inf \left\{ I(\varphi) = \operatorname{var}_g T \circ \varphi + \int_{\Omega} f(x, \varphi(x), \nabla \varphi(x)) dx \right. \\ \left. = \operatorname{var}_g T \circ \varphi + \int_{\Omega} \left[\frac{\nu}{2} (T(\varphi) - R)^2 + W(\nabla \varphi(x)) \right] dx \right\}, \end{aligned} \quad (P)$$

with $\varphi \in \operatorname{Id} + W_0^{1,4}(\Omega, \mathbb{R}^2)$ and $f(x, \varphi, \xi) = \frac{\nu}{2} (T(\varphi) - R)^2 + W_{SVK}(\xi) + \mu (\det \xi - 1)^2 = \frac{\nu}{2} (T(\varphi) - R)^2 + W(\xi)$. Also, $\varphi \in \operatorname{Id} + W_0^{1,4}(\Omega, \mathbb{R}^2)$ means that $\varphi = \operatorname{Id}$ on $\partial\Omega$ and $\varphi \in W^{1,4}(\Omega, \mathbb{R}^2)$. $W^{1,4}(\Omega, \mathbb{R}^2)$ denotes the Sobolev space of functions $\varphi \in L^4(\Omega, \mathbb{R}^2)$ with distributional derivatives up to order 1 which also belong to $L^4(\Omega)$. Note that from generalized Hölder's inequality, if $\varphi \in W^{1,4}(\Omega, \mathbb{R}^2)$, then $\det \nabla \varphi \in L^2(\Omega)$. It is clear later that $W^{1,4}(\Omega, \mathbb{R}^2)$ is a suitable functional space for the considered problem. Now we justify that $\operatorname{var}_g T \circ \varphi$ is well-defined. In [1], Ambrosio and Dal Maso prove a general chain rule for the distribution derivatives of the composite function $v(x) = f(u(x))$, where $u : \mathbb{R}^n \rightarrow \mathbb{R}^m$ has bounded variation and $f : \mathbb{R}^m \rightarrow \mathbb{R}^k$ is Lipschitz continuous. A simpler result is given when $u \in W^{1,p}(\Omega, \mathbb{R}^m)$ for some p , $1 \leq p \leq +\infty$ as follows:

Corollary 4.1.1 ([1, Corollary 3.2])

Let $p \in [1, +\infty]$, $u \in W^{1,p}(\Omega, \mathbb{R}^m)$ (open set $\Omega \subset \mathbb{R}^n$) and let $f : \mathbb{R}^m \rightarrow \mathbb{R}^k$ be a Lipschitz continuous function such that $f(0) = 0$. Then $v = f(u)$ belongs to $W^{1,p}(\Omega, \mathbb{R}^k)$, for almost every $x \in \Omega$ the restriction of f to the affine space

$$T_x^u = \{y \in \mathbb{R}^m : y = u(x) + \langle \nabla u(x), z \rangle \text{ for some } z \in \mathbb{R}^n\}$$

is differentiable at $u(x)$ and,

$$\nabla v = \nabla(f|_{T_x^u})(u) \nabla u \text{ a.e. in } \Omega.$$

Assuming $T(0) = 0$, it follows that $T \circ \varphi \in W^{1,4}(\Omega) := W^{1,4}(\Omega, \mathbb{R}) \subset BV(\Omega)$. As $g \leq w^*$ with $w^* = 1$, $BV(\Omega) \subset BV(\Omega, g)$ and $T \circ \varphi \in BV(\Omega, g)$.

4.1.3 Mathematical obstacle and derivation of a relaxed problem

We start by expressing the main technical difficulty related to this problem that led us to introduce a relaxed problem related to (P) . It is this relaxed problem that is then studied throughout the chapter.

Proposition 4.1.2

Function f is not quasiconvex (see [17, Chapter 9] for a complete review of this notion).

Proof: The proof is based on the argument that the stored energy function W is not rank-1 convex and consequently neither quasiconvex, nor polyconvex. To prove this statement, a technique similar to the one applied by Raoult in [37] to demonstrate that the stored energy function of a Saint Venant-Kirchhoff material is not rank-1 convex is employed. The Saint Venant-Kirchhoff stored energy function reads equivalently

$$W_{SVK}(\xi) = \frac{\lambda}{8} (\|\xi\|^2 - 2)^2 + \frac{\mu}{4} \|\xi^T \xi - I\|^2.$$

The characteristic polynomial of $\xi^T \xi$ is defined by

$$\chi_{\xi^T \xi}(X) = X^2 - \text{tr}(\xi^T \xi) X + \det \xi^T \xi$$

and using Cayley-Hamilton theorem, it can be proved that

$$(\det \xi)^2 = \frac{1}{2} \|\xi\|^4 - \frac{1}{2} \|\xi^T \xi\|^2.$$

After some intermediate computations, one then has:

$$W(\xi) = \frac{\lambda + 2\mu}{8} \|\xi\|^4 - \frac{\lambda + \mu}{2} \|\xi\|^2 + \Phi(\det \xi) + \frac{\lambda + \mu}{2}$$

with Φ the convex mapping defined by $\Phi : s \mapsto \frac{\mu}{2} s^2 - 2\mu s + \mu$. For the sake of simplicity, we set: $W(\xi) = a_1 \|\xi\|^4 + a_2 \|\xi\|^2 + \Phi(\det \xi) + \frac{\lambda + \mu}{2}$ with $a_1 > 0$ and $a_2 < 0$.

We argue by contradiction and assume that W is rank-one convex. Let us set $\xi = \varepsilon I$ and $\xi' = \varepsilon \text{diag}(1, 3)$ with $\varepsilon > 0$. Obviously, $\text{rank}(\xi - \xi') = 1$ and according to the

hypothesis of rank-1 convexity, one should have:

$$W\left(\frac{\xi + \xi'}{2}\right) \leq \frac{1}{2}W(\xi) + \frac{1}{2}W(\xi'). \quad (4.5)$$

Standard computations give that

$$\begin{aligned} W(\xi) &= 4a_1 \varepsilon^4 + 2a_2 \varepsilon^2 + \Phi(\varepsilon^2) + \frac{\lambda + \mu}{2}, \\ W(\xi') &= 100a_1 \varepsilon^4 + 10a_2 \varepsilon^2 + \Phi(3\varepsilon^2) + \frac{\lambda + \mu}{2}, \\ W\left(\frac{\xi + \xi'}{2}\right) &= 25a_1 \varepsilon^4 + 5a_2 \varepsilon^2 + \Phi(2\varepsilon^2) + \frac{\lambda + \mu}{2}. \end{aligned}$$

Inequality (4.5) thus amounts to:

$$\left(27a_1 + \frac{\mu}{2}\right) \varepsilon^2 + a_2 \geq 0,$$

which raises a contradiction for ε small enough.

Then by definition (see [17, Chapitre 9, p. 432]), for almost every $x \in \Omega$ and for every $(\varphi, \xi) \in \mathbb{R}^2 \times \mathbb{R}^4$, the quasiconvex envelope of f with respect to the last variable, denoted by Qf , is defined by:

$$Qf(x, \varphi, \xi) = \inf \left\{ \frac{1}{\text{meas}(D)} \int_D f(x, \varphi, \xi + \nabla \Phi(y)) dy : \Phi \in W_0^{1,\infty}(D, \mathbb{R}^2) \right\},$$

$D \subset \mathbb{R}^2$ being a bounded open set. Consequently, in our case,

$$Qf(x, \varphi, \xi) = \frac{\nu}{2} (T(\varphi) - R)^2 + QW(\xi).$$

It ensues that $Qf \neq f$ and f is not quasiconvex. ■

Proposition 4.1.2 raises a drawback of a theoretical nature since we cannot obtain the weak lower semicontinuity of the introduced functional. The idea is thus to replace the original problem (P) by a relaxed one denoted by (QP) formulated in terms of the quasiconvex envelope Qf of f . We draw the reader's attention on the fact that the introduced problem (QP) is not the relaxed problem associated to (P) in the sense of Dacorogna ([17, chapter 9], definition that applies to problems phrased in the form of integral).

As stressed in [25], the derivation of the relaxed problem associated to a given problem in the sense of Dacorogna entails the computation of the quasiconvex envelope of a function defined on a space of matrices, which is generally an hopeless task. We dwell on this point at the end of subsection 4.1.4 and the proposed relaxation technique is justified. In any case, one has $\inf(QP) \leq \inf(P)$. The infimum of (QP) is reached and with additional hypotheses the equality $\inf(QP) = \inf(P)$ can hold.

4.1.4 Theoretical results

In what follows, we start by establishing the explicit expression of the quasiconvex envelope of f and derive the considered relaxed problem.

Proposition 4.1.3

The quasiconvex envelope Qf of f is defined by $Qf(x, \varphi, \xi) = \frac{\nu}{2} (T(\varphi) - R)^2 + QW(\xi)$

with $QW(\xi) = \begin{cases} W(\xi) & \text{if } \|\xi\|^2 \geq 2\frac{\lambda + \mu}{\lambda + 2\mu}, \\ \Psi(\det \xi) & \text{if } \|\xi\|^2 < 2\frac{\lambda + \mu}{\lambda + 2\mu}, \end{cases}$ and Ψ , the convex mapping such that

$$\Psi : t \mapsto -\frac{\mu}{2} t^2 + \mu (t - 1)^2 + \frac{\mu(\lambda + \mu)}{2(\lambda + 2\mu)}.$$

The relaxed problem (QP) is chosen to be:

$$\inf \left\{ \bar{I}(\varphi) = \text{var}_g T \circ \varphi + \int_{\Omega} Qf(x, \varphi(x), \nabla \varphi(x)) dx \right\}, \quad (\text{QP})$$

with $\varphi \in Id + W_0^{1,4}(\Omega, \mathbb{R}^2)$.

Proof: As previously shown, $Qf(x, \varphi, \xi) = \frac{\nu}{2} (T(\varphi) - R)^2 + QW(\xi)$.

After some intermediate computations, one has

$$W(\xi) = \beta (\|\xi\|^2 - \alpha)^2 + \psi(\det \xi)$$

with $\alpha = 2\frac{\lambda + \mu}{\lambda + 2\mu}$ and $\beta = \frac{\lambda + 2\mu}{8}$.

Let us denote by $W_1 : \xi \mapsto \beta (\|\xi\|^2 - \alpha)^2$ and by $g : \xi \mapsto \psi(\det \xi)$. It is well-known that $QW_1(\xi) = W_1(\xi)$ if $\|\xi\|^2 \geq \alpha$ and $QW_1(\xi) = 0$ if $\|\xi\|^2 < \alpha$. Also, it is not difficult to see that $QW_1 + g \leq QW$. Indeed, $QW_1 = Q(W - g)$ and for any $D \subset \mathbb{R}^2$ bounded open set,

$$\begin{aligned} \frac{1}{\text{meas}(D)} \int_D g(\xi + \nabla \Phi(y)) dy &= \frac{1}{\text{meas}(D)} \int_D \Psi(\det(\xi + \nabla \Phi(y))) dy, \\ &\geq \Psi \left(\frac{1}{\text{meas}(D)} \int_D \det(\xi + \nabla \Phi(y)) dy \right), \end{aligned}$$

from Jensen's inequality. In addition, from [17, lemma 5.5, p. 160],

$$\frac{1}{\text{meas}(D)} \int_D \det(\xi + \nabla \Phi(y)) dy = \det \xi, \text{ so:}$$

$$\frac{1}{\text{meas}(D)} \int_D g(\xi + \nabla \Phi(y)) dy \geq \psi(\det \xi).$$

Consequently, according to the definition of the quasiconvex envelope of a function, it follows that $QW_1 + g \leq QW$.

The most difficult part of the proof lies in the derivation of the inequality $QW \leq QW_1 + g$ when $\|\xi\|^2 < \alpha$, the case $\|\xi\|^2 \geq \alpha$ being obvious. As the following inequality holds, $QW \leq RW \leq W$ with RW the rank one convex envelope of W , it suffices to prove that $RW \leq QW_1 + g$. Let us consider $\xi \in \mathbb{R}^4$ such that $0 < \|\xi\|^2 < \alpha$. In [5, lemma 3.2], Bousselsal proves that one can always decompose ξ into $\xi = \lambda \xi_1 + (1 - \lambda) \xi_2$ with $\lambda \in]0, 1[$ and such that $\text{rank}(\xi_1 - \xi_2) \leq 1$, $\|\xi_1\|^2 = \|\xi_2\|^2 = \alpha$ and $\det \xi_1 = \det \xi_2 = \det \xi$. With this decomposition it is now easy to conclude. By definition of the rank-one convexity,

$$RW(\xi) \leq \lambda W(\xi_1) + (1 - \lambda) W(\xi_2) = \psi(\det(\xi)) = QW_1(\xi) + g(\xi).$$

We provide a detailed review of the quasiconvex envelop of W in Chapter 6.

Remark 4.1.4

This judicious rewriting of $W(\xi)$ into $W(\xi) = \beta (\|\xi\|^2 - \alpha)^2 + \psi(\det \xi)$ allows to see that $W^{1,4}(\Omega, \mathbb{R}^2)$ is a suitable functional space for φ . Indeed, it can easily be proved that

$$\begin{cases} \beta (\|\xi\|^2 - \alpha)^2 \leq \beta \|\xi\|^4 + \beta \alpha^2, \\ \psi(\det \xi) \leq \mu (\det \xi)^2 + 3\mu + \frac{\mu(\lambda + \mu)}{2(\lambda + 2\mu)}, \end{cases}$$

so that if $\varphi \in W^{1,4}(\Omega, \mathbb{R}^2)$, $\int_{\Omega} f(x, \varphi(x), \nabla \varphi(x)) dx < \infty$. Recall that from generalized Hölder's inequality, if $\varphi \in W^{1,4}(\Omega, \mathbb{R}^2)$, then $\det \nabla \varphi \in L^2(\Omega)$.

Remark 4.1.5

In fact, we can prove a stronger result, namely, that the polyconvex envelope of W , PW , coincides with the quasiconvex envelope of W : $PW = QW$.

Remark 4.1.6

We understand better through this proof, the choice of the weighting parameter balancing the component $(\det \xi - 1)^2$; it has been chosen in order that the mapping ψ is convex.

Remark 4.1.7

We emphasize that the extension of the model to the 3D case is not straightforward. Indeed, in three dimensions, the expression of $W_{SVK}(\xi)$ involves the cofactor matrix denoted by $\text{Cof} \xi$ as follows:

$$W_{SVK}(\xi) = \frac{\lambda}{8} \left(\|\xi\|^2 - \left(3 + \frac{2\mu}{\lambda} \right) \right)^2 + \frac{\mu}{4} (\|\xi\|^4 - 2 \|\text{Cof} \xi\|^2) - \frac{\mu}{4\lambda} (2\mu + 3\lambda),$$

and it is not clear that one can derive the explicit expression of the quasiconvex envelope QW of W .

We now prove that the infimum of (QP) is attained. Note that one always has $\inf(QP) \leq \inf(P)$.

Theorem 4.1.2

Assume that there exists $\widehat{\varphi} \in \text{Id} + W_0^{1,4}(\Omega, \mathbb{R}^2)$ such that $\bar{I}(\widehat{\varphi}) < +\infty$. Then the infimum of (QP) is attained.

Before giving the sketch of the proof, we introduce a useful lemma.

Lemma 4.1.3 (Generalized Poincaré's inequality, taken from [18, p. 106–107])

Let Ω be a Lipschitz bounded domain in \mathbb{R}^N . Let $p \in [1, +\infty[$ and let \mathcal{N} be a continuous semi-norm on $W^{1,p}(\Omega)$; that is, a norm on the constant functions. Then there exists a constant $C > 0$ depending only on Ω , N and p such that:

$$\|u\|_{W^{1,p}(\Omega)} \leq C \left(\left(\int_{\Omega} |\nabla u(x)|^p dx \right)^{\frac{1}{p}} + \mathcal{N}(u) \right).$$

In practice, we will take $\mathcal{N}(u) = \int_{\partial\Omega} |u(x)| d\sigma$, (Ω being of class \mathcal{C}^1).

Proof of Theorem 4.1.2 :

We assume that there exists $\widehat{\varphi} \in \text{Id} + W_0^{1,4}(\Omega, \mathbb{R}^2)$ such that $\bar{I}(\widehat{\varphi}) < +\infty$.

The first step rests upon the derivation of the following coerciveness inequality:

$$Qf(x, \varphi, \xi) \geq \frac{\mu}{4} (\det \xi)^2 + \frac{\beta}{2} \|\xi\|^4 - \beta\alpha^2 - 3\mu + \frac{\mu(\lambda + \mu)}{2(\lambda + 2\mu)}, \quad (4.6)$$

ensuring that the infimum is finite.

Then we introduce a minimizing sequence $(\varphi^k) \in \text{Id} + W_0^{1,4}(\Omega, \mathbb{R}^2)$. We can always assume that $\bar{I}(\varphi^k) \leq 1 + \bar{I}(\widehat{\varphi})$. From estimation (4.6) and the generalized Poincaré's inequality, it follows that φ^k is bounded in $W^{1,4}(\Omega, \mathbb{R}^2)$ and $\det(\nabla\varphi^k)$ is bounded in $L^2(\Omega)$. We can thus extract a subsequence, still denoted by (φ^k) , such that:

$$\begin{cases} \varphi^k \rightharpoonup \bar{\varphi} \text{ in } W^{1,4}(\Omega, \mathbb{R}^2), \\ \det(\nabla\varphi^k) \rightharpoonup \bar{\delta} \text{ in } L^2(\Omega). \end{cases}$$

From Theorem 1.14, p. 16 of [17], if $\varphi^k \rightharpoonup \varphi$ in $W^{1,4}(\Omega, \mathbb{R}^2)$, then $\det(\nabla\varphi^k) \rightharpoonup \det(\nabla\varphi)$ in $L^2(\Omega)$, yielding to $\bar{\delta} = \det(\nabla\bar{\varphi})$ by uniqueness of the weak limit in $L^2(\Omega)$. The last step consists in letting k tend to $+\infty$.

The mapping $F \mapsto h(F) = \begin{cases} \beta (\|F\|^2 - \alpha)^2 & \text{if } \|F\|^2 \geq \alpha \\ 0 & \text{if } \|F\|^2 < \alpha \end{cases}$ is continuous and convex

on $M_2(\mathbb{R}) \sim \mathbb{R}^4$.

Let (Ψ_k) be a given sequence that strongly converges to Ψ in $W^{1,4}(\Omega, \mathbb{R}^2)$ (so $\nabla\Psi_k \rightarrow \nabla\Psi$ in $L^4(\Omega, M_2(\mathbb{R}))$). One can always extract a subsequence still denoted by (Ψ_k) such that $\nabla\Psi_k \rightarrow \nabla\Psi$ almost everywhere. According to the continuity of h , it follows that:

$$h(\nabla\Psi_k(x)) \rightarrow h(\nabla\Psi(x))$$

and Fatou's lemma ensures that:

$$\liminf_{k \rightarrow +\infty} \int_{\Omega} h(\nabla\Psi_k(x)) dx \geq \int_{\Omega} h(\nabla\Psi(x)) dx.$$

By employing this technique, one proves that functional J defined on

$W^{1,4}(\Omega, \mathbb{R}^2) \times L^2(\Omega)$ by $J(\Phi, \delta) = \int_{\Omega} \mathbb{W}^*(\nabla\Phi, \delta) dx$ with

$$\mathbb{W}^*(\nabla\Phi, \delta) = \begin{cases} \beta (\|\nabla\Phi\|^2 - \alpha)^2 + \psi(\delta) & \text{if } \|\nabla\Phi\|^2 \geq \alpha \\ \psi(\delta) & \text{if } \|\nabla\Phi\|^2 < \alpha \end{cases} \text{ is convex (thanks to the ar-}$$

gument of polyconvexity) and strongly sequentially lower semicontinuous since \mathbb{W}^* is convex and continuous. It is thus weakly lower semicontinuous and

$$J(\bar{\varphi}, \det(\nabla\bar{\varphi})) \leq \liminf_{k \rightarrow +\infty} J(\varphi^k, \det(\nabla\varphi^k)).$$

The Rellich-Kondrachov embedding theorem gives that $W^{1,4}(\Omega, \mathbb{R}^2) \overset{c}{\hookrightarrow} C^0(\bar{\Omega}, \mathbb{R}^2)$ with compact injection, so (φ^k) uniformly converges to $\bar{\varphi}$ and of course in $L^1(\Omega, \mathbb{R}^2)$. Due to the hypothesis of Lipschitz continuity of T , $T \circ \varphi^k$ strongly converges to $T \circ \bar{\varphi}$ in $L^1(\Omega)$ and finally in $L^1(\Omega, g)$. The semicontinuity theorem ([2, Theorem 3.2]) enables us to conclude that:

$$\text{var}_g T \circ \bar{\varphi} \leq \liminf_{k \rightarrow +\infty} \text{var}_g T \circ \varphi^k,$$

and Lebesgue's dominated convergence theorem that

$$\lim_{k \rightarrow +\infty} \|T \circ \varphi^k - R\|_{L^2(\Omega)}^2 = \|T \circ \bar{\varphi} - R\|_{L^2(\Omega)}^2,$$

and conclusively,

$$\bar{I}(\bar{\varphi}) \leq \liminf_{k \rightarrow +\infty} \bar{I}(\varphi^k).$$

It remains to prove that $\bar{\varphi} \in \text{Id} + W_0^{1,4}(\Omega, \mathbb{R}^2)$, which is guaranteed due to the continuity of the trace map. ■

We now concentrate upon the relation between $\inf(QP)(= \min(QP))$ and $\inf(P)$ when additional hypotheses are assumed. In this prospect, we investigate the auxiliary problem (4.7) studied in [19] and defined by:

$$\inf \left\{ \mathcal{F}(\varphi) = \int_{\Omega} f(x, \varphi(x), \nabla \varphi(x)) dx : \varphi \in \text{Id} + W_0^{1,4}(\Omega, \mathbb{R}^2) \right\}, \quad (4.7)$$

with f given in (P). The following results can be established successively (see [19]):

Proposition 4.1.8

The relaxed problem in the sense of Dacorogna associated to (4.7) is defined by:

$$\inf \left\{ \bar{\mathcal{F}}(\varphi) = \int_{\Omega} Qf(x, \varphi(x), \nabla \varphi(x)) dx : \varphi \in \text{Id} + W_0^{1,4}(\Omega, \mathbb{R}^2) \right\}, \quad (4.8)$$

with Qf given in Proposition (4.1.3).

Theorem 4.1.4

The infimum of (4.8) is attained. Let then $\varphi^* \in W^{1,4}(\Omega, \mathbb{R}^2)$ be a minimizer of the relaxed problem (4.8). Then there exists a sequence $\{\varphi_\nu\}_{\nu=1}^{\infty} \subset \varphi^* + W_0^{1,4}(\Omega, \mathbb{R}^2)$ such that $\varphi_\nu \rightarrow \varphi^*$ in $L^4(\Omega, \mathbb{R}^2)$ as $\nu \rightarrow +\infty$ and $\mathcal{F}(\varphi_\nu) \rightarrow \bar{\mathcal{F}}(\varphi^*)$ as $\nu \rightarrow +\infty$, yielding to $\min(4.8) = \inf(4.7)$.

Moreover, the following holds: $\varphi_\nu \rightharpoonup \varphi^*$ in $W^{1,4}(\Omega, \mathbb{R}^2)$ as $\nu \rightarrow +\infty$.

Remark 4.1.9

In fact, the result is even stronger and can be stated as follows (see [17, Theorem 9.8]). Let $4 \leq q \leq \infty$ and $u \in W^{1,q}(\Omega, \mathbb{R}^2)$. Then there exists a sequence $\{u_\nu\}_{\nu=1}^\infty \subset u + W_0^{1,q}(\Omega, \mathbb{R}^2)$ such that:

$$u_\nu \rightarrow u \text{ in } L^q(\Omega, \mathbb{R}^2) \text{ as } \nu \rightarrow \infty,$$

$$\int_{\Omega} f(x, u_\nu(x), \nabla u_\nu(x)) dx \rightarrow \int_{\Omega} Qf(x, u(x), \nabla u(x)) dx,$$

as $\nu \rightarrow +\infty$. In addition to the above conclusions, the following holds:

$$u_\nu \rightharpoonup u \text{ in } W^{1,4}(\Omega, \mathbb{R}^2) \text{ as } \nu \rightarrow +\infty.$$

With these elements in hand, we now provide a result relating $\inf(QP)(= \min(QP))$ and $\inf(P)$ when additional hypotheses are assumed.

Proposition 4.1.10

Let us assume that $T \in W^{2,\infty}(\mathbb{R}^2, \mathbb{R})$, ∇T being Lipschitz continuous with Lipschitz constant κ' .

Let $\bar{\varphi} \in Id + W_0^{1,4}(\Omega, \mathbb{R}^2)$ be a minimizer of the relaxed problem (QP). Due to Remark 4.1.9, there exists a sequence $\{\varphi_\nu\}_{\nu=1}^\infty \subset \bar{\varphi} + W_0^{1,4}(\Omega, \mathbb{R}^2)$ such that

$$\varphi_\nu \rightharpoonup \bar{\varphi} \text{ in } W^{1,4}(\Omega, \mathbb{R}^2) \text{ as } \nu \rightarrow \infty$$

and

$$\int_{\Omega} f(x, \varphi_\nu(x), \nabla \varphi_\nu(x)) dx \rightarrow \int_{\Omega} Qf(x, \bar{\varphi}(x), \nabla \bar{\varphi}(x)) dx.$$

If moreover $\nabla \varphi_\nu$ strongly converges to $\nabla \bar{\varphi}$ in $L^1(\Omega, M_2(\mathbb{R}))$, then one has $I(\varphi_\nu) \rightarrow \bar{I}(\bar{\varphi})$ as $\nu \rightarrow \infty$ and therefore $\inf(QP) = \min(QP) = \inf(P)$.

Proof: The mapping $T \circ \varphi$ belongs to $W^{1,4}(\Omega) := W^{1,4}(\Omega, \mathbb{R})$ and since T has continuous first order partial derivatives, the chain rule holds almost everywhere on Ω . Also, as $T \circ \varphi \in W^{1,1}(\Omega)$, Ω being bounded, it also belongs to $W^{1,1}(\Omega, g)$ and the norms on $BV(\Omega, g)$ and $W^{1,1}(\Omega, g)$ are equivalent, i.e., $\text{var}_g T \circ \varphi = \int_{\Omega} |\nabla(T \circ \varphi)|g(x) dx$. We now aim to estimate:

$$|\text{var}_g T \circ \varphi_\nu - \text{var}_g T \circ \bar{\varphi}| = \left| \int_{\Omega} |\nabla(T \circ \varphi_\nu)|g(x) dx - \int_{\Omega} |\nabla(T \circ \bar{\varphi})|g(x) dx \right|.$$

We denote by $x = (x_1, x_2)$. Then

$$\begin{aligned} |\text{var}_g T \circ \varphi_\nu - \text{var}_g T \circ \bar{\varphi}| &\leq \int_{\Omega} |\nabla(T \circ \varphi_\nu) - \nabla(T \circ \bar{\varphi})|g(x) dx, \\ &\leq \int_{\Omega} \left(\left| \nabla T(\varphi_\nu) \frac{\partial \varphi_\nu}{\partial x_1} - \nabla T(\bar{\varphi}) \frac{\partial \bar{\varphi}}{\partial x_1} \right| + \left| \nabla T(\varphi_\nu) \frac{\partial \varphi_\nu}{\partial x_2} - \nabla T(\bar{\varphi}) \frac{\partial \bar{\varphi}}{\partial x_2} \right| \right) dx. \end{aligned}$$

We focus on the former component, the reasoning being the same for the latter one.

$$\begin{aligned}
\int_{\Omega} \left| \nabla T(\varphi_{\nu}) \frac{\partial \varphi_{\nu}}{\partial x_1} - \nabla T(\bar{\varphi}) \frac{\partial \bar{\varphi}}{\partial x_1} \right| dx &\leq \int_{\Omega} \left| \nabla T(\varphi_{\nu}) \left(\frac{\partial \varphi_{\nu}}{\partial x_1} - \frac{\partial \bar{\varphi}}{\partial x_1} \right) \right| dx \\
&\quad + \int_{\Omega} |\nabla T(\bar{\varphi}) - \nabla T(\varphi_{\nu})| \left| \frac{\partial \bar{\varphi}}{\partial x_1} \right| dx, \\
&\leq \|\nabla T\|_{L^{\infty}(\mathbb{R}^2, \mathbb{R}^2)} \left\| \frac{\partial \varphi_{\nu}}{\partial x_1} - \frac{\partial \bar{\varphi}}{\partial x_1} \right\|_{L^1(\Omega, \mathbb{R}^2)} \\
&\quad + \kappa' \|\bar{\varphi} - \varphi_{\nu}\|_{L^4(\Omega, \mathbb{R}^2)} \left\| \frac{\partial \bar{\varphi}}{\partial x_1} \right\|_{L^{\frac{4}{3}}(\Omega, \mathbb{R}^2)},
\end{aligned}$$

from Hölder's inequality and owing to the hypotheses on T . The conclusion is straightforward. \blacksquare

We now propose a numerical method for the resolution of the relaxed problem. It is motivated by a prior related work by Negrón Marrero ([34]).

4.2 Numerical method of resolution

4.2.1 Description and Analysis of the Proposed Numerical Method

In [34], Negrón Marrero describes and analyzes a numerical method that detects singular minimizers and avoids the Lavrentiev phenomenon for three dimensional problems in non-linear elasticity. This method consists in decoupling the function φ from its gradient and in formulating a related decoupled problem under inequality constraints. With this in mind, we introduce two auxiliary variables: \tilde{T} simulating the deformed Template $T \circ \varphi$ and V simulating the Jacobian deformation field $\nabla \varphi$ (-the underlying idea being to remove the nonlinearity in the derivatives of the deformation-) and derive a functional minimization problem phrased in terms of the variables φ , V and \tilde{T} . Nevertheless, our approach is different from that in [34] in several points: first, we do not formulate a minimization problem under constraints but incorporate L^p -type penalizations ($p = 1$ or 2 - the choice of the L^1 -penalization is discussed in Subsection 4.2.2) in the functional to be minimized. In [34], the author focuses on the decoupled discretized problem (discretized with the finite element method - the paper provides neither numerical applications, nor details of the implementation) for which the existence of minimizers is guaranteed, while we consider the continuous problem. Also, the author assumes that the finite element approximations satisfy some convergence hypotheses. Moreover, in our case, (as we work in two dimensions) less regularity is required for the formulation of the penalization (see in particular Remark 4.2.1).

The decoupled problem is thus defined by means of the following functional:

$$\begin{aligned}
\bar{I}_{\gamma}(\varphi, V, \tilde{T}) = &\text{var}_g \tilde{T} + \frac{\nu}{2} \|T(\varphi) - R\|_{L^2(\Omega)}^2 + \int_{\Omega} QW(V) dx \\
&+ \frac{\gamma}{2} \|V - \nabla \varphi\|_{L^2(\Omega, M_2)}^2 + \gamma \|\tilde{T} - T \circ \varphi\|_{L^1(\Omega)}. \tag{4.9}
\end{aligned}$$

We set $\widehat{\mathcal{W}} = \text{Id} + W_0^{1,2}(\Omega, \mathbb{R}^2)$ and $\widehat{\chi} = \{V \in L^4(\Omega, M_2(\mathbb{R}))\}$. The decoupled problem consists in minimizing (4.9) on $\widehat{\mathcal{W}} \times \widehat{\chi} \times BV(\Omega, g)$. Then the following theorem holds.

Theorem 4.2.1

Let (γ_j) be an increasing sequence of positive real numbers such that $\lim_{j \rightarrow +\infty} \gamma_j = +\infty$.

Let also $(\varphi_k(\gamma_j), V_k(\gamma_j), \tilde{T}_k(\gamma_j))$ be a minimizing sequence of the decoupled problem with $\gamma = \gamma_j$. Then there exist a subsequence denoted by

$(\varphi_{N(\gamma_{\zeta(j)})}(\gamma_{\zeta(j)}), V_{N(\gamma_{\zeta(j)})}(\gamma_{\zeta(j)}), \tilde{T}_{N(\gamma_{\zeta(j)})}(\gamma_{\zeta(j)}))$ of $(\varphi_k(\gamma_j), V_k(\gamma_j), \tilde{T}_k(\gamma_j))$ and a minimizer $\bar{\varphi}$ of \bar{I} ($\bar{\varphi} \in \text{Id} + W_0^{1,4}(\Omega, \mathbb{R}^2)$) such that:

$$\lim_{j \rightarrow +\infty} \bar{I}_{\gamma_{\zeta(j)}} \left(\varphi_{N(\gamma_{\zeta(j)})}(\gamma_{\zeta(j)}), V_{N(\gamma_{\zeta(j)})}(\gamma_{\zeta(j)}), \tilde{T}_{N(\gamma_{\zeta(j)})}(\gamma_{\zeta(j)}) \right) = \bar{I}(\bar{\varphi}).$$

Proof: Let $\epsilon > 0$ be given, $\epsilon \in]0, \epsilon_0]$, $\epsilon_0 > 0$ fixed. Without loss of generality, we assume that $\text{meas}(\Omega) = 1$. There exists $\widehat{\varphi}_\epsilon \in \mathcal{W} = \text{Id} + W_0^{1,4}(\Omega, \mathbb{R}^2)$ such that:

$$\begin{aligned} \inf_{(\varphi, V, \tilde{T}) \in \widehat{\mathcal{W}} \times \widehat{\mathcal{X}} \times BV(\Omega, g)} \bar{I}_\gamma(\varphi, V, \tilde{T}) &\leq \bar{I}_\gamma(\widehat{\varphi}_\epsilon, \nabla \widehat{\varphi}_\epsilon, T \circ \widehat{\varphi}_\epsilon) = \bar{I}(\widehat{\varphi}_\epsilon), \\ &< \inf_{\varphi \in \mathcal{W}} \bar{I}(\varphi) + \epsilon \leq \inf_{\varphi \in \mathcal{W}} \bar{I}(\varphi) + \epsilon_0. \end{aligned}$$

Consequently,

$$\inf_{(\varphi, V, \tilde{T}) \in \widehat{\mathcal{W}} \times \widehat{\mathcal{X}} \times BV(\Omega, g)} \bar{I}_\gamma(\varphi, V, \tilde{T}) \leq \inf_{\varphi \in \mathcal{W}} \bar{I}(\varphi) + \epsilon. \quad (4.10)$$

The second part of the proof consists in taking an increasing sequence (γ_j) of positive real numbers such that $\lim_{j \rightarrow +\infty} \gamma_j = +\infty$. We then consider a minimizing sequence denoted by $(\varphi_k(\gamma_j), V_k(\gamma_j), \tilde{T}_k(\gamma_j))$ for the decoupled problem with $\gamma = \gamma_j$, that is:

$$\lim_{k \rightarrow +\infty} \bar{I}_{\gamma_j} \left(\varphi_k(\gamma_j), V_k(\gamma_j), \tilde{T}_k(\gamma_j) \right) = \inf_{(\varphi, V, \tilde{T}) \in \widehat{\mathcal{W}} \times \widehat{\mathcal{X}} \times BV(\Omega, g)} \bar{I}_{\gamma_j}(\varphi, V, \tilde{T}).$$

In particular, $\forall \epsilon > 0, \exists N(\epsilon, \gamma_j) \in \mathbb{N}, \forall k \in \mathbb{N}$,

$$\left(k \geq N(\epsilon, \gamma_j) \implies \bar{I}_{\gamma_j} \left(\varphi_k(\gamma_j), V_k(\gamma_j), \tilde{T}_k(\gamma_j) \right) \leq \inf_{(\varphi, V, \tilde{T}) \in \widehat{\mathcal{W}} \times \widehat{\mathcal{X}} \times BV(\Omega, g)} \bar{I}_{\gamma_j}(\varphi, V, \tilde{T}) + \epsilon \right).$$

Let us take in particular $\epsilon = \frac{1}{\gamma_j}$. There exists $N(\gamma_j) \in \mathbb{N}$ such that $\forall k \in \mathbb{N}$,

$$\left(k \geq N(\gamma_j) \implies \bar{I}_{\gamma_j} \left(\varphi_k(\gamma_j), V_k(\gamma_j), \tilde{T}_k(\gamma_j) \right) \leq \inf_{(\varphi, V, \tilde{T}) \in \widehat{\mathcal{W}} \times \widehat{\mathcal{X}} \times BV(\Omega, g)} \bar{I}_{\gamma_j}(\varphi, V, \tilde{T}) + \frac{1}{\gamma_j} \right).$$

We then set $k = N(\gamma_j)$ and we obtain:

$$\begin{aligned} \bar{I}_{\gamma_j} \left(\varphi_{N(\gamma_j)}(\gamma_j), V_{N(\gamma_j)}(\gamma_j), \tilde{T}_{N(\gamma_j)}(\gamma_j) \right) &\leq \inf_{(\varphi, V, \tilde{T}) \in \widehat{\mathcal{W}} \times \widehat{\mathcal{X}} \times BV(\Omega, g)} \bar{I}_{\gamma_j}(\varphi, V, \tilde{T}) + \frac{1}{\gamma_j}, \\ &\leq \inf_{\varphi \in \mathcal{W}} \bar{I}(\varphi) + \frac{2}{\gamma_j} \leq \inf_{\varphi \in \mathcal{W}} \bar{I}(\varphi) + \frac{2}{\gamma_0} < +\infty, \end{aligned}$$

(4.11)

from (5.10).

Similarly to the coercivity inequality obtained in the proof of Theorem 4.1.2, the following inequality holds:

$$\frac{\mu}{4} (\det(V))^2 + \frac{\beta}{2} \|V\|^4 - \beta \alpha^2 - 3\mu + \frac{\mu(\lambda + \mu)}{2(\lambda + 2\mu)} \leq QW(V).$$

As a consequence,

$\left\{ \begin{array}{l} V_{N(\gamma_j)}(\gamma_j) \text{ is uniformly bounded in } L^4(\Omega, M_2) \text{ (so in } L^2(\Omega, M_2) \text{ with } M_2 = M_2(\mathbb{R}) \sim \mathbb{R}^4) \text{ and} \\ \det(V_{N(\gamma_j)}(\gamma_j)) \text{ is uniformly bounded in } L^2(\Omega). \end{array} \right.$

We can thus extract a subsequence denoted by $(V_{N(\gamma_{\Psi(j)})}(\gamma_{\Psi(j)}))$ such that:

$$\left\{ \begin{array}{l} V_{N(\gamma_{\Psi(j)})}(\gamma_{\Psi(j)}) \xrightarrow{j \rightarrow +\infty} \bar{V} \text{ in } L^4(\Omega, M_2), \\ \det(V_{N(\gamma_{\Psi(j)})}(\gamma_{\Psi(j)})) \xrightarrow{j \rightarrow +\infty} \bar{\delta} \text{ in } L^2(\Omega). \end{array} \right.$$

In addition,

$$\frac{\gamma_{\Psi(j)}}{2} \|V_{N(\gamma_{\Psi(j)})}(\gamma_{\Psi(j)}) - \nabla \varphi_{N(\gamma_{\Psi(j)})}(\gamma_{\Psi(j)})\|_{L^2(\Omega, M_2)}^2 \leq \beta \alpha^2 + 3\mu - \frac{\mu(\lambda + \mu)}{2(\lambda + 2\mu)} + \inf_{\varphi \in \mathcal{W}} \bar{I}(\varphi) + \frac{2}{\gamma_0},$$

so,

$$\|V_{N(\gamma_{\Psi(j)})}(\gamma_{\Psi(j)}) - \nabla \varphi_{N(\gamma_{\Psi(j)})}(\gamma_{\Psi(j)})\|_{L^2(\Omega, M_2)}^2 \leq \frac{2}{\gamma_0} \left(\beta \alpha^2 + 3\mu - \frac{\mu(\lambda + \mu)}{2(\lambda + 2\mu)} + \inf_{\varphi \in \mathcal{W}} \bar{I}(\varphi) + \frac{2}{\gamma_0} \right),$$

and

$$\begin{aligned} & | \|\nabla \varphi_{N(\gamma_{\Psi(j)})}(\gamma_{\Psi(j)})\|_{L^2(\Omega, M_2)} - \|V_{N(\gamma_{\Psi(j)})}(\gamma_{\Psi(j)})\|_{L^2(\Omega, M_2)} | \\ & \leq \|V_{N(\gamma_{\Psi(j)})}(\gamma_{\Psi(j)}) - \nabla \varphi_{N(\gamma_{\Psi(j)})}(\gamma_{\Psi(j)})\|_{L^2(\Omega, M_2)}, \\ & \leq \left(\frac{2}{\gamma_0} \left(\beta \alpha^2 + 3\mu - \frac{\mu(\lambda + \mu)}{2(\lambda + 2\mu)} + \inf_{\varphi \in \mathcal{W}} \bar{I}(\varphi) + \frac{2}{\gamma_0} \right) \right)^{\frac{1}{2}}. \end{aligned}$$

The sequence $(\varphi_{N(\gamma_{\Psi(j)})}(\gamma_{\Psi(j)}))$ is thus uniformly bounded in $W^{1,2}(\Omega, \mathbb{R}^2)$ according to the generalized Poincaré inequality. (Recall that $\varphi_{N(\gamma_{\Psi(j)})}(\gamma_{\Psi(j)}) = \text{Id}$ on $\partial\Omega$). We can therefore extract a subsequence denoted by $(\varphi_{N(\gamma_{\Psi \circ g(j)})}(\gamma_{\Psi \circ g(j)}))$ such that:

$$\varphi_{N(\gamma_{\Psi \circ g(j)})}(\gamma_{\Psi \circ g(j)}) \xrightarrow{j \rightarrow +\infty} \bar{\varphi} \text{ in } W^{1,2}(\Omega, \mathbb{R}^2).$$

Similarly, $\text{var}_g \tilde{T}_{N(\gamma_{\Psi \circ g(j)})}(\gamma_{\Psi \circ g(j)})$ is bounded independently of j as well as $\|\tilde{T}_{N(\gamma_{\Psi \circ g(j)})}(\gamma_{\Psi \circ g(j)})\|_{L^1(\Omega)}$. For the latter case, the uniform bound is obtained remarking that

$$\|T \circ \varphi_{N(\gamma_{\Psi \circ g(j)})}(\gamma_{\Psi \circ g(j)})\|_{L^1(\Omega)} \leq \kappa \|\varphi_{N(\gamma_{\Psi \circ g(j)})}(\gamma_{\Psi \circ g(j)})\|_{L^1(\Omega, \mathbb{R}^2)}.$$

As function g satisfies $g \leq 1$, it follows that $\tilde{T}_{N(\gamma_{\Psi \circ g(j)})}(\gamma_{\Psi \circ g(j)})$ is uniformly bounded in $L^1(\Omega, g)$ and consequently in $BV(\Omega, g)$ (- this space being equipped with the norm $\|\cdot\|_{BV(\Omega, g)} = \|\cdot\|_{L^1(\Omega, g)} + \text{var}_g \cdot$).

We now need the following theorem from [2].

Theorem 4.2.2 (*Theorem 3.4 of [2]*)

Let Ω be an open set in \mathbb{R}^n . Suppose $w \in \text{Lip}(\Omega)$, $w \in A_1$ is a weight function. Let $u \in BV(\Omega, w)$, then there exists a sequence $\{u_k\} \subset C^\infty(\Omega) \cap BV(\Omega, w)$ such that:

- (i) $\|u_k - u\|_{L^1(\Omega, w)} \rightarrow 0$ as $k \rightarrow +\infty$.
- (ii) $\text{var}_w u_k \rightarrow \text{var}_w u$ as $k \rightarrow +\infty$.

From Theorem 4.2.2, for each j , there exists $\{g_j\}$ such that $g_j \in C^\infty(\Omega)$ and

$$\begin{cases} \int_{\Omega} g |\tilde{T}_{N(\gamma_{\Psi \circ g(j)})}(\gamma_{\Psi \circ g(j)}) - g_j| dx \leq \frac{1}{j}, \\ \sup_j \int_{\Omega} g |\nabla g_j| dx < \infty. \end{cases}$$

As function g satisfies $0 < c \leq g$, it follows that:

$$\begin{cases} \int_{\Omega} |\tilde{T}_{N(\gamma_{\Psi \circ g(j)})}(\gamma_{\Psi \circ g(j)}) - g_j| dx \leq \frac{1}{cj}, \\ \sup_j \int_{\Omega} |\nabla g_j| dx < \infty. \end{cases}$$

Consequently, there exist $\tilde{T} \in BV(\Omega) \subset BV(\Omega, g)$ and a subsequence of $\{g_j\}$ still denoted by $\{g_j\}$ such that:

$$g_j \rightarrow \tilde{T} \text{ in } L^1(\Omega), \text{ so in } L^1(\Omega, g).$$

But,

$$\|\tilde{T}_{N(\gamma_{\Psi \circ g(j)})}(\gamma_{\Psi \circ g(j)}) - \tilde{T}\|_{L^1(\Omega, g)} \leq \|\tilde{T}_{N(\gamma_{\Psi \circ g(j)})}(\gamma_{\Psi \circ g(j)}) - g_j\|_{L^1(\Omega, g)} + \|g_j - \tilde{T}\|_{L^1(\Omega, g)},$$

so it implies that $\tilde{T}_{N(\gamma_{\Psi \circ g(j)})}(\gamma_{\Psi \circ g(j)}) \rightarrow \tilde{T}$ in $L^1(\Omega, g)$. We have proved that there exists a subsequence of $\tilde{T}_{N(\gamma_{\Psi \circ g(j)})}(\gamma_{\Psi \circ g(j)})$ denoted by $\tilde{T}_{N(\gamma_{\zeta(j)})}(\gamma_{\zeta(j)}) := \tilde{T}_{N(\gamma_{\Psi \circ g \circ h(j)})}(\gamma_{\Psi \circ g \circ h(j)})$ and a function \tilde{T} in $BV(\Omega, g)$ such that $\tilde{T}_{N(\gamma_{\zeta(j)})}(\gamma_{\zeta(j)}) \rightarrow \tilde{T}$ in $L^1(\Omega, g)$ and so in $L^1(\Omega)$.

Let us now set $x_j = \tilde{T}_{N(\gamma_{\zeta(j)})}(\gamma_{\zeta(j)}) - T \circ \varphi_{N(\gamma_{\zeta(j)})}(\gamma_{\zeta(j)})$. Since,

$$\begin{aligned} & \|\tilde{T}_{N(\gamma_{\zeta(j)})}(\gamma_{\zeta(j)}) - T \circ \varphi_{N(\gamma_{\zeta(j)})}(\gamma_{\zeta(j)})\|_{L^1(\Omega)} \\ & \leq \frac{1}{\gamma_{\zeta(j)}} \left(\beta\alpha^2 + 3\mu - \frac{\mu(\lambda + \mu)}{2(\lambda + 2\mu)} + \inf_{\varphi \in \mathcal{W}} \bar{I}(\varphi) + \frac{2}{\gamma_0} \right), \end{aligned}$$

it implies that $x_j \xrightarrow{j \rightarrow +\infty} 0$ in $L^1(\Omega)$ and consequently, $\tilde{T}_{N(\gamma_{\zeta(j)})}(\gamma_{\zeta(j)}) \rightarrow T \circ \bar{\varphi}$ in $L^1(\Omega)$ as

$$\begin{aligned} \|\tilde{T}_{N(\gamma_{\zeta(j)})}(\gamma_{\zeta(j)}) - T \circ \bar{\varphi}\|_{L^1(\Omega)} & \leq \|\tilde{T}_{N(\gamma_{\zeta(j)})}(\gamma_{\zeta(j)}) - T \circ \varphi_{N(\gamma_{\zeta(j)})}(\gamma_{\zeta(j)})\|_{L^1(\Omega)} \\ & \quad + \|T \circ \varphi_{N(\gamma_{\zeta(j)})}(\gamma_{\zeta(j)}) - T \circ \bar{\varphi}\|_{L^1(\Omega)}, \\ & \leq \|\tilde{T}_{N(\gamma_{\zeta(j)})}(\gamma_{\zeta(j)}) - T \circ \varphi_{N(\gamma_{\zeta(j)})}(\gamma_{\zeta(j)})\|_{L^1(\Omega)} \\ & \quad + \kappa \|\varphi_{N(\gamma_{\zeta(j)})}(\gamma_{\zeta(j)}) - \bar{\varphi}\|_{L^1(\Omega, \mathbb{R}^2)}, \end{aligned}$$

and $\varphi_{N(\gamma_{\zeta(j)})}(\gamma_{\zeta(j)})$ strongly converges to $\bar{\varphi}$ in $L^1(\Omega, \mathbb{R}^2)$. By uniqueness of the limit, it yields to $\tilde{T} = T \circ \bar{\varphi}$. Also, as $\tilde{T}_{N(\gamma_{\zeta(j)})}(\gamma_{\zeta(j)}) \in BV(\Omega, g)$ and $\tilde{T}_{N(\gamma_{\zeta(j)})}(\gamma_{\zeta(j)}) \rightarrow T \circ \bar{\varphi}$

in $L^1(\Omega, g)$ as $j \rightarrow +\infty$, $\text{var}_g T \circ \bar{\varphi} \leq \liminf_{j \rightarrow +\infty} \text{var}_g \tilde{T}_{N(\gamma_{\zeta(j)})}(\gamma_{\zeta(j)})$.

To summarize at this stage,

$$\begin{cases} V_{N(\gamma_{\zeta(j)})}(\gamma_{\zeta(j)}) \xrightarrow{j \rightarrow +\infty} \bar{V} \text{ in } L^4(\Omega, M_2), \\ \det(V_{N(\gamma_{\zeta(j)})}(\gamma_{\zeta(j)})) \xrightarrow{j \rightarrow +\infty} \bar{\delta} \text{ in } L^2(\Omega), \\ \varphi_{N(\gamma_{\zeta(j)})}(\gamma_{\zeta(j)}) \xrightarrow{j \rightarrow +\infty} \bar{\varphi} \text{ in } W^{1,2}(\Omega, \mathbb{R}^2), \\ \text{and } \tilde{T}_{N(\gamma_{\zeta(j)})}(\gamma_{\zeta(j)}) \xrightarrow{j \rightarrow +\infty} T \circ \bar{\varphi} \text{ in } L^1(\Omega). \end{cases}$$

Let us now set $z_j = \nabla \varphi_{N(\gamma_{\zeta(j)})}(\gamma_{\zeta(j)}) - V_{N(\gamma_{\zeta(j)})}(\gamma_{\zeta(j)})$. Since

$$\begin{aligned} & \|V_{N(\gamma_{\zeta(j)})}(\gamma_{\zeta(j)}) - \nabla \varphi_{N(\gamma_{\zeta(j)})}(\gamma_{\zeta(j)})\|_{L^2(\Omega, M_2)}^2 \leq \\ & \frac{2}{\gamma_{\zeta(j)}} \left(\beta \alpha^2 + 3\mu - \frac{\mu(\lambda + \mu)}{2(\lambda + 2\mu)} + \inf_{\varphi \in \mathcal{W}} \bar{I}(\varphi) + \frac{2}{\gamma_0} \right), \end{aligned}$$

it implies that $z_j \xrightarrow{j \rightarrow +\infty} 0$ in $L^2(\Omega, M_2)$ and consequently,

$$\nabla \varphi_{N(\gamma_{\zeta(j)})}(\gamma_{\zeta(j)}) \xrightarrow{j \rightarrow +\infty} \bar{V} \text{ in } L^2(\Omega, M_2).$$

Indeed, $\forall \Phi \in L^2(\Omega, M_2)$, $\int_{\Omega} z_j : \Phi \, dx \xrightarrow{j \rightarrow +\infty} 0$. So,

$$\int_{\Omega} \left(\nabla \varphi_{N(\gamma_{\zeta(j)})}(\gamma_{\zeta(j)}) - V_{N(\gamma_{\zeta(j)})}(\gamma_{\zeta(j)}) \right) : \Phi \, dx \xrightarrow{j \rightarrow +\infty} 0.$$

But $V_{N(\gamma_{\zeta(j)})}(\gamma_{\zeta(j)}) \xrightarrow{j \rightarrow +\infty} \bar{V}$ in $L^4(\Omega, M_2)$ so in $L^2(\Omega, M_2)$ and $\forall \Phi \in L^2(\Omega, M_2)$,

$$\int_{\Omega} \nabla \varphi_{N(\gamma_{\zeta(j)})}(\gamma_{\zeta(j)}) : \Phi \, dx \xrightarrow{j \rightarrow +\infty} \int_{\Omega} \bar{V} : \Phi \, dx.$$

In addition, $\nabla \varphi_{N(\gamma_{\zeta(j)})}(\gamma_{\zeta(j)}) \xrightarrow{j \rightarrow +\infty} \nabla \bar{\varphi}$ in $L^2(\Omega, M_2)$, and by uniqueness of the weak limit in $L^2(\Omega, M_2)$, $\nabla \bar{\varphi} = \bar{V} \in L^4(\Omega, M_2)$.

As previously mentioned, $V_{N(\gamma_{\zeta(j)})}(\gamma_{\zeta(j)}) = \nabla \varphi_{N(\gamma_{\zeta(j)})}(\gamma_{\zeta(j)}) - z_j$ with $z_j \xrightarrow{j \rightarrow +\infty} 0$ in $L^2(\Omega, M_2)$. Consequently,

$$\det(V_{N(\gamma_{\zeta(j)})}(\gamma_{\zeta(j)})) = \det(\nabla \varphi_{N(\gamma_{\zeta(j)})}(\gamma_{\zeta(j)})) + d_j,$$

with

$$\begin{aligned} d_j = & (z_j)_{11}(z_j)_{22} - (z_j)_{21}(z_j)_{12} - (z_j)_{22} \frac{\partial \varphi_{N(\gamma_{\zeta(j)})}^1(\gamma_{\zeta(j)})}{\partial x} \\ & - (z_j)_{11} \frac{\partial \varphi_{N(\gamma_{\zeta(j)})}^2(\gamma_{\zeta(j)})}{\partial y} + (z_j)_{21} \frac{\partial \varphi_{N(\gamma_{\zeta(j)})}^1(\gamma_{\zeta(j)})}{\partial y} \\ & + (z_j)_{12} \frac{\partial \varphi_{N(\gamma_{\zeta(j)})}^2(\gamma_{\zeta(j)})}{\partial x}, \end{aligned}$$

$((z_j)_{kl})$ denoting the element of the k^{th} row and the l^{th} column of the matrix z_j and with $\varphi_{N(\gamma_{\zeta(j)})}(\gamma_{\zeta(j)}) = \left(\varphi_{N(\gamma_{\zeta(j)})}^1(\gamma_{\zeta(j)}), \varphi_{N(\gamma_{\zeta(j)})}^2(\gamma_{\zeta(j)}) \right)$. The following inequality holds:

$$\int_{\Omega} |d_j| \, dx \leq \frac{1}{2} \|z_j\|_{L^2(\Omega, M_2)}^2 + \|z_j\|_{L^2(\Omega, M_2)} \|\nabla \varphi_{N(\gamma_{\zeta(j)})}(\gamma_{\zeta(j)})\|_{L^2(\Omega, M_2)},$$

$\|\nabla\varphi_{N(\gamma_{\zeta(j)})}(\gamma_{\zeta(j)})\|_{L^2(\Omega, M_2)}$ being bounded independently of j . As a consequence, $d_j \xrightarrow{j \rightarrow +\infty} 0$ in $L^1(\Omega)$. Let us now gather all the previous results:

$$\begin{cases} \det(V_{N(\gamma_{\zeta(j)})}(\gamma_{\zeta(j)})) \xrightarrow{j \rightarrow +\infty} \bar{\delta} \text{ in } L^2(\Omega), \\ \varphi_{N(\gamma_{\zeta(j)})}(\gamma_{\zeta(j)}) \xrightarrow{j \rightarrow +\infty} \bar{\varphi} \text{ in } W^{1,2}(\Omega, \mathbb{R}^2), \\ \text{and } \det(V_{N(\gamma_{\zeta(j)})}(\gamma_{\zeta(j)})) = \det(\nabla\varphi_{N(\gamma_{\zeta(j)})}(\gamma_{\zeta(j)})) + d_j \text{ with } d_j \xrightarrow{j \rightarrow +\infty} 0 \text{ in } L^1(\Omega). \end{cases}$$

From Theorem 1.14 from [17], if $\varphi_{N(\gamma_{\zeta(j)})}(\gamma_{\zeta(j)}) \xrightarrow{j \rightarrow +\infty} \bar{\varphi}$ in $W^{1,2}(\Omega, \mathbb{R}^2)$, then $\det(\nabla\varphi_{N(\gamma_{\zeta(j)})}(\gamma_{\zeta(j)})) \xrightarrow{j \rightarrow +\infty} \det(\nabla\bar{\varphi})$ in the sense of distributions.

Also, $\forall \Phi \in \mathcal{D}(\Omega)$,

$$\int_{\Omega} \det(V_{N(\gamma_{\zeta(j)})}(\gamma_{\zeta(j)})) \Phi \, dx \xrightarrow{j \rightarrow +\infty} \int_{\Omega} \bar{\delta} \Phi \, dx,$$

since $\det(V_{N(\gamma_{\zeta(j)})}(\gamma_{\zeta(j)}))$ weakly converges to $\bar{\delta}$ in $L^2(\Omega)$.

In addition:

$$\int_{\Omega} \det(V_{N(\gamma_{\zeta(j)})}(\gamma_{\zeta(j)})) \Phi \, dx = \int_{\Omega} \det(\nabla\varphi_{N(\gamma_{\zeta(j)})}(\gamma_{\zeta(j)})) \Phi \, dx + \int_{\Omega} d_j \Phi \, dx,$$

and

$$\begin{cases} \int_{\Omega} \det(\nabla\varphi_{N(\gamma_{\zeta(j)})}(\gamma_{\zeta(j)})) \Phi \, dx \xrightarrow{j \rightarrow +\infty} \int_{\Omega} \det(\nabla\bar{\varphi}) \Phi \, dx, \\ \left| \int_{\Omega} d_j \Phi \, dx \right| \leq \|d_j\|_{L^1(\Omega)} \|\Phi\|_{C^0(\bar{\Omega})} \xrightarrow{j \rightarrow +\infty} 0 \text{ from Hölder's inequality.} \end{cases}$$

Consequently, $\forall \Phi \in \mathcal{D}(\Omega)$,

$$\int_{\Omega} \bar{\delta} \Phi \, dx = \int_{\Omega} \det(\nabla\bar{\varphi}) \Phi \, dx$$

and $\det(\nabla\bar{\varphi}) = \bar{\delta}$ in the sense of distributions. As $\det(\nabla\bar{\varphi}) \in L^2(\Omega)$ (since $\bar{\varphi} \in W^{1,4}(\Omega, \mathbb{R}^2)$ -recall that if Φ^n weakly converges to Φ in $W^{1,p}$ and $\Phi^n = Id$ on $\partial\Omega$, then $\Phi = Id$ on $\partial\Omega$ -) and as $\bar{\delta} \in L^2(\Omega)$, it results in $\det(\nabla\bar{\varphi}) = \bar{\delta}$ almost everywhere.

The mapping $J(V, \delta) = \int_{\Omega} \mathbb{W}^*(V, \delta) \, dx$ with

$$\mathbb{W}^*(V, \delta) = \begin{cases} \beta (\|V\|^2 - \alpha)^2 + \Psi(\delta) & \text{if } \|V\|^2 \geq \alpha \\ \Psi(\delta) & \text{if } \|V\|^2 < \alpha \end{cases} \text{ is defined on } L^4(\Omega, M_2) \times L^2(\Omega).$$

It is convex and strongly sequentially lower semi-continuous since \mathbb{W}^* is convex and continuous. It is thus weakly sequentially lower semi-continuous.

The Rellich-Kondrachov compact embedding theorem gives that $W^{1,2}(\Omega, \mathbb{R}^2) \subset_c L^q(\Omega, \mathbb{R}^2)$, $\forall q \in [1, +\infty[$. In particular, $\varphi_{N(\gamma_{\zeta(j)})}(\gamma_{\zeta(j)})$ strongly converges to $\bar{\varphi}$ in $L^2(\Omega, \mathbb{R}^2)$. As T is assumed to be Lipschitz continuous with Lipschitz constant κ , it can be proved that:

$$\lim_{j \rightarrow +\infty} \int_{\Omega} \left(T \left(\varphi_{N(\gamma_{\zeta(j)})}(\gamma_{\zeta(j)}) \right) - R \right)^2 \, dx = \int_{\Omega} (T(\bar{\varphi}) - R)^2 \, dx.$$

By passing to the limit when j goes to $+\infty$, it yields to:

$$\inf_{\varphi \in \mathcal{W}} \bar{I}(\varphi) \leq \bar{I}(\bar{\varphi}) \leq \liminf_{j \rightarrow +\infty} \bar{I}_{\gamma_{\zeta(j)}} \left(\varphi_{N(\gamma_{\zeta(j)})}(\gamma_{\zeta(j)}), V_{N(\gamma_{\zeta(j)})}(\gamma_{\zeta(j)}), \tilde{T}_{N(\gamma_{\zeta(j)})}(\gamma_{\zeta(j)}) \right),$$

since

$$\begin{aligned} & \text{var}_g \tilde{T}_{N(\gamma_{\zeta(j)})}(\gamma_{\zeta(j)}) + \frac{\nu}{2} \|T(\varphi_{N(\gamma_{\zeta(j)})}(\gamma_{\zeta(j)})) - R\|_{L^2(\Omega)}^2 + \int_{\Omega} QW(V_{N(\gamma_{\zeta(j)})}(\gamma_{\zeta(j)})) dx \\ & \leq \bar{I}_{\gamma_{\zeta(j)}} \left(\varphi_{N(\gamma_{\zeta(j)})}(\gamma_{\zeta(j)}), V_{N(\gamma_{\zeta(j)})}(\gamma_{\zeta(j)}), \tilde{T}_{N(\gamma_{\zeta(j)})}(\gamma_{\zeta(j)}) \right). \end{aligned}$$

In conclusion, we have obtained the two following inequalities:

$$\left\{ \begin{array}{l} \inf_{\varphi \in \mathcal{W}} \bar{I}(\varphi) \leq \bar{I}(\bar{\varphi}) \leq \liminf_{j \rightarrow +\infty} \bar{I}_{\gamma_{\zeta(j)}} \left(\varphi_{N(\gamma_{\zeta(j)})}(\gamma_{\zeta(j)}), V_{N(\gamma_{\zeta(j)})}(\gamma_{\zeta(j)}), \tilde{T}_{N(\gamma_{\zeta(j)})}(\gamma_{\zeta(j)}) \right) \quad \text{and} \\ \bar{I}_{\gamma_{\zeta(j)}} \left(\varphi_{N(\gamma_{\zeta(j)})}(\gamma_{\zeta(j)}), V_{N(\gamma_{\zeta(j)})}(\gamma_{\zeta(j)}), \tilde{T}_{N(\gamma_{\zeta(j)})}(\gamma_{\zeta(j)}) \right) \leq \inf_{\varphi \in \mathcal{W}} \bar{I}(\varphi) + \frac{2}{\gamma_{\zeta(j)}} \end{array} \right. ,$$

that is,

$$\limsup_{j \rightarrow +\infty} \bar{I}_{\gamma_{\zeta(j)}} \left(\varphi_{N(\gamma_{\zeta(j)})}(\gamma_{\zeta(j)}), V_{N(\gamma_{\zeta(j)})}(\gamma_{\zeta(j)}), \tilde{T}_{N(\gamma_{\zeta(j)})}(\gamma_{\zeta(j)}) \right) \leq \inf_{\varphi \in \mathcal{W}} \bar{I}(\varphi),$$

and finally:

$$\lim_{j \rightarrow +\infty} \bar{I}_{\gamma_{\zeta(j)}} \left(\varphi_{N(\gamma_{\zeta(j)})}(\gamma_{\zeta(j)}), V_{N(\gamma_{\zeta(j)})}(\gamma_{\zeta(j)}), \tilde{T}_{N(\gamma_{\zeta(j)})}(\gamma_{\zeta(j)}) \right) = \bar{I}(\bar{\varphi}) = \inf_{\varphi \in \mathcal{W}} \bar{I}(\varphi). \quad \blacksquare$$

Remark 4.2.1

We remark that we gain some regularity: indeed, $\varphi_{N(\gamma_{\zeta(j)})}(\gamma_{\zeta(j)})$ is only $W^{1,2}(\Omega, \mathbb{R}^2)$ and $\tilde{T}_{N(\gamma_{\zeta(j)})}(\gamma_{\zeta(j)}) \in BV(\Omega, g)$ but when passing to the limit when $j \rightarrow +\infty$, we prove that $\varphi_{N(\gamma_{\zeta(j)})}(\gamma_{\zeta(j)}) \rightharpoonup \bar{\varphi}$ in $W^{1,2}(\Omega, \mathbb{R}^2)$ with $\bar{\varphi} \in W^{1,4}(\Omega, \mathbb{R}^2)$ and $\tilde{T}_{N(\gamma_{\zeta(j)})}(\gamma_{\zeta(j)}) \rightarrow T \circ \bar{\varphi}$ in $L^1(\Omega)$ with $T \circ \bar{\varphi} \in W^{1,4}(\Omega)$.

Inspired by this theoretical result, we now turn to the discretization of the considered problem.

4.2.2 Numerical Scheme

The algorithm requires the evaluation of the Template T at $\varphi(x)$. We thus assume that T is a smooth mapping that has been obtained by interpolating the image data provided on the grid. As an additional convention, T is supposed to vanish outside the domain, *i.e.*, $T(x) = 0$ if $x \notin \Omega$. As suggested by Modersitzki in [33], Chapter 3, subsection 3.6.1, for the interpolation stage we apply a multiscale interpolation technique which includes a weighting parameter controlling smoothness versus data proximity. Also, for the sake of optimization, a multilevel representation of the data is adopted (see Chapter 3, section 3.7 of [33]).

We first solve $\inf_{\tilde{T}} E(\tilde{T}) = \text{var}_g \tilde{T} + \gamma \|\tilde{T} - T \circ \varphi\|_{L^1(\Omega)}$, for fixed φ , the minimization being based on a convex regularization as done in [6], on the dual formulation of the weighted total variation and on Chambolle's projection algorithm ([9]). An important result (see again [10] and [6]) is that if $T \circ \varphi$ is a characteristic function, if \tilde{T} is a minimizer of E then for almost every $\mu_0 \in [0, 1]$, one has that the characteristic function $1_{\{x | \tilde{T}(x) > \mu_0\}}$ is a global minimizer of E .

Then we solve (for fixed \tilde{T}): $\inf_{\varphi, V} \bar{\mathcal{J}}_\epsilon(\varphi, V) + \frac{\gamma}{2} \|\nabla\varphi - V\|_{L^2(\Omega, M_2(\mathbb{R}))}^2 + \gamma \|\tilde{T} - T \circ \varphi\|_{L^1(\Omega)}$, with

$$\begin{aligned} \bar{\mathcal{J}}_\epsilon(\varphi, V) = & \int_{\Omega} W(V) H_\epsilon(\|V\|^2 - \alpha) \, dx \\ & + \int_{\Omega} \Psi(\det V) H_\epsilon(\alpha - \|V\|^2) \, dx + \frac{\nu}{2} \int_{\Omega} (T(\varphi) - R)^2 \, dx, \end{aligned}$$

where γ is a positive constant big enough to ensure that V and $\nabla\varphi$, respectively, \tilde{T} and $T \circ \varphi$ are sufficiently close in the sense of the L^2 -norm, respectively the L^1 -norm. H_ϵ is the regularized one-dimensional Heaviside function defined by $H_\epsilon : z \mapsto \frac{1}{2} \left(1 + \frac{2}{\pi} \operatorname{Arctan} \frac{z}{\epsilon}\right)$. The edge detector function g is defined by

$$g(s) = \frac{1}{1 + as^2} \text{ where } a \text{ is a positive constant.}$$

These schemes are easy to implement and very fast compared with usual ones.

Fixing φ and V , we minimize the following functional with respect to \tilde{T} :

$$\inf_{\tilde{T}} \left\{ \operatorname{var}_g \tilde{T} + \gamma \|\tilde{T} - T \circ \varphi\|_{L^1(\Omega)} \right\}. \quad (4.12)$$

Following the same strategy as Bresson *et al.*'s one in [6], we introduce an auxiliary variable f (different from the f in section 4.1) such that the problem amounts to minimizing:

$$\inf_{\tilde{T}, f} \left\{ \operatorname{var}_g \tilde{T} + \gamma \|f\|_{L^1(\Omega)} + \frac{1}{2\theta} \|\tilde{T} - T \circ \varphi + f\|_{L^2(\Omega)}^2 \right\},$$

problem decoupled into the two following subproblems:

$$\inf_{\tilde{T}} \left\{ \operatorname{var}_g \tilde{T} + \frac{1}{2\theta} \|\tilde{T} - T \circ \varphi + f\|_{L^2(\Omega)}^2 \right\}, \quad (4.13)$$

$$\inf_f \left\{ \gamma \|f\|_{L^1(\Omega)} + \frac{1}{2\theta} \|\tilde{T} - T \circ \varphi + f\|_{L^2(\Omega)}^2 \right\}. \quad (4.14)$$

Proposition 4.2.2

The solution of (4.13) is given by

$$\tilde{T} = T \circ \varphi - f - \Pi_{\theta K} (T \circ \varphi - f),$$

where Π represents the orthogonal projection, and K is the closure of $\{\operatorname{div} \xi : \xi \in \mathcal{C}_c^1(\Omega, \mathbb{R}^2), |\xi(x)| \leq g(x), \forall x \in \Omega\}$, $|\cdot|$ being the Euclidean norm in \mathbb{R}^2 .

Proof: The proof is inspired by [22]. Writing the associated Euler-Lagrange equation, \tilde{T} is solution of (4.13) is equivalent to :

$$0 \in \partial \operatorname{var}_g(\tilde{T}) + \frac{1}{\theta} (\tilde{T} - T \circ \varphi + f),$$

where $\partial \operatorname{var}_g$ is the sub-differential of var_g .

Equivalently,

$$\begin{aligned} & -\frac{1}{\theta} (\tilde{T} - T \circ \varphi + f) \in \partial \operatorname{var}_g(\tilde{T}) \\ \iff & \tilde{T} \in \partial \operatorname{var}_g^* \left(-\frac{\tilde{T} - T \circ \varphi + f}{\theta} \right), \end{aligned}$$

where var_g^* is the Legendre-Fenchel transform of var_g .

Therefore,

$$\begin{aligned} 0 &\in -\tilde{T} + \partial \text{var}_g^* \left(\frac{T \circ \varphi - \tilde{T} - f}{\theta} \right) \\ \iff 0 &\in \frac{T \circ \varphi - \tilde{T} - f}{\theta} - \frac{T \circ \varphi - f}{\theta} + \frac{1}{\theta} \partial \text{var}_g^* \left(\frac{T \circ \varphi - \tilde{T} - f}{\theta} \right). \end{aligned}$$

We get that $w = \frac{T \circ \varphi - \tilde{T} - f}{\theta}$ is a minimizer of

$$\frac{1}{2} \left\| w - \left(\frac{T \circ \varphi - f}{\theta} \right) \right\|_{L^2(\Omega)}^2 + \frac{1}{\theta} \text{var}_g^*(w).$$

According to general convex analysis results, the Legendre-Fenchel transform of a convex and one-homogeneous functional is the characteristic function of a closed convex set K :

$$\text{var}_g^*(v) = \chi_K(v) = \begin{cases} 0 & \text{if } v \in K \\ +\infty & \text{otherwise.} \end{cases}$$

Then $w = \Pi_K \left(\frac{T \circ \varphi - f}{\theta} \right) = \frac{1}{\theta} \Pi_{\theta K} (T \circ \varphi - f)$, where Π_K represents the orthogonal projection on K , and K is the closure of

$$\{ \text{div } \xi : \xi \in C_c^1(\Omega, \mathbb{R}^2), |\xi(x)| \leq g(x), \forall x \in \Omega \}.$$

Hence the solution is given by

$$\tilde{T} = T \circ \varphi - f - \Pi_{\theta K} (T \circ \varphi - f). \quad \blacksquare$$

Proposition 4.2.3

The solution of (4.14) is given by

$$f = \begin{cases} T \circ \varphi - \tilde{T} - \theta\gamma & \text{if } T \circ \varphi - \tilde{T} \geq \theta\gamma, \\ T \circ \varphi - \tilde{T} + \theta\gamma & \text{if } T \circ \varphi - \tilde{T} \leq -\theta\gamma, \\ 0 & \text{otherwise.} \end{cases}$$

Remark 4.2.4

Numerically, computing $\Pi_{\theta K} (T \circ \varphi - f)$ amounts to solving:

$$\min \{ \|\theta \text{div } p - (T \circ \varphi - f)\|_{L^2(\Omega)}^2 : |p(x)|^2 - g(x)^2 \leq 0 \}.$$

The Karush-Kuhn-Tucker conditions yield to the following equation satisfied by p :

$$g(x) \nabla(\theta \text{div } p - (T \circ \varphi - f)) - |\nabla(\theta \text{div } p - (T \circ \varphi - f))| p = 0.$$

The previous equation can be solved by a fixed point method:

$$\begin{cases} p^0 = 0, \\ p^{n+1} = \frac{p^n + \tau \nabla(\text{div } p^n - (T \circ \varphi - f)/\theta)}{1 + \frac{\tau}{g(x)} |\nabla(\text{div } p^n - (T \circ \varphi - f)/\theta)|}. \end{cases}$$

The Euler-Lagrange equation for φ is defined by:

$$0 = \nu(T \circ \varphi - R)\nabla T(\varphi) - \gamma\Delta\varphi + \gamma \begin{pmatrix} \operatorname{div} V_1 \\ \operatorname{div} V_2 \end{pmatrix} - \frac{1}{\theta}(f - T \circ \varphi + \tilde{T})\nabla T(\varphi),$$

and the system of equations for V is:

$$\begin{cases} 0 = 2\beta c_0 V_{11} (2H_\varepsilon(c_0) + c_0\delta_\varepsilon(c_0)) + \mu V_{22}(\det V - 2) + \gamma(V_{11} - \frac{\partial\varphi_1}{\partial x}), \\ 0 = 2\beta c_0 V_{12} (2H_\varepsilon(c_0) + c_0\delta_\varepsilon(c_0)) - \mu V_{21}(\det V - 2) + \gamma(V_{12} - \frac{\partial\varphi_1}{\partial y}), \\ 0 = 2\beta c_0 V_{21} (2H_\varepsilon(c_0) + c_0\delta_\varepsilon(c_0)) - \mu V_{12}(\det V - 2) + \gamma(V_{21} - \frac{\partial\varphi_2}{\partial x}), \\ 0 = 2\beta c_0 V_{22} (2H_\varepsilon(c_0) + c_0\delta_\varepsilon(c_0)) + \mu V_{11}(\det V - 2) + \gamma(V_{22} - \frac{\partial\varphi_2}{\partial y}), \end{cases}$$

where $c_0 = (\|V\|^2 - \alpha)$, V_i denotes the i^{th} row of V and $V = (V_{ij})_{1 \leq i, j \leq 2}$.

These equations are solved by a gradient descent method using an implicit scheme of finite differences for φ and a semi-implicit scheme for V .

Remark 4.2.5

In practice, we take two different parameters γ :

$$\inf_{\varphi, V} \bar{\mathcal{J}}_\varepsilon(\varphi, V) + \gamma_1 \|\tilde{T} - T \circ \varphi\|_{L^1(\Omega)} + \frac{\gamma_2}{2} \|\nabla\varphi - V\|_{L^2(\Omega, M_2(\mathbb{R}))}^2.$$

4.3 Numerical experiments

We now present some results. Prior to this, we introduce the regriding technique employed, comment on the choice of the tuning parameters and propose an assessment of the registration accuracy.

4.3.1 Regriding technique, choice of the parameters and registration accuracy

The deformation must remain physically and mechanically meaningful, and reflect material properties: self-penetration of the matter (indicating that the transformation is not injective) should be prohibited. The penalty term $(\det \nabla\varphi - 1)^2$ does not guarantee that the Jacobian determinant remains positive. That is the reason why we have implemented the regriding algorithm proposed by Christensen and his collaborators in [12] to ensure the positivity of the Jacobian. Indeed, we have chosen the regriding method described in [12] because the implementation is quite simple and is performed simultaneously with the resolution. The method consists in monitoring the values of the Jacobian at each step of the descent gradient. If the Jacobian drops below a defined threshold, then the process is reinitialized taking as new Template the previous computed deformed Template.

Algorithm 1 Regridding method.

1. Initialization: $V^0 = I$, $\varphi^0 = \text{Id}$, regrid_count=0.

2. For $k = 0, 1, \dots$

$$(\varphi^{k+1}, V^{k+1}) = \arg \min_{\varphi, V} \bar{\mathcal{J}}_\varepsilon(\varphi, V) + \frac{\gamma}{2} \|\nabla\varphi - V\|_{L^2(\Omega, M_2(\mathbb{R}))}^2 + \gamma \|\tilde{T} - T \circ \varphi\|_{L^1(\Omega)}$$

if $\det \nabla\varphi^{k+1} < \text{tol}$

- regrid_count=regrid_count+1
- $T = T \circ \varphi^k$
- save $\text{tab}_\varphi(\text{regrid_count}) = \varphi^k$, $\varphi^{k+1} = \text{Id}$, $V^{k+1} = I$

3. If regrid_count>0

$$\varphi^{\text{final}} = \text{tab}_\varphi(1) \circ \dots \circ \text{tab}_\varphi(\text{regrid_count})$$

An alternative method would consist in applying a correction step when the Jacobian is not positive as done by Ozeré and Le Guyader in [35].

For each pair, we provide the Reference and the Template images, the deformed Template, that is to say $T \circ \varphi$, the deformed grid associated with φ (Reference to Template, straightforwardly given by φ), the deformed grid associated with φ^{-1} (Template to Reference, computed using interpolation techniques) and the distortion map drawing the displacement vectors attached to the grid points of the Reference image and pointing towards non-grid points after registration. We also display the segmentation of the Reference image obtained thanks to \tilde{T} . For applications not requiring regridding steps (see Figs. 4.4 and 4.6), we display the components V_{11} , V_{12} , V_{21} , and V_{22} versus $\frac{\partial\varphi_1}{\partial x}$, $\frac{\partial\varphi_1}{\partial y}$, $\frac{\partial\varphi_2}{\partial x}$, and $\frac{\partial\varphi_2}{\partial y}$ respectively.

For all applications, the ranges of the parameters are the same. Parameter ν balancing the intensity L^2 distance is between 0.5 and 1, the Lamé coefficient λ is set to 10. The physical meaning of Lamé's parameter λ is not straightforward: Lamé's parameter λ is related to the bulk modulus which measures the substance resistance to uniform compression. This numerical value of λ is not physically inconsistent. The Lamé coefficient μ is between 1000 and 3500. It is the shear modulus, that is to say that μ measures the resistance of the material. From our experience, the parameter that proves to be the most sensitive is the Lamé parameter μ . It can be seen as a measure of rigidity. The greater parameter μ is, the more rigid the deformation is (which can be relevant if we aim to obtain a smooth and topology-preserving deformation map). The issue is thus to find a proper trade-off between accurate image alignment (which means authorizing large deformations) and topology or orientation preservation (which means monitoring the Jacobian determinant by limiting shrinkage and growth). To get a clearer picture of the range of the different parameters, a table summarizes the selected values.

	ν	θ	γ_1	γ_2	μ	λ	a
Letter C	1	1	0.1	60 000	3500	10	1
Triangle	1.5	1	0.1	90 000	500	10	1
Mouse brain 1	0.5	1	0.1	80 000	1000	10	10
Mouse brain 2	0.5	1	0.1	80 000	2000	10	10
Slice of brain	1	1	0.1	80 000	1000	10	10
Heart ED-ES	1	0.1	0.1	90 000	1000	10	10
Heart slices 120-140	2	0.1	0.1	40 000	500	10	10

Table 4.1: Values of involved parameters

In order to obtain the segmentation of the Reference image, we display the contour corresponding to the level line $\{\tilde{T} = 0.3\}$ of \tilde{T} .

To assess registration and segmentation accuracy, we compute the Dice coefficient ([20]) which measures set agreement (after binarizing R , $T \circ \varphi$ and \tilde{T} by thresholding). The Dice similarity coefficient is a measurement of spatial overlap widely used for comparing segmentation results. The formula is given by:

$$\text{Dice}(A, B) = 2|A \cap B|/(|A| + |B|),$$

where A and B are two sets and where $|\cdot|$ denotes the cardinality. The more $\text{Dice}(A, B)$ is close to 1, the better is the matching between the two sets. We compute the Dice coefficient between R and $T \circ \varphi$ to measure the quality of the registration, as well as between R and \tilde{T} to evolve the quality of the segmentation.

	$\text{Dice}(R, T)$	$\text{Dice}(R, T \circ \varphi)$	$\text{Dice}(R, \tilde{T})$
Letter C	0.878	0.968	0.975
Triangle	0.900	0.990	0.993
Mouse brain 1	0.939	0.988	0.988
Mouse brain 2	0.921	0.982	0.983
Slice of brain	0.797	0.967	0.972
Heart ED-ES	0.771	0.929	0.942
Heart slices 120-140	0.777	0.931	0.942

Table 4.2: Dice coefficients.

4.3.2 Letter C

First, the method is applied on an academic example (Fig 6.1) taken from [13] for mapping a disk to the letter C, demonstrating the ability of the algorithm to handle large deformations.

Note that with linear elasticity model, diffusion model or curvature-based model, registration cannot be successfully accomplished (see [32]). As in [13], the right part of the disk is stretched into the shape of the interior edge of the letter C, and then moves outward to align the interior boundary of the letter C. Nevertheless, our deformation field is smoother (see in particular [13, p. 88]). In [7], the authors also apply their method on a similar example. We can notice that the deformed Template cannot reach the end of the hollow of the C, while our method handles very well deep concavities. At last, compared to [27], the algorithm requires fewer regridding corrections (2 versus 4 in [27]) and the range of the Jacobian determinant is smaller.

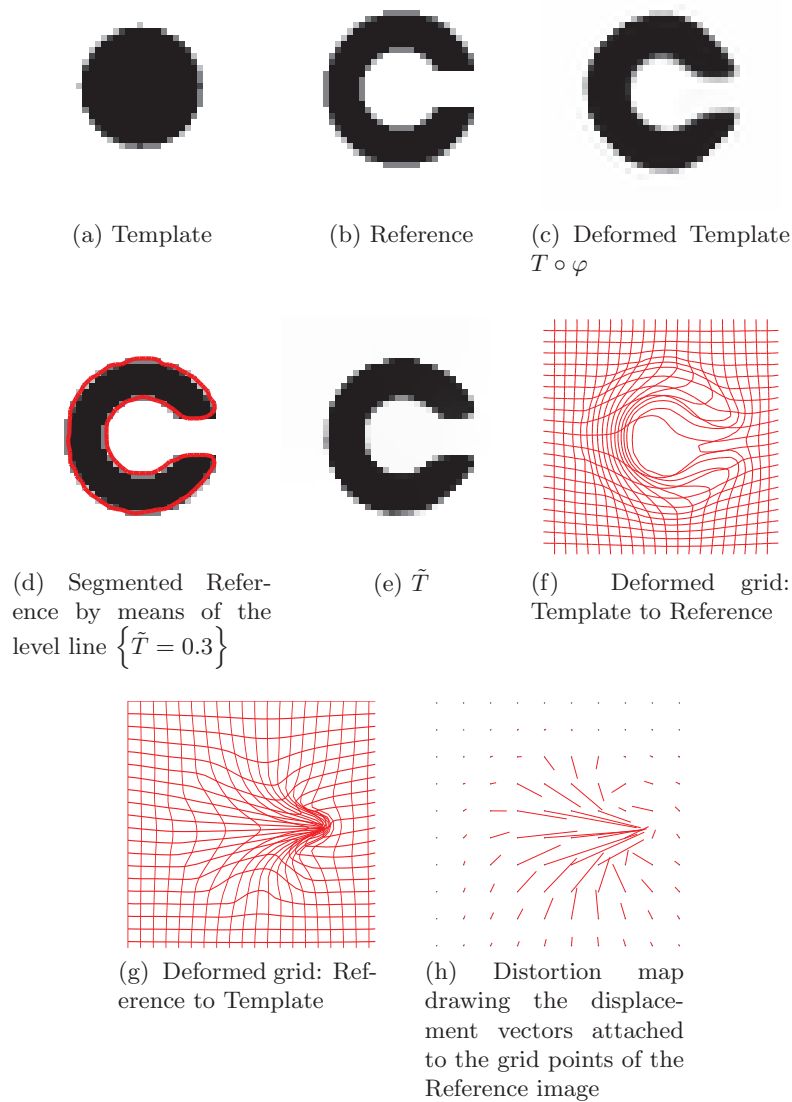


Figure 4.1: **Mapping of a disk to letter C.**

Execution time: 19 seconds for 40×40 pixel images. 2 regridding steps. $\min \det \nabla \varphi = 0.002$, $\max \det \nabla \varphi = 2.32$.

4.3.3 Noisy triangle

Another toy example is provided to emphasize again the capability of the model to generate large deformations even on data corrupted by noise. The algorithm produces both a smooth deformation field and a simplified (thus here denoised) version of the Reference image allowing for its segmentation.

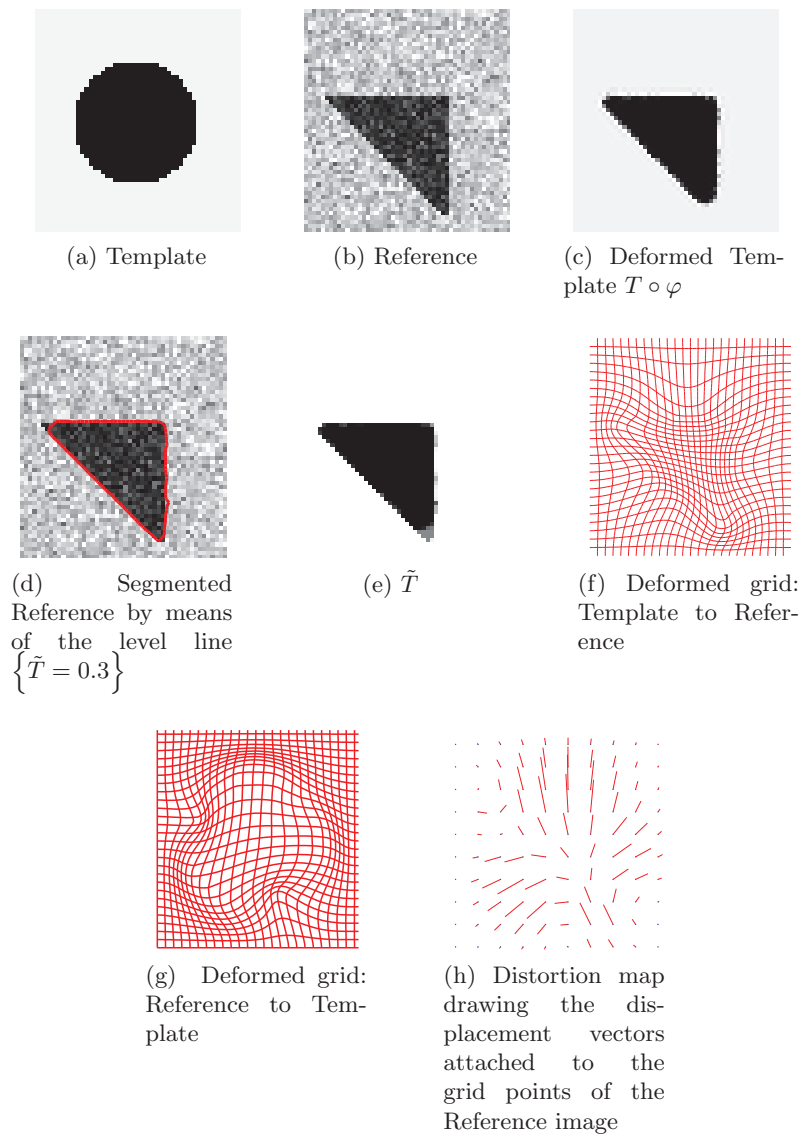


Figure 4.2: **Mapping of a disk to a noisy triangle.**

Execution time: 53 seconds for 54×50 pixel images. $\min \det \nabla \varphi = 0.37$, $\max \det \nabla \varphi = 2.25$.

4.3.4 Mouse brain gene expression data

Then the method was applied on medical images (Figs 6.3, 6.4) with the goal to map a 2D slice of mouse brain gene expression data (Template T) to its corresponding 2D slice of the mouse brain atlas, in order to facilitate the integration of anatomic, genetic and physiologic observations from multiple subjects in a common space. Since genetic mutations and knock-out strains of mice provide critical models for a variety of human diseases, such linkage between genetic information and anatomical structure is important. The data are provided by the Center for Computational Biology, UCLA. The mouse atlas acquired from the LONI database was pre-segmented. The gene expression data were segmented manually to facilitate data processing in other applications. Some algorithms have been developed to automatically segment the brain area of gene expression data. The non-brain regions have been removed to produce better matching. Our method qualitatively performs as the one in [28] and produces a smooth deformation field but also provides both a simplified version of the Reference image and its segmentation. In order to assess the closeness of V and $\nabla\varphi$ and to underline that we have indeed a good match between these two variables, we display their components in Fig. 4.4 and Fig. 4.6. Compared to the results obtained in [27], [28] or [19], the deformation grid is more regular and does not exhibit shrinkage or growth. For Fig. 6.3, the Jacobian determinants mass around the value 1 (range [0.63,1.28]) versus [0.28,2.09] in [27], [0.15,2.40] in [28] or [0.09,2.47] in [19]. The same remark can be done for Fig. 6.4: the Jacobian determinants remain close to 1 (range [0.68, 1.42]) versus [0.03,3.48] in [27], [0.18,3.23] in [28] or [0.01,2.18] in [19]. At last, contrary to [27], no regriding correction is required.

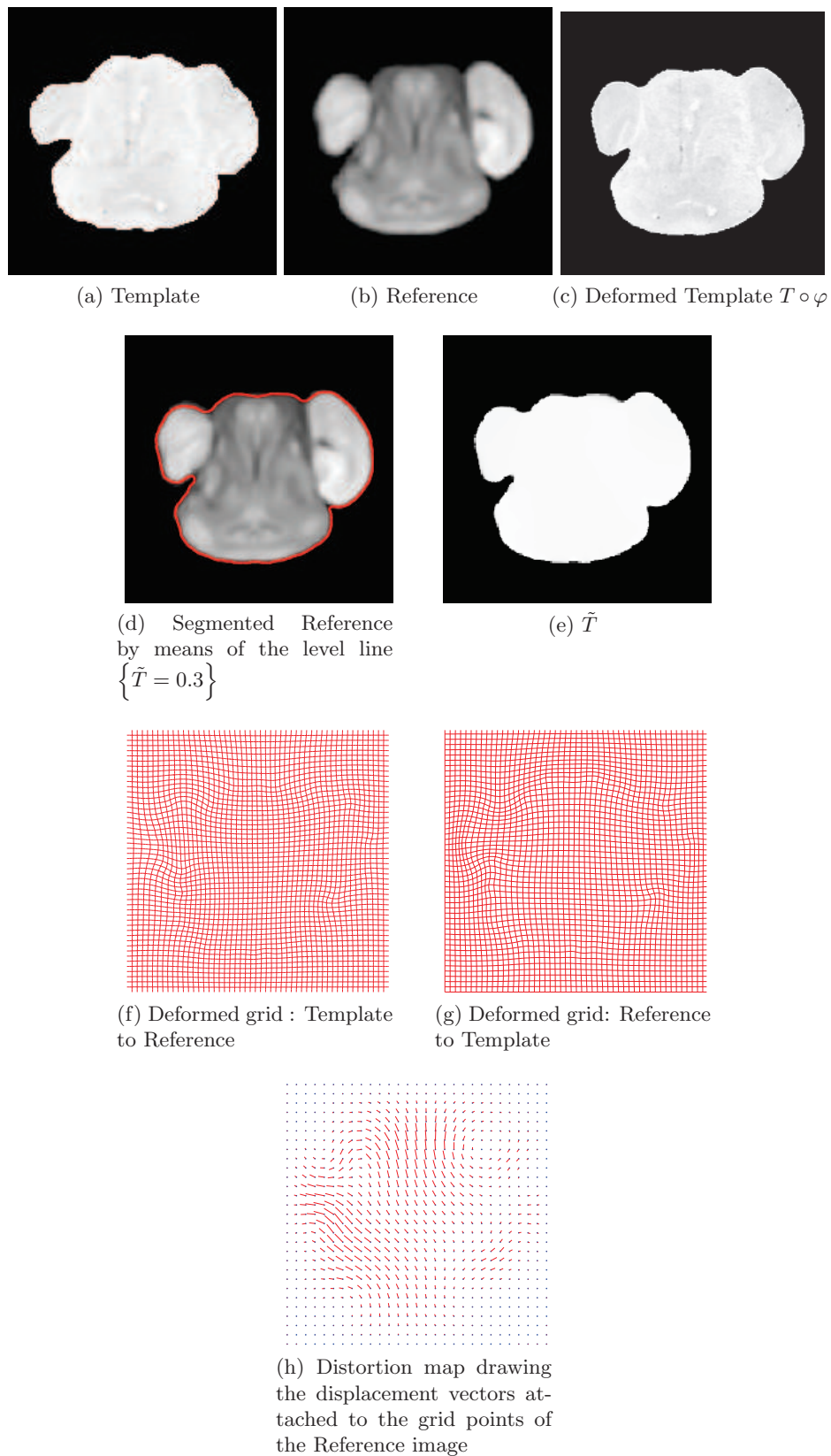


Figure 4.3: Mapping of a 2D slice of mouse brain gene expression data to its counterpart in an atlas.

Execution time: 5 minutes for 200×200 pixel images. $\min \det \nabla \varphi = 0.63$, $\max \det \nabla \varphi = 1.28$.

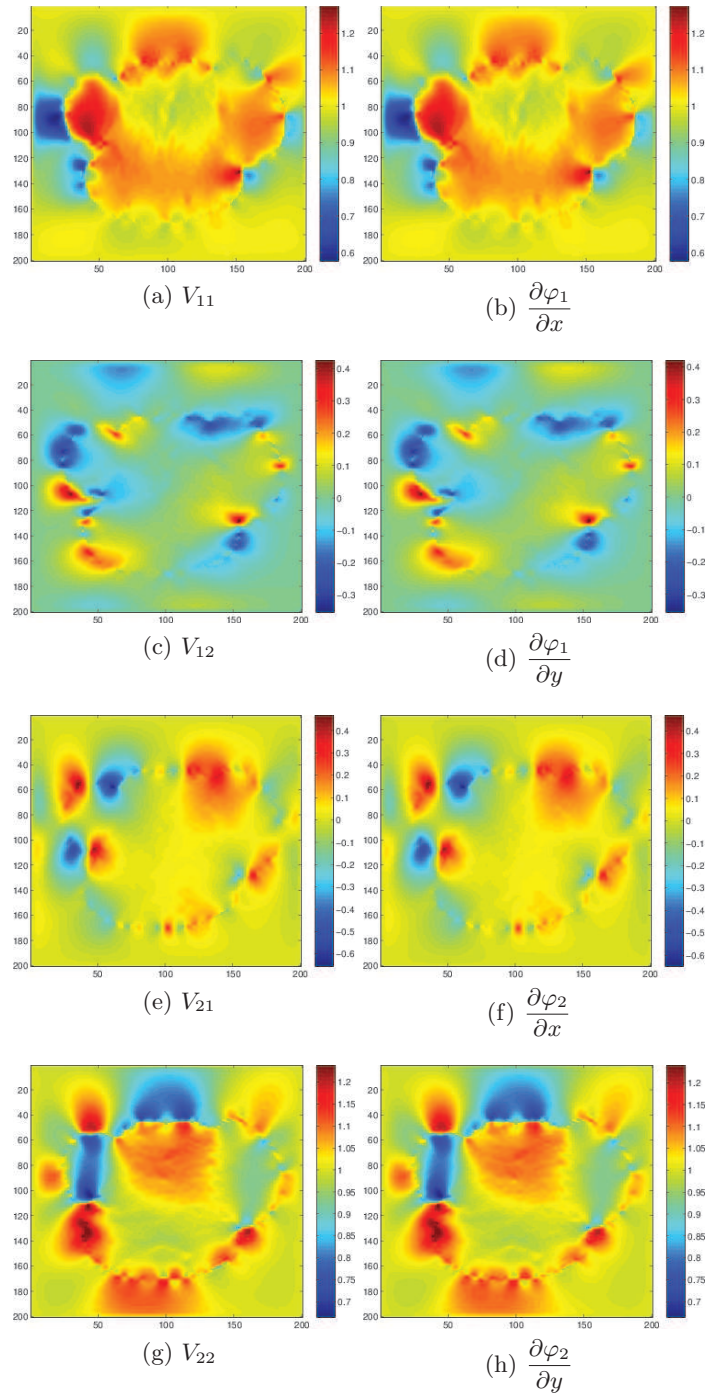


Figure 4.4: Display of V_{11} versus $\frac{\partial \varphi_1}{\partial x}$, V_{12} versus $\frac{\partial \varphi_1}{\partial y}$, V_{21} versus $\frac{\partial \varphi_2}{\partial x}$, V_{22} versus $\frac{\partial \varphi_2}{\partial y}$ related to the application of Fig. 6.3. $\|V_{11} - \frac{\partial \varphi_1}{\partial x}\|_{\infty} = 0.09$, $\|V_{12} - \frac{\partial \varphi_1}{\partial y}\|_{\infty} = 0.03$, $\|V_{21} - \frac{\partial \varphi_2}{\partial x}\|_{\infty} = 0.06$, $\|V_{22} - \frac{\partial \varphi_2}{\partial y}\|_{\infty} = 0.07$

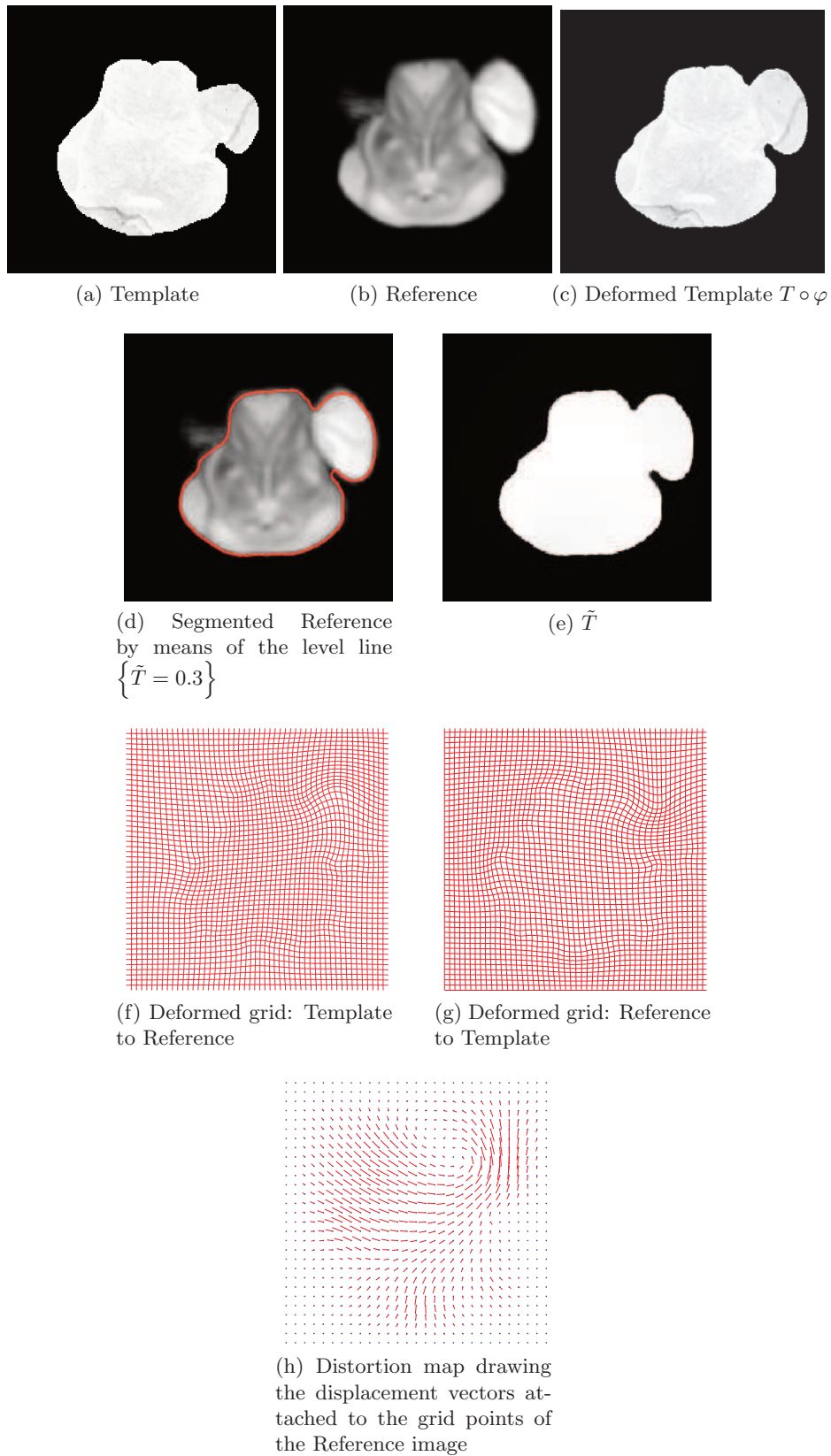


Figure 4.5: Mapping of a 2D slice of mouse brain gene expression data to its counterpart in an atlas.

Execution time: 3 minutes for 200×200 pixel images. $\min \det \nabla \varphi = 0.68$, $\max \det \nabla \varphi = 1.42$.

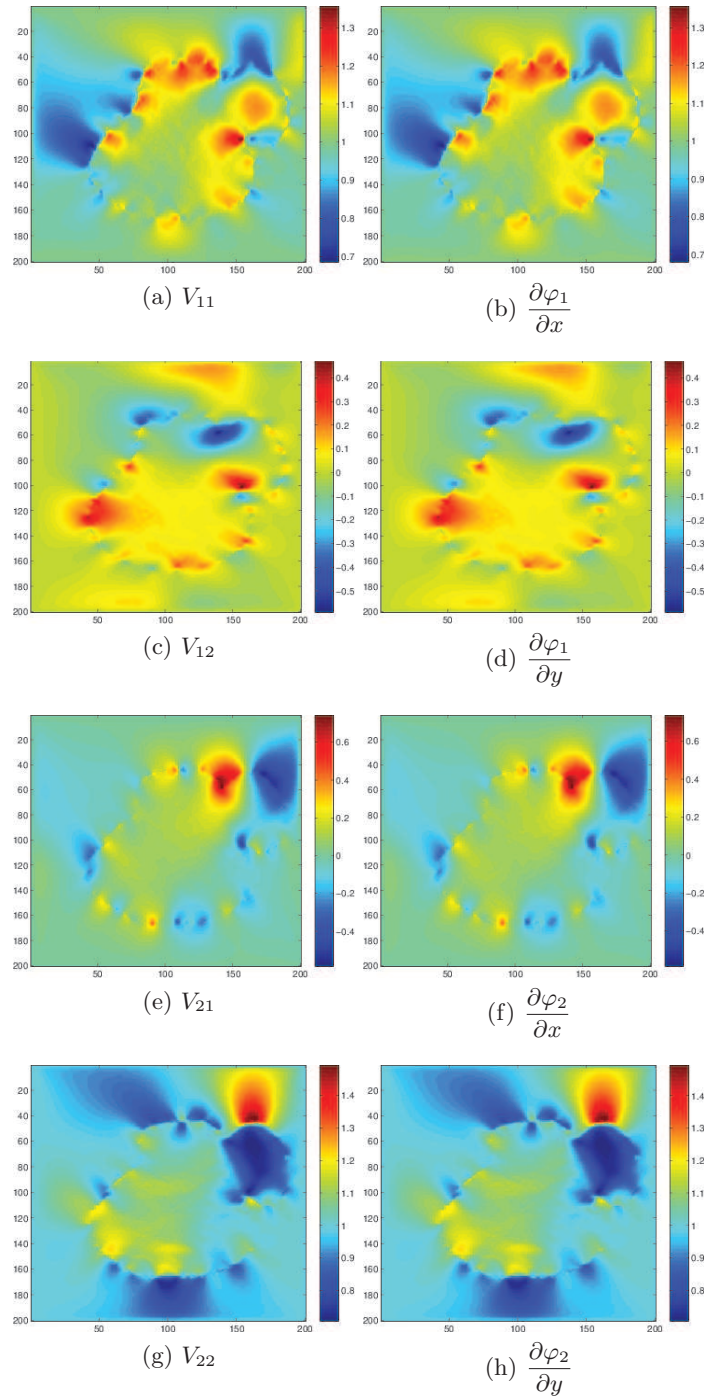


Figure 4.6: Display of V_{11} versus $\frac{\partial \varphi_1}{\partial x}$, V_{12} versus $\frac{\partial \varphi_1}{\partial y}$, V_{21} versus $\frac{\partial \varphi_2}{\partial x}$, V_{22} versus $\frac{\partial \varphi_2}{\partial y}$ related to the application of Fig. 6.4. $\|V_{11} - \frac{\partial \varphi_1}{\partial x}\|_\infty = 0.09$, $\|V_{12} - \frac{\partial \varphi_1}{\partial y}\|_\infty = 0.03$, $\|V_{21} - \frac{\partial \varphi_2}{\partial x}\|_\infty = 0.06$, $\|V_{22} - \frac{\partial \varphi_2}{\partial y}\|_\infty = 0.07$

4.3.5 Slices of the brain

The method has also been applied to complex slices of brain data (Fig 4.7) (courtesy of Laboratory Of Neuro-Imaging, UCLA). We aim to register a torus to the slice of brain with topology preservation to demonstrate the ability of the algorithm to handle complex topologies. The results are very satisfactory on this example since the deformed Template matches very well the convolutions of the brain. The interior contour of the right part of the torus moves to the upper boundary of the hole, while the exterior contour moves towards the upper envelope, entailing large deformations since the thickness of this part of the brain is much greater than the thickness of the torus.

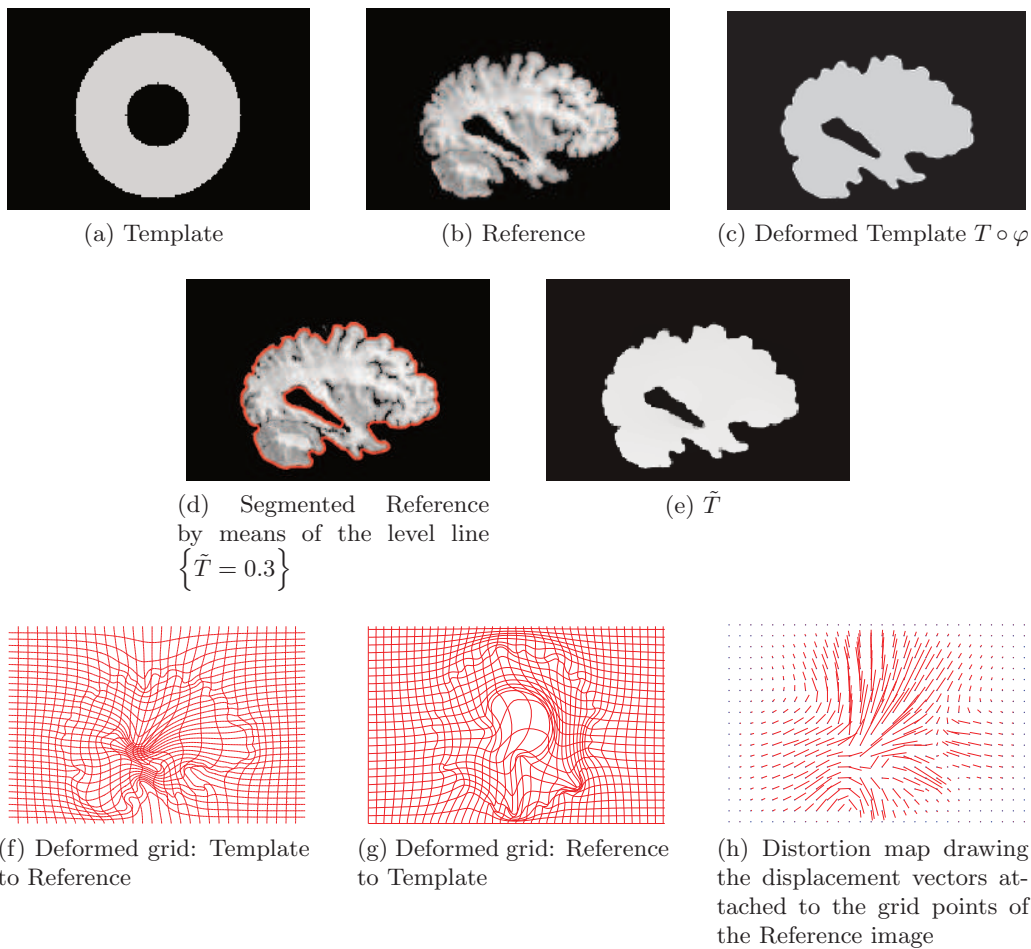


Figure 4.7: **Mapping of a torus to a slice of a brain.**

Execution time: 5 minutes for 128×192 pixel images. 2 regriding steps. $\min \det \nabla \varphi = 0.06$, $\max \det \nabla \varphi = 14.8$.

4.3.6 MRI images of cardiac cycle

Finally, numerical simulations on MRI images of a patient cardiac cycle have been carried out. We were supplied with a whole cardiac MRI examination of a patient (courtesy of the LITIS, University of Rouen, France). It is made of 280 images divided into 14 levels of slice and 20 images per cardiac cycle. The numbering of the images goes from 0 to 279, and includes both the slice number and the time index. The image 0 is set at the upper part of the heart and the sequence from image 0 to image 19 contains the whole cardiac cycle for this slice. The sequence from images 20 to 39 contains the whole cardiac cycle for the slice underneath the previous one and so on. A cardiac cycle is composed of a contraction phase (40% of the cycle duration), followed by a dilation phase (60% of the cycle duration). The first image of the sequence (frames 0, 20, 40, etc.) is when the heart is most dilated (end diastole - ED) and the 8th of the sequence (end systole - ES) is when the heart is most contracted. It thus seemed relevant, in order to assess the accuracy of the proposed algorithm in handling large deformations, to register a pair of the type: Reference corresponding to end diastole (ED), that is the first image of a sequence, and Template corresponding to end systole (ES), that is the 8th frame of the same sequence. Besides, due to the patient's breathing, images from a slice to another are not stackable (whereas they should be) so we also registered pairs of the form 120-140, that thus correspond to two images taken when the heart is most dilated but at different levels of slice.

We provide extra numerical results on the webpage <http://lmi.insa-rouen.fr/31.html>

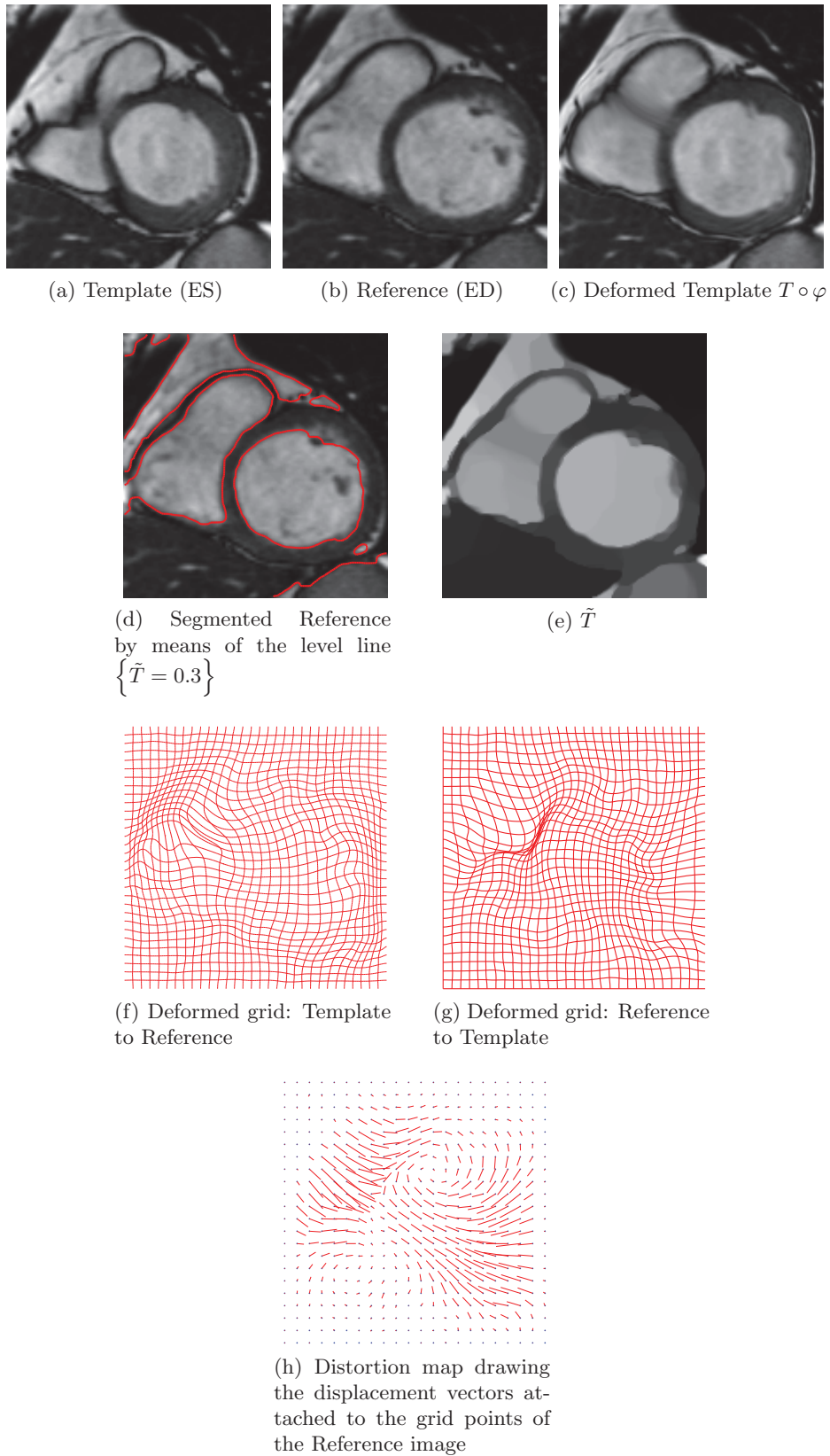
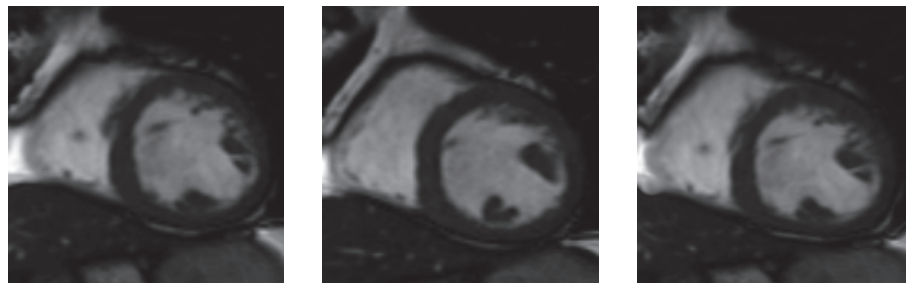
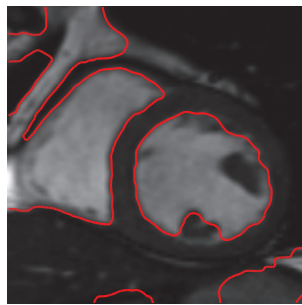


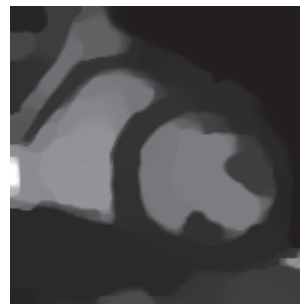
Figure 4.8: **Mapping of MRI images. Reference corresponding to end diastole (ED) and Template corresponding to end systole (ES) of a same sequence.** Execution time: 13 minutes for 150×150 pixel images. 1 regriding step. $\min \det \nabla \varphi = 0.01$, $\max \det \nabla \varphi = 3.83$.



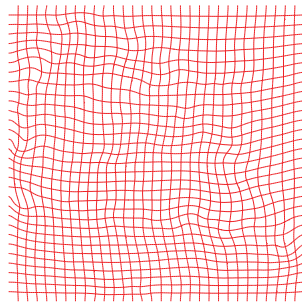
(a) Template (ED) at a given slice (b) Reference (ED) at a different slice (c) Deformed Template $T \circ \varphi$



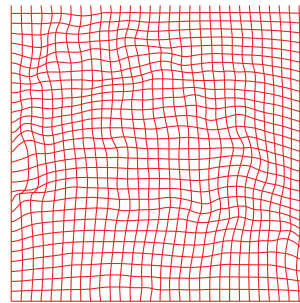
(d) Segmented Reference by means of the level line $\{\tilde{T} = 0.3\}$



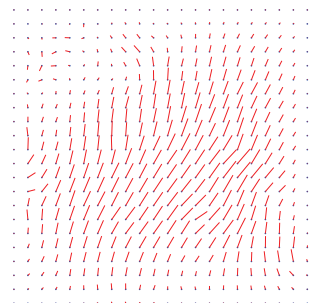
(e) \tilde{T}



(f) Deformed grid: Template to Reference



(g) Deformed grid: Reference to Template



(h) Distortion map drawing the displacement vectors attached to the grid points of the Reference image

Figure 4.9: Mapping of MRI images. Heart slices of the form 120-140 corresponding to two images taken when the heart is most dilated but at different levels of slice.

Execution time: 15 minutes for 150×150 pixel images. $\min \det \nabla \varphi = 0.18$, $\max \det \nabla \varphi = 2.92$.

4.3.7 Comparisons with prior related works

The question of comparing the proposed model with prior ones is legitimate but difficult to address since the goal of the model is twofold (producing a smooth deformation map and obtaining a simplified version of the Reference image yielding to its segmentation) and since encompassing 3 levels of discussion :

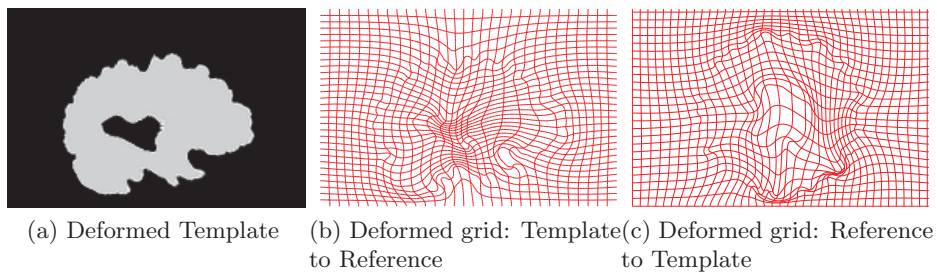
1. the relevance of the nonlinear elasticity based regularizer compared to classical regularization terms (diffusion, biharmonic, linear elasticity models) that lead to linear terms with respect to derivatives in the Euler-Lagrange equations,
2. the relevance of the dissimilarity measure based on the weighted total variation,
3. the accuracy of the segmentation, which is already addressed in subsections 4.3.2 and 4.3.4.

To tackle the two previous points (keeping in mind that we implement the computer codes ex-nihilo by ourselves) in depth, we have investigated several angles of inquiry.

Due to the large amount of literature in the field of registration, we had to make a choice as for the alternative methods to be compared with our model. First, we decided to focus on non parametric registration methods, category of methods we are familiar with. In [28], Lin *et al.* first review the most common and simplest regularization terms (diffusion, biharmonic, linear elasticity models) that lead to linear terms with respect to derivatives in the Euler-Lagrange equations. Then they introduce a nonlinear elasticity regularization based on the basic Saint Venant-Kirchhoff stored energy function in order to allow for larger and smoother deformations. The first conclusion is that, by comparison with image registration models involving linear regularization, the nonlinear-elasticity-based model renders better ground truth, produces larger mutual information and requires fewer numerical corrections such as regriding steps. The second conclusion is that the biharmonic model is more comparable to the nonlinear elasticity model, which motivates us to further examine its behaviour compared with our model. Three kinds of experiments have been conducted: the first kind consisted in replacing the nonlinear-elasticity-based regularizer by the biharmonic one, keeping the dissimilarity measure untouched. The second kind of experiments consisted both in replacing the nonlinear-elasticity-based regularizer by the biharmonic one and in removing the weighted total variation in order to assess its relevance. In both cases (even if including the weighted total variation yields to better results, see the webpage), the obtained deformed Template exhibits artefacts on the boundary of the brain slice, and the hole is not satisfactorily reproduced (after 40000 iterations for this algorithm versus 100 iterations for our model, see Fig. 4.10). To conclude, in order to assess the relevance of the weighted total variation (in addition to allowing for the segmentation of the Reference image), we turned it off in the original nonlinear-elasticity-based model. We see that including the weighted total variation term increases the speed of convergence of the algorithm. For a same number of iterations, the L^2 -fidelity term alone cannot achieve the joint registration/segmentation process (Fig. 4.11). Moreover, in the regions where the matching is achieved, the circumvolutions of the brain are not as clearly reproduced as in the model including the weighted total variation.



Figure 4.10: Obtained result with the biharmonic model after 40000 iterations



(d) Zoom on the circumvolutions when weighted TV is on



(e) Zoom on the circumvolutions when weighted TV is off

Figure 4.11: Obtained results when the weighted total variation is turned off in the nonlinear elasticity based model. The thin concavities are better delineated when the weighted total variation is on.

Remark 4.3.1

Two alternative models have been experimented and give similar results. These are analogously built on Bresson *et al.*'s ones in [6]. The first one consists in minimizing the following functional :

$$\mathcal{G}(\tilde{T}, V) = \nu \int_{\Omega} |\tilde{T} - R| dx + \text{var}_g(\tilde{T}) + \int_{\Omega} QW(V) dx \quad (4.15)$$

$$\begin{aligned} \text{subjected to } \|\tilde{T} - T \circ \varphi\|_{L^2(\Omega)}^2 &\leq \varepsilon, \\ \|\nabla \varphi - V\|_{L^2(\Omega, M_2)}^2 &\leq \varepsilon, \end{aligned} \quad (4.16)$$

with the idea to let ε tend to 0. The second one, also based on [6], employs Chan-Vese segmentation principles:

$$\mathcal{H}(\tilde{T}, V) = \nu \int_{\Omega} ((c_1 - R)^2 - (c_2 - R)^2) \tilde{T} dx + \text{var}_g(\tilde{T}) + \int_{\Omega} QW(V) dx \quad (4.17)$$

$$\begin{aligned} \text{subjected to } \|\tilde{T} - T \circ \varphi\|_{L^1(\Omega)} &\leq \varepsilon, \\ \|\nabla \varphi - V\|_{L^2(\Omega, M_2)}^2 &\leq \varepsilon, \end{aligned} \quad (4.18)$$

$$\text{where } c_1 = \frac{\int_{\Omega} R(x)H(\tilde{T})}{\int_{\Omega} H(\tilde{T})} \text{ and } c_2 = \frac{\int_{\Omega} R(x)(1 - H(\tilde{T}))}{\int_{\Omega} (1 - H(\tilde{T}))}.$$

This is still a work in progress.

Conclusion

We therefore have designed functionals for image joint registration/segmentation problem, not only based on intensity differences but also on weighted total variation in order to favor shape alignment rather than intensity matching. Moreover, we overcome the obstacle of non quasiconvexity of the stored energy function of Saint Venant-Kirchhoff using a relaxed problem associated with the original one. Then we provide theoretical results as existence of minimizers for the relaxed problem and equality of the two infima under certain conditions. Also a Γ -convergence result for the decoupled problem is established.

Our future work consists in extending the problem to the 3D case, using the formulation of the Saint Venant-Kirchhoff stored function in terms of the singular values of $\nabla \varphi$ and a finite element approach for the numerical discretization as done by Le Dret in [26].

Acknowledgment: We would like to thank Dr. Caroline Petitjean (LITIS, Université de Rouen, France) for providing us with the cardiac cycle MRI images. Her help has been much appreciated and has been decisive.

- [1] L. AMBROSIO AND G. DAL MASO, *A general chain rule for distributional derivatives*, Proceedings of the American Mathematical Society, 108 (1990), pp. 691–702.
- [2] A. BALDI, *Weighted BV functions*, Houston Journal of Mathematics, 27 (2001), pp. 683–705.
- [3] M. BEG, M. MILLER, A. TROUVÉ, AND L. YOUNES, *Computing Large Deformation Metric Mappings via Geodesic Flows of Diffeomorphisms*, International Journal of Computer Vision, 61 (2005), pp. 139–157.
- [4] G. BELLETTINI, G. BOUCHITTÉ, AND I. FRAGALÀ, *Bv functions with respect to a measure and relaxation of metric integral functionals*, Journal of convex analysis, 6 (1999), pp. 349–366.
- [5] M. BOUSSELSAL, *Étude de Quelques Problèmes de Calcul des Variations Liés à la Mécanique*, PhD thesis, University of Metz, France, 1993.
- [6] X. BRESSON, S. ESEDOĞLU, P. VANDERGHEYNST, J.-P. THIRAN, AND S. OSHER, *Fast Global Minimization of the Active Contour/Snake Model*, J. Math. Imaging Vis., 68 (2007), pp. 151–167.
- [7] M. BURGER, J. MODERSITZKI, AND L. RUTHOTTO, *A hyperelastic regularization energy for image registration*, SIAM Journal on Scientific Computing, 35 (2013), pp. B132–B148.
- [8] V. CASELLES, R. KIMMEL, AND G. SAPIRO, *Geodesic Active Contours*, Int. J. Comput. Vis., 22 (1993), pp. 61–87.
- [9] A. CHAMBOLLE, *An algorithm for total variation minimization and applications*, J. Math. Imaging Vis., 20 (2004), pp. 89–97.
- [10] T. CHAN, S. ESEDOĞLU, AND M. NIKOLOVA, *Algorithms for finding global minimizers of image segmentation and denoising models*, SIAM J. Appl. Math., 66 (2006), pp. 1632–1648.
- [11] T. CHAN AND L. VESE, *Active Contours Without Edges*, IEEE Trans. Image Process., 10 (2001), pp. 266–277.

- [12] G. CHRISTENSEN, R. RABBITT, AND M. MILLER, *Deformable Templates Using Large Deformation Kinematics*, IEEE Trans. Image Process., 5 (1996), pp. 1435–1447.
- [13] G. E. CHRISTENSEN, *Deformable shape models for anatomy*, PhD thesis, Washington University, Sever Institute of technology, USA, 1994.
- [14] H. CHUI AND A. RANGARAJAN, *A new point matching algorithm for non-rigid registration*, Computer Vision and Image Understanding, 89 (2003), pp. 114–141.
- [15] P. CIARLET, *Elasticité Tridimensionnelle*, Masson, 1985.
- [16] ———, *Mathematical Elasticity, Volume I: Three-dimensional elasticity*, Amsterdam etc., North-Holland, 1988.
- [17] B. DACOROGNA, *Direct Methods in the Calculus of Variations, Second Edition*, Springer, 2008.
- [18] F. DEMENGEL AND G. DEMENGEL, *Functional Spaces for the Theory of Elliptic Partial Differential Equations*, Springer, 2012.
- [19] R. DERFOUL AND C. LE GUYADER, *A relaxed problem of registration based on the Saint Venant-Kirchhoff material stored energy for the mapping of mouse brain gene expression data to a neuroanatomical mouse atlas*, SIAM Journal on Imaging Sciences, 7 (2014), pp. 2175–2195.
- [20] L. R. DICE, *Measures of the Amount of Ecologic Association Between Species*, Ecology, 26 (1945), pp. 297–302.
- [21] M. DROSKE AND M. RUMPF, *A Variational Approach to Non-Rigid Morphological Registration*, SIAM J. Appl. Math., 64 (2004), pp. 668–687.
- [22] J. DURAN, B. COLL, AND C. SBERT, *Chambolle’s projection algorithm for total variation denoising*, Image Processing On Line, 2013 (2013), pp. 311–331.
- [23] A. GOOYA, K. POHL, M. BILELLO, L. CIRILLO, G. BIROS, E. MELHEM, AND C. DAVATZIKOS, *GLISTR: Glioma Image Segmentation and Registration*, Medical Imaging, IEEE Transactions on, 31 (2012), pp. 1941–1954.
- [24] E. HABER, S. HELDMANN, AND J. MODERSITZKI, *A computational framework for image-based constrained registration*, Linear Algebra and its Applications, 431 (2009), pp. 459–470. Special Issue in honor of Henk van der Vorst.
- [25] N. KERDID, H. LE DRET, AND A. SAÏDI, *Numerical approximation for a non-linear membrane problem*, International Journal of Non-Linear Mechanics, 43 (2008), pp. 908–914.
- [26] H. LE DRET AND A. RAOULT, *The quasi-convex envelope of the Saint Venant-Kirchhoff stored energy function.*, Proceedings of the Royal Society of Edinburgh: Section A Mathematics, 125 (1995), pp. 1179–1192.
- [27] C. LE GUYADER AND L. VESE, *A combined segmentation and registration framework with a nonlinear elasticity smoother*, Computer Vision and Image Understanding, 115 (2011), pp. 1689–1709.

- [28] T. LIN, C. LE GUYADER, I. DINOVI, P. THOMPSON, A. TOGA, AND L. VESE, *Gene Expression Data to Mouse Atlas Registration Using a Nonlinear Elasticity Smoother and Landmark Points Constraints*, J. Sci. Comput., 50 (2012), pp. 586–609.
- [29] N. LORD, J. HO, B. VEMURI, AND S. EISENSCHENK, *Simultaneous Registration and Parcellation of Bilateral Hippocampal Surface Pairs for Local Asymmetry Quantification*, IEEE Trans. Med. Imaging, 26 (2007), pp. 471–478.
- [30] M. MILLER, A. TROUVÉ, AND L. YOUNES, *On the Metrics and Euler-Lagrange Equations of Computational Anatomy*, Annu. Rev. B. Eng., 4 (2002), pp. 375–405.
- [31] M. I. MILLER AND L. YOUNES, *Group actions, homeomorphisms, and matching: A general framework*, International Journal of Computer Vision, 41 (2001), pp. 61–84.
- [32] J. MODERSITZKI, *Numerical Methods for Image Registration*, Oxford University Press, 2004.
- [33] ———, *FAIR: Flexible Algorithms for Image Registration*, Society for Industrial and Applied Mathematics (SIAM), 2009.
- [34] P. NEGRÓN MARRERO, *A numerical method for detecting singular minimizers of multidimensional problems in nonlinear elasticity*, Numerische Mathematik, 58 (1990), pp. 135–144.
- [35] S. OZERÉ AND C. LE GUYADER, *Topology preservation for image-registration-related deformation fields*, Communications in Mathematical Sciences, 13 (2015), pp. 1135–1161.
- [36] R. RABBITT, J. WEISS, G. CHRISTENSEN, AND M. MILLER, *Mapping of Hyperelastic Deformable Templates Using the Finite Element Method*, in Proceedings SPIE, vol. 2573, SPIE, 1995, pp. 252–265.
- [37] A. RAOULT, *Non-polyconvexity of the stored energy function of a Saint Venant-Kirchhoff material*, Aplikace Matematiky, 31 (1986), pp. 417–419.
- [38] L. RUDIN, S. OSHER, AND E. FATEMI, *Nonlinear Total Variation Based Noise Removal Algorithms*, Phys. D, 60 (1992), pp. 259–268.
- [39] D. SHEN AND C. DAVATZIKOS, *HAMMER: hierarchical attribute matching mechanism for elastic registration*, Medical Imaging, IEEE Transactions on, 21 (2002), pp. 1421–1439.
- [40] A. SOTIRAS, C. DAVATZIKOS, AND N. PARAGIOS, *Deformable medical image registration: A survey*, Medical Imaging, IEEE Transactions on, 32 (2013), pp. 1153–1190.
- [41] T. W. TANG AND A. C. CHUNG, *Non-rigid image registration using graph-cuts*, in Medical Image Computing and Computer-Assisted Intervention—MICCAI 2007, Springer, 2007, pp. 916–924.
- [42] B. VEMURI, J. YE, Y. CHEN, AND C. LEONARD, *Image Registration via level-set motion: Applications to atlas-based segmentation*, Medical Image Analysis, 7 (2003), pp. 1–20.

- [43] F. WANG, B. C. VEMURI, A. RANGARAJAN, AND S. J. EISENSCHENK, *Simultaneous nonrigid registration of multiple point sets and atlas construction*, Pattern Analysis and Machine Intelligence, IEEE Transactions on, 30 (2008), pp. 2011–2022.
- [44] W. M. WELLS, P. VIOLA, H. ATSUMI, S. NAKAJIMA, AND R. KIKINIS, *Multi-modal volume registration by maximization of mutual information*, Medical image analysis, 1 (1996), pp. 35–51.
- [45] A. YEZZI, L. ZOLLEI, AND T. KAPUR, *A variational framework for joint segmentation and registration*, in Mathematical Methods in Biomedical Image Analysis, IEEE-MMBIA, 2001, pp. 44–51.

CHAPTER 5

NONLOCAL JOINT SEGMENTATION REGISTRATION MODEL

In this chapter, we address the issue of designing a theoretically well-motivated joint segmentation-registration method capable of handling large deformations. The shapes to be matched are implicitly modeled by level set functions and are evolved in order to minimize a functional containing both a nonlinear-elasticity-based regularizer and a criterion that forces the evolving shape to match intermediate topology-preserving segmentation results.

The chapter is organized as follows. First, we present the mathematical modelling and we introduce the nonlinear-elasticity-based regularizer. Then we are concerned with the design of the fidelity term inspired by a topology-preserving segmentation model. Next, we proceed with the study of theoretical results encompassing existence of minimizers, a Γ -convergence result and the existence of a weak viscosity solution of the related evolution problem. Finally, we provide a discretization method and implementation details as well as some numerical results.

Introduction

Image segmentation aims to partition a given image into meaningful constituents or to find boundaries delineating such objects (see [1, Chapter 4] for instance, for a relevant analysis of this problem), while registration, given two images called Template and Reference, consists in determining a smooth deformation field φ such that the deformed Template is aligned with the Reference. According to the modalities of the involved images, the goal of registration might differ: for images of the same modality, the purpose of registration is to match the geometrical features, the shapes and the intensity level distribution of the Reference with those of the Template. When the images have been acquired through different mechanisms and have different modalities, registration aims to correlate both images in terms of shapes and salient components, while preserving the modality of the Template image. In this paper, instead of considering these two tasks, segmentation and registration, as independent ones, we propose to jointly treat them: the segmentation result obtained at intermediate steps will serve as a target to reach in the registration process and will guide it. The scope of the proposed work is thus first to devise a theoretically well-motivated registration model in a variational formulation, authorizing large and smooth deformations. In particular, classical

regularizers such as linear elasticity (see [6]) are not suitable for this kind of problems involving large deformations since assuming small strains and the validity of Hooke's law. In addition, to handle a large class of images, we propose defining a geometric dissimilarity measure based on shape comparisons thanks to successive segmentation results that will serve as inputs in our registration model. Thus the algorithm produces both a smooth mapping between the two shapes as well as a segmentation of the Reference image. The idea of combining segmentation and registration is not new. Prior related works suggest to take advantage of both processes: in [28], a curve evolution approach is used and phrased in terms of level set functions. In [26], Vemuri *et al.* propose a coupled PDE model to perform both segmentation and registration. In the first PDE, the level sets of the source image are evolved along their normals with a speed defined as the difference between the target and the evolving source image. In [18], the model combines a matching criterion based on the active contours without edges ([9]) and a nonlinear-elasticity-based regularizer. In [19], Lord *et al.* propose a unified method that simultaneously treats segmentation and registration based on metric structure comparisons. In [15], Droske *et al.* aim to match the edges and the normals of the two images by applying a Mumford-Shah type free discontinuity problem. More recently, Ozeré *et al.* ([22]) have introduced a variational joint segmentation/registration model combining a measure of dissimilarity based on weighted total variation and a regularizer based on the stored energy function of a Saint Venant-Kirchhoff material.

5.1 Mathematical Modelling

Making the same assumptions as those in the previous chapters, let us denote by:

- Ω a connected bounded open subset of \mathbb{R}^2 with Lipschitz boundary $\partial\Omega$,
- $R : \bar{\Omega} \rightarrow \mathbb{R}$, representing the Reference image,
- $T : \bar{\Omega} \rightarrow \mathbb{R}$, the Template image assumed to be compactly supported and Lipschitz continuous (we denote by k_T the Lipschitz constant),
- $\varphi : \bar{\Omega} \rightarrow \mathbb{R}^2$ the sought deformation with prescribed values on the boundary: $\varphi = \text{Id}$ on $\partial\Omega$.

The shape contained in the Template image is supposed to be modeled by a Lipschitz continuous function Φ_0 whose zero level line is the shape boundary. Denoting by \mathcal{C} the zero level set of Φ_0 and by $w \subset \Omega$ the open set it delineates, Φ_0 is chosen such that

$$\begin{aligned}\mathcal{C} &= \{x \in \Omega \mid \Phi_0(x) = 0\}, \\ w &= \{x \in \Omega \mid \Phi_0(x) > 0\}, \\ \Omega \setminus \bar{w} &= \{x \in \Omega \mid \Phi_0(x) < 0\}.\end{aligned}$$

For theoretical and numerical purposes, we may consider a linear extension operator (see [5, p. 158]) $P : W^{1,\infty}(\Omega) \rightarrow W^{1,\infty}(\mathbb{R}^2)$ such that for all $\Phi \in W^{1,\infty}(\Omega)$,

- (i) $P\Phi|_{\Omega} = \Phi$,
- (ii) $\|P\Phi\|_{L^\infty(\mathbb{R}^2)} \leq C \|\Phi\|_{L^\infty(\Omega)}$,
- (iii) $\|P\Phi\|_{W^{1,\infty}(\mathbb{R}^2)} \leq C \|\Phi\|_{W^{1,\infty}(\Omega)}$, with C depending only on Ω .

By this extension process, we consider then that $\Phi_0 \in W^{1,\infty}(\mathbb{R}^2)$ to ensure that $\Phi_0 \circ \varphi$ – with φ introduced later – is always defined.

Let $\varphi : \bar{\Omega} \rightarrow \mathbb{R}^2$ be the sought deformation. A deformation is a smooth mapping that is orientation-preserving and injective, except possibly on $\partial\Omega$. We also denote by u the associated displacement such that $\varphi = \text{Id} + u$, Id denoting the identity mapping. The deformation gradient is $\nabla\varphi = I + \nabla u$, $\bar{\Omega} \rightarrow M_2(\mathbb{R})$, the set $M_2(\mathbb{R})$ being the set of all real square matrices of order 2 identified to \mathbb{R}^4 .

The idea is thus to find a smooth deformation field φ such that the zero level line of $\Phi_0 \circ \varphi$ gives a relevant partition of the Reference image R , relating then segmentation and registration. The model is phrased as a functional minimization problem with unknown φ ; it combines a smoother on the deformation field, and a distance measure criterion between $\Phi_0 \circ \varphi$ and an input resulting from the topology-preserving segmentation process of Le Guyader and Vese ([17]).

In many applications, such as medical imaging, topology preservation is a desirable property: when the shape to be detected has a known topology (e.g. spherical topology for the brain), or when the resulting shape must be homeomorphic to the initial one. In other words, an initial contour should be deformed without change of topology as merging or breaking. We expect this property to be inherited by the registration process. This measure constitutes an alternative to classical intensity-based/information-theoretic-based matching measures, mutual information – suitable when dealing with images that have been acquired through different sensors –, measures based on the comparison of gradient vector fields of both images, metric structure comparisons, mass-preserving measures, etc. The proposed matching criterion is complemented by a nonlinear-elasticity-based regularizer on the deformation field φ . To allow large and nonlinear deformations, we propose to view the shapes to be warped as isotropic, homogeneous, hyperelastic materials and more precisely as Saint Venant-Kirchhoff materials (see [11] for further details and [7] for an alternative hyperelastic model). A motivation for this choice is that the stored energy function of such materials is the simplest one that agrees with the generic expression of the stored energy of an isotropic, homogeneous, hyperelastic material. To ensure that the distribution of the deformation Jacobian determinants does not exhibit shrinkages or growths, we propose complementing the model by a term controlling that the Jacobian determinant remains close to 1. At this stage, the considered regularizer would be, setting $F = \nabla\varphi$

$$W(F) = W_{SVK}(F) + \mu (\det F - 1)^2,$$

with $W_{SVK}(F) = \frac{\lambda}{2} (\text{tr } E)^2 + \mu \text{tr } E^2$, the stored energy function of a Saint Venant-Kirchhoff material, λ and μ the Lamé coefficients, $E = (F^T F - I)/2$ the Green-Saint Venant stress tensor measuring the deviation between φ and a rigid deformation, and with the following notation $A : B = \text{tr } A^T B$, the matrix inner product and $\|A\| = \sqrt{A : A}$ the related matrix norm (Frobenius norm).

Nevertheless, the stored energy function W written as is exhibits undesirable properties: it is not rank-1 convex (as the density W_{SVK}), and consequently neither quasiconvex, nor polyconvex, which raises a drawback of theoretical nature since we cannot obtain the weak lower semicontinuity of the introduced functional. The idea is thus to replace W by its quasiconvex envelope QW (see [13] for a deeper presentation of these notions). In general, deriving the explicit expression of this envelope is an hopeless task, but in this case, using

Jensen's inequality and a decomposition result by Bousssalsal ([4]), one can establish that

$$QW(F) = \begin{cases} W(F) = \beta (\|F\|^2 - \alpha)^2 + \psi(\det F) & \text{if } \|F\|^2 \geq \alpha, \\ \psi(\det F) & \text{if } \|F\|^2 < \alpha, \end{cases}$$

with $\alpha = 2 \frac{\lambda + \mu}{\lambda + 2\mu}$, $\beta = \frac{\lambda + 2\mu}{8}$ and ψ the convex mapping defined by

$$\psi : t \mapsto -\frac{\mu}{2}t^2 + \mu(t-1)^2 + \frac{\mu(\lambda + \mu)}{2(\lambda + 2\mu)}.$$

Remark 5.1.1

In fact, we can prove a stronger result, namely, that the polyconvex envelope of W , PW , coincides with the quasiconvex envelope of W : $PW = QW$.

Ultimately, we propose to consider the following minimization problem, with $T > 0$ fixed

$$\inf \left\{ \bar{I}(\varphi) = \int_{\Omega} f(x, \varphi(x), \nabla \varphi(x)) dx : \varphi \in \text{Id} + W_0^{1,4}(\Omega, \mathbb{R}^2) \right\}, \quad (5.1)$$

with $f(x, \varphi, \xi) = \frac{\nu}{2} \|\Phi_0 \circ \varphi - \tilde{\Phi}(\cdot, T)\|^2 + QW(\xi)$ and $\tilde{\Phi}$ a solution of the evolution equation stemming from the topology-preserving segmentation model by Le Guyader and Vese ([17])

$$\begin{cases} \frac{\partial \tilde{\Phi}}{\partial t} = |\nabla \tilde{\Phi}| \left[\text{div} \left(\tilde{g}(|\nabla R|) \frac{\nabla \tilde{\Phi}}{|\nabla \tilde{\Phi}|} \right) \right] + 4 \frac{\mu'}{d^2} \bar{H}(\tilde{\Phi}(x) + l) \bar{H}(l - \tilde{\Phi}(x)) \\ \int_{\Omega} \left[\langle x - y, \nabla \tilde{\Phi}(y) \rangle e^{-\|x-y\|_2^2/d^2} \bar{H}(\tilde{\Phi}(y) + l) \bar{H}(l - \tilde{\Phi}(y)) \right] dy, \\ \tilde{\Phi}(x, 0) = \Phi_0(x), \\ \frac{\partial \tilde{\Phi}}{\partial \vec{\nu}} = 0, \quad \text{on } \partial\Omega. \end{cases} \quad (E)$$

Function \tilde{g} is an edge-detector function satisfying

- (i) $\tilde{g}(0) = 1$,
- (ii) \tilde{g} strictly decreasing,
- (iii) $\lim_{r \rightarrow +\infty} \tilde{g}(r) = 0$.

This evolution equation results from the minimization of functional $J(\tilde{\Phi}) + \mu' L(\tilde{\Phi})$ ($\mu' > 0$, tuning parameter), combination of $J(\tilde{\Phi}) = \int_{\Omega} \tilde{g}(|\nabla R|) |D\bar{H}(\tilde{\Phi})|$ coming from the classical geodesic active contour model ([8]) (\bar{H} being the one-dimensional Heaviside function) and L , related to the topological constraint:

$$L(\tilde{\Phi}) = - \int_{\Omega} \int_{\Omega} \left[\exp \left(-\frac{\|x-y\|_2^2}{d^2} \right) \langle \nabla \tilde{\Phi}(x), \nabla \tilde{\Phi}(y) \rangle \bar{H}(\tilde{\Phi}(x) + l) \bar{H}(l - \tilde{\Phi}(x)) \right. \\ \left. \bar{H}(\tilde{\Phi}(y) + l) \bar{H}(l - \tilde{\Phi}(y)) \right] dx dy. \quad (5.2)$$

The Euclidean scalar product in \mathbb{R}^2 is denoted by $\langle \cdot, \cdot \rangle$ and $\|\cdot\|_2$ is the associated norm. A geometrical observation motivates the introduction of L . Indeed, in the case when Φ is a

signed-distance function, $|\nabla\Phi| = 1$ and the unit outward normal vector to the zero level line at point x is $-\nabla\Phi(x)$. Let us now consider two points $(x, y) \in \Omega \times \Omega$ belonging to the zero level line of Φ , close enough to each other, and let $-\nabla\Phi(x)$ and $-\nabla\Phi(y)$ be the two unit outward normal vectors to the contour at these points. When the contour is about to merge or split, that is, when the topology of the evolving contour is to change, then $\langle \nabla\Phi(x), \nabla\Phi(y) \rangle \simeq -1$. This remark justifies the construction of L .

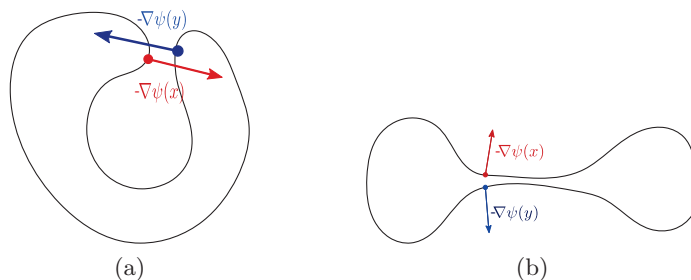


Figure 5.1: Geometrical characterization of points in a zone where the curve is to split, merge, or have a contact point.

The registration process is then fed by the knowledge of the segmentation of the Reference image at time T . In practice, we may apply several times this step.

Also, $\varphi \in \text{Id} + W_0^{1,4}(\Omega, \mathbb{R}^2)$ means that $\varphi = \text{Id}$ —the identity mapping— on $\partial\Omega$ and $\varphi \in W^{1,4}(\Omega, \mathbb{R}^2)$. $W^{1,4}(\Omega, \mathbb{R}^2)$ denotes the Sobolev space of functions $\varphi \in L^4(\Omega, \mathbb{R}^2)$ with distributional derivatives up to order 1 which also belong to $L^4(\Omega)$. (The rewriting of $W(F)$ into $\beta (\|F\|^2 - \alpha)^2 + \Psi(\det F)$ allows to see that $W^{1,4}(\Omega, \mathbb{R}^2)$ is a suitable functional space for the considered minimization problem (5.1): from Hölder's inequality, if $\varphi \in W^{1,4}(\Omega, \mathbb{R}^2)$, then $\det \nabla\varphi \in L^2(\Omega)$).

In the next section, we prove that the infimum of problem (5.1) is attained and that if $\bar{\varphi}$ is a solution of (5.1), then there exists a minimizing sequence $\{\varphi_\nu\}$ of problem (P) defined by

$$\inf_{\varphi \in \text{Id} + W_0^{1,4}(\Omega, \mathbb{R}^2)} I(\varphi) \quad \text{with } I(\varphi) = \frac{\nu}{2} \|\Phi_0 \circ \varphi - \tilde{\Phi}(\cdot, T)\|_{L^2(\Omega)}^2 + \int_{\Omega} W(\nabla\varphi) dx,$$

(i.e., the functional expressed in terms of the Saint Venant-Kirchhoff stored energy function) such that φ_ν weakly converges to $\bar{\varphi}$ and $I(\varphi_\nu) \rightarrow \bar{I}(\bar{\varphi})$. The solutions of (5.1) are considered as generalized solutions of (P) , in the sense of weak convergence. We also ensure that $\tilde{\Phi}(\cdot, T)$ is well-defined, using the viscosity solution theoretical framework.

5.2 Theoretical results

5.2.1 Existence of minimizers and relaxation theorem

We state the main theoretical result related to the existence of minimizers, following arguments similar to those used in [14].

Theorem 5.2.1

The infimum of (5.1) is attained. Let then $\bar{\varphi} \in W^{1,4}(\Omega, \mathbb{R}^2)$ be a minimizer of the relaxed problem (5.1). Then there exists a sequence $\{\varphi_\nu\}_{\nu=1}^\infty \subset \bar{\varphi} + W_0^{1,4}(\Omega, \mathbb{R}^2)$ such that $\varphi_\nu \rightarrow \bar{\varphi}$ in $L^4(\Omega, \mathbb{R}^2)$ as $\nu \rightarrow \infty$ and $I(\varphi_\nu) \rightarrow \bar{I}(\bar{\varphi})$ as $\nu \rightarrow \infty$. Moreover, the following holds: $\varphi_\nu \rightarrow \bar{\varphi}$ in $W^{1,4}(\Omega, \mathbb{R}^2)$ as $\nu \rightarrow \infty$.

It means in particular that
$$I(\varphi) = \min_{\varphi \in \text{Id} + W_0^{1,4}(\Omega, \mathbb{R}^2)} \bar{I}(\varphi),$$

as $QW \leq W$. The solutions of (5.1) are considered as generalized solutions of problem (P).

Proof: The proof is similar to the one of Theorem 6.1.8 in Chapter 6. ■

We now investigate the well-definedness of $\tilde{\Phi}(\cdot, T)$.

5.2.2 Well-definedness of $\tilde{\Phi}$

Problem (E) is hard to handle from a theoretical point of view. A suitable setting would be the one of the viscosity solution theory ([12]) (owing to the nonlinearity induced by the modified mean curvature term), but the dependency of the nonlocal term on the gradient $\nabla \tilde{\Phi}(y)$ and the failure to fulfill the monotony property in $\tilde{\Phi}$ make it difficult. For this reason, for the theoretical part, we consider a slightly modified problem: we assume that the topological constraint is only applied to the zero level line. Assuming that $\tilde{\Phi}$ is a signed-distance function, the topological constraint L is then rephrased as

$$L(\tilde{\Phi}) = - \int_{\Omega} \int_{\Omega} \left[\exp \left(- \frac{\|x - y\|_2^2}{d^2} \right) \langle \nabla \tilde{\Phi}(x), \nabla \tilde{\Phi}(y) \rangle \delta(\tilde{\Phi}(x)) \delta(\tilde{\Phi}(y)) \right] dx dy,$$

with δ the Dirac measure.

The evolution equation coming from the Euler-Lagrange equation associated to $J(\tilde{\Phi}) + \mu L(\tilde{\Phi})$ is computed. It can be formally obtained as follows: let us denote by $\Gamma(\nu) = \mathcal{J}(\nu) + \mu \mathcal{L}(\nu)$ with $\mathcal{J}(\nu) = J(\tilde{\Phi} + \nu \Psi)$ and $\mathcal{L}(\nu) = L(\tilde{\Phi} + \nu \Psi)$, ν being a small parameter and Ψ a function like $\tilde{\Phi}$. A minimizer $\tilde{\Phi}$ will satisfy $\Gamma'(0) = \mathcal{J}'(0) + \mu \mathcal{L}'(0) = 0$ for all functions Ψ .

We set $G(x - y) = \exp \left(- \frac{\|x - y\|_2^2}{d^2} \right)$ and $h(\nabla \tilde{\Phi}(x), \nabla \tilde{\Phi}(y)) = - \langle \nabla \tilde{\Phi}(x), \nabla \tilde{\Phi}(y) \rangle$. We will use the following notations $h = h(z_1, z_2, z_3, z_4)$ and we will denote by $\nabla_{z_1 z_2} h = (h_{z_1}, h_{z_2})^T$ and $\nabla_{z_3 z_4} h = (h_{z_3}, h_{z_4})^T$.

$$\mathcal{L}(\nu) = \int_{\Omega} \int_{\Omega} G(x - y) h \left(\nabla \tilde{\Phi}(x) + \nu \nabla \Psi(x), \nabla \tilde{\Phi}(y) + \nu \nabla \Psi(y) \right) \delta(\tilde{\Phi}(x) + \nu \Psi(x)) \delta(\tilde{\Phi}(y) + \nu \Psi(y)) dx dy.$$

One has,

$$\begin{aligned} \mathcal{L}'(0) &= \int_{\Omega} \int_{\Omega} G(x-y) h \left(\nabla \tilde{\Phi}(x), \nabla \tilde{\Phi}(y) \right) \\ &\quad \left(\delta'(\tilde{\Phi}(x)) \delta(\tilde{\Phi}(y)) \Psi(x) + \delta'(\tilde{\Phi}(y)) \delta(\tilde{\Phi}(x)) \Psi(y) \right) dx dy \\ &+ \int_{\Omega} \int_{\Omega} G(x-y) \delta(\tilde{\Phi}(x)) \delta(\tilde{\Phi}(y)) \\ &\quad \left(\langle \nabla_{z_1 z_2} h(\nabla \tilde{\Phi}(x), \nabla \tilde{\Phi}(y)), \nabla \Psi(x) \rangle + \langle \nabla_{z_3 z_4} h(\nabla \tilde{\Phi}(x), \nabla \tilde{\Phi}(y)), \nabla \Psi(y) \rangle \right) dx dy. \end{aligned}$$

Switching x and y and assuming we can interchange the order of integration, we obtain

$$\begin{aligned} \mathcal{L}'(0) &= 2 \int_{\Omega} \left\{ \int_{\Omega} \left[G(x-y) h(\nabla \tilde{\Phi}(x), \nabla \tilde{\Phi}(y)) \delta'(\tilde{\Phi}(x)) \delta(\tilde{\Phi}(y)) \right] dy \right\} \Psi(x) dx \\ &\quad + 2 \int_{\Omega} \int_{\Omega} G(x-y) \delta(\tilde{\Phi}(x)) \delta(\tilde{\Phi}(y)) \langle \nabla_{z_1 z_2} h(\nabla \tilde{\Phi}(x), \nabla \tilde{\Phi}(y)), \nabla \Psi(x) \rangle dx dy, \end{aligned}$$

and integrating by parts and setting the necessary boundary conditions to zero,

$$\begin{aligned} \mathcal{L}'(0) &= 2 \int_{\Omega} \left\{ \int_{\Omega} \left[G(x-y) h(\nabla \tilde{\Phi}(x), \nabla \tilde{\Phi}(y)) \delta'(\tilde{\Phi}(x)) \delta(\tilde{\Phi}(y)) \right] dy \right\} \Psi(x) dx \\ &\quad - 2 \int_{\Omega} \left\{ \int_{\Omega} \operatorname{div} \left(G(x-y) \delta(\tilde{\Phi}(x)) \delta(\tilde{\Phi}(y)) \nabla_{z_1 z_2} h(\nabla \tilde{\Phi}(x), \nabla \tilde{\Phi}(y)) \right) dy \right\} \Psi(x) dx. \end{aligned}$$

Finally, we obtain the following Euler-Lagrange equation

$$-\delta(\tilde{\Phi}(x)) \operatorname{div} \left(\tilde{g}(|\nabla R|) \frac{\nabla \tilde{\Phi}}{|\nabla \tilde{\Phi}|} \right) - \frac{4\mu}{d^2} \delta(\tilde{\Phi}(x)) \int_{\Omega} \left(\langle x-y, \nabla \tilde{\Phi}(y) \rangle e^{-\frac{\|x-y\|_2^2}{d^2}} \delta(\tilde{\Phi}(y)) \right) dy = 0.$$

Then applying an integration by parts, a gradient descent method and a rescaling by replacing $\delta(\tilde{\Phi})$ by $|\nabla \tilde{\Phi}|$, yields to the evolution problem (defined on \mathbb{R}^2 for the space coordinates for the sake of simplicity)

$$\frac{\partial \tilde{\Phi}}{\partial t} = |\nabla \tilde{\Phi}| \left\{ \operatorname{div} \left(\tilde{g}(|\nabla R|) \frac{\nabla \tilde{\Phi}}{|\nabla \tilde{\Phi}|} \right) + c_0 * \left[\tilde{\Phi}(\cdot, t) \right] \right\}, \quad (5.3)$$

with $\left[\tilde{\Phi}(\cdot, t) \right]$ the characteristic function of the set $\left\{ \tilde{\Phi}(\cdot, t) \geq 0 \right\}$ and

$$c_0 : \begin{cases} \mathbb{R}^2 \rightarrow \mathbb{R} \\ x \mapsto \frac{4\mu}{d^2} \left(2 - \frac{2}{d^2} \|x\|_2^2 \right) \exp \left(-\frac{\|x\|_2^2}{d^2} \right) \end{cases}. \quad (5.4)$$

Remark 5.2.1

A sample of experiments shows that this simplified model qualitatively performs in a similar way to [17] (see [16] in particular).

We now describe the general framework our equation falls within, recall the definition of weak solutions in this context, give the general existence theorem (in the unbounded case) introduced by Barles *et al.* ([2]) and check whether it applies to the considered problem (5.3). Note that the proposed result, which is a result of existence of weak solutions to problem (5.3)– with no restriction on time T – is different from the one obtained in [16], which is a short-time existence/uniqueness result in the classical sense.

General framework

We follow the notations of [2]. Let us consider the class of nonlocal and nonlinear parabolic equations which can be rewritten as

$$\begin{cases} u_t = H[\mathbb{1}_{\{u \geq 0\}}](x, t, u, Du, D^2u) & \text{in } \mathbb{R}^N \times (0, T), \\ u(\cdot, 0) = u_0 & \text{in } \mathbb{R}^N, \end{cases} \quad (5.5)$$

where u_t , Du and D^2u stand respectively for the time derivative, gradient and Hessian matrix with respect to the space variable x of $u : \mathbb{R}^N \times [0, T] \rightarrow \mathbb{R}$, and where $\mathbb{1}_A$ denotes the indicator function of a set A . The initial datum u_0 is a bounded and Lipschitz continuous function on \mathbb{R}^N .

For any indicator function $\chi : \mathbb{R}^N \times [0, T] \rightarrow \mathbb{R}$, or more generally for any $\chi \in L^\infty(\mathbb{R}^N \times [0, T]; [0, 1])$, $H[\chi]$ denotes a function of $(x, t, r, p, A) \in \mathbb{R}^N \times [0, T] \times \mathbb{R} \times \mathbb{R}^N \setminus \{0\} \times \mathcal{S}_N$ where \mathcal{S}_N is the set of real, $N \times N$ symmetric matrices.

For almost any $t \in [0, T]$, $(x, r, p, A) \mapsto H[\chi](x, t, r, p, A)$ is a continuous function on $\mathbb{R}^N \times \mathbb{R} \times \mathbb{R}^N \setminus \{0\} \times \mathcal{S}_N$ with a possible singularity at $p = 0$, while $t \mapsto H[\chi](x, t, r, p, A)$ is a bounded measurable function for all $(x, r, p, A) \in \mathbb{R}^N \times \mathbb{R} \times \mathbb{R}^N \setminus \{0\} \times \mathcal{S}_N$.

The equation is said to be degenerate elliptic if, for any $\chi \in L^\infty(\mathbb{R}^N \times [0, T]; [0, 1])$, for any $(x, r, p) \in \mathbb{R}^N \times \mathbb{R} \times \mathbb{R}^N \setminus \{0\}$, for almost every $t \in [0, T]$ and for all $A, B \in \mathcal{S}_N$, one has:

$$H[\chi](x, t, r, p, A) \leq H[\chi](x, t, r, p, B) \text{ if } A \leq B,$$

with \leq the usual partial ordering for symmetric matrices.

The notion of viscosity solutions for equations with a measurable dependence in time (called L^1 -viscosity solution) is needed to define weak solutions. For a complete presentation of the theory, the reader may refer to [3]. The following definition of weak solutions is introduced in [2].

Definition 5.2.2 (Taken from [2])

Let $u : \mathbb{R}^N \times [0, T] \rightarrow \mathbb{R}$ be a continuous function. u is said to be a weak solution of (5.5) if there exists $\chi \in L^\infty(\mathbb{R}^N \times [0, T]; [0, 1])$ such that:

i) u is a L^1 -viscosity solution of

$$\begin{cases} u_t(x, t) = H[\chi](x, t, u, Du, D^2u) & \text{in } \mathbb{R}^N \times (0, T), \\ u(\cdot, 0) = u_0 & \text{in } \mathbb{R}^N. \end{cases} \quad (5.6)$$

ii) For almost all $t \in [0, T]$,

$$\mathbb{1}_{\{u(\cdot, t) > 0\}} \leq \chi(\cdot, t) \leq \mathbb{1}_{\{u(\cdot, t) \geq 0\}} \text{ a.e. in } \mathbb{R}^N. \quad (5.7)$$

Moreover, we say that u is a classical solution of (5.5) if in addition, for almost every $t \in [0, T]$,

$$\mathbb{1}_{\{u(\cdot, t) > 0\}} = \mathbb{1}_{\{u(\cdot, t) \geq 0\}} \text{ a.e in } \mathbb{R}^N.$$

We now state some assumptions (still following [2]) that are needed to establish the result of existence of at least one weak solution to general problem (5.5).

[A1] i) For any $\chi \in X \subset L^\infty(\mathbb{R}^N \times [0, T]; [0, 1])$, equation (5.6) has a bounded uniformly continuous L^1 -viscosity solution u . Moreover, there exists a constant $L > 0$ independent of $\chi \in X$ such that $|u|_\infty \leq L$.

ii) For any fixed $\chi \in X$, a comparison principle holds for equation (5.6): if u is a bounded, upper semi-continuous L^1 -viscosity subsolution of (5.6) in $\mathbb{R}^N \times (0, T)$ and v is a bounded, lower semi-continuous L^1 -viscosity supersolution of (5.6) in $\mathbb{R}^N \times (0, T)$ with $u(\cdot, 0) \leq v(\cdot, 0)$ in \mathbb{R}^N , then $u \leq v$ in $\mathbb{R}^N \times (0, T)$.

[A2] i) For any compact subset $K \subset \mathbb{R}^N \times \mathbb{R} \times \mathbb{R}^N \setminus \{0\} \times \mathcal{S}^N$, there exists a (locally bounded) modulus of continuity $m_K : [0, T] \times \mathbb{R}^+ \rightarrow \mathbb{R}^+$ such that $m_K(\cdot, \varepsilon) \rightarrow 0$ in $L^1(0, T)$ as $\varepsilon \rightarrow 0$, and

$$\begin{aligned} & |H[\chi](x_1, t, r_1, p_1, A_1) - H[\chi](x_2, t, r_2, p_2, A_2)| \leq \\ & m_K(t, |x_1 - x_2| + |r_1 - r_2| + |p_1 - p_2| + |A_1 - A_2|), \end{aligned}$$

for any $\chi \in X$, for almost all $t \in [0, T]$ and all $(x_1, r_1, p_1, A_1), (x_2, r_2, p_2, A_2) \in K$.

ii) There exists a bounded function $h(x, t, r)$, which is continuous in x and r for almost every t and measurable in t , such that: for any neighborhood V of $(0, 0)$ in $\mathbb{R}^N \setminus \{0\} \times \mathcal{S}^N$ and any compact subset $K \subset \mathbb{R}^N \times \mathbb{R}$, there exists a modulus of continuity $m_{K,V} : [0, T] \times \mathbb{R}^+ \rightarrow \mathbb{R}^+$ such that $m_{K,V}(\cdot, \varepsilon) \rightarrow 0$ in $L^1(0, T)$ as $\varepsilon \rightarrow 0$, and

$$|H[\chi](x, t, r, p, A) - h(x, t, r)| \leq m_{K,V}(t, |p| + |A|),$$

for any $\chi \in X$, for almost all $t \in [0, T]$, all $(x, r) \in K$ and $(p, A) \in V$.

iii) If $\chi_n \rightharpoonup \chi$ weakly-* in $L^\infty(\mathbb{R}^N \times [0, T]; [0, 1])$ with $\chi_n, \chi \in X$ for all n , then for all $(x, t, r, p, A) \in \mathbb{R}^N \times [0, T] \times \mathbb{R} \times \mathbb{R}^N \setminus \{0\} \times \mathcal{S}^N$,

$$\int_0^1 H[\chi_n](x, s, r, p, A) ds \xrightarrow{n \rightarrow +\infty} \int_0^1 H[\chi](x, s, r, p, A) ds,$$

locally uniformly for $t \in [0, T]$

[A3] For any $\chi \in X$, for almost every $t \in [0, T]$, for all $(x, p, A) \in \mathbb{R}^N \times \mathbb{R}^N \setminus \{0\} \times \mathcal{S}^N$, and for any $r_1 \leq r_2$,

$$H[\chi](x, t, r_1, p, A) \geq H[\chi](x, t, r_2, p, A).$$

The general existence theorem proposed by Barles *et al.* ([2]) is then:

Theorem 5.2.3 (General existence theorem by Barles *et al.* [2])

Assume that [A1], [A2] and [A3] hold. Then there exists at least a weak solution to (5.5).

Existence of weak solutions of the considered evolution problem

Equipped with these theoretical elements, we now state the main theoretical result regarding the existence of at least one weak solution to problem (5.3).

Theorem 5.2.4

Assuming that $g := \tilde{g}(|\nabla R|)$, $g^{\frac{1}{2}}$ and ∇g are bounded and Lipschitz continuous on \mathbb{R}^2 , problem (5.3) admits at least one weak solution.

Proof: First, one can easily check that setting $C(p) := (I - \frac{p \otimes p}{|p|^2})$,

$$H[\chi](x, t, p, A) = g(x) \operatorname{tr}(C(p)A) + \langle \nabla g(x), p \rangle + |p| \int_{\mathbb{R}^2} c_0(x-y) \chi(y, t) dy.$$

We give the sketch of the proof by mainly checking that the assumptions of Theorem 5.2.3 are fulfilled.

For assumption [A1], we have both to prove the existence of a L^1 -viscosity solution and a comparison principle (following the Perron method). This result is obtained by combining the results of Bourgoing in [3] and Nunziante in [21].

Let us now focus on assumption [A2] i).

$M > 0$ denotes a positive constant that may change line to line and that may depend on K , g , ∇g , $\|c_0\|_{L^1(\mathbb{R}^2)}$ or $\|\nabla c_0\|_{L^1(\mathbb{R}^2)}$. Recall that (x_i, p_i, A_i) belongs to the compact subset K . One then has

$$\begin{aligned} |\langle \nabla g(x_1), p_1 \rangle - \langle \nabla g(x_2), p_2 \rangle| &= |\langle \nabla g(x_1) - \nabla g(x_2), p_1 \rangle + \langle \nabla g(x_2), p_1 - p_2 \rangle| \\ &\leq M (|x_1 - x_2| + |p_1 - p_2|), \end{aligned}$$

due to the properties of ∇g . Also,

$$\begin{aligned} &\left| |p_1| \int_{\mathbb{R}^2} c_0(x_1 - y) \chi(y, t) dy - |p_2| \int_{\mathbb{R}^2} c_0(x_2 - y) \chi(y, t) dy \right| \\ &\leq \left| |p_1| - |p_2| \right| \left| \int_{\mathbb{R}^2} c_0(x_1 - y) \chi(y, t) dy \right| \\ &\quad + |p_2| \left| \int_{\mathbb{R}^2} (c_0(x_1 - y) - c_0(x_2 - y)) \chi(y, t) dy \right|, \\ &\leq |p_1 - p_2| \|c_0\|_{L^1(\mathbb{R}^2)} \|\chi\|_{L^\infty(\mathbb{R}^2 \times [0, T])} \\ &\quad + |p_2| \left| \int_{\mathbb{R}^2} \left(\int_0^1 \langle \nabla c_0((x_2 - y) + s(x_1 - x_2)), x_1 - x_2 \rangle ds \right) \chi(y, t) dy \right|. \end{aligned}$$

A change of variable in the integral allows to conclude that

$$\begin{aligned} & \left| |p_1| \int_{\mathbb{R}^2} c_0(x_1 - y) \chi(y, t) dy - |p_2| \int_{\mathbb{R}^2} c_0(x_2 - y) \chi(y, t) dy \right| \\ & \leq |p_1 - p_2| \|c_0\|_{L^1(\mathbb{R}^2)} \|\chi\|_{L^\infty(\mathbb{R}^2 \times [0, T])} \\ & \quad + |p_2| |x_1 - x_2| \|\chi\|_{L^\infty(\mathbb{R}^2 \times [0, T])} \|\nabla c_0\|_{L^1(\mathbb{R}^2)}, \\ & \leq M (|p_1 - p_2| + |x_1 - x_2|). \end{aligned}$$

It remains to estimate $|g(x_1) \text{tr}(C(p_1)A_1) - g(x_2) \text{tr}(C(p_2)A_2)|$. One has

$$\begin{aligned} & |g(x_1) \text{tr}(C(p_1)A_1) - g(x_2) \text{tr}(C(p_2)A_2)| \leq |g(x_1) - g(x_2)| |\text{tr}(C(p_1)A_1)| \\ & \quad + g(x_2) |\text{tr}(C(p_1)A_1) - \text{tr}(C(p_2)A_2)|, \\ & \leq M |x_1 - x_2| \|C(p_1)\|_F \|A_1\|_F + g(x_2) |\text{tr}((C(p_1) - C(p_2))A_1) \\ & \quad + \text{tr}(C(p_2)(A_1 - A_2))|, \end{aligned}$$

$\|\cdot\|_F$ denoting the Frobenius norm. Remarking that $\|C(p_1)\|_F = 1$ and that one has $\|A_1\|_F \leq \sqrt{2}\|A_1\|_2 = \sqrt{2}|A_1|$, it yields to

$$\begin{aligned} |g(x_1) \text{tr}(C(p_1)A_1) - g(x_2) \text{tr}(C(p_2)A_2)| & \leq M (|x_1 - x_2| + |A_1 - A_2|) \\ & \quad + g(x_2) |\text{tr}((C(p_1) - C(p_2))A_1)|. \end{aligned} \quad (5.8)$$

One can notice that $C(p) = \sigma(p)\sigma(p)^T$ with $\sigma(p) = \begin{pmatrix} \frac{p_{02}}{|p|} & 0 \\ \frac{-p_{01}}{|p|} & 0 \end{pmatrix}$, $p = (p_{01}, p_{02})^T \neq 0$.

Consequently,

$$\begin{aligned} & g(x_2) |\text{tr}((C(p_1) - C(p_2))A_1)| \leq \\ & M |\text{tr}((\sigma(p_1) - \sigma(p_2))\sigma(p_1)^T A_1) + \text{tr}(\sigma(p_2)(\sigma(p_1)^T - \sigma(p_2)^T)A_1)|. \end{aligned}$$

Focusing on the first term of the right part of the inequality, the result being similar for the second component, one obtains

$$\begin{aligned} |\text{tr}((\sigma(p_1) - \sigma(p_2))\sigma(p_1)^T A_1)| & \leq \|A_1\|_F \|\sigma(p_1) - \sigma(p_2)\|_F \|\sigma(p_1)^T\|_F, \\ & \leq M \left| \frac{p_1}{|p_1|} - \frac{p_2}{|p_2|} \right| \leq \frac{|p_1 - p_2|}{\min(|p_1|, |p_2|)}, \end{aligned}$$

so

$$|\text{tr}((\sigma(p_1) - \sigma(p_2))\sigma(p_1)^T A_1)| \leq M |p_1 - p_2|.$$

Including this result in equation (5.8) yields to the desired estimation.

The two remaining assumptions are checked using the same arguments as above and taking h the null function for assumption [A2] ii) and by definition of the L^∞ -weak * convergence for assumption [A2] iii).

Assumption [A3] is obviously fulfilled, $H[\chi]$ being independent of r in the considered problem. ■

5.3 Numerical Method of Resolution

In [20], Negrón Marrero describes and analyzes a numerical method that detects singular minimizers and avoids the Lavrentiev phenomenon for three dimensional problems in non-linear elasticity. This method consists in decoupling the function φ from its gradient and in formulating a related decoupled problem under inequality constraint. In the same spirit, we introduce an auxiliary variable V simulating the Jacobian deformation field $\nabla\varphi$ (–the underlying idea being to remove the nonlinearity in the derivatives of the deformation–) and derive a functional minimization problem phrased in terms of the two variables φ and V . The decoupled problem is thus defined by means of the following functional:

$$\bar{I}_\gamma(\varphi, V) = \frac{\nu}{2} \|\Phi_0 \circ \varphi - \tilde{\Phi}(\cdot, T)\|_{L^2(\Omega)}^2 + \int_{\Omega} QW(V) dx + \frac{\gamma}{2} \|V - \nabla\varphi\|_{L^2(\Omega, M_2)}^2, \quad (5.9)$$

the idea being to let γ tend to $+\infty$. Let us now denote by $\widehat{\mathcal{W}}$ the functional space defined by $\widehat{\mathcal{W}} = \text{Id} + W_0^{1,2}(\Omega, \mathbb{R}^2)$ and by $\widehat{\mathcal{X}}$, the functional space $\widehat{\mathcal{X}} = \{V \in L^4(\Omega, M_2)\}$. The decoupled problem consists in minimizing (5.9) on $\widehat{\mathcal{W}} \times \widehat{\mathcal{X}}$. Then the following theorem holds.

Theorem 5.3.1

Let (γ_j) be an increasing sequence of positive real numbers such that $\lim_{j \rightarrow +\infty} \gamma_j = +\infty$. Let also $(\varphi_k(\gamma_j), V_k(\gamma_j))$ be a minimizing sequence of the decoupled problem with $\gamma = \gamma_j$. Then there exist a subsequence denoted by $(\varphi_{N(\gamma_{\psi \circ \zeta(j)})(\gamma_{\psi \circ \zeta(j)})}, V_{N(\gamma_{\psi \circ \zeta(j)})(\gamma_{\psi \circ \zeta(j)})})$ of $(\varphi_k(\gamma_j), V_k(\gamma_j))$ and a minimizer $\bar{\varphi}$ of \bar{I} ($\bar{\varphi} \in \text{Id} + W_0^{1,4}(\Omega, \mathbb{R}^2)$) such that:

$$\lim_{j \rightarrow +\infty} \bar{I}_{\gamma_{\psi \circ \zeta(j)}} \left(\varphi_{N(\gamma_{\psi \circ \zeta(j)})(\gamma_{\psi \circ \zeta(j)})}, V_{N(\gamma_{\psi \circ \zeta(j)})(\gamma_{\psi \circ \zeta(j)})} \right) = \bar{I}(\bar{\varphi}).$$

Proof: Let $\epsilon > 0$ be given, $\epsilon \in]0, \epsilon_0]$, $\epsilon_0 > 0$ fixed. There exists $\widehat{\varphi}_\epsilon \in \mathcal{W} = \text{Id} + W_0^{1,4}(\Omega, \mathbb{R}^2)$ such that:

$$\begin{aligned} \inf_{(\varphi, V) \in \widehat{\mathcal{W}} \times \widehat{\mathcal{X}}} \bar{I}_\gamma(\varphi, V) &\leq \bar{I}_\gamma(\widehat{\varphi}_\epsilon, \nabla \widehat{\varphi}_\epsilon) = \bar{I}(\widehat{\varphi}_\epsilon) \\ &< \inf_{\varphi \in \mathcal{W}} \bar{I}(\varphi) + \epsilon \leq \inf_{\varphi \in \mathcal{W}} \bar{I}(\varphi) + \epsilon_0. \end{aligned}$$

Consequently,

$$\inf_{(\varphi, V) \in \widehat{\mathcal{W}} \times \widehat{\mathcal{X}}} \bar{I}_\gamma(\varphi, V) \leq \inf_{\varphi \in \mathcal{W}} \bar{I}(\varphi) + \epsilon. \quad (5.10)$$

The second part of the proof consists in taking an increasing sequence (γ_j) of positive real numbers such that $\lim_{j \rightarrow +\infty} \gamma_j = +\infty$. We then consider a minimizing sequence denoted by $(\varphi_k(\gamma_j), V_k(\gamma_j))$ for the decoupled problem with $\gamma = \gamma_j$, that is:

$$\lim_{k \rightarrow +\infty} \bar{I}_{\gamma_j}(\varphi_k(\gamma_j), V_k(\gamma_j)) = \inf_{(\varphi, V) \in \widehat{\mathcal{W}} \times \widehat{\mathcal{X}}} \bar{I}_{\gamma_j}(\varphi, V).$$

In particular, $\forall \epsilon > 0, \exists N(\epsilon, \gamma_j) \in \mathbb{N}, \forall k \in \mathbb{N}$,

$$\left(k \geq N(\epsilon, \gamma_j) \implies \bar{I}_{\gamma_j}(\varphi_k(\gamma_j), V_k(\gamma_j)) \leq \inf_{(\varphi, V) \in \widehat{\mathcal{W}} \times \widehat{\mathcal{X}}} \bar{I}_{\gamma_j}(\varphi, V) + \epsilon \right).$$

Let us take in particular $\epsilon = \frac{1}{\gamma_j}$. There exists $N(\gamma_j) \in \mathbb{N}$ such that $\forall k \in \mathbb{N}$,

$$\left(k \geq N(\gamma_j) \implies \bar{I}_{\gamma_j}(\varphi_k(\gamma_j), V_k(\gamma_j)) \leq \inf_{(\varphi, V) \in \widehat{\mathcal{W}} \times \widehat{\mathcal{X}}} \bar{I}_{\gamma_j}(\varphi, V) + \frac{1}{\gamma_j} \right).$$

We then set $k = N(\gamma_j)$ and we obtain:

$$\begin{aligned} \bar{I}_{\gamma_j}(\varphi_{N(\gamma_j)}(\gamma_j), V_{N(\gamma_j)}(\gamma_j)) &\leq \inf_{(\varphi, V) \in \widehat{\mathcal{W}} \times \widehat{\mathcal{X}}} \bar{I}_{\gamma_j}(\varphi, V) + \frac{1}{\gamma_j}, \\ &\leq \inf_{\varphi \in \mathcal{W}} \bar{I}(\varphi) + \frac{2}{\gamma_j} \leq \inf_{\varphi \in \mathcal{W}} \bar{I}(\varphi) + \frac{2}{\gamma_0} < +\infty, \end{aligned} \quad (5.11)$$

from (5.10).

Similarly to the coercivity inequality obtained in the proof of Theorem 5.2.1, the following inequality holds:

$$\frac{\mu}{4} (\det(V))^2 + \frac{\beta}{2} \|V\|^4 - \beta \alpha^2 - 3\mu + \frac{\mu(\lambda + \mu)}{2(\lambda + 2\mu)} \leq QW(V).$$

As a consequence,

$\left\{ \begin{array}{l} V_{N(\gamma_j)}(\gamma_j) \text{ is uniformly bounded in } L^4(\Omega, M_2) \text{ (so in } L^2(\Omega, M_2) \text{ with } M_2 = M_2(\mathbb{R}) \sim \mathbb{R}^4) \text{ and} \\ \det(V_{N(\gamma_j)}(\gamma_j)) \text{ is uniformly bounded in } L^2(\Omega). \end{array} \right.$

We can thus extract a subsequence denoted by $(V_{N(\gamma_{\Psi(j)})}(\gamma_{\Psi(j)}))$ such that:

$$\left\{ \begin{array}{l} V_{N(\gamma_{\Psi(j)})}(\gamma_{\Psi(j)}) \xrightarrow{j \rightarrow +\infty} \bar{V} \text{ in } L^4(\Omega, M_2), \\ \det(V_{N(\gamma_{\Psi(j)})}(\gamma_{\Psi(j)})) \xrightarrow{j \rightarrow +\infty} \bar{\delta} \text{ in } L^2(\Omega). \end{array} \right.$$

In addition,

$$\begin{aligned} \frac{\gamma_{\Psi(j)}}{2} \|V_{N(\gamma_{\Psi(j)})}(\gamma_{\Psi(j)}) - \nabla \varphi_{N(\gamma_{\Psi(j)})}(\gamma_{\Psi(j)})\|_{L^2(\Omega, M_2)}^2 &\leq \left(\beta \alpha^2 + 3\mu - \frac{\mu(\lambda + \mu)}{2(\lambda + 2\mu)} \right) \text{meas}(\Omega) \\ &\quad + \inf_{\varphi \in \mathcal{W}} \bar{I}(\varphi) + \frac{2}{\gamma_0}, \end{aligned}$$

so,

$$\begin{aligned} \|V_{N(\gamma_{\Psi(j)})}(\gamma_{\Psi(j)}) - \nabla \varphi_{N(\gamma_{\Psi(j)})}(\gamma_{\Psi(j)})\|_{L^2(\Omega, M_2)}^2 &\leq \frac{2}{\gamma_0} \left(\left(\beta \alpha^2 + 3\mu - \frac{\mu(\lambda + \mu)}{2(\lambda + 2\mu)} \right) \text{meas}(\Omega) \right. \\ &\quad \left. + \inf_{\varphi \in \mathcal{W}} \bar{I}(\varphi) + \frac{2}{\gamma_0} \right) \end{aligned}$$

and

$$\begin{aligned} &| \|\nabla \varphi_{N(\gamma_{\Psi(j)})}(\gamma_{\Psi(j)})\|_{L^2(\Omega, M_2)} - \|V_{N(\gamma_{\Psi(j)})}(\gamma_{\Psi(j)})\|_{L^2(\Omega, M_2)} | \\ &\leq \|V_{N(\gamma_{\Psi(j)})}(\gamma_{\Psi(j)}) - \nabla \varphi_{N(\gamma_{\Psi(j)})}(\gamma_{\Psi(j)})\|_{L^2(\Omega, M_2)} \\ &\leq \left(\frac{2}{\gamma_0} \left(\left(\beta \alpha^2 + 3\mu - \frac{\mu(\lambda + \mu)}{2(\lambda + 2\mu)} \right) \text{meas}(\Omega) + \inf_{\varphi \in \mathcal{W}} \bar{I}(\varphi) + \frac{2}{\gamma_0} \right) \right)^{\frac{1}{2}}. \end{aligned}$$

The sequence $(\varphi_{N(\gamma_{\Psi(j)})}(\gamma_{\Psi(j)}))$ is thus uniformly bounded in $W^{1,2}(\Omega, \mathbb{R}^2)$ according to the generalized Poincaré inequality. (Recall that $\varphi_{N(\gamma_{\Psi(j)})}(\gamma_{\Psi(j)}) = \text{Id}$ on $\partial\Omega$). We can therefore extract a subsequence denoted by $(\varphi_{N(\gamma_{\Psi \circ \zeta(j)})}(\gamma_{\Psi \circ \zeta(j)}))$ such that:

$$\varphi_{N(\gamma_{\Psi \circ \zeta(j)})}(\gamma_{\Psi \circ \zeta(j)}) \xrightarrow{j \rightarrow +\infty} \bar{\varphi} \text{ in } W^{1,2}(\Omega, \mathbb{R}^2).$$

To summarize at this stage,

$$\begin{cases} V_{N(\gamma_{\Psi \circ \zeta(j)})}(\gamma_{\Psi \circ \zeta(j)}) \xrightarrow{j \rightarrow +\infty} \bar{V} \text{ in } L^4(\Omega, M_2), \\ \det(V_{N(\gamma_{\Psi \circ \zeta(j)})}(\gamma_{\Psi \circ \zeta(j)})) \xrightarrow{j \rightarrow +\infty} \bar{\delta} \text{ in } L^2(\Omega), \\ \varphi_{N(\gamma_{\Psi \circ \zeta(j)})}(\gamma_{\Psi \circ \zeta(j)}) \xrightarrow{j \rightarrow +\infty} \bar{\varphi} \text{ in } W^{1,2}(\Omega, \mathbb{R}^2). \end{cases}$$

For the sake of clarity, we denote by $h(j) := \Psi \circ \zeta(j)$.

Let us now set $z_j = \nabla \varphi_{N(\gamma_{h(j)})}(\gamma_{h(j)}) - V_{N(\gamma_{h(j)})}(\gamma_{h(j)})$.

Since

$$\|V_{N(\gamma_{h(j)})}(\gamma_{h(j)}) - \nabla \varphi_{N(\gamma_{h(j)})}(\gamma_{h(j)})\|_{L^2(\Omega, M_2)} \leq \frac{1}{\gamma_{h(j)}} \left(\left(\beta \alpha^2 + 3\mu - \frac{\mu(\lambda + \mu)}{2(\lambda + 2\mu)} \right) \text{meas}(\Omega) + \inf_{\varphi \in \mathcal{W}} \bar{I}(\varphi) + \frac{2}{\gamma_0} \right),$$

it implies that $z_j \xrightarrow{j \rightarrow +\infty} 0$ in $L^2(\Omega, M_2)$ and consequently,

$$\nabla \varphi_{N(\gamma_{h(j)})}(\gamma_{h(j)}) \xrightarrow{j \rightarrow +\infty} \bar{V} \text{ in } L^2(\Omega, M_2).$$

Indeed, $\forall \Phi \in L^2(\Omega, M_2)$, $\int_{\Omega} z_j : \Phi \, dx \xrightarrow{j \rightarrow +\infty} 0$. So,

$$\int_{\Omega} \left(\nabla \varphi_{N(\gamma_{h(j)})}(\gamma_{h(j)}) - V_{N(\gamma_{h(j)})}(\gamma_{h(j)}) \right) : \Phi \, dx \xrightarrow{j \rightarrow +\infty} 0.$$

But $V_{N(\gamma_{h(j)})}(\gamma_{h(j)}) \xrightarrow{j \rightarrow +\infty} \bar{V}$ in $L^4(\Omega, M_2)$ so in $L^2(\Omega, M_2)$ and $\forall \Phi \in L^2(\Omega, M_2)$,

$$\int_{\Omega} \nabla \varphi_{N(\gamma_{h(j)})}(\gamma_{h(j)}) : \Phi \, dx \xrightarrow{j \rightarrow +\infty} \int_{\Omega} \bar{V} : \Phi \, dx.$$

In addition, $\nabla \varphi_{N(\gamma_{h(j)})}(\gamma_{h(j)}) \xrightarrow{j \rightarrow +\infty} \nabla \bar{\varphi}$ in $L^2(\Omega, M_2)$, and by uniqueness of the weak limit in $L^2(\Omega, M_2)$, $\nabla \bar{\varphi} = \bar{V} \in L^4(\Omega, M_2)$.

As previously mentioned, $V_{N(\gamma_{h(j)})}(\gamma_{h(j)}) = \nabla \varphi_{N(\gamma_{h(j)})}(\gamma_{h(j)}) - z_j$ with $z_j \xrightarrow{j \rightarrow +\infty} 0$ in $L^2(\Omega, M_2)$. Consequently,

$$\det(V_{N(\gamma_{h(j)})}(\gamma_{h(j)})) = \det(\nabla \varphi_{N(\gamma_{h(j)})}(\gamma_{h(j)})) + d_j,$$

with

$$\begin{aligned} d_j = & (z_j)_{11}(z_j)_{22} - (z_j)_{21}(z_j)_{12} - (z_j)_{22} \frac{\partial \varphi_{N(\gamma_{h(j)})}^1(\gamma_{h(j)})}{\partial x} \\ & - (z_j)_{11} \frac{\partial \varphi_{N(\gamma_{h(j)})}^2(\gamma_{h(j)})}{\partial y} + (z_j)_{21} \frac{\partial \varphi_{N(\gamma_{h(j)})}^1(\gamma_{h(j)})}{\partial y} \\ & + (z_j)_{12} \frac{\partial \varphi_{N(\gamma_{h(j)})}^2(\gamma_{h(j)})}{\partial x}, \end{aligned}$$

$((z_j)_{kl})$ denoting the element of the k^{th} row and the l^{th} column of the matrix z_j and with $\varphi_{N(\gamma_{h(j)})}(\gamma_{h(j)}) = \left(\varphi_{N(\gamma_{h(j)})}^1(\gamma_{h(j)}), \varphi_{N(\gamma_{h(j)})}^2(\gamma_{h(j)}) \right)$. The following inequality holds:

$$\int_{\Omega} |d_j| dx \leq \frac{1}{2} \|z_j\|_{L^2(\Omega, M_2)}^2 + \|z_j\|_{L^2(\Omega, M_2)} \|\nabla \varphi_{N(\gamma_{h(j)})}(\gamma_{h(j)})\|_{L^2(\Omega, M_2)},$$

$\|\nabla \varphi_{N(\gamma_{h(j)})}(\gamma_{h(j)})\|_{L^2(\Omega, M_2)}$ being bounded independently of j . As a consequence, $d_j \xrightarrow{j \rightarrow +\infty} 0$ in $L^1(\Omega)$. Let us now gather all the previous results:

$$\begin{cases} \det(V_{N(\gamma_{h(j)})}(\gamma_{h(j)})) \xrightarrow{j \rightarrow +\infty} \bar{\delta} \text{ in } L^2(\Omega), \\ \varphi_{N(\gamma_{h(j)})}(\gamma_{h(j)}) \xrightarrow{j \rightarrow +\infty} \bar{\varphi} \text{ in } W^{1,2}(\Omega, \mathbb{R}^2), \\ \text{and } \det(V_{N(\gamma_{h(j)})}(\gamma_{h(j)})) = \det(\nabla \varphi_{N(\gamma_{h(j)})}(\gamma_{h(j)})) + d_j \text{ with } d_j \xrightarrow{j \rightarrow +\infty} 0 \text{ in } L^1(\Omega). \end{cases}$$

From Theorem 1.14 from [13], if $\varphi_{N(\gamma_{h(j)})}(\gamma_{h(j)}) \xrightarrow{j \rightarrow +\infty} \bar{\varphi}$ in $W^{1,2}(\Omega, \mathbb{R}^2)$, then $\det(\nabla \varphi_{N(\gamma_{h(j)})}(\gamma_{h(j)})) \xrightarrow{j \rightarrow +\infty} \det(\nabla \bar{\varphi})$ in the sense of distributions.

Also, $\forall \Phi \in \mathcal{D}(\Omega)$,

$$\int_{\Omega} \det(V_{N(\gamma_{h(j)})}(\gamma_{h(j)})) \Phi dx \xrightarrow{j \rightarrow +\infty} \int_{\Omega} \bar{\delta} \Phi dx,$$

since $\det(V_{N(\gamma_{h(j)})}(\gamma_{h(j)}))$ weakly converges to $\bar{\delta}$ in $L^2(\Omega)$.

In addition:

$$\int_{\Omega} \det(V_{N(\gamma_{h(j)})}(\gamma_{h(j)})) \Phi dx = \int_{\Omega} \det(\nabla \varphi_{N(\gamma_{h(j)})}(\gamma_{h(j)})) \Phi dx + \int_{\Omega} d_j \Phi dx$$

and

$$\begin{cases} \int_{\Omega} \det(\nabla \varphi_{N(\gamma_{h(j)})}(\gamma_{h(j)})) \Phi dx \xrightarrow{j \rightarrow +\infty} \int_{\Omega} \det(\nabla \bar{\varphi}) \Phi dx, \\ \left| \int_{\Omega} d_j \Phi dx \right| \leq \|d_j\|_{L^1(\Omega)} \|\Phi\|_{C^0(\bar{\Omega})} \xrightarrow{j \rightarrow +\infty} 0 \text{ from Hölder's inequality.} \end{cases}$$

Consequently, $\forall \Phi \in \mathcal{D}(\Omega)$,

$$\int_{\Omega} \bar{\delta} \Phi dx = \int_{\Omega} \det(\nabla \bar{\varphi}) \Phi dx$$

and $\det(\nabla \bar{\varphi}) = \bar{\delta}$ in the sense of distributions. As $\det(\nabla \bar{\varphi}) \in L^2(\Omega)$ (since $\bar{\varphi} \in W^{1,4}(\Omega, \mathbb{R}^2)$ -recall that if Φ^n weakly converges to Φ in $W^{1,p}$ and $\Phi^n = \text{Id}$ on $\partial\Omega$, then $\Phi = \text{Id}$ on $\partial\Omega$ -) and as $\bar{\delta} \in L^2(\Omega)$, it results in $\det(\nabla \bar{\varphi}) = \bar{\delta}$ almost everywhere.

The mapping $J(V, \delta) = \int_{\Omega} \mathbb{W}^*(V, \delta) dx$ with

$$\mathbb{W}^*(V, \delta) = \begin{cases} \beta (\|V\|^2 - \alpha)^2 + \Psi(\delta) & \text{if } \|V\|^2 \geq \alpha \\ \Psi(\delta) & \text{if } \|V\|^2 < \alpha \end{cases} \text{ is defined on } L^4(\Omega, M_2) \times L^2(\Omega).$$

It is convex and strongly sequentially lower semi-continuous since \mathbb{W}^* is convex and continuous. It is thus weakly sequentially lower semi-continuous.

The Rellich-Kondrachov compact embedding theorem gives that $W^{1,2}(\Omega, \mathbb{R}^2) \subset L^q(\Omega, \mathbb{R}^2)$, $\forall q \in [1, +\infty[$. In particular, $\varphi_{N(\gamma_{h(j)})}(\gamma_{h(j)})$ strongly converges to $\bar{\varphi}$ in $L^2(\Omega, \mathbb{R}^2)$. As Φ_0 is assumed to be Lipschitz continuous, it can be proved that:

$$\lim_{j \rightarrow +\infty} \int_{\Omega} \left(\Phi_0 \left(\varphi_{N(\gamma_{h(j)})}(\gamma_{h(j)}) \right) - \tilde{\Phi}(\cdot, T) \right)^2 dx = \int_{\Omega} \left(\Phi_0(\bar{\varphi}) - \tilde{\Phi}(\cdot, T) \right)^2 dx.$$

By passing to the limit when j goes to $+\infty$, it yields to:

$$\inf_{\varphi \in \mathcal{W}} \bar{I}(\varphi) \leq \bar{I}(\bar{\varphi}) \leq \liminf_{j \rightarrow +\infty} \bar{I}_{\gamma_{h(j)}} \left(\varphi_{N(\gamma_{h(j)})}(\gamma_{h(j)}), V_{N(\gamma_{h(j)})}(\gamma_{h(j)}) \right),$$

since

$$\begin{aligned} \frac{\nu}{2} \|\Phi_0(\varphi_{N(\gamma_{h(j)})}(\gamma_{h(j)})) - \tilde{\Phi}(\cdot, T)\|_{L^2(\Omega)}^2 + \int_{\Omega} QW(V_{N(\gamma_{h(j)})}(\gamma_{h(j)})) dx \\ \leq \bar{I}_{\gamma_{h(j)}} \left(\varphi_{N(\gamma_{h(j)})}(\gamma_{h(j)}), V_{N(\gamma_{h(j)})}(\gamma_{h(j)}) \right). \end{aligned}$$

In conclusion, we have obtained the two following inequalities:

$$\begin{cases} \inf_{\varphi \in \mathcal{W}} \bar{I}(\varphi) \leq \bar{I}(\bar{\varphi}) \leq \liminf_{j \rightarrow +\infty} \bar{I}_{\gamma_{h(j)}} \left(\varphi_{N(\gamma_{h(j)})}(\gamma_{h(j)}), V_{N(\gamma_{h(j)})}(\gamma_{h(j)}) \right) \text{ and} \\ \bar{I}_{\gamma_{h(j)}} \left(\varphi_{N(\gamma_{h(j)})}(\gamma_{h(j)}), V_{N(\gamma_{h(j)})}(\gamma_{h(j)}) \right) \leq \inf_{\varphi \in \mathcal{W}} \bar{I}(\varphi) + \frac{2}{\gamma_{h(j)}}, \end{cases}$$

that is,

$$\limsup_{j \rightarrow +\infty} \bar{I}_{\gamma_{h(j)}} \left(\varphi_{N(\gamma_{h(j)})}(\gamma_{h(j)}), V_{N(\gamma_{h(j)})}(\gamma_{h(j)}) \right) \leq \inf_{\varphi \in \mathcal{W}} \bar{I}(\varphi),$$

and finally:

$$\boxed{\lim_{j \rightarrow +\infty} \bar{I}_{\gamma_{h(j)}} \left(\varphi_{N(\gamma_{h(j)})}(\gamma_{h(j)}), V_{N(\gamma_{h(j)})}(\gamma_{h(j)}) \right) = \bar{I}(\bar{\varphi}) = \inf_{\varphi \in \mathcal{W}} \bar{I}(\varphi).}$$

■

5.4 Discretization and Implementation

5.4.1 Introduction of an AOS scheme for the evolution problem

For the discretization of the evolution problem (E), an Additive Operator Splitting (AOS) scheme is implemented (see the seminal work [27] and [17]), requiring a linear computational cost at each step. The matrices involved in the sub-problems are monotone and their inverse matrices are such that the sum of the coefficients of each row is equal to 1. The scheme is thus unconditionally stable for the L^∞ -norm.

First of all, we recall the classical scheme of discretization of $\text{div}(c\nabla\Phi)$

$$\begin{aligned} \text{div}(c\nabla\Phi) &\simeq \partial_x \left(c_{i,j} \frac{\Phi_{i+\frac{1}{2},j} - \Phi_{i-\frac{1}{2},j}}{h} \right) + \partial_y \left(c_{i,j} \frac{\Phi_{i,j+\frac{1}{2}} - \Phi_{i,j-\frac{1}{2}}}{h} \right) \\ &\simeq c_{i+\frac{1}{2},j} \frac{\Phi_{i+1,j} - \Phi_{i,j}}{h^2} - c_{i-\frac{1}{2},j} \frac{\Phi_{i,j} - \Phi_{i-1,j}}{h^2} \\ &\quad + c_{i,j+\frac{1}{2}} \frac{\Phi_{i,j+1} - \Phi_{i,j}}{h^2} - c_{i,j-\frac{1}{2}} \frac{\Phi_{i,j} - \Phi_{i,j-1}}{h^2}, \end{aligned}$$

where $c_{i\pm\frac{1}{2},j}$ and $c_{i,j\pm\frac{1}{2}}$ are determined by bilinear interpolation. We use a vectorial representation of our function $\tilde{\Phi}$ by concatenation of the rows. Now we denote by $\tilde{\Phi} \in \mathbb{R}^{M \times N}$, where M is the number of rows and N is the number of columns. Thus $\tilde{\Phi}_i^n$ corresponds to an approximation of $\tilde{\Phi}(x_i, t_n)$.

We apply a semi-implicit finite differences scheme and using the previous discretization of $\text{div}(c\nabla\Phi)$ with $c(x) = \frac{\tilde{g}(|\nabla R(x)|)}{|\nabla\tilde{\Phi}(x)|}$, we obtain the following discretization:

$$\begin{aligned} \tilde{\Phi}_i^{n+1} = & \tilde{\Phi}_i^n + \tau |\nabla\tilde{\Phi}|_i^n \sum_{j \in \Lambda(i)} \frac{\left(\frac{g}{|\nabla\tilde{\Phi}|}\right)_i^n + \left(\frac{g}{|\nabla\tilde{\Phi}|}\right)_j^n}{2} \frac{\tilde{\Phi}_j^{n+1} - \tilde{\Phi}_i^{n+1}}{h^2} \\ & + \frac{4\mu'\tau}{d^2} H_\varepsilon(\tilde{\Phi}_i^n + l) H_\varepsilon(l - \tilde{\Phi}_i^n) \int_{\Omega} \langle x - y, \nabla\tilde{\Phi}^n(y) \rangle e^{-\|x-y\|_2^2/d^2} \\ & H_\varepsilon(\tilde{\Phi}^n(y) + l) H_\varepsilon(l - \tilde{\Phi}^n(y)) dy, \end{aligned}$$

where τ is the time step, $\Lambda(i)$ corresponds to the neighbours of i and H_ε is a C^∞ -regularization of the Heaviside function:

$$H_\varepsilon(x) = \frac{1}{2} \left(1 + \frac{2}{\pi} \arctan\left(\frac{x}{\varepsilon}\right) \right).$$

If we directly implement this scheme, the term $|\nabla\tilde{\Phi}|$ can be a problem in particular when $|\nabla\tilde{\Phi}| = 0$. That is the reason why Weickert *et al.* in [27] propose to replace the arithmetic mean by the harmonic mean. Thus we obtain:

$$\begin{aligned} \tilde{\Phi}_i^{n+1} = & \tilde{\Phi}_i^n + \tau |\nabla\tilde{\Phi}|_i^n \sum_{j \in \Lambda(i)} \frac{2}{\left(\frac{|\nabla\tilde{\Phi}|}{g}\right)_i^n + \left(\frac{|\nabla\tilde{\Phi}|}{g}\right)_j^n} \frac{\tilde{\Phi}_j^{n+1} - \tilde{\Phi}_i^{n+1}}{h^2} \\ & + \frac{4\mu'\tau}{d^2} H_\varepsilon(\tilde{\Phi}_i^n + l) H_\varepsilon(l - \tilde{\Phi}_i^n) \int_{\Omega} \langle x - y, \nabla\tilde{\Phi}^n(y) \rangle e^{-\|x-y\|_2^2/d^2} \\ & H_\varepsilon(\tilde{\Phi}^n(y) + l) H_\varepsilon(l - \tilde{\Phi}^n(y)) dy. \end{aligned}$$

If $|\nabla\tilde{\Phi}|_i^n = 0$ or $g_i = 0$, we set $\tilde{\Phi}_i^{n+1} = \tilde{\Phi}_i^n$. The previous equation can be rewritten as follows:

$$\begin{aligned} \tilde{\Phi}^{n+1} = & \tilde{\Phi}^n + \tau \sum_{l \in \{x, y\}} A_l(\tilde{\Phi}^n) \tilde{\Phi}^{n+1} \\ & + \frac{4\mu'\tau}{d^2} H_\varepsilon(\tilde{\Phi}^n + l) H_\varepsilon(l - \tilde{\Phi}^n) \int_{\Omega} \langle x - y, \nabla\tilde{\Phi}^n(y) \rangle e^{-\|x-y\|_2^2/d^2} \\ & H_\varepsilon(\tilde{\Phi}^n(y) + l) H_\varepsilon(l - \tilde{\Phi}^n(y)) dy \end{aligned}$$

with

$$a_{ij_x}(\tilde{\Phi}^n) \begin{cases} |\nabla\tilde{\Phi}|_i^n \frac{2}{\left(\frac{|\nabla\tilde{\Phi}|}{g}\right)_i^n + \left(\frac{|\nabla\tilde{\Phi}|}{g}\right)_j^n}, & j \in \Lambda_x(i), \\ -|\nabla\tilde{\Phi}|_i^n \sum_{m \in \Lambda_x(i)} \frac{2}{\left(\frac{|\nabla\tilde{\Phi}|}{g}\right)_i^n + \left(\frac{|\nabla\tilde{\Phi}|}{g}\right)_m^n}, & i = j, \\ 0 & \text{otherwise.} \end{cases}$$

$\Lambda_x(i)$ is the set of neighbors of i in the direction x . Matrix $A_y(\tilde{\Phi}^n)$ is determined in the same way. For the sake of conciseness, we denote by $G_{topo}(\tilde{\Phi}^n)$, the term corresponding to the topological constraint:

$$G_{topo}(\tilde{\Phi}^n) = \frac{4\mu'\tau}{d^2} H_\varepsilon(\tilde{\Phi}^n + l) H_\varepsilon(l - \tilde{\Phi}^n) \int_{\Omega} \langle x - y, \nabla \tilde{\Phi}^n(y) \rangle e^{-\|x-y\|_2^2/d^2} H_\varepsilon(\tilde{\Phi}^n(y) + l) H_\varepsilon(l - \tilde{\Phi}^n(y)) dy.$$

Therefore, we have to solve the following linear system:

$$\left(I - \tau \sum_{l \in \{x,y\}} A_l(\tilde{\Phi}^n) \right) \tilde{\Phi}^{n+1} = \tilde{\Phi}^n + G_{topo}(\tilde{\Phi}^n). \quad (5.12)$$

Let us consider the matrix $\left(I - \tau \sum_{l \in \{x,y\}} A_l(\tilde{\Phi}^n) \right)$, where I is the identity matrix. This matrix is strictly diagonally dominant, pentadiagonal, tridiagonal per block (and so invertible). However, due to the structure of the matrix, the computation cost remains high: the matrix is sparse by bands with at most 5 non zero coefficients per row. The resolution requires the use of iterative methods whose convergence is slow owing to the condition number of the matrix that increases when τ increases. That is the reason why Weickert *et al.* ([27]) propose to apply an AOS (Additive Operator Splitting) scheme. Instead of applying the following scheme:

$$\tilde{\Phi}^{n+1} = \left(I - \tau \sum_{l \in \{x,y\}} A_l(\tilde{\Phi}^n) \right)^{-1} \left(\tilde{\Phi}^n + G_{topo}(\tilde{\Phi}^n) \right),$$

Weickert *et al.* consider the following AOS scheme:

$$\tilde{\Phi}^{n+1} = \frac{1}{2} \sum_{l \in \{x,y\}} \left(I - 2\tau A_l(\tilde{\Phi}^n) \right)^{-1} \left(\tilde{\Phi}^n + G_{topo}(\tilde{\Phi}^n) \right), \quad (5.13)$$

Let us set $B_l(\tilde{\Phi}^n) = I - 2\tau A_l(\tilde{\Phi}^n)$. We obtain two disconnected linear systems that are both tridiagonal if one reorders the nodes of the mesh in a different way for the second system. Matrix $B_l(\tilde{\Phi}^n)$ is strictly diagonally dominant and monotone. Therefore, we can solve the systems computing by means of Thomas algorithm with a linear complexity. The algorithm can be summarized as follows:

Algorithm 2 Algorithm for the AOS scheme.

1. Solve $\left(I - 2\tau A_x(\tilde{\Phi}^n) \right) v^{n+1} = \tilde{\Phi}^n + G_{topo}(\tilde{\Phi}^n)$
 2. Solve $\left(I - 2\tau A_y(\tilde{\Phi}^n) \right) w^{n+1} = \tilde{\Phi}^n + G_{topo}(\tilde{\Phi}^n)$
 3. $\tilde{\Phi}^{n+1} = \frac{1}{2}(v^{n+1} + w^{n+1})$.
-

We observe that the AOS schemes separate the treatment of the axis x and y , and are additive. Moreover, these schemes are unconditionally stable.

Remark 5.4.1

In practice, we also add a balloon force term: $k\tilde{g}(|\nabla R|)|\nabla\tilde{\Phi}|$ in order to increase the speed of convergence. A classical discretization of the gradient can lead to the creation of loops. The condition of entropy of Sethian [24] prevents the curve from propagating where it has already been and thus avoids loop formation. The hyperbolic conservation laws enable to obtain the discretization of the gradient:

$$\begin{aligned} \left(|\nabla\tilde{\Phi}|_i^n\right)^2 &\simeq \left[\max(D^-x\tilde{\Phi}_i^n, 0)^2 + \min(D^+x\tilde{\Phi}_i^n, 0)^2 \right. \\ &\quad \left. + \max(D^-y\tilde{\Phi}_i^n, 0)^2 + \min(D^+y\tilde{\Phi}_i^n, 0)^2 \right], \quad \text{if } k < 0 \\ &\simeq \left[\max(D^+x\tilde{\Phi}_i^n, 0)^2 + \min(D^-x\tilde{\Phi}_i^n, 0)^2 \right. \\ &\quad \left. + \max(D^+y\tilde{\Phi}_i^n, 0)^2 + \min(D^-y\tilde{\Phi}_i^n, 0)^2 \right], \quad \text{if } k > 0. \end{aligned}$$

Lastly, we have assumed that $\tilde{\Phi}$ is a signed distance function. Thus we need to periodically apply a reinitialization process. We have used the scheme obtained by Russo and Smereka in [23], defined by:

$$\tilde{\Phi}_{i,j}^{n+1} = \begin{cases} \tilde{\Phi}_{i,j}^n - \frac{\Delta t}{\Delta x} (\text{sign}(\tilde{\Phi}_{i,j}^0)|\tilde{\Phi}_{i,j}^n| - D_{i,j}) & \text{if } \tilde{\Phi}_{i,j}^0\tilde{\Phi}_{i-1,j}^0 < 0 \text{ or } \tilde{\Phi}_{i,j}^0\tilde{\Phi}_{i+1,j}^0 < 0 \\ & \text{or } \tilde{\Phi}_{i,j}^0\tilde{\Phi}_{i,j-1}^0 < 0 \text{ or } \tilde{\Phi}_{i,j}^0\tilde{\Phi}_{i,j+1}^0 < 0, \\ \tilde{\Phi}_{i,j}^n - \Delta t \text{ sign}(\tilde{\Phi}_{i,j}^0)G(\tilde{\Phi})_{i,j} & \text{otherwise,} \end{cases}$$

with $D_{i,j}$, the distance of node (i, j) from the interface and where, if $\tilde{\Phi}_{i,j}^0 > 0$,

$$\begin{aligned} G(\tilde{\Phi})_{i,j} &= \left(\max \left((\max(D_x^- \tilde{\Phi}_{i,j}, 0))^2, (\min(D_x^+ \tilde{\Phi}_{i,j}, 0))^2 \right) \right. \\ &\quad \left. + \max \left((\max(D_y^- \tilde{\Phi}_{i,j}, 0))^2, (\min(D_y^+ \tilde{\Phi}_{i,j}, 0))^2 \right) - 1 \right)^{\frac{1}{2}}, \end{aligned}$$

and if $\tilde{\Phi}_{i,j}^0 < 0$,

$$\begin{aligned} G(\tilde{\Phi})_{i,j} &= \left(\max \left((\min(D_x^- \tilde{\Phi}_{i,j}, 0))^2, (\max(D_x^+ \tilde{\Phi}_{i,j}, 0))^2 \right) \right. \\ &\quad \left. + \max \left((\min(D_y^- \tilde{\Phi}_{i,j}, 0))^2, (\max(D_y^+ \tilde{\Phi}_{i,j}, 0))^2 \right) - 1 \right)^{\frac{1}{2}}. \end{aligned}$$

- for the resolution of $Ru = y$: $(N - 1)$ multiplications, $N - 1$ subtractions and N divisions are required.

Thus the global cost is $3N - 3$ subtractions and $5N - 4$ multiplications/divisions.

5.4.3 Euler-Lagrange equations for functional \bar{I}_γ

The Euler-Lagrange equation associated with (5.9) in φ is defined by:

$$\nu(\Phi_0 \circ \varphi - \tilde{\Phi}(\cdot, T))\nabla\Phi_0(\varphi) + \gamma \begin{pmatrix} \operatorname{div} V_1 \\ \operatorname{div} V_2 \end{pmatrix} - \gamma\Delta\varphi = 0,$$

and the system of equations for V is given by:

$$\begin{cases} 0 = 2\beta c_0 V_{11} (2H_\varepsilon(c_0) + c_0\delta_\varepsilon(c_0)) + \mu V_{22}(\det V - 2) + \gamma(V_{11} - \frac{\partial\varphi_1}{\partial x}), \\ 0 = 2\beta c_0 V_{12} (2H_\varepsilon(c_0) + c_0\delta_\varepsilon(c_0)) - \mu V_{21}(\det V - 2) + \gamma(V_{12} - \frac{\partial\varphi_1}{\partial y}), \\ 0 = 2\beta c_0 V_{21} (2H_\varepsilon(c_0) + c_0\delta_\varepsilon(c_0)) - \mu V_{12}(\det V - 2) + \gamma(V_{21} - \frac{\partial\varphi_2}{\partial x}), \\ 0 = 2\beta c_0 V_{22} (2H_\varepsilon(c_0) + c_0\delta_\varepsilon(c_0)) + \mu V_{11}(\det V - 2) + \gamma(V_{22} - \frac{\partial\varphi_2}{\partial y}), \end{cases}$$

where $c_0 = (\|V\|^2 - \alpha)$, V_i denotes the i^{th} row of V and $V = (V_{ij})_{1 \leq i, j \leq 2}$.

The equation for φ is discretized using an implicit finite difference scheme with a 5 point centered scheme for the Laplacian and the equation for V is discretized using a semi-implicit finite difference scheme. The construction of the matrix of the linear system and its resolution is similar to the one described in Chapter 6.

5.5 Numerical results

In this section, we present some numerical results. For each example, we provide the Template and Reference images superimposed with the initial contour given by Φ_0 , the deformed Template, the Reference image segmented by $\tilde{\Phi}$ (result of the segmentation process) and by $\Phi_0 \circ \varphi$. As well, both deformed grids (from Template to Reference and from Reference to Template) and the displacement vector field are displayed.

5.5.1 Letter C

The method is applied on a first academic example inspired from [10] for mapping a disk to the letter C, demonstrating the ability of the algorithm to handle large deformations. First, we illustrate the segmentation process by giving some intermediate steps of the algorithm (60, 120, 180, 210 and 300 iterations) that can be used for the registration process.

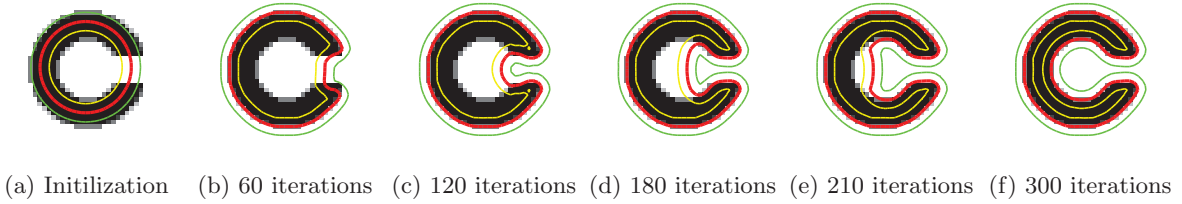


Figure 5.2: Evolution of the level sets of $\tilde{\Phi}$. Display of the zero level line (red) and the levels 2 and -2 (green and yellow).

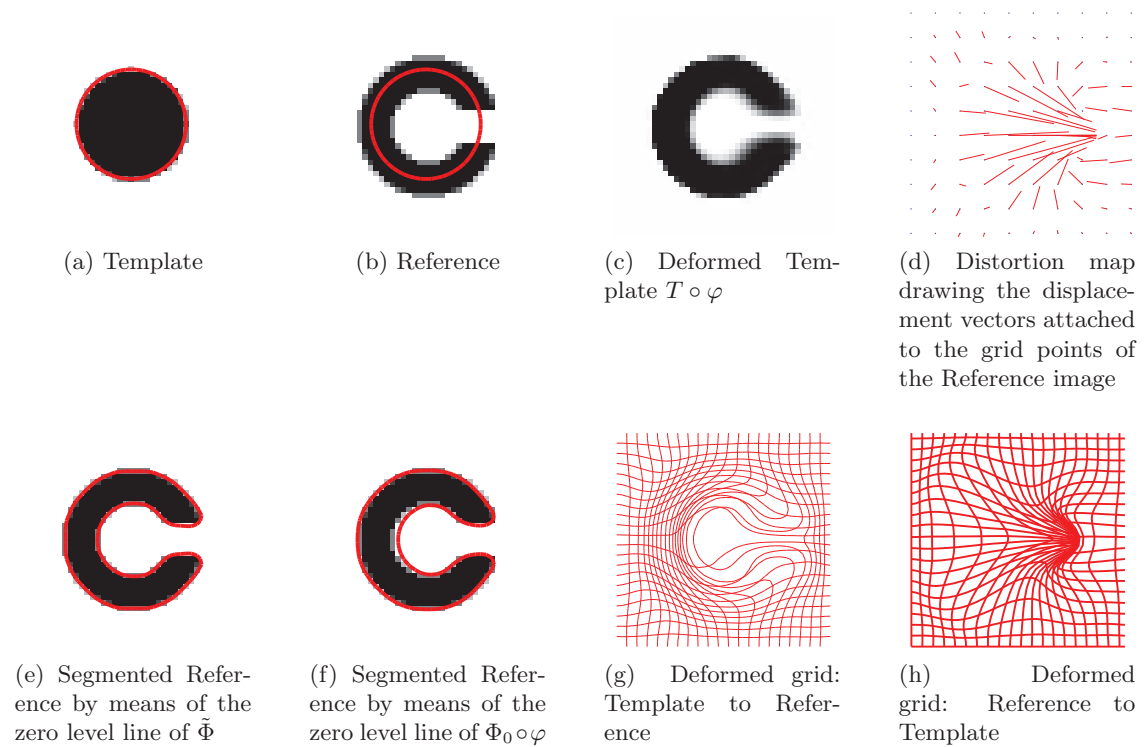


Figure 5.3: Mapping of a disk to letter C.

Execution time: 16 seconds for 40×40 pixel images. $\min \det \nabla \varphi = 0.0005$, $\max \det \nabla \varphi = 2.51$.

5.5.2 Triangle

The method is applied on another toy example to emphasize again the capability of the model to generate large deformations even on noisy data.

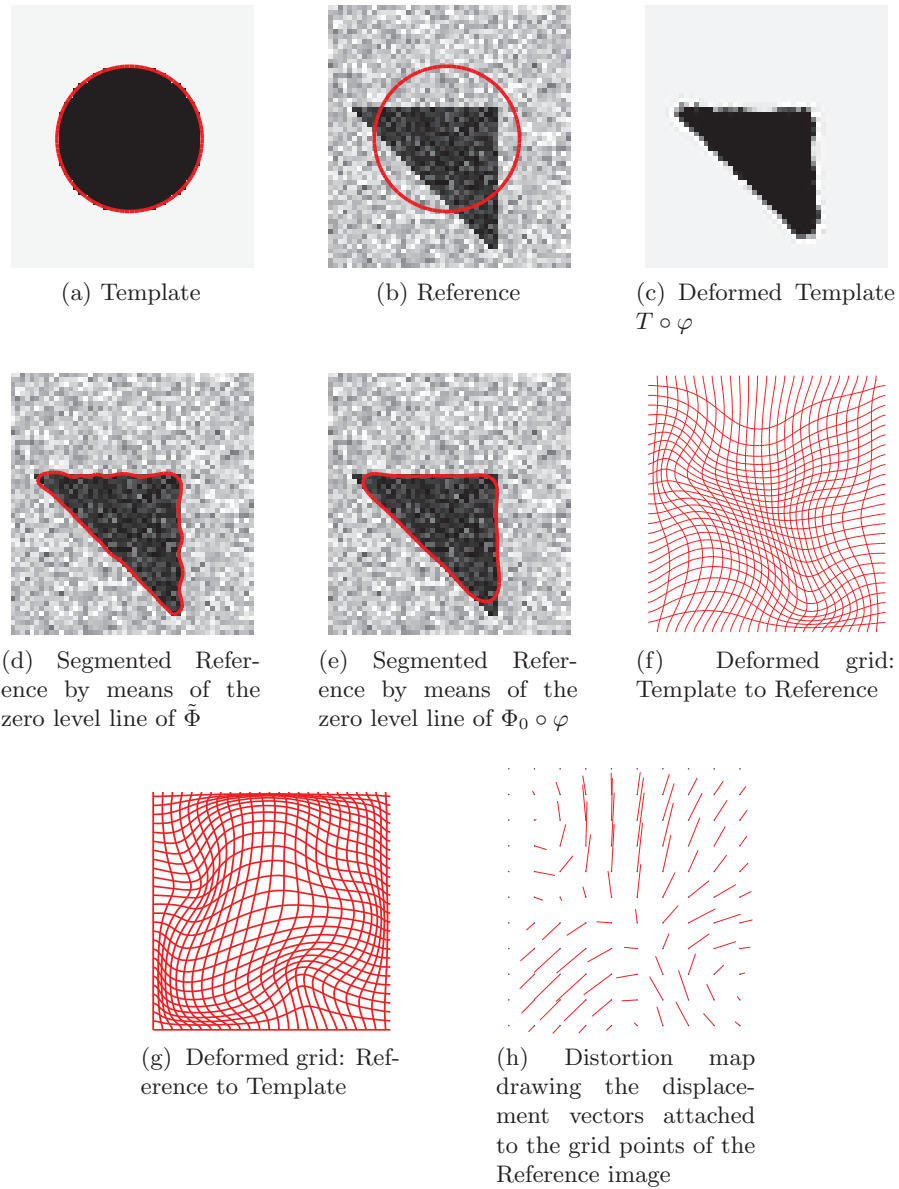


Figure 5.4: **Mapping of a disk to a triangle.**

Execution time: 13 seconds for 54×50 pixel images. $\min \det \nabla \varphi = 0.026$, $\max \det \nabla \varphi = 2.95$.

5.5.3 Mouse brain gene expression

The method has been applied on medical images with the goal to map a 2D slice of mouse brain gene expression data (Template T) to its corresponding 2D slice of mouse brain atlas in order to facilitate the integration of anatomic, genetic and physiologic observations from multiple subjects in a common space. Since genetic mutations and knock-out strains of mice provide critical models for a variety of human diseases, such linkage between genetic information and anatomical structure is important. The data are provided by the Center for Computational Biology, UCLA. The mouse atlas acquired from the LONI database was pre-segmented. The gene expression data were segmented manually to facilitate data processing in other applications. Some algorithms have been developed to automatically segment the brain area of gene expression data. The non-brain regions have been removed to produce better matching.

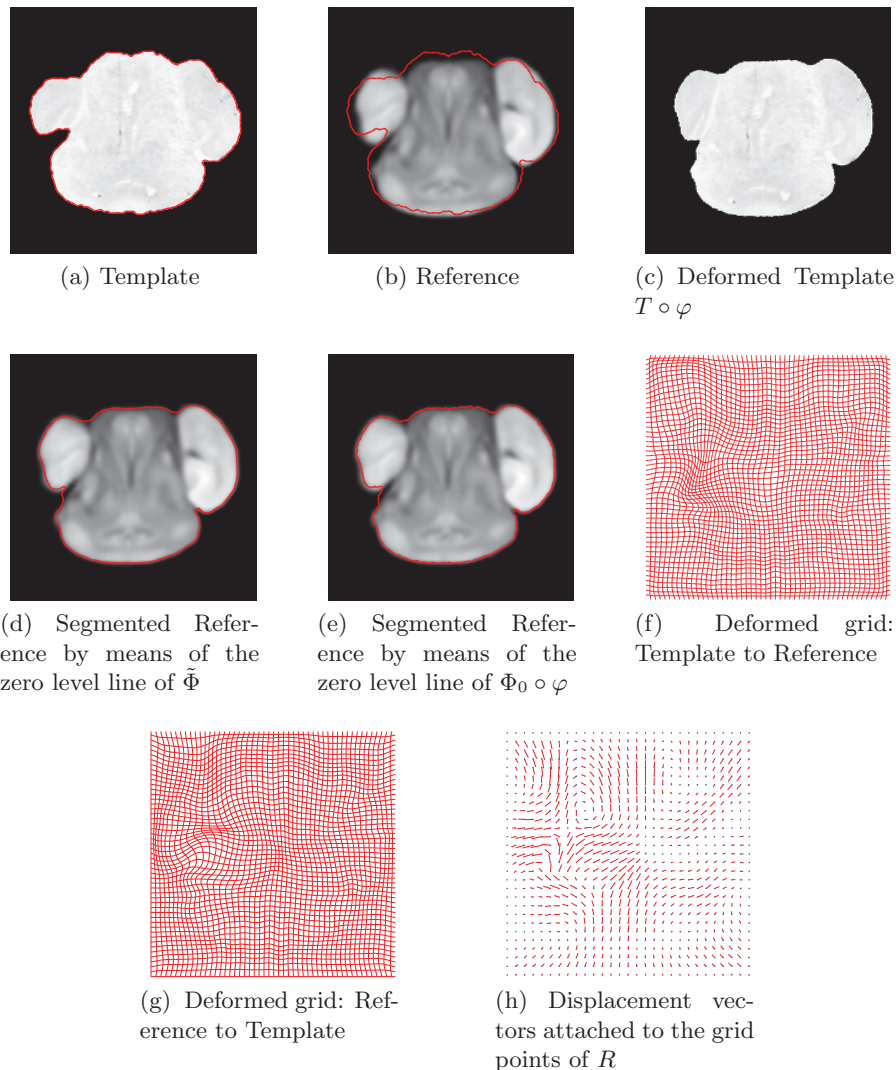


Figure 5.5: Mapping of a mouse brain gene expression to an atlas.

Execution time: 10 minutes for 200×200 pixel images. $\min \det \nabla \varphi = 0.36$, $\max \det \nabla \varphi = 2.18$.

5.5.4 Slices of brain

We also applied the method to complex slices of brain data (courtesy of Laboratory Of Neuro-Imaging, UCLA). We aim to register a disk to the slice of brain. The results demonstrate the ability of the obtained contour to fit very well the convolutions of the brain.

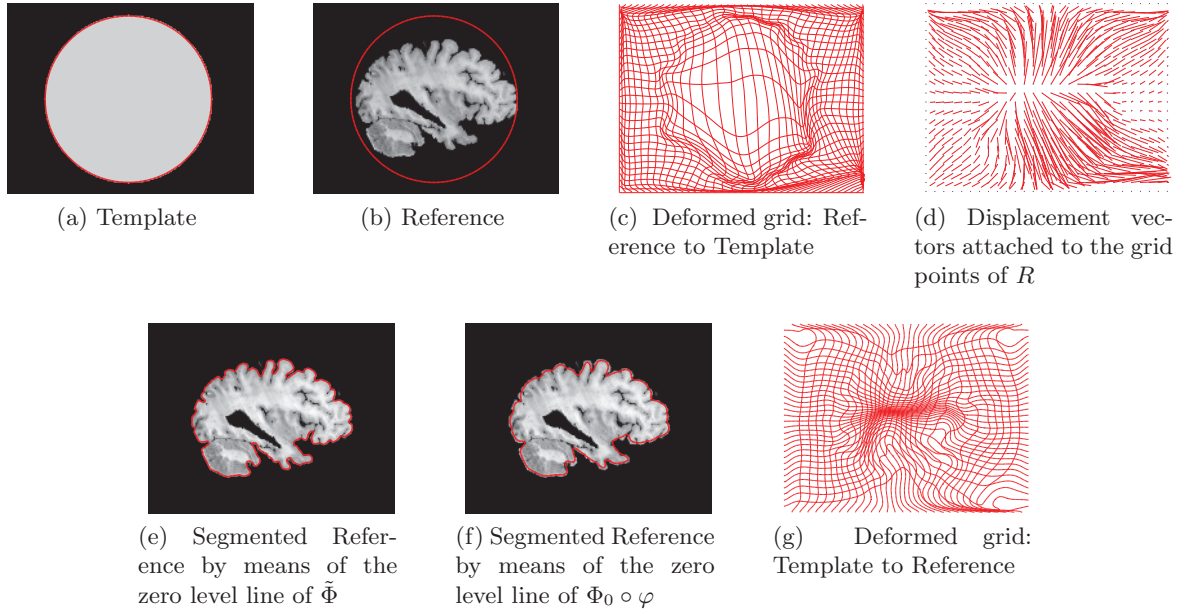


Figure 5.6: **Mapping of a disk to a slice of brain.** Execution time: 9 minutes for 148×192 pixel images.

Conclusion

We therefore have designed a functional for image joint registration/segmentation problem based on the comparison of level sets so that the registration process does not depend on the intensity differences but only on shape alignment. Moreover, we overcome the obstacle of non quasiconvexity of the stored energy function of Saint Venant-Kirchhoff using the relaxed problem associated with the original one. We also study the well-definedness of the evolution problem, study involving the theory of viscosity solutions. Numerically, the model enables us to obtain large deformations and an accurate segmentation. The only limitation of this model comes from the evolution equation: this segmentation method is sensitive to the initial condition and the direction of propagation is enforced by the parameter balancing the balloon force term. The initial condition being the contour of the object in the Template image, we may have tuned, in certain circumstances, the parameter balancing the balloon force during the evolution process.

- [1] G. AUBERT AND P. KORNPBST, *Mathematical Problems in Image processing: Partial Differential Equations and the Calculus of Variations*, vol. 147 of Applied Mathematical Sciences, Springer-Verlag, 2001.
- [2] G. BARLES, P. CARDALIAGUET, O. LEY, AND A. MONTEILLET, *Existence of weak solutions for general nonlocal and nonlinear second-order parabolic equations*, *Nonlinear Analysis: Theory, Methods & Applications*, 71 (2009), pp. 2801–2810.
- [3] M. BOURGOING, *Viscosity solutions of fully nonlinear second order parabolic equations with L^1 dependence in time and neumann boundary conditions*, *Discrete Contin. Dyn. Syst.*, 21 (2008), pp. 763–800.
- [4] M. BOUSSELSAL, *Etude de quelques problèmes de calcul des variations liés à la mécanique*, PhD thesis, Université de Metz, 1993.
- [5] H. BRÉZIS, *Analyse Fonctionnelle, Théorie et Applications*, Dunod, Paris, 2005.
- [6] C. BROIT, *Registration of Deformed Images*, PhD thesis, Université de Pennsylvania, USA, 1981.
- [7] M. BURGER, J. MODERSITZKI, AND L. RUTHOTTO, *A hyperelastic regularization energy for image registration*, *SIAM Journal on Scientific Computing*, 35 (2013), pp. B132–B148.
- [8] V. CASELLES, R. KIMMEL, AND G. SAPIRO, *Geodesic active contours*, *International journal of computer vision*, 22 (1997), pp. 61–79.
- [9] T. F. CHAN AND L. VESE, *Active contours without edges*, *IEEE T. Image Processing*, 10 (2001), pp. 266–277.
- [10] G. E. CHRISTENSEN, *Deformable shape models for anatomy*, PhD thesis, Washington University, Sever Institute of technology, USA, 1994.
- [11] P. G. CIARLET, *Elasticité tridimensionnelle*, Masson, 1985.
- [12] M. G. CRANDALL, H. ISHII, AND P.-L. LIONS, *User’s guide to viscosity solutions of second order partial differential equations*, *Bulletin of the American Mathematical Society*, 27 (1992), pp. 1–67.

- [13] B. DACOROGNA, *Direct methods in the calculus of variations*, vol. 78 of Applied Mathematical Sciences, Springer, 2008.
- [14] R. DERFOUL AND C. LE GUYADER, *A Relaxed Problem of Registration Based on the Saint Venant–Kirchhoff Material Stored Energy for the Mapping of Mouse Brain Gene Expression Data to a Neuroanatomical Mouse Atlas*, SIAM Journal on Imaging Sciences, 7 (2014), pp. 2175–2195.
- [15] M. DROSKE AND M. RUMPF, *Multiscale joint segmentation and registration of image morphology*, Pattern Analysis and Machine Intelligence, IEEE Transactions on, 29 (2007), pp. 2181–2194.
- [16] N. FORCADEL AND C. LE GUYADER, *A short time existence/uniqueness result for a nonlocal topology-preserving segmentation model*, Journal of Differential Equations, 253 (2012), pp. 977–995.
- [17] C. LE GUYADER AND L. VESE, *Self-repelling snakes for topology-preserving segmentation models*, Image Processing, IEEE Transactions on, 17 (2008), pp. 767–779.
- [18] C. LE GUYADER AND L. A. VESE, *A combined segmentation and registration framework with a nonlinear elasticity smoother*, Computer Vision and Image Understanding, 115 (2011), pp. 1689–1709.
- [19] N. LORD, J. HO, B. C. VEMURI, S. EISENSCHENK, ET AL., *Simultaneous registration and parcellation of bilateral hippocampal surface pairs for local asymmetry quantification*, Medical Imaging, IEEE Transactions on, 26 (2007), pp. 471–478.
- [20] P. V. N. MARRERO, *A numerical method for detecting singular minimizers of multidimensional problems in nonlinear elasticity*, Numerische Mathematik, 58 (1990), pp. 135–144.
- [21] D. NUNZIANTE, *Existence and uniqueness of unbounded viscosity solutions of parabolic equations with discontinuous time-dependence*, Nonlinear Analysis: Theory, Methods & Applications, 18 (1992), pp. 1033–1062.
- [22] S. OZERÉ, C. GOUT, AND C. LE GUYADER, *Joint segmentation/registration model by shape alignment via weighted total variation minimization and nonlinear elasticity*, Accepted for publication in Siam Imaging Sciences, (July 2015).
- [23] G. RUSSO AND P. SMEREKA, *A Remark on Computing Distance Functions*, Journal of Computational Physics, 163 (2000), pp. 51 – 67.
- [24] J. A. SETHIAN, *Level set methods and fast marching methods: evolving interfaces in computational geometry, fluid mechanics, computer vision, and materials science*, vol. 3, Cambridge university press, 1999.
- [25] A. SOTIRAS, C. DAVATZIKOS, AND N. PARAGIOS, *Deformable medical image registration: A survey*, Medical Imaging, IEEE Transactions on, 32 (2013), pp. 1153–1190.
- [26] B. C. VEMURI, J. YE, Y. CHEN, AND C. M. LEONARD, *Image registration via level-set motion: Applications to atlas-based segmentation*, Medical image analysis, 7 (2003), pp. 1–20.

- [27] J. WEICKERT AND G. KÜHNE, *Fast methods for implicit active contour models*, Springer, 2003.
- [28] A. YEZZI, L. ZÖLLEI, AND T. KAPUR, *A variational framework for joint segmentation and registration*, in *Mathematical Methods in Biomedical Image Analysis*, 2001. MMBIA 2001. IEEE Workshop on, IEEE, 2001, pp. 44–51.

CHAPTER 6

REGISTRATION PROBLEM BASED ON GEOMETRIC CONSTRAINTS AND SAINT VENANT-KIRCHHOFF MATERIAL

In this chapter, we introduce a registration model under constraints based on nonlinear elasticity theory. In particular, we choose to view the shapes to be matched as hyperelastic, isotropic and homogeneous materials. The choice of a hyperelastic material can be explained by two reasons: on the one hand, this kind of regularizer enables us to handle large and nonlinear deformations, on the other hand, in the literature, biological tissues are often modelled as hyperelastic materials.

Moreover, we introduce geometrical constraints, that is to say that we seek to match pairs of control points on the Reference image and the Template image.

The chapter is organized as follows. In a first section, we present the mathematical modelling of our method based on the stored energy function of the Saint Venant-Kirchhoff material. We formulate our problem as a functional minimization problem. Next, we establish theoretical results such as the existence of so-called generalized solutions (solutions of an associated relaxed problem). We also establish a convergence result when the number of control points increases to infinity. Finally, we are concerned with the discretization and the implementation of the model, and we conclude the chapter with some numerical experiments.

Introduction

Image registration is a fundamental task encountered in a large range of applications such as medical imaging, when comparing an image to an atlas or when fusing two images. Given two images, registration consists in determining an optimal diffeomorphic transformation φ such that the deformed Template image is aligned with the Reference. For images of the same modality, the goal of registration is to correlate the geometrical features and the intensity level distribution of the Reference and those of the deformed Template. When the images have been acquired through different mechanisms and have different modalities, registration aims to correlate both images while preserving the modality of the Template image. Sometimes, in medical image registration, geometrical constraints such as landmark points can complement the image data. In this case, relevant points on the Reference image are manually selected and

their counterparts on the Template are identified by an expert (see [19] for details and [17] for applications to registration of mouse brain gene expression data to an atlas). This prior knowledge allows, in particular, to increase the reliability of the obtained results. The quality of the obtained deformation can thus be measured by comparing the position of the landmark points on the Template and the position of the associated deformed landmark points. In this chapter, we propose a nonlinear elasticity based registration method including geometrical constraints manually selected on the images. The energy to be minimized consists of three terms: the L^2 distance of the grey levels, the elasticity-based regularizer and the geometrical constraint term (denoted respectively by Fid , Reg , $Const$). The minimization problem can be written in the form

$$\inf_{\varphi} \{Fid(\varphi) + Reg(\varphi) + Const(\varphi)\}.$$

To allow large deformations, we introduce a nonlinear-elasticity-based smoother (see [8], [9] for further details), the theory of linear elasticity being unsuitable in this case since assuming small strains and the validity of Hooke's law. We propose viewing the shapes to be warped as isotropic, homogeneous, hyperelastic materials and more precisely as Saint Venant-Kirchhoff materials. Note that rubber, filled elastomers, biological tissues are often modeled within the hyperelastic framework, which motivates our modelling.

For the sake of completeness, we would like to refer the reader to previous works related to registration based on nonlinear elasticity principles. In [13], Droske and Rumpf address the issue of non-rigid registration of multi-modal image data. The matching criterion includes first order derivatives of the deformation and is complemented by a nonlinear elastic regularization based on a polyconvex stored energy function, which is different from our proposed approach. We also mention the combined segmentation/registration model introduced by Le Guyader and Vese ([16]) in which the shapes to be matched are viewed as Ciarlet-Geymonat materials, the works [2] and [18] for a variational registration method for large deformations (Large Deformation Diffeomorphic Metric Mapping - LDDMM), and refer to [22] for a much related work that also uses nonlinear elasticity regularization but implemented by the finite element method.

In [5], the authors design an hyperelastic regularizer. More precisely, they build an hyperelastic stored energy function penalizing variations of lengths and areas, and add a penalty term on the Jacobian determinant such that the energy tends to infinity as $\det \nabla \varphi$ tends to 0 and such that shrinkage and growth have the same price. The numerical implementation is based on a discretize-then-optimize strategy and the authors use a generalized Gauss-Newton scheme to compute a numerical minimizer.

6.1 Mathematical modelling

6.1.1 Preliminaries

Before introducing the model, let us make a short reminder on nonlinear elasticity and on the Saint Venant-Kirchhoff material. Denoting by φ a deformation, we recall that the right Cauchy-Green strain tensor is defined by

$$C = \nabla \varphi^T \nabla \varphi = F^T F \in \mathcal{S}^2$$

with $\mathcal{S}^2 = \{A \in M_2(\mathbb{R}), A = A^T\}$, set of all real symmetric matrices of order 2. Physically, the right Cauchy-Green tensor can be interpreted as a quantifier of the square of local change

in distances due to deformation. The Green-Saint Venant strain tensor is defined by

$$E = \frac{1}{2}(\nabla u + \nabla u^T + \nabla u^T \nabla u).$$

Associated with a given deformation $\varphi = \text{Id} + u$, it is a measure of the deviation between φ and a rigid deformation. We also provide the following notations:

- $A : B = \text{tr } A^T B$ the matrix inner product
- $\|A\| = \sqrt{A : A}$, the related matrix norm (Frobenius norm).

The stored energy function of an isotropic, homogeneous, hyperelastic material, if the reference configuration is a natural state, is of the form:

$$W(F) = \widehat{W}(E) = \frac{\lambda}{2} (\text{tr } E)^2 + \mu \text{tr } E^2 + o(\|E\|^2), \quad F^T F = I + 2E, \quad (6.1)$$

with I the identity matrix. The Saint Venant-Kirchhoff material is the simplest homogeneous, isotropic, hyperelastic material with a natural reference configuration complying with the previous expansion (6.1). The stored energy function is defined by

$$W_{SVK}(F) = \widehat{W}_{SVK}(E) = \frac{\lambda}{2} (\text{tr } E)^2 + \mu \text{tr}(E^2).$$

The coefficients λ and μ are the Lamé constants. The first Lamé parameter λ has no straightforward physical interpretation, but is related to the bulk modulus. The second Lamé parameter μ is the shear modulus. That is to say that μ measures the resistance of a material: the greater μ , the stronger the applied force to obtain the same deformation. If a material had a null shear modulus, it would not be stable.

6.1.2 Depiction of the model

We focus on a registration problem based on the L^2 -norm of the difference between the Template and the Reference images. Concerning the regularizer, we choose a nonlinear elastic regularizer, in particular, the stored energy function of a Saint Venant-Kirchhoff material. Moreover, from a numerical viewpoint, this choice of regularizer enables us to deal with high-magnitude deformations. Also, we add a penalty term to force the Jacobian to be close to 1 in order to obtain a homogeneous deformation that is to say to prevent the deformation map from exhibiting contractions and expansions that are too large.

Moreover, we propose to include geometrical constraints to match some interest points. Indeed, we manually choose a finite number of points on the Template image and on the Reference image and we want every point on the Reference image to be mapped to its counterpart on the Template image.

Let us denote by:

- Ω a connected bounded open subset of \mathbb{R}^2 with Lipschitz boundary $\partial\Omega$,
- $R : \bar{\Omega} \rightarrow \mathbb{R}$, the Reference image,
- $T : \bar{\Omega} \rightarrow \mathbb{R}$, a Lipschitz continuous function (we denote by k_T the Lipschitz constant) with compact support, representing the Template image,
- $\varphi : \bar{\Omega} \rightarrow \mathbb{R}^2$ the sought deformation with $\varphi = \text{Id}$ on $\partial\Omega$.

Geometrical constraints

The geometrical constraints correspond to selected landmark points on R and their corresponding counterpart on T . We denote by $\omega = (\omega_1, \dots, \omega_N) \in (\mathbb{R}^2)^N$, the landmark points on R and $\tilde{\omega} = (\tilde{\omega}_1, \dots, \tilde{\omega}_N) \in (\mathbb{R}^2)^N$ their counterparts on T .

We define the linear mapping ρ by:

$$\begin{aligned} \rho : W^{1,4}(\Omega, \mathbb{R}^2) &\longrightarrow (\mathbb{R}^2)^N \\ \varphi &\longmapsto (\varphi(\omega_1), \dots, \varphi(\omega_N))^T. \end{aligned}$$

We justify the choice of the functional space $W^{1,4}(\Omega, \mathbb{R}^2)$ in the sequel. The mapping ρ is well defined since we have the continuous embedding $W^{1,4}(\Omega, \mathbb{R}^2) \hookrightarrow C^0(\bar{\Omega}, \mathbb{R}^2)$. The purpose is to minimize

$$\langle \rho(\varphi) - \tilde{\omega} \rangle_{2N}^2,$$

with respect to φ where $\langle \cdot \rangle_{2N}$ is the Euclidean norm in \mathbb{R}^{2N} and N is the number of constraints.

In fact, we aim to minimize the distance between $\varphi(\omega_i)$ and $\tilde{\omega}_i$, $i = 1 \dots N$, ie, we search for the deformation such that the points in the Reference image are mapped to the points of the Template image through this smooth deformation. We can notice that minimizing $\langle \rho(\varphi) - \tilde{\omega} \rangle_{2N}^2$ with respect to φ is equivalent to minimizing $\langle \rho(\varphi) \rangle_{2N}^2 - 2\langle \rho(\varphi), \tilde{\omega} \rangle_{2N}$.

Elastic regularization

As already mentioned, we choose to view the shapes to be matched as Saint Venant-Kirchhoff materials. In addition, we complement the stored energy function W_{SVK} by the term $\mu(\det \nabla \varphi - 1)^2$ controlling that the Jacobian remains close to 1. The weighting of the determinant component by parameter μ is justified in the proof of 6.1.1.

We set $W(\nabla \varphi) = W_{SVK}(\nabla \varphi) + \mu(\det \nabla \varphi - 1)^2$ where W_{SVK} is the stored energy function of a Saint Venant-Kirchhoff material, defined by

$$W_{SVK}(F) = \widehat{W}_{SVK}(E) = \frac{\lambda}{2}(\text{tr } E)^2 + \mu \text{tr}(E^2), \quad \text{with } E = \frac{1}{2}(F^T F - I).$$

We first rewrite $W_{SVK}(\nabla \varphi)$ in a more simplified way. In two dimensions, we have:

$$\begin{aligned} W_{SVK}(F) &= \frac{\lambda}{2}(\text{tr } E)^2 + \mu \text{tr}(E^2), \\ &= \frac{\lambda}{8}(\|F\|^2 - 2)^2 + \frac{\mu}{4}(\|F^T F\|^2 - 2\|F\|^2 + 2), \\ &= \underbrace{-\frac{\lambda + \mu}{2}}_{a_1 < 0} \|F\|^2 + \underbrace{\frac{\lambda + 2\mu}{8}}_{a_2} \|F\|^4 - \frac{\mu}{2}(\det F)^2 + \frac{\lambda + \mu}{2}. \end{aligned} \tag{6.2}$$

Indeed, considering the characteristic polynomial $\chi_{F^T F}$ of $F^T F$, we have:

$$\chi_{F^T F}(X) = X^2 - \text{tr}(F^T F)X + \det(F^T F)I.$$

Moreover, according to Cayley-Hamilton theorem, $\chi_{F^T F}(F^T F) = 0$, then $(F^T F)^2 - \text{tr}(F^T F)F^T F + \det(F^T F)I = 0$.

Passing to the trace we obtain: $\|F^T F\|^2 - \|F\|^4 + 2(\det F)^2 = 0$. Replacing $\|F^T F\|^2$ by $\|F\|^4 - 2(\det F)^2$, we obtain the desired expression of W_{SVK} .

Therefore,

$$W(F) = a_1 \|F\|^2 + a_2 \|F\|^4 + \frac{\lambda + \mu}{2} + \phi(\det F),$$

with $\phi : s \mapsto -\frac{\mu}{2}s^2 + \mu(s-1)^2$.

Functional to be minimized

Finally, we aim to minimize the following functional:

$$\inf_{\varphi \in \mathcal{W}} \left\{ I(\varphi) = \frac{\nu}{2} \int_{\Omega} (T \circ \varphi - R)^2 dx + \int_{\Omega} W(\nabla \varphi) dx + \eta \langle \rho(\varphi) \rangle_{2N}^2 - 2\eta \langle \rho(\varphi), \tilde{\omega} \rangle_{2N} \right\} \quad (\text{P})$$

with $\mathcal{W} = \left\{ \varphi \in \text{Id} + W_0^{1,4}(\Omega, \mathbb{R}^2) \right\}$, where ν, η are positive parameters. $\varphi \in \text{Id} + W_0^{1,4}(\Omega, \mathbb{R}^2)$ means that $\varphi = \text{Id}$ on $\partial\Omega$ and $\varphi \in W^{1,4}(\Omega, \mathbb{R}^2)$, $W^{1,4}(\Omega, \mathbb{R}^2)$ denoting the Sobolev space of functions $\varphi \in L^4(\Omega, \mathbb{R}^2)$ with distributional derivatives up to order 1 which also belong to $L^2(\Omega)$.

The functional is well defined for $\varphi \in W^{1,4}(\Omega, \mathbb{R}^2)$. Indeed, we have the continuous embedding $W^{1,4}(\Omega, \mathbb{R}^2) \hookrightarrow C^0(\bar{\Omega}, \mathbb{R}^2)$ ensuring that the geometrical term makes sense and the generalized Hölder inequality ([4]) guarantees that $\det \nabla \varphi \in L^2(\Omega)$.

6.1.3 Mathematical obstacle and relaxed problem

We are faced with a theoretical problem with problem (P).

Proposition 6.1.1

W is not rank 1-convex.

Proof: The proof is based on the same technique as the one applied by A. Raoult in [23].

Let $\varepsilon > 0$. We set $F = \varepsilon I$ and $F' = \varepsilon \text{diag}(1, 3)$. Then $F - F' = \begin{pmatrix} 0 & 0 \\ 0 & -2\varepsilon \end{pmatrix}$ and we

have $\text{rank}(F - F') = 1$.

We have $\det F = \varepsilon^2$, $\det F' = 3\varepsilon^2$, $\|F\|^2 = 2\varepsilon^2$, $\|F'\|^2 = 10\varepsilon^2$, $\det\left(\frac{F+F'}{2}\right) = 2\varepsilon^2$, $\left\|\frac{F+F'}{2}\right\|^2 = 5\varepsilon^2$.

We argue by contradiction and assume that W is rank 1-convex, then

$$W\left(\frac{F+F'}{2}\right) \leq \frac{1}{2} (W(F) + W(F')),$$

$$\begin{aligned}
\iff 5a_1\varepsilon^2 + 25a_2\varepsilon^4 - 2\mu\varepsilon^4 + \mu(2\varepsilon^2 - 1)^2 &\leq \frac{1}{2}\left(2a_1\varepsilon^2 + 4a_2\varepsilon^4 - \frac{\mu}{2}\varepsilon^4 + \mu(\varepsilon^2 - 1)^2\right. \\
&\quad \left.+ 10a_1\varepsilon^2 + 100a_2\varepsilon^4 - \frac{9}{2}\mu\varepsilon^4 + \mu(3\varepsilon^2 - 1)^2\right), \\
\iff \varepsilon^2(5a_1 - 4\mu) + \varepsilon^4(25a_2 + 2\mu) &\leq \frac{1}{2}\left(\varepsilon^2(12a_1 - 8\mu) + \varepsilon^4(104a_2 + 5\mu)\right), \\
\iff a_1\varepsilon^2 + 27a_2\varepsilon^4 + \frac{1}{2}\mu\varepsilon^4 &\geq 0, \\
\iff \underbrace{a_1}_{<0} + \varepsilon^2\left(27a_2 + \frac{1}{2}\mu\right) &\geq 0.
\end{aligned}$$

which raises a contradiction for ε small enough. ■

The stored energy function W is not rank 1-convex so it is not quasiconvex, which raises a drawback of theoretical nature since we cannot obtain the weak sequential lower semicontinuity of the functional (quasiconvexity is a necessary and sufficient condition to get weak lower semicontinuity). This prevents us from applying the direct method. As stressed by Dacorogna ([10, page 17]), the general rule is that in this case the considered problem has no minimizers.

Proposition 6.1.2

The stored energy function $W(F)$ can be written as follows:

$$W(F) = \beta(\|F\|^2 - \alpha)^2 + \psi(\det F),$$

with $\beta > 0$, $\alpha > 0$, and where ψ is a convex function.

Proof:

$$\begin{aligned}
W(F) &= a_2\|F\|^4 + a_1\|F\|^2 + \phi(\det F) + \frac{\lambda + \mu}{2}, \\
&= a_2\left(\|F\|^2 - \left(-\frac{a_1}{2a_2}\right)\right)^2 - a_2\left(\frac{a_1}{2a_2}\right)^2 + \frac{\lambda + \mu}{2} + \phi(\det F), \\
&= \beta(\|F\|^2 - \alpha)^2 + \psi(\det F),
\end{aligned}$$

with $\beta = a_2 = \frac{\lambda + 2\mu}{8}$, $\alpha = -\frac{a_1}{2a_2} = 2\frac{\lambda + \mu}{\lambda + 2\mu}$
and $\psi : s \mapsto -\frac{\mu}{2}s^2 + \mu(s - 1)^2 + \underbrace{\frac{\mu(\lambda + \mu)}{2(\lambda + 2\mu)}}_{\gamma}$ convex. ■

Theorem 6.1.1 (*Bousselsal [3, Theorem 3.1]*)

Let $W : \mathbb{R}^{n \times n} \rightarrow \mathbb{R}$. Let $\psi : \mathbb{R} \rightarrow \mathbb{R}$ be a convex function such that

$$W(F) = \beta(\|F\|^2 - \alpha)^2 + \psi(\det F), \quad \alpha, \beta \in \mathbb{R}_+^*.$$

Then

$$PW(F) = QW(F) = RW(F) = \begin{cases} W(F) & \text{if } \|F\|^2 \geq \alpha \\ \psi(\det F) & \text{if } \|F\|^2 < \alpha. \end{cases}$$

Before proving Theorem 6.1.1, we give the following lemmas:

Lemma 6.1.2 (*Bousselsal [3, Lemma 3.1]*)

Let $f : \mathbb{R}^{n \times n} \rightarrow \mathbb{R}$ and $\psi : \mathbb{R} \rightarrow \mathbb{R}$ such that

$$f(F) = \psi(\det F).$$

Then

$$f \text{ polyconvex} \iff f \text{ quasiconvex} \iff f \text{ rank-1 convex} \iff \psi \text{ convex}.$$

Proof (taken from [3]): By definition, we have f polyconvex $\iff \psi$ convex.

Moreover, we know that f polyconvex $\implies f$ quasiconvex $\implies f$ rank-1 convex.

Thus we just need to prove that f rank-1 convex $\implies \psi$ convex.

Let A and $B \in \mathbb{R}^{n \times n}$ be such that $\text{rank}(A - B) \leq 1$.

We suppose that f is rank 1-convex then for $\lambda \in [0, 1]$:

$$\begin{aligned} f(\lambda A + (1 - \lambda)B) &\leq \lambda f(A) + (1 - \lambda)f(B) \\ \iff \psi(\det(\lambda A + (1 - \lambda)B)) &\leq \lambda \psi(\det A) + (1 - \lambda)\psi(\det B) \end{aligned}$$

We use the following lemma.

Lemma 6.1.3 (*Dacorogna [10, Lemma 5.5]*)

Let $\xi \in \mathbb{R}^{N \times n}$ and $T : \mathbb{R}^{N \times n} \rightarrow \mathbb{R}^{\tau(n, N)}$ is such that $T(\xi) = (\xi, \text{adj}_2 \xi, \dots, \text{adj}_{n \wedge N})$ with $\tau(n, N) = \sum_{s=1}^{n \wedge N} \sigma(s)$ where $\sigma(s) = \binom{N}{s} \binom{n}{s}$.

For every $\xi, \eta \in \mathbb{R}^{N \times n}$ with $\text{rank}(\xi - \eta) \leq 1$ and for every $\lambda \in [0, 1]$, the following identity holds:

$$T(\lambda \xi + (1 - \lambda)\eta) = \lambda T(\xi) + (1 - \lambda)T(\eta).$$

Then we obtain that $\det(\lambda A + (1 - \lambda)B) = \lambda \det A + (1 - \lambda) \det B$. Therefore

$$\psi(\lambda \det A + (1 - \lambda) \det B) \leq \lambda \psi(\det A) + (1 - \lambda)\psi(\det B).$$

Then ψ is convex. ■

Lemma 6.1.4 (*Bousselsal [3, Lemma 3.2]*)

Let $F \in \mathbb{R}^{n \times n}$ be such that $0 \leq \|F\|^2 < \alpha$. Then there exist $B, C \in \mathbb{R}^{n \times n}, \lambda \in]0, 1[$ such that

$$\begin{aligned} F &= \lambda B + (1 - \lambda)C, \\ \text{rank}(B - C) &\leq 1, \\ \|B\|^2 &= \|C\|^2 = \alpha, \\ \det F &= \det B = \det C. \end{aligned}$$

Proof (taken from [3]):

If $\text{rank}(F) = 1$, the result is immediate taking $B = -\sqrt{\alpha} \frac{F}{\|F\|}, C = \sqrt{\alpha} \frac{F}{\|F\|}$

and $\lambda = \frac{1}{2} \left(1 - \frac{\|F\|}{\sqrt{\alpha}}\right)$.

If $\text{rank}(F) = 0$, which means that F is the null matrix, it suffices to take for example $B = (B_1, 0, \dots, 0)$ with $B_1 = \sqrt{\alpha}(1, 0, \dots, 0)^T, C = -B$, and $\lambda = \frac{1}{2}$.

If $\text{rank}(F) \neq 1$, we denote by F_j the j^{th} column of F . Then there exists j_0 such that $F_{j_0} \neq 0$. We can suppose that $F_2 \neq 0$ without loss of generality, then we set $E = aG$ with $G = (F_2, 0, \dots, 0) \in \mathbb{R}^{n \times n}, a \neq 0$.

We choose

$$\begin{aligned} B &= F - (1 - \lambda)E, \\ C &= F + \lambda E. \end{aligned}$$

Matrix E has rank equal to 1, and we have $F = \lambda B + (1 - \lambda)C$ and $\text{rank}(B - C) \leq 1$. Moreover, $\det F = \det B = \det C$.

It remains to prove that $\|B\|^2 = \|C\|^2 = \alpha$, which is equivalent to

$$\begin{cases} \|F\|^2 - 2(1 - \lambda)(F, E) + (1 - \lambda)^2 \|E\|^2 = \alpha \\ \|F\|^2 + 2\lambda(F, E) + \lambda^2 \|E\|^2 = \alpha, \end{cases}$$

$$\iff \begin{cases} \|F\|^2 - 2(1 - \lambda)a(F, G) + (1 - \lambda)^2 a^2 \|G\|^2 = \alpha & (6.3) \\ \|F\|^2 + 2\lambda a(F, G) + \lambda^2 a^2 \|G\|^2 = \alpha. & (6.4) \end{cases}$$

We set $\Sigma = 2(F, G)$, (\cdot, \cdot) denoting the inner product.

The last step consists in finding $\lambda \in]0, 1[$ and a such that (6.3) and (6.4) are satisfied.

We can notice that if $\bar{\lambda}$ and $\bar{\lambda} - 1$ are solutions of (6.4), then (6.3) is satisfied. This is the case if

$$\begin{aligned} \bar{\lambda} + \bar{\lambda} - 1 &= \frac{-a\Sigma}{a^2 \|G\|^2}, \\ \iff \bar{\lambda} &= \frac{1}{2} \left(1 - \frac{a\Sigma}{a^2 \|G\|^2}\right). \end{aligned}$$

The equations are satisfied if

$$\begin{aligned} \bar{\lambda}(\bar{\lambda} - 1) &= \frac{\|F\|^2 - \alpha}{a^2 \|G\|^2}, \\ \iff \left(\frac{a\Sigma}{a^2 \|G\|^2}\right)^2 &+ \frac{4(\alpha - \|F\|^2)}{a^2 \|G\|^2} = 1. \end{aligned}$$

We assume that we can find an $a \in \mathbb{R}$ such that

$$\left(\frac{a\Sigma}{a^2\|G\|^2} \right)^2 + \frac{4(\alpha - \|F\|^2)}{a^2\|G\|^2} = 1 \quad (6.5)$$

then

$$-1 \leq \frac{a\Sigma}{a^2\|G\|^2} \leq 1$$

and so $\bar{\lambda} \in]0, 1[$. It remains to be proved that there exists $a \in \mathbb{R}$ such that (6.5) holds. To do so, we notice that

- if $a \rightarrow 0$ the left member of (6.5) tends to $+\infty$,
- if $a \rightarrow +\infty$ the left member of (6.5) tends to 0.

By continuity, there exists a value of a such that (6.5) is satisfied. Therefore, we obtain the desired result. ■

Theorem 6.1.5 (*Bousselsal [3, Theorem 3.2]*)

We assume that g is a non-negative function such that $g = 0$ on $\|F\|^2 = \alpha$, and g is convex outside $B_\alpha = \{F : \|F\|^2 \leq \alpha\}$.

Then

$$Cg = Pg = Qg = Rg = \begin{cases} g & \text{outside } B_\alpha \\ 0 & \text{inside } B_\alpha. \end{cases}$$

Proof: We denote by

$$\tilde{g} = \begin{cases} g & \text{outside } B_\alpha \\ 0 & \text{inside } B_\alpha. \end{cases}$$

By construction, we have $\tilde{g} \leq g$.

We begin by proving that the function \tilde{g} is convex.

On the one hand, if $\lambda F_1 + (1 - \lambda)F_2 \in B_\alpha$, $\lambda \in [0, 1]$, and since $\tilde{g} \geq 0$, we have

$$0 = \tilde{g}(\lambda F_1 + (1 - \lambda)F_2) \leq \lambda \tilde{g}(F_1) + (1 - \lambda) \tilde{g}(F_2).$$

On the other hand, we focus on the outside of B_α .

Function g is convex outside B_α and non-negative so if there exists a convex function \hat{g} such that $\hat{g} = g$ outside B_α , necessarily by convexity of \hat{g} , $\hat{g} \leq 0$ on B_α .

If $\lambda F_1 + (1 - \lambda)F_2 \notin B_\alpha$, we have

$$\tilde{g}(\lambda F_1 + (1 - \lambda)F_2) = \hat{g}(\lambda F_1 + (1 - \lambda)F_2)$$

and

$$\hat{g}(\lambda F_1 + (1 - \lambda)F_2) \leq \lambda \hat{g}(F_1) + (1 - \lambda) \hat{g}(F_2) \leq \lambda \tilde{g}(F_1) + (1 - \lambda) \tilde{g}(F_2).$$

Therefore, we have proved that

$$\tilde{g}(\lambda F_1 + (1 - \lambda)F_2) \leq \lambda \tilde{g}(F_1) + (1 - \lambda) \tilde{g}(F_2)$$

for all $F_1, F_2 \in \mathbb{R}^{n \times n}$, $\lambda \in [0, 1]$, then \tilde{g} is convex.

Next, if h is a convex function such that $h \leq g$, by convexity, we also have $h \leq \tilde{g}$ and by definition of the convex envelop $Cg = \tilde{g}$. Since $Cg \leq Pg \leq Qg \leq Rg \leq g$ and $\tilde{g} = g$ outside B_α , then

$$Cg = Pg = Qg = Rg = g \text{ outside } B_\alpha.$$

Inside B_α , we have $Cg = \tilde{g} = 0$. Moreover, according to lemma 6.1.4, for $F \in B_\alpha$, there exist $B, C \in (\mathbb{R}^{n \times n})^2$ and $\lambda \in]0, 1[$ such that $F = \lambda B + (1 - \lambda)C$, $\text{rank}(B - C) \leq 1$ and $\|B\|^2 = \|C\|^2 = \alpha$.

Therefore,

$$Rg(F) = Rg(\lambda B + (1 - \lambda)C) \leq \lambda Rg(B) + (1 - \lambda)Rg(C) \leq \lambda g(B) + (1 - \lambda)g(C).$$

But, $g(C) = g(B) = 0$, since $\|B\|^2 = \|C\|^2 = \alpha$, so $Rg(F) \leq 0$. We obtain

$$0 = Cg \leq Rg \leq 0 \text{ inside } B_\alpha.$$

In conclusion,

$$Cg = Pg = Qg = Rg = \tilde{g}. \quad \blacksquare$$

Proof of Theorem 6.1.1 (from [3]):

Let $f(F) = \psi(\det F)$ and $g(F) = \beta(\|F\|^2 - \alpha)^2$ then $W(F) = f(F) + g(F)$. The function ψ being convex, f is polyconvex. According to Theorem 6.1.5, we can deduce that

$$Cg(F) = Pg(F) = Qg(F) = Rg(F) = \begin{cases} g(F) & \text{if } \|F\|^2 \geq \alpha \\ 0 & \text{if } \|F\|^2 < \alpha. \end{cases}$$

Moreover, $g = W - f \geq Cg = Pg$ and f is polyconvex so $f + Pg$ is polyconvex and $W \geq f + Pg = f + Cg$ then by definition of the polyconvex envelop, we obtain:

$$PW(F) \geq (f + Cg)(F) = \begin{cases} W(F) & \text{if } \|F\|^2 \geq \alpha \\ f(F) & \text{if } \|F\|^2 < \alpha. \end{cases}$$

In particular we have

$$PW(F) = RW(F) = W(F) \text{ if } \|F\|^2 \geq \alpha$$

and

$$f(F) \leq PW(F) \leq QW(F) \leq RW(F) \text{ if } \|F\|^2 < \alpha.$$

It remains to prove the inequality $RW(F) \leq f(F)$ in the case $\|F\|^2 < \alpha$.

According to lemma 6.1.4, there exist $B, C \in \mathbb{R}^{n \times n}$ and $\lambda \in]0, 1[$ such that $F = \lambda B + (1 - \lambda)C$, $\text{rank}(B - C) \leq 1$, $\det B = \det C = \det F$, and $\|B\|^2 = \|C\|^2 = \alpha$. By definition, $RW(F)$ is rank-one convex, we obtain:

$$RW(F) \leq \lambda RW(B) + (1 - \lambda)RW(C) \leq \lambda W(B) + (1 - \lambda)W(C) = \lambda f(B) + (1 - \lambda)f(C) = \psi(\det F)$$

According to the two previous inequalities, we can conclude that $RW(F) = f(F)$ if $\|F\|^2 < \alpha$. Therefore,

$$PW(F) = QW(F) = RW(F) = \begin{cases} W(F) & \text{if } \|F\|^2 \geq \alpha \\ \psi(\det F) & \text{if } \|F\|^2 < \alpha. \end{cases} \quad \blacksquare$$

Remark 6.1.3

We can show the same result using Dacorogna's arguments.

Alternative proof: The proof is based on a property of invariance of the considered stored energy function. We first recall a few definitions.

Definition 6.1.6 (Dacorogna [10])

- The set of *orthogonal matrices* is denoted by $O(n)$. It is the set of matrices $R \in M_n(\mathbb{R})$ such that

$$RR^t = I.$$

- The set of *special orthogonal matrices*, denoted by $SO(n)$, is the subset of $O(n)$ such that the matrices satisfy

$$\det R = 1.$$

- Let $\xi \in M_n(\mathbb{R})$. The *singular values* of ξ , denoted by

$$0 \leq \lambda_1 \leq \dots \leq \lambda_n,$$

are defined to be the square root of the eigenvalues of the symmetric positive semidefinite matrix $\xi\xi^t \in M_n(\mathbb{R})$.

- The *signed singular values* of ξ , denoted by

$$0 \leq |\mu_1(\xi)| \leq \mu_2(\xi) \leq \dots \leq \mu_n(\xi),$$

are defined by

$$\mu_1(\xi) = \lambda_1(\xi) \operatorname{sign}(\det \xi) \quad \text{and} \quad \mu_j(\xi) = \lambda_j(\xi), \quad \forall j = 2, \dots, n.$$

- A function $f : M_n(\mathbb{R}) \rightarrow [-\infty, +\infty]$ is said to be $SO(n) \times SO(n)$ invariant if:

$$\forall \xi \in M_n(\mathbb{R}), \forall Q, R \in SO(n) \times SO(n), f(Q\xi R) = f(\xi).$$

According to the singular value theorem (Theorem 13.3 in [10]), for all $\xi \in M_n(\mathbb{R})$, we can find Q and R in $SO(n)$ such that $\xi = Q\Lambda R$ where $\Lambda = \operatorname{diag}(\operatorname{sign}(\det \xi)\lambda_1, \lambda_2, \dots, \lambda_n)$. In terms of singular values, function W can be rewritten

$$W(\xi) = \beta(\lambda_1^2 + \lambda_2^2 - \alpha)^2 + \psi(\operatorname{sign}(\det \xi)\lambda_1\lambda_2) = \beta(\lambda_1^2 + \lambda_2^2 - \alpha)^2 + \psi(\mu_1\mu_2).$$

Let

$$g(\xi) = \begin{cases} W(\xi) & \text{if } \|\xi\|^2 \geq \alpha \\ \psi(\xi) & \text{if } \|\xi\|^2 < \alpha. \end{cases}$$

In view of the general results, we have:

$$PW \leq QW \leq RW \leq W.$$

Therefore, we only need to prove that

$$RW(\xi) = PW(\xi) = g(\xi), \quad \forall \xi \in M_n(\mathbb{R}).$$

The stored energy function $W(\xi)$ is $SO(2) \times SO(2)$ invariant as function of the trace and the determinant. Indeed,

$$\begin{cases} \|\xi\|^2 = \text{tr}(\xi^T \xi), \\ \|Q\xi R\|^2 = \text{tr}(R^T \xi^T Q^T Q \xi R) = \text{tr}(R^T \xi^T \xi R) = \text{tr}(\xi^T \xi R R^T) = \|\xi\|^2, \\ \det(Q\xi R) = \det(\xi). \end{cases}$$

Hence, according to Theorem 6.20 in [10], PW , QW and RW are $SO(2) \times SO(2)$ invariant. Therefore, we can restrict ourselves to the case of matrices of the form:

$$\xi = \begin{pmatrix} x & 0 \\ 0 & y \end{pmatrix} \text{ where } |x| \leq y.$$

Then we have: $\det \xi = xy$ and $\|\xi\|^2 = x^2 + y^2$.

Before proceeding further, it is convenient to introduce the two following functions defined on \mathbb{R}^2 by

$$\begin{cases} \chi(x, y) = \beta(x^2 + y^2 - \alpha)^2 + \mu(xy - 1)^2 - \frac{\mu}{2}x^2y^2 + \gamma \\ \phi(x, y) = \beta[x^2 + y^2 - \alpha]_+^2 + \mu(xy - 1)^2 - \frac{\mu}{2}x^2y^2 + \gamma \end{cases}$$

$$\text{with } [z]_+^2 = \begin{cases} z^2 & \text{if } z \geq 0 \\ 0 & \text{otherwise.} \end{cases}$$

A simple calculation leads to $W \begin{pmatrix} x & 0 \\ 0 & y \end{pmatrix} = \chi(x, y)$ and $g \begin{pmatrix} x & 0 \\ 0 & y \end{pmatrix} = \phi(x, y)$. According to Definition 5.42 of [10], ϕ is polyconvex, then g is polyconvex ([10, Theorem 5.43]). Since $g(\xi) \leq W(\xi)$ and $PW = \sup\{h \leq W, h \text{ polyconvex}\}$, we have

$$g(\xi) \leq PW(\xi).$$

Case 1: $\|\xi\|^2 < \alpha$.

Let us set

$$\xi_1 = \begin{pmatrix} x & 0 \\ -\sqrt{\alpha - (x^2 + y^2)} & y \end{pmatrix}, \quad \xi_2 = \begin{pmatrix} x & 0 \\ \sqrt{\alpha - (x^2 + y^2)} & y \end{pmatrix}$$

Then

$$\begin{cases} \xi = \frac{1}{2}\xi_1 + \frac{1}{2}\xi_2, \\ \|\xi_1\|^2 = \|\xi_2\|^2 = \alpha, \\ \text{and } \text{rank}(\xi_1 - \xi_2) = 1. \end{cases}$$

This implies that

$$g(\xi) \leq PW(\xi) \leq RW(\xi) \leq \frac{1}{2}RW(\xi_1) + \frac{1}{2}RW(\xi_2) \leq \frac{1}{2}W(\xi_1) + \frac{1}{2}W(\xi_2) = g(\xi).$$

Case 2: $\|\xi\|^2 \geq \alpha$.

$$W(\xi) = g(\xi) \leq PW(\xi) \leq QW(\xi) \leq RW(\xi) \leq W(\xi),$$

which concludes the proof. ■

As established in Proposition 6.1.1, the functional to be minimized is not quasiconvex, therefore we cannot prove the existence of minimizers of the functional using the direct method. Indeed, quasiconvexity is a necessary and sufficient condition to get (sequentially) weak lower semicontinuity. To overcome this issue, we propose to deal with a relaxed problem associated with the original problem obtained by taking the quasiconvex envelop of W . In the sequel, we prove that the initial and this relaxed problem both admit the same infimum.

6.1.4 Theoretical results

Definition 6.1.7 (Dacorogna [10])

Given the problem

$$\inf \left\{ I(u) = \int_{\Omega} f(x, u(x), \nabla u(x)) dx : u \in u_0 + W^{1,p}(\Omega, \mathbb{R}^N) \right\}, \quad (\text{P})$$

where

- $\Omega \subset \mathbb{R}^n, n \geq 1$, is a bounded open set,
- $u : \Omega \rightarrow \mathbb{R}^N, N \geq 1$ and $u_0 \in W^{1,p}(\Omega, \mathbb{R}^N)$ is a given function,
- $f : \Omega \times \mathbb{R}^N \times \mathbb{R}^{N \times n}, f = f(x, u, \xi)$, is a given non-quasiconvex function.

There is a way of defining generalized solutions of (P) via the so-called *relaxed problem*

$$\inf \left\{ \bar{I}(u) = \int_{\Omega} Qf(x, u(x), \nabla u(x)) dx : u \in u_0 + W^{1,p}(\Omega, \mathbb{R}^N) \right\}, \quad (\text{QP})$$

where Qf is the quasiconvex envelop of f with respect to the last variable.

Applying this definition to our problem, we can define a relaxed problem (not exactly the relaxed problem in the sense of Dacorogna since our functional cannot be written in integral form). Therefore, we define our relaxed problem.

Proposition 6.1.4

The relaxed problem associated to (P) we consider hereafter is defined by:

$$\inf_{\varphi \in \mathcal{W}} \left\{ \bar{I}(\varphi) = \frac{\nu}{2} \int_{\Omega} (T \circ \varphi(x) - R(x))^2 dx + \int_{\Omega} QW(\nabla \varphi) dx + \eta \langle \rho(\varphi) \rangle_{2N}^2 - 2\eta \langle \rho(\varphi), \tilde{\omega} \rangle_{2N} \right\} \quad (\text{QP})$$

where $\mathcal{W} = \left\{ \varphi \in \text{Id} + W_0^{1,4}(\Omega, \mathbb{R}^2) \right\}$, and QW is the quasiconvex envelop of W given by:

$$QW(F) = \begin{cases} \beta(\|F\|^2 - \alpha)^2 + \psi(\det F) & \text{if } \|F\|^2 \geq \alpha, \\ \psi(\det F) & \text{if } \|F\|^2 < \alpha, \end{cases}$$

with $\psi : s \mapsto -\frac{\mu}{2}s^2 + \mu(s-1)^2 + \gamma$ convex.

Theorem 6.1.8

Assume that \bar{I} is proper. Then functional \bar{I} admits minimizers in \mathcal{W} .

Proof: The proof is divided into three steps.

Coercivity inequality

In the first step, we demonstrate that the infimum is finite by establishing a coercivity inequality.

First, we have

$$\beta(\|\nabla \varphi\|^2 - \alpha)^2 \geq \frac{\beta}{2} \|\nabla \varphi\|^4 - \beta \alpha^2.$$

It could be recalled that $\psi(s) = -\frac{\mu}{2}s^2 + \mu(s-1)^2 + \gamma = \frac{\mu}{4}s^2 + \frac{\mu}{4}s^2 - 2\mu s + \mu + \gamma \geq \frac{\mu}{4}s^2 - 3\mu + \gamma$. Consequently,

$$QW(\nabla \varphi) \geq \frac{\beta}{2} \|\nabla \varphi\|^4 - \beta \alpha^2 + \frac{\mu}{4} (\det \nabla \varphi)^2 - 3\mu + \gamma. \quad (6.6)$$

We know that $W^{1,4}(\Omega, \mathbb{R}^2)$ is continuously embedded in $\mathcal{C}^0(\bar{\Omega}, \mathbb{R}^2)$ endowed with the norm $\|\varphi\|_{\mathcal{C}^0(\bar{\Omega}, \mathbb{R}^2)} = \sup_{x \in \bar{\Omega}} \langle \varphi(x) \rangle_2$.

That is to say that there exists a constant C depending only on Ω such that

$$\forall \varphi \in W^{1,4}(\Omega, \mathbb{R}^2), \|\varphi\|_{\mathcal{C}^0(\bar{\Omega}, \mathbb{R}^2)} \leq C \|\varphi\|_{W^{1,4}(\Omega, \mathbb{R}^2)}.$$

Since the term $\langle \rho(\varphi) \rangle_{2N}^2$ is positive, we just have to bound from below the term $-2\eta \langle \rho(\varphi), \tilde{\omega} \rangle_{2N}$. Indeed,

$$\begin{aligned} \langle \rho(\varphi), \tilde{\omega} \rangle_{2N} &\leq \langle \rho(\varphi) \rangle_{2N} \langle \tilde{\omega} \rangle_{2N} \text{ (by Cauchy-Schwartz)} \\ &\leq \sqrt{N} \langle \tilde{\omega} \rangle_{2N} \|\varphi\|_{C^0(\bar{\Omega}, \mathbb{R}^2)} \\ &\leq C_1(N, \Omega) \|\varphi\|_{W^{1,4}(\Omega, \mathbb{R}^2)}. \end{aligned}$$

Hence,

$$\bar{I}(\varphi) \geq C_2 \|\nabla \varphi\|_{L^4(\Omega, M_2)}^4 - C_1 \|\varphi\|_{W^{1,4}(\Omega, \mathbb{R}^2)} + \frac{\mu}{4} \|\det \nabla \varphi\|_{L^2(\Omega)}^2 + K,$$

where $C_2 = \frac{\beta}{2}$, and $K \in \mathbb{R}$. The constant K may change line to line. We use the generalized Poincaré inequality ([15]):

$$\|\varphi\|_{L^4(\Omega, \mathbb{R}^2)}^4 \leq c \left(\|\nabla \varphi\|_{L^4(\Omega, M_2)}^4 + \left| \int_{\partial\Omega} \varphi d\sigma \right|^4 \right).$$

Since φ is known on $\partial\Omega$,

$$\|\varphi\|_{W^{1,4}(\Omega, \mathbb{R}^2)}^4 \leq (c+1) \|\nabla \varphi\|_{L^4(\Omega, M_2)}^4 + k,$$

which implies that

$$\bar{I}(\varphi) \geq \frac{C_2}{c+1} \left(\|\varphi\|_{W^{1,4}(\Omega, \mathbb{R}^2)}^4 - C'_1 \|\varphi\|_{W^{1,4}(\Omega, \mathbb{R}^2)} + \frac{\mu(c+1)}{4C_2} \|\det \nabla \varphi\|_{L^2(\Omega)}^2 \right) + K.$$

Using Young inequality, $ab \leq \frac{a^p}{p} + \frac{b^q}{q}$, taking $a = \|\varphi\|_{W^{1,4}(\Omega, \mathbb{R}^2)}$, $b = C'_1$, $p = 4$, $q = \frac{4}{3}$, we obtain

$$C'_1 \|\varphi\|_{W^{1,4}(\Omega, \mathbb{R}^2)} \leq \frac{1}{4} \|\varphi\|_{W^{1,4}(\Omega, \mathbb{R}^2)}^4 + C_q.$$

To conclude,

$$\boxed{\bar{I}(\varphi) \geq C_3 \left(\|\varphi\|_{W^{1,4}(\Omega, \mathbb{R}^2)}^4 + \|\det \nabla \varphi\|_{L^2(\Omega)}^2 \right) + K.} \quad (6.7)$$

Therefore, the infimum of \bar{I} is finite.

Convergence of a minimizing sequence in \mathcal{W}

Let $(\varphi_k) \in \mathcal{W}$ be a minimizing sequence of the problem, that is:

$$\bar{I}(\varphi_k) \longrightarrow \inf_{\Psi \in \mathcal{W}} \bar{I}(\Psi) \text{ when } k \longrightarrow +\infty.$$

We have assumed that \bar{I} is proper so $\exists \tilde{\varphi} \in \mathcal{W}$ such that $\bar{I}(\tilde{\varphi}) < +\infty$. For k large enough: $\bar{I}(\varphi_k) \leq \bar{I}(\tilde{\varphi}) + 1$. Thanks to the coercivity inequality,

$$C_3 \left(\|\varphi_k\|_{W^{1,4}(\Omega, \mathbb{R}^2)}^4 + \|\det \nabla \varphi_k\|_{L^2(\Omega)}^2 \right) + K \leq \bar{I}(\varphi_k) \leq \bar{I}(\tilde{\varphi}) + 1,$$

and we can deduce that

$$\begin{cases} \varphi_k \text{ is bounded in } W^{1,4}(\Omega, \mathbb{R}^2) \text{ independently of } k, \\ \det(\nabla\varphi_k) \text{ is bounded in } L^2(\Omega) \text{ independently of } k. \end{cases} \quad (6.8)$$

Therefore, we can extract a subsequence of φ_k (still denoted by φ_k) such that:

$$\begin{cases} \varphi_k \rightharpoonup \bar{\varphi} \text{ in } W^{1,4}(\Omega, \mathbb{R}^2), \\ \det(\nabla\varphi_k) \rightharpoonup \delta \text{ in } L^2(\Omega). \end{cases} \quad (6.9)$$

We have the following theorem:

Theorem 6.1.9 ([10, Theorem 8.20])

Let Ω be a bounded open set, $1 < p < \infty$, and let

$$u_\nu \rightharpoonup u \text{ in } W^{1,p}(\Omega, \mathbb{R}^N).$$

- Let $N = n = 2$ and $p \geq 2$. Then

$$\det \nabla u_\nu \rightharpoonup \det \nabla u \text{ in } \mathcal{D}'(\Omega),$$

and if $p > 2$, then

$$\det \nabla u_\nu \rightharpoonup \det \nabla u \text{ in } L^{p/2}(\Omega).$$

- Let $N = n = 3$. If $p \geq 2$ then

$$\text{adj}_2 \nabla u_\nu \rightharpoonup \text{adj}_2 \nabla u \text{ in } \mathcal{D}'(\Omega, \mathbb{R}^9),$$

and if $p > 2$, then

$$\text{adj}_2 \nabla u_\nu \rightharpoonup \text{adj}_2 \nabla u \text{ in } L^{p/2}(\Omega, \mathbb{R}^9).$$

If $p \geq 3$, then

$$\det \nabla u_\nu \rightharpoonup \det \nabla u \text{ in } \mathcal{D}'(\Omega),$$

and if $p > 3$, then

$$\det \nabla u_\nu \rightharpoonup \det \nabla u \text{ in } L^{p/3}(\Omega).$$

- Let $N = n$ and $p \geq n$. Then

$$\det \nabla u_\nu \rightharpoonup \det \nabla u \text{ in } \mathcal{D}'(\Omega),$$

and if $p > n$, then

$$\det \nabla u_\nu \rightharpoonup \det \nabla u \text{ in } L^{p/n}(\Omega).$$

- Let $N, n \geq 2, 2 \leq s \leq n \wedge N = \min(n, N)$ and $p \geq s$. Then

$$\text{adj}_s \nabla u_\nu \rightharpoonup \text{adj}_s \nabla u \text{ in } \mathcal{D}'(\Omega, \mathbb{R}^{\sigma(s)}),$$

where $\sigma(s) = \binom{N}{s} \binom{n}{s} = \frac{N!n!}{(s!)^2(N-s)!(n-s)!}$.

Furthermore, if $p > s$, then

$$\text{adj}_s \nabla u_\nu \rightharpoonup \text{adj}_s \nabla u \text{ in } L^{p/s}(\Omega, \mathbb{R}^{\sigma(s)}),$$

- Let $N, n \geq 2, 2 \leq s \leq n \wedge N$ and assume that

$$\text{adj}_{s-1} \nabla u_\nu \rightharpoonup \text{adj}_{s-1} \nabla u \text{ in } L^r(\Omega, \mathbb{R}^{\sigma(s-1)}),$$

where $r > 1$ with $\frac{1}{p} + \frac{1}{r} \leq 1$. Then

$$\text{adj}_s \nabla u_\nu \rightharpoonup \text{adj}_s \nabla u \text{ in } \mathcal{D}'(\Omega, \mathbb{R}^{\sigma(s)}).$$

Hence, by uniqueness of the weak limit in $L^2(\Omega)$, we can conclude that $\delta = \det(\nabla \bar{\varphi})$.

Lower semicontinuity of \bar{I}

Let $J(\Psi, \delta)$ be the functional defined by

$$J(\Psi, \delta) = \int_{\Omega} W^*(\nabla \Psi(x), \delta(x)) dx$$

$$\text{with } W^*(\nabla \Psi, \delta) = \begin{cases} \beta(\|\nabla \Psi\|^2 - \alpha)^2 + \psi(\delta) & \text{if } \|\nabla \Psi\|^2 \geq \alpha, \\ \psi(\delta) & \text{otherwise.} \end{cases}$$

J is defined on $W^{1,4}(\Omega, \mathbb{R}^2) \times L^2(\Omega)$ with values in \mathbb{R} .

It is convex and strongly sequentially lower semi-continuous since W^* is convex and continuous.

Thus it is weakly lower semicontinuous and

$$J(\bar{\varphi}, \det \nabla \bar{\varphi}) \leq \liminf_{k \rightarrow +\infty} J(\varphi_k, \det \nabla \varphi_k).$$

We recall that $W^{1,4}(\Omega, \mathbb{R}^2) \hookrightarrow \mathcal{C}^0(\bar{\Omega}, \mathbb{R}^2)$ with compact embedding so (φ_k) strongly converges to $\bar{\varphi}$ in $\mathcal{C}^0(\bar{\Omega}, \mathbb{R}^2)$, therefore, φ_k uniformly converges to $\bar{\varphi}$ and we have:

$$|\langle \rho(\varphi_k) - \rho(\bar{\varphi}), \tilde{w} \rangle_{2N}| \leq \underbrace{\langle \rho(\varphi_k) - \rho(\bar{\varphi}) \rangle_{2N}}_{\downarrow k \rightarrow +\infty} \langle \tilde{w} \rangle_{2N} \text{ and } \langle \rho(\varphi_k) \rangle_{2N}^2 \longrightarrow \langle \rho(\bar{\varphi}) \rangle_{2N}^2.$$

$$0$$

$$\text{According to Fatou's Lemma: } \int_{\Omega} (T \circ \bar{\varphi} - R)^2 dx \leq \liminf_{k \rightarrow +\infty} \int_{\Omega} (T \circ \varphi_k - R)^2 dx.$$

Finally,

$$\bar{I}(\bar{\varphi}) \leq \liminf_{k \rightarrow +\infty} \bar{I}(\varphi_k).$$

The space \mathcal{W} is a closed affine subspace of $W^{1,4}(\Omega, \mathbb{R}^2)$ by continuity of the trace on $\partial\Omega$, then \mathcal{W} is a strongly closed convex subspace. According to Theorem III.7 in [4], \mathcal{W} is a weakly closed convex subspace. Therefore, we obtain that $\bar{\varphi} \in \mathcal{W}$, that is to say that: $\bar{\varphi} = \text{Id}$ on $\partial\Omega$.

To conclude, the relaxed problem admits at least one solution $\bar{\varphi} \in \mathcal{W}$. ■

6.1.5 Relaxation theorem

Theorem 6.1.10

Let $\bar{\varphi} \in W^{1,4}(\Omega, \mathbb{R}^2)$ be a minimizer of the relaxed problem (QP). Then there exists a sequence

$$\{\varphi_k\}_{k=1}^\infty \subset \bar{\varphi} + W_0^{1,4}(\Omega, \mathbb{R}^2) \text{ such that } \varphi_k \xrightarrow{k \rightarrow \infty} \bar{\varphi} \text{ in } L^4(\Omega, \mathbb{R}^2)$$

and

$$I(\varphi_k) \longrightarrow \bar{I}(\bar{\varphi}).$$

Moreover, the following holds:

$$\varphi_k \rightharpoonup \bar{\varphi} \text{ in } W^{1,4}(\Omega, \mathbb{R}^2).$$

Solutions of problem (QP) are said to be generalized solutions of problem (P).

Proof: The proof is based on Theorem 9.8 in [10] and on the compact embedding of $W^{1,4}(\Omega, \mathbb{R}^2)$ in $C^0(\bar{\Omega}, \mathbb{R}^2)$ for the geometric constraints. ■

6.2 A convergence result

In this section, we establish a result of convergence when the number of geometrical constraints increases to infinity. The proof is based on prior related works developed in [1] dedicated to applications of D^m -splines in the theory of approximation.

Let D be a subset of $]0, +\infty[$ admitting 0 as accumulation point (this implies that $0 \in \bar{D}$). For each $d \in D$, let A^d be a set of $N = N(d)$ distinct points of $\bar{\Omega}$. We assume that

$$\sup_{x \in \Omega} \delta(x, A^d) = d, \tag{6.10}$$

where δ is the Euclidean distance in \mathbb{R}^2 . Let us observe that the left-hand side of (6.10) is just the Hausdorff distance between A^d and $\bar{\Omega}$. Consequently, it implies that D is bounded and that this distance tends to 0 as d does. Thus d is the radius of the largest sphere included in Ω that contains no point from A^d (Hausdorff distance).

For all $d \in D$, we denote by ρ^d the mapping defined by:

$$\rho^d : \begin{cases} W^{1,4}(\Omega, \mathbb{R}^2) \rightarrow (\mathbb{R}^2)^{N(d)} \\ \varphi \mapsto \rho^d(\varphi) = ((\varphi(a))_{a \in A^d})^T \end{cases} .$$

We denote by $\tilde{\omega}^d = (\tilde{\omega}_1, \dots, \tilde{\omega}_{N(d)})$ the corresponding landmark points on the Template image T .

Theorem 6.2.1

Assume that there exists $\hat{\varphi} \in W^{1,4}(\Omega, \mathbb{R}^2)$ such that for any $d \in D$, $\rho^d(\hat{\varphi}) = \tilde{\omega}^d$, $\hat{\varphi} = \text{Id}$ on $\partial\Omega$. For any $d \in D$, let us denote by φ^d a minimizer of (QP). Under the above assumptions, we have:

$$\lim_{d \rightarrow 0} \|\varphi^d - \hat{\varphi}\|_{C^0(\bar{\Omega}, \mathbb{R}^2)} = 0.$$

Proof: The proof is divided into three steps.

First step: We start by proving that the sequence $(\varphi^d)_{d \in D \cap]0, \eta']}$ (η' fixed) is bounded in $W^{1,4}(\Omega, \mathbb{R}^2)$ independently of d . By definition of a minimizer, we have:

$$\begin{aligned} \frac{\nu}{2} \int_{\Omega} (T \circ \varphi^d - R)^2 dx + \int_{\Omega} QW(\nabla \varphi^d) dx + \eta \langle \rho^d(\varphi^d) - \tilde{\omega}^d \rangle_{2N(d)}^2 \leq \frac{\nu}{2} \int_{\Omega} (T \circ \hat{\varphi} - R)^2 dx \\ + \int_{\Omega} QW(\nabla \hat{\varphi}) dx \end{aligned}$$

Using the coercivity inequality previously established ($\forall V \in L^4(\Omega, M_2)$, $QW(V) \geq -\mu + \gamma < 0$), we obtain that

$$\begin{cases} \varphi^d \text{ is bounded in } W^{1,4}(\Omega, \mathbb{R}^2) \text{ independently of } d, \\ \det \nabla \varphi^d \text{ is bounded in } L^2(\Omega) \text{ independently of } d. \end{cases}$$

Therefore, we can extract a subsequence (φ^{d_l}) that weakly converges to φ^* in $W^{1,4}(\Omega, \mathbb{R}^2)$:

$$(\varphi^{d_l}) \rightharpoonup \varphi^* \text{ in } W^{1,4}(\Omega, \mathbb{R}^2), \text{ with } \lim_{l \rightarrow +\infty} d_l = 0.$$

Second step: The second step consists in proving that $\varphi^* = \hat{\varphi}$.

We argue by contradiction, by assuming that $\varphi^* \neq \hat{\varphi}$. It means that there exists a non-empty open subset of Ω denoted by \aleph and a positive real $\alpha > 0$ such that

$$\forall x \in \aleph, \langle \hat{\varphi}(x) - \varphi^*(x) \rangle_2 > \alpha.$$

Let us set

$$\xi = 1 + \text{E} \left[\frac{1}{\eta \alpha^2} \left(\frac{\nu}{2} \int_{\Omega} (T \circ \hat{\varphi} - R)^2 dx + \int_{\Omega} QW(\nabla \hat{\varphi}) dx + \mu - \gamma \right) \right],$$

where E denotes the integer part.

Let $B_0 = \{p_{01}, \dots, p_{0\xi}\}$ be a subset of ξ distinct points of \aleph , we have:

$$\forall i = 1, \dots, \xi, \exists \left(p_{0i}^d \right)_{d \in D} \left(\forall d \in D, p_{0i}^d \in A^d \right) \text{ and } \left(p_{0i} = \lim_{d \rightarrow 0} p_{0i}^d \right)$$

For all $d \in D$, let B_0^d be the set $\{p_{01}^d, \dots, p_{0\xi}^d\}$. As $B_0^d \subset A^d$, we have:

$$\eta \sum_{i=1}^{\xi} \langle \varphi^{d_i}(p_{0i}^{d_i}) - \hat{\varphi}(p_{0i}^{d_i}) \rangle_2^2 \leq \frac{\nu}{2} \int_{\Omega} (T \circ \hat{\varphi} - R)^2 dx + \int_{\Omega} QW(\nabla \hat{\varphi}) dx + \mu - \gamma. \quad (6.11)$$

Moreover,

$$\begin{aligned} \langle \varphi^{d_i}(p_{0i}^{d_i}) - \varphi^*(p_{0i}) \rangle_2 &= \langle \varphi^{d_i}(p_{0i}^{d_i}) - \varphi^{d_i}(p_{0i}) + \varphi^{d_i}(p_{0i}) - \varphi^*(p_{0i}) \rangle_2, \\ &\leq \langle \varphi^{d_i}(p_{0i}^{d_i}) - \varphi^{d_i}(p_{0i}) \rangle_2 + \langle \varphi^{d_i}(p_{0i}) - \varphi^*(p_{0i}) \rangle_2. \end{aligned}$$

On the one hand, according to the compact embedding $W^{1,4}(\Omega, \mathbb{R}^2) \hookrightarrow C^{0, \frac{1}{2}}(\bar{\Omega}, \mathbb{R}^2)$, there exists a constant k_2 such that

$$\langle \varphi^{d_i}(p_{0i}^{d_i}) - \varphi^{d_i}(p_{0i}) \rangle_2 \leq k_2 \langle p_{0i}^{d_i} - p_{0i} \rangle_2^{\frac{1}{2}}.$$

But $\lim_{l \rightarrow +\infty} d_l = 0$ and $p_{0i} = \lim_{d \rightarrow 0} p_{0i}^d$, then

$$\lim_{l \rightarrow +\infty} \langle \varphi^{d_i}(p_{0i}^{d_i}) - \varphi^{d_i}(p_{0i}) \rangle_2 = 0.$$

On the other hand, according to Rellich-Kondrachov Theorem, we have the compact embedding $W^{1,4}(\Omega, \mathbb{R}^2) \hookrightarrow C^0(\bar{\Omega}, \mathbb{R}^2)$. Therefore, weak convergence in $W^{1,4}(\Omega, \mathbb{R}^2)$ implies uniform convergence:

$$\lim_{l \rightarrow +\infty} \langle \varphi^{d_i}(p_{0i}) - \varphi^*(p_{0i}) \rangle_2 = 0.$$

Hence,

$$\lim_{l \rightarrow +\infty} \langle \varphi^{d_i}(p_{0i}^{d_i}) - \varphi^*(p_{0i}) \rangle_2 = 0,$$

That is to say

$$\lim_{l \rightarrow +\infty} \varphi^{d_i}(p_{0i}^{d_i}) = \varphi^*(p_{0i}).$$

Letting $l \rightarrow +\infty$ in (6.11), we conclude that

$$\eta \sum_{i=1}^{\xi} \langle \varphi^*(p_{0i}) - \hat{\varphi}(p_{0i}) \rangle_2^2 \leq \frac{\nu}{2} \int_{\Omega} (T \circ \hat{\varphi} - R)^2 dx + \int_{\Omega} QW(\nabla \hat{\varphi}) dx + \mu - \gamma,$$

and then

$$\eta \alpha^2 \xi \leq \frac{\nu}{2} \int_{\Omega} (T \circ \hat{\varphi} - R)^2 dx + \int_{\Omega} QW(\nabla \hat{\varphi}) dx + \mu - \gamma,$$

which is in contradiction with the definition of ξ .

Therefore, $\varphi^* = \hat{\varphi}$ and (φ^{d_i}) weakly converges to $\hat{\varphi}$ in $W^{1,4}(\Omega, \mathbb{R}^2)$ and uniformly as a result.

Third step: We now prove that $(\varphi^d)_{d \in D \cap]0, \eta[}$ uniformly converges to $\hat{\varphi}$ arguing by contradiction.

We suppose that $\|\varphi^d - \hat{\varphi}\|_{C^0(\bar{\Omega}, \mathbb{R}^2)}$ does not tend to 0 when $d \rightarrow 0$, that is to say, that there exists a constant $\alpha > 0$ and a sequence $(d_k)_{k \in \mathbb{N}}$ such that $\lim_{k \rightarrow +\infty} d_k = 0$ and

$$\forall k \in \mathbb{N}, \|\varphi^{d_k} - \hat{\varphi}\|_{C^0(\bar{\Omega}, \mathbb{R}^2)} > \alpha. \quad (6.12)$$

Following the same previous steps, we build a subsequence of (φ^{d_k}) uniformly converging to $\hat{\varphi}$, which is in contradiction with the hypothesis (6.12). ■

6.3 Discretization and Implementation

6.3.1 Augmented Lagrangian

The computation of the Euler-Lagrange equations satisfied by u (we recall that $\varphi = \text{Id} + u$) turns out to be cumbersome. That is the reason why we introduce an auxiliary variable V , such that $V = \nabla \varphi$. Therefore, we consider the following constrained optimization problem

$$\begin{aligned} \min_{\varphi, V} \bar{\mathcal{J}}_\varepsilon(\varphi, V) \\ \text{such that } V = \nabla \varphi, \end{aligned} \quad (6.13)$$

with

$$\begin{aligned} \bar{\mathcal{J}}_\varepsilon(\varphi, V) = \frac{\nu}{2} \int_{\Omega} (T \circ \varphi(x) - R(x))^2 dx + \int_{\Omega} \beta (\|V\|^2 - \alpha)^2 \text{H}_\varepsilon(\|V\|^2 - \alpha) + \psi(\det V) dx \\ + \eta \langle \rho(\varphi) - \tilde{\omega} \rangle_{2N}^2. \end{aligned}$$

The function H_ε is the regularized one-dimensional Heaviside function, defined by

$$\text{H}_\varepsilon : z \mapsto \frac{1}{2} \left(1 + \frac{2}{\pi} \text{Arctan} \frac{z}{\varepsilon} \right) \text{ and we denote by } \delta_\varepsilon \text{ the regularized Dirac defined by}$$

$$\delta_\varepsilon : z \mapsto \frac{\varepsilon/\pi}{z^2 + \varepsilon^2}.$$

We propose to solve (6.13) by an augmented Lagrangian method which aims to solve:

$$\min_{\varphi, V} \max_{\beta} \mathcal{L}_{\alpha, \varepsilon}(\varphi, V, \beta) = \bar{\mathcal{J}}_\varepsilon(\varphi, V) + \frac{\alpha}{2} \int_{\Omega} \|V - \nabla \varphi\|^2 dx + \int_{\Omega} \beta : (V - \nabla \varphi) dx,$$

where $\beta \in M_2(\mathbb{R})$ is the Lagrangian multiplier (we think that there is confusion with the previously introduced coefficient β) and α is a positive constant.

The goal is thus to search for a saddle point of $\mathcal{L}_{\alpha, \varepsilon}$. We can summarize the algorithm as follows:

Algorithm 3 Augmented Lagrangian Method.

1. Initialization: $\beta^0 = 0$, $V^0 = I$, $\varphi^0 = \text{Id}$.

2. For $k = 0, 1, \dots$

$$(\varphi^{k+1}, V^{k+1}) = \arg \min_{\varphi, V} \mathcal{L}_{\alpha, \varepsilon}(\varphi, V, \beta^k) \quad (6.14)$$

Update $\beta^{k+1} = \beta^k + \alpha(V^{k+1} - \nabla \varphi^{k+1})$.

To solve (6.14), the problem is divided into two subproblems:

$$\min_V \int_{\Omega} QW(V) dx + \frac{\alpha}{2} \|V - \nabla\varphi\|^2 + \int_{\Omega} \beta : V dx, \quad (6.15)$$

for fixed φ , and then

$$\min_{\varphi} \frac{\nu}{2} \int_{\Omega} (T \circ \varphi(x) - R(x))^2 dx + \frac{\alpha}{2} \|V - \nabla\varphi\|^2 - \int_{\Omega} \beta : \nabla\varphi dx + \eta \langle \rho(\varphi) - \tilde{\omega} \rangle_{2N}^2, \quad (6.16)$$

for fixed V .

Numerically, the Euler-Lagrange equations in V and φ are alternatively solved using a gradient descent method, parameterizing the descent direction by an artificial time $t \geq 0$. We set $V = \begin{pmatrix} V_{11} & V_{12} \\ V_{21} & V_{22} \end{pmatrix}$ and $\beta = \begin{pmatrix} \beta_{11} & \beta_{12} \\ \beta_{21} & \beta_{22} \end{pmatrix}$.

The Euler-Lagrange equations for problem (6.15) are given by:

$$\left\{ \begin{array}{l} \frac{\partial \mathcal{L}_{\alpha,\varepsilon}}{\partial V_{11}} = \mu V_{22}(\det V - 2) + 4\beta(\|V\|^2 - \alpha)V_{11} \mathbf{H}_{\varepsilon}(\|V\|^2 - \alpha) + \\ \quad 2\beta(\|V\|^2 - \alpha)^2 V_{11} \delta_{\varepsilon}(\|V\|^2 - \alpha) + \beta_{11} + \alpha(V_{11} - \frac{\partial \varphi_1}{\partial x}) = 0, \\ \frac{\partial \mathcal{L}_{\alpha,\varepsilon}}{\partial V_{12}} = -\mu V_{21}(\det V - 2) + 4\beta(\|V\|^2 - \alpha)V_{12} \mathbf{H}_{\varepsilon}(\|V\|^2 - \alpha) \\ \quad + 2\beta(\|V\|^2 - \alpha)^2 V_{12} \delta_{\varepsilon}(\|V\|^2 - \alpha) + \beta_{12} + \alpha(V_{12} - \frac{\partial \varphi_1}{\partial y}) = 0, \\ \frac{\partial \mathcal{L}_{\alpha,\varepsilon}}{\partial V_{21}} = -\mu V_{12}(\det V - 2) + 4\beta(\|V\|^2 - \alpha)V_{21} \mathbf{H}_{\varepsilon}(\|V\|^2 - \alpha) \\ \quad + 2\beta(\|V\|^2 - \alpha)^2 V_{21} \delta_{\varepsilon}(\|V\|^2 - \alpha) + \beta_{21} + \alpha(V_{21} - \frac{\partial \varphi_2}{\partial x}) = 0, \\ \frac{\partial \mathcal{L}_{\alpha,\varepsilon}}{\partial V_{22}} = \mu V_{11}(\det V - 2) + 4\beta(\|V\|^2 - \alpha)V_{22} \mathbf{H}_{\varepsilon}(\|V\|^2 - \alpha) \\ \quad + 2\beta(\|V\|^2 - \alpha)^2 V_{22} \delta_{\varepsilon}(\|V\|^2 - \alpha) + \beta_{22} + \alpha(V_{22} - \frac{\partial \varphi_2}{\partial y}) = 0. \end{array} \right.$$

The descent gradient method gives:

$$\left\{ \begin{array}{l} \frac{\partial V_{11}}{\partial t} = -\frac{\partial \mathcal{L}_{\alpha,\varepsilon}}{\partial V_{11}}, \\ \frac{\partial V_{12}}{\partial t} = -\frac{\partial \mathcal{L}_{\alpha,\varepsilon}}{\partial V_{12}}, \\ \frac{\partial V_{21}}{\partial t} = -\frac{\partial \mathcal{L}_{\alpha,\varepsilon}}{\partial V_{21}}, \\ \frac{\partial V_{22}}{\partial t} = -\frac{\partial \mathcal{L}_{\alpha,\varepsilon}}{\partial V_{22}}, \end{array} \right.$$

and using semi-implicit finite difference schemes with a time step dt , we obtain the following discretized equations for V :

$$\left\{ \begin{array}{l} (1 + \alpha dt)V_{11}^{k+1} = V_{11}^k - dt \left[\mu V_{22}^k (\det V^k - 2) + 4\beta (\|V^k\|^2 - \alpha) V_{11}^k H_\varepsilon(\|V^k\|^2 - \alpha) \right. \\ \quad \left. + 2\beta (\|V^k\|^2 - \alpha)^2 V_{11}^k \delta_\varepsilon(\|V^k\|^2 - \alpha) + \beta_{11} - \alpha \frac{\partial \varphi_1}{\partial x} \right], \\ (1 + \alpha dt)V_{12}^{k+1} = V_{12}^k - dt \left[-\mu V_{21}^k (\det V^k - 2) + 4\beta (\|V^k\|^2 - \alpha) V_{12}^k H_\varepsilon(\|V^k\|^2 - \alpha) \right. \\ \quad \left. + 2\beta (\|V^k\|^2 - \alpha)^2 V_{12}^k \delta_\varepsilon(\|V^k\|^2 - \alpha) + \beta_{12} - \alpha \frac{\partial \varphi_1}{\partial y} \right], \\ (1 + \alpha dt)V_{21}^{k+1} = V_{21}^k - dt \left[-\mu V_{12}^k (\det V^k - 2) + 4\beta (\|V^k\|^2 - \alpha) V_{21}^k H_\varepsilon(\|V^k\|^2 - \alpha) \right. \\ \quad \left. + 2\beta (\|V^k\|^2 - \alpha)^2 V_{21}^k \delta_\varepsilon(\|V^k\|^2 - \alpha) + \beta_{21} - \alpha \frac{\partial \varphi_2}{\partial x} \right], \\ (1 + \alpha dt)V_{22}^{k+1} = V_{22}^k - dt \left[\mu V_{11}^k (\det V^k - 2) + 4\beta (\|V^k\|^2 - \alpha) V_{22}^k H_\varepsilon(\|V^k\|^2 - \alpha) \right. \\ \quad \left. + 2\beta (\|V^k\|^2 - \alpha)^2 (V_{22}^k \delta_\varepsilon(\|V^k\|^2 - \alpha) + \beta_{22} - \alpha \frac{\partial \varphi_2}{\partial y}) \right]. \end{array} \right.$$

The Euler-Lagrange equations for (6.16) are given by

$$\nu(T \circ \varphi - R)\nabla T(\varphi) + 2\eta \sum_{i=1}^N (\varphi(\omega_i) - \tilde{\omega}_i) \delta_{\omega_i} + \alpha \begin{pmatrix} \operatorname{div} V_1 \\ \operatorname{div} V_2 \end{pmatrix} - \alpha \Delta \varphi + \begin{pmatrix} \operatorname{div} \beta_1 \\ \operatorname{div} \beta_2 \end{pmatrix} = 0,$$

where V_1 and V_2 are respectively the first row and the second row of V , and β_1 and β_2 are the first row and the second row of β .

The equations are discretized using an implicit finite difference scheme with a 5 point scheme for the Laplacian (in practice, we search for u instead of φ). That is to say that we have to solve a linear system of the form:

$$AU_l^{k+1} = B(U_l^k),$$

with $A \in M_{(M-2) \times (N-2)}(\mathbb{R})$, $U_l^{k+1}, U_l^k, B \in \mathbb{R}^{(M-2) \times (N-2)}$, $l = 1, 2$. We denote by M, N the dimensions of the grid which correspond to the image size. We only solve U_l^k for $i = 2 \dots M - 1$, $j = 2 \dots N - 1$ since the displacement is supposed to be null on the boundary.

$$U_l^k = \begin{pmatrix} u_{l,2,2}^k \\ u_{l,3,2}^k \\ \vdots \\ u_{l,i,2}^k \\ \vdots \\ u_{l,i-1,j}^k \\ u_{l,i,j}^k \\ u_{l,i+1,j}^k \\ \vdots \\ u_{l,M-1,N-1}^k \end{pmatrix}, \quad U_l^{k+1} = \begin{pmatrix} u_{l,2,2}^{k+1} \\ u_{l,3,2}^{k+1} \\ \vdots \\ u_{l,i,2}^{k+1} \\ \vdots \\ u_{l,i-1,j}^{k+1} \\ u_{l,i,j}^{k+1} \\ u_{l,i+1,j}^{k+1} \\ \vdots \\ u_{l,M-1,N-1}^{k+1} \end{pmatrix}$$

$$B(U_l^k) = U_l^k + dt \left(-\nu(T \circ \varphi_k - R) \frac{\partial T}{\partial x_l}(\varphi^k) - \alpha \operatorname{div} V_l - \operatorname{div} \beta_l - 2\eta \sum_{i=1}^N \left(\varphi^k(\omega_i) - \tilde{\omega}_i \right)_l \delta_{\omega_i} \right)$$

Matrix A is a symmetric block tridiagonal matrix:

$$A = \left(\begin{array}{ccccc} D & -\gamma I_{M-2} & \mathbb{0}_{M-2} & \dots & \mathbb{0}_{M-2} \\ -\gamma I_{M-2} & D & -\gamma I_{M-2} & \mathbb{0}_{M-2} & \vdots \\ \mathbb{0}_{M-2} & -\gamma I_{M-2} & \ddots & \ddots & \mathbb{0}_{M-2} \\ \vdots & \mathbb{0}_{M-2} & \ddots & D & -\gamma I_{M-2} \\ \mathbb{0}_{M-2} & \dots & \mathbb{0}_{M-2} & -\gamma I_{M-2} & D \end{array} \right) \Bigg\} (N-2)$$

with

$$D = \begin{pmatrix} d & -\gamma & 0 & 0 \\ -\gamma & d & \ddots & 0 \\ 0 & \ddots & \ddots & -\gamma \\ 0 & 0 & -\gamma & d \end{pmatrix} \in M_{(M-2)}(\mathbb{R}).$$

Also $d = 1 + 4 \frac{\alpha dt}{h^2}$, $\gamma = \frac{\alpha dt}{h^2}$ where h is the spatial step and I_{M-2} is the identity matrix and $\mathbb{0}_{M-2}$ the zero matrix of order $M-2$.

6.3.2 Implementation details

The algorithm requires the evaluation of the Template T at $\varphi(x)$. We thus assume that T is a smooth mapping that has been obtained by interpolating the image data provided on the grid. As an additional convention, T is supposed to vanish outside the domain, *i.e.*, $T(x) = 0$ if $x \notin \Omega$. As suggested by Modersitzki in [20], Chapter 3, subsection 3.6.1, for the interpolation stage we apply a multiscale interpolation technique which includes a weighting parameter controlling smoothness versus data proximity. Also, for the sake of optimization, a multilevel representation of the data is adopted (see Chapter 3, section 3.7 of [20]).

Concerning the resolution of the linear system, the matrix being sparse we choose to keep in memory only non-zero elements. Indeed, if we store the whole matrix in the case of a 200×200 pixel image, the matrix will be composed of $(198 \times 198)^2$ elements. The data we use are double precision, then there are coded on 8 bytes. The necessary memory to store the whole matrix is then more than 12 Gigabytes. That is the reason why we have chosen a method enabling us to store only non-zero elements. The necessary memory to store non-zero element is about 1 Megabyte. The library MUMPS enables us to store only non-zero elements and in the case of a symmetric matrix, only the upper or lower triangular part. We also store the corresponding coordinates of the non-zero elements in integer tables. Moreover, the library MUMPS uses MPI to parallelize the computations during the resolution of the linear system.

6.4 Numerical experiments

First, we have experimented our method on an academic example which consists in mapping a disk to the letter C, this example being inspired from [7]. We compute for each example, the average distance between the landmarks:

$$LD = \frac{1}{N} \langle \rho(\varphi) - \tilde{\omega} \rangle_{2N}.$$

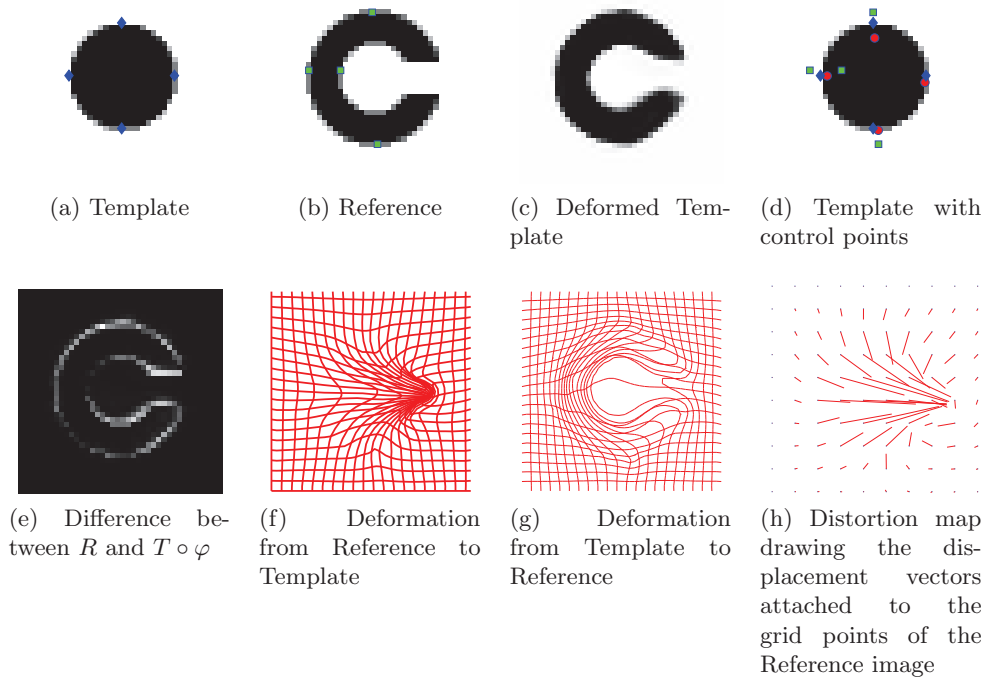
In each case, we display the Template image with the control points in blue diamonds, the Reference image with the control points in green squares, and the deformed Template $T \circ \varphi$. Then, on the Template image, we display the deformed control points $\rho(\varphi)$ in red circles. The green points move to red spots and these red spots should be as close as possible to the blue spots. We also provide the deformation from Template to Reference and the deformation from Reference to Template, as well as the displacement vector field, and the difference between R and $T \circ \varphi$.

Concerning the parameters, the Lamé coefficients are fixed to $\mu = 3000$ and $\lambda = 10$, the time step is $dt = 0.01$ and the space step is $h = 1$. Finally, the weight of the geometrical term is between 20000 and 60000 and $\nu = 1$.

For this example, we also estimate the contribution of the geometrical constraints by comparing the mutual information with and without the geometrical term. In information theory, the mutual information (MI) between two random variables is a measure of the variable mutual dependence and is defined as follows:

$$MI_{X,Y} = \int_Y \int_X p(x,y) \log \left(\frac{p(x,y)}{p(x)p(y)} \right) dx dy,$$

where $p(x,y)$ is the joint probability density function of X and Y , and $p(x)$ and $p(y)$ are the marginal probability density functions of X and Y respectively. Mutual information quantifies the dependence between X and Y , that is, in our case, the intensity maps of R and $T \circ \varphi$. Larger mutual information indicates better registration.

Figure 6.1: **Letter_C**.

Execution time: 2 seconds for 40×40 pixel images. 2 regriding steps. $\min \det \nabla \varphi = 0.002$, $\max \det \nabla \varphi = 2.31$. $LD = 0.89$.

$MI_{R,T}$	$MI_{R,T \circ \varphi}$ with constraints	$MI_{R,T \circ \varphi}$ without constraint	$MI_{R,R}$
0.1342	0.1506	0.1437	0.1559

Table 6.1: Mutual Information.

We observe that the geometrical constraints enable us to obtain a slightly better result, as the mutual information is greater with this term.

In this example, we observe that the algorithm can deal with large deformations, but due to these large deformations the Jacobian may become negative, that is the reason why we have applied the regriding step proposed by Christensen and his collaborators in [6]. The method consists in monitoring the values of the Jacobian at each step of the descent gradient. If the Jacobian drops below a defined threshold, then the process is reinitialized taking as new Template the previous computed deformed Template.

Algorithm 4 Regridding method.

1. Initialization: $\beta^0 = 0$, $V^0 = I$, $\varphi^0 = \text{Id}$, $\text{regrid_count}=0$.
 2. For $k = 0, 1, \dots$

$$(\varphi^{k+1}, V^{k+1}) = \arg \min_{\varphi, V} \mathcal{L}_{\alpha, \varepsilon}(\varphi, V, \beta^k)$$

if $\det \nabla \varphi^{k+1} < \text{tol}$

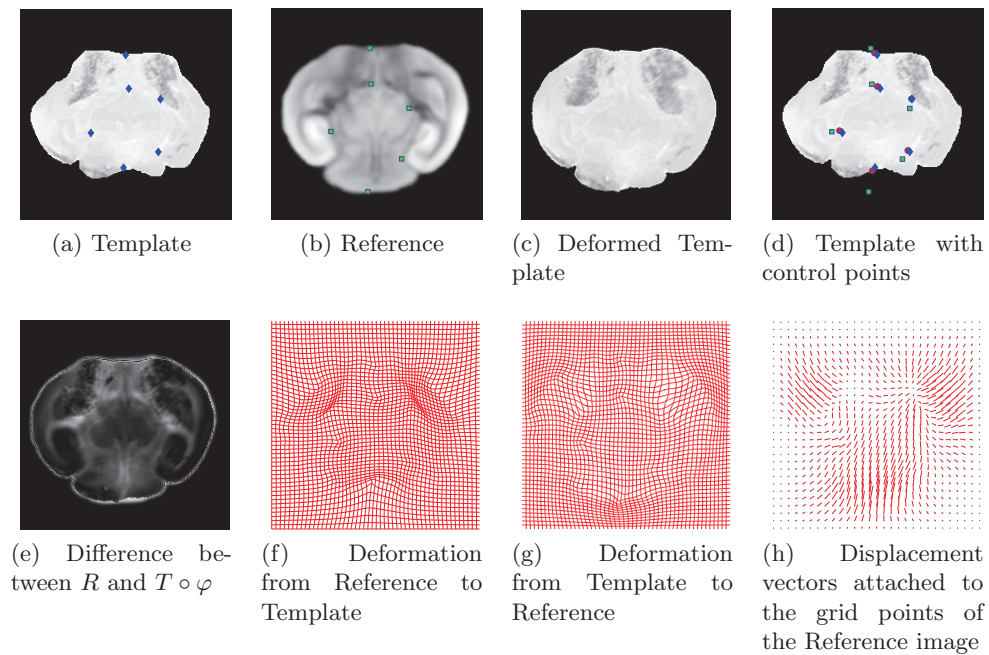
 - $\text{regrid_count}=\text{regrid_count}+1$
 - $T = T \circ \varphi^k$
 - save $\text{tab_}\varphi(\text{regrid_count})=\varphi^k$, $\varphi^{k+1} = \text{Id}$, $V^{k+1} = I$, $\beta^k = 0$.

Update $\beta^{k+1} = \beta^k + \alpha(V^{k+1} - \nabla \varphi^{k+1})$.
 3. If $\text{regrid_count}>0$

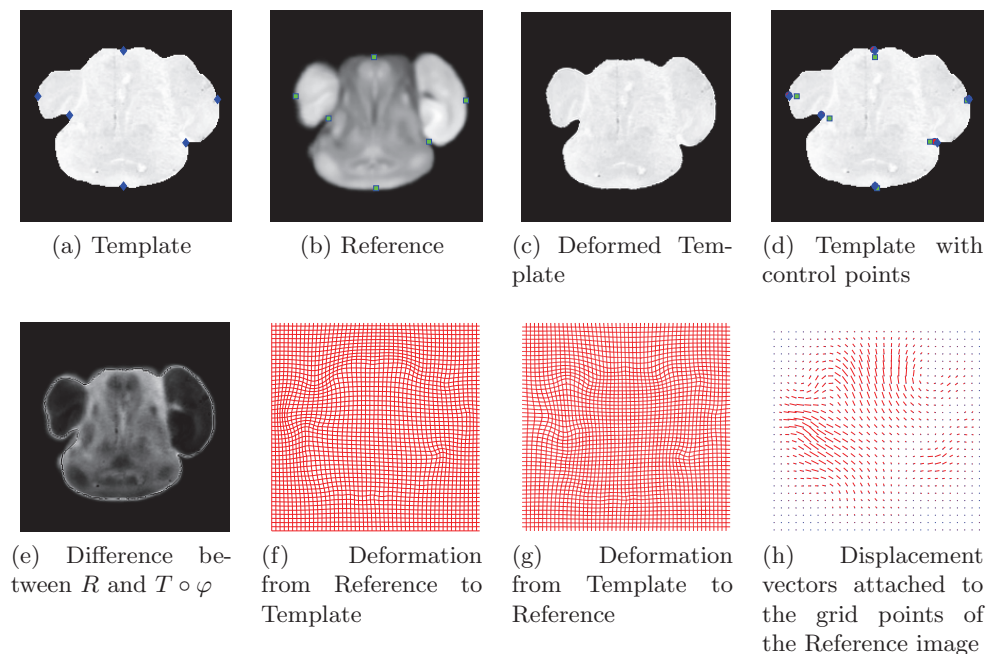
$$\varphi^{\text{final}} = \text{tab_}\varphi(1) \circ \dots \circ \text{tab_}\varphi(\text{regrid_count})$$
-

An alternative method would consist in applying a correction step when the Jacobian is negative as done in Chapter 3 ([21]).

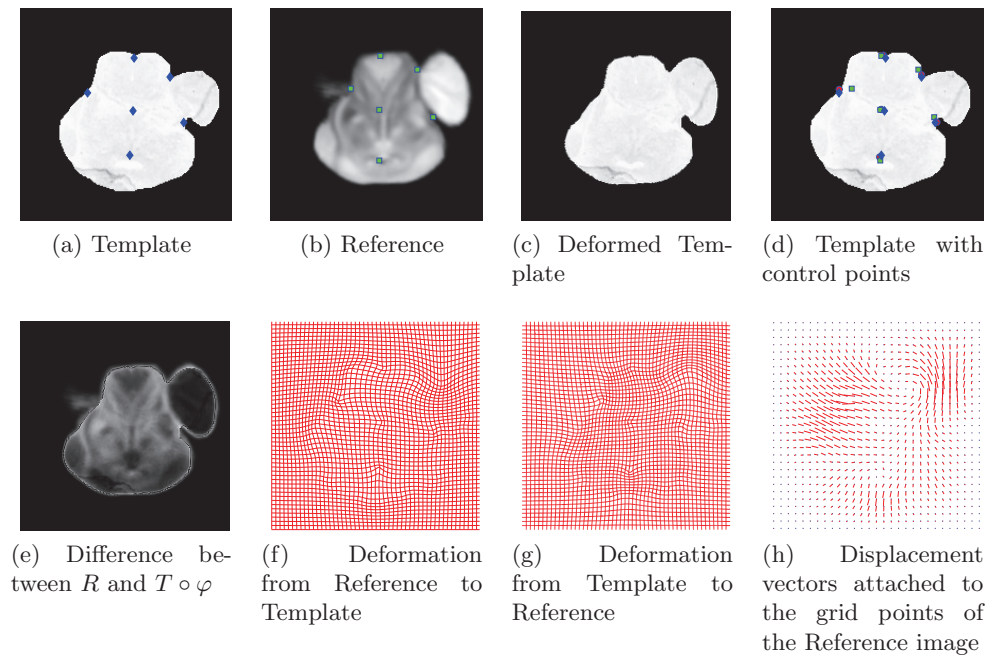
Then we have applied the method on medical images (Figs 6.2, 6.3, 6.4) with the goal to map a 2D slice of mouse brain gene expression data (Template T) to its corresponding 2D slice of the mouse brain atlas, in order to facilitate the integration of anatomic, genetic and physiologic observations from multiple subjects in a common space. Since genetic mutations and knock-out strains of mice provide critical models for a variety of human diseases, such linkage between genetic information and anatomical structure is important. The data are provided by the Center for Computational Biology, UCLA. The mouse atlas acquired from the LONI database was pre-segmented.

Figure 6.2: **Atlas08**.

Execution time: 22 seconds for 200×200 pixel images. $\min \det \nabla \varphi = 0.16$, $\max \det \nabla \varphi = 2.17$. $LD = 1.21$.

Figure 6.3: **Atlas11**.

Execution time: 16 seconds for 200×200 pixel images. $\min \det \nabla \varphi = 0.58$, $\max \det \nabla \varphi = 1.36$. $LD = 0.58$.

Figure 6.4: **Atlas12**.

Execution time: 23 seconds for 200×200 pixel images. $\min \det \nabla \varphi = 0.27$, $\max \det \nabla \varphi = 1.62$. $LD = 1.12$.

Conclusion

In this chapter, we have proposed a registration model under geometrical constraints. We have proved the existence of generalized solutions and a convergence result when the number of landmark points increases to infinity. Numerically, the model enables us to obtain large deformations thanks to the nonlinear elasticity-based regularization, and the constraints improve the similarity between the Reference image and the deformed Template.

- [1] R. ARCANGÉLI, M. C. L. DE SILANES, AND J. J. TORRENS, *An extension of a bound for functions in sobolev spaces, with applications to (m, s) -spline interpolation and smoothing*, *Numerische Mathematik*, 107 (2007), pp. 181–211.
- [2] M. BEG, M. MILLER, A. TROUVÉ, AND L. YOUNES, *Computing Large Deformation Metric Mappings via Geodesic Flows of Diffeomorphisms*, *International Journal of Computer Vision*, 61 (2005), pp. 139–157.
- [3] M. BOUSSELSAL, *Etude de quelques problèmes de calcul des variations liés à la mécanique*, PhD thesis, Université de Metz, 1993.
- [4] H. BRÉZIS, *Analyse Fonctionnelle, Théorie et Applications. 1999*, Dunod, Paris, 1999.
- [5] M. BURGER, J. MODERSITZKI, AND L. RUTHOTTO, *A hyperelastic regularization energy for image registration*, *SIAM Journal on Scientific Computing*, 35 (2013), pp. B132–B148.
- [6] G. CHRISTENSEN, R. RABBITT, AND M. MILLER, *Deformable Templates Using Large Deformation Kinematics*, *IEEE Trans. Image Process.*, 5 (1996), pp. 1435–1447.
- [7] G. E. CHRISTENSEN, *Deformable shape models for anatomy*, PhD thesis, Washington University, Sever Institute of technology, USA, 1994.
- [8] P. CIARLET, *Élasticité tridimensionnelle*, *Recherches en mathématiques appliquées*, Masson, 1986.
- [9] ———, *Mathematical Elasticity: Three-dimensional elasticity*, vol. 1, North-Holland, 1993.
- [10] B. DACOROGNA, *Direct methods in the calculus of variations*, vol. 78, Springer, 2007.
- [11] R. DERFOUL AND C. LE GUYADER, *A constrained registration problem based on Ciarlet-Geymonat stored energy*, in *SPIE Medical Imaging*, International Society for Optics and Photonics, 2014, pp. 90343Q–90343Q.
- [12] R. DERFOUL AND C. LE GUYADER, *A relaxed problem of registration based on the Saint Venant-Kirchhoff material stored energy for the mapping of mouse brain gene expression data to a neuroanatomical mouse atlas*, *SIAM Journal on Imaging Sciences*, 7 (2014), pp. 2175–2195.

- [13] M. DROSKE AND M. RUMPF, *A Variational Approach to Non-Rigid Morphological Registration*, SIAM J. Appl. Math., 64 (2004), pp. 668–687.
- [14] N. KERDID, H. LE DRET, AND A. SAÏDI, *Numerical approximation for a non-linear membrane problem*, International Journal of Non-Linear Mechanics, 43 (2008), pp. 908–914.
- [15] H. LE DRET, *Notes de Cours de DEA. Méthodes mathématiques en élasticité*, (2003–2004).
- [16] C. LE GUYADER AND L. VESE, *A combined segmentation and registration framework with a nonlinear elasticity smoother*, Computer Vision and Image Understanding, 115 (2011), pp. 1689–1709.
- [17] T. LIN, E.-F. LEE, I. DINOV, C. LE GUYADER, P. THOMPSON, A. TOGA, AND L. VESE, *A landmark-based nonlinear elasticity model for mouse atlas registration*, in Biomedical Imaging: From Nano to Macro, 2008. ISBI 2008. 5th IEEE International Symposium on, 2008, pp. 788–791.
- [18] M. MILLER, A. TROUVÉ, AND L. YOUNES, *On the Metrics and Euler-Lagrange Equations of Computational Anatomy*, Annu. Rev. B. Eng., 4 (2002), pp. 375–405.
- [19] J. MODERSITZKI, *Numerical Methods for Image Registration*, Oxford University Press, 2004.
- [20] ———, *FAIR: Flexible Algorithms for Image Registration*, Society for Industrial and Applied Mathematics (SIAM), 2009.
- [21] S. OZERÉ AND C. LE GUYADER, *Topology preservation for image-registration-related deformation fields*, Communications in Mathematical Sciences, 13 (2015), pp. 1135–1161.
- [22] R. RABBITT, J. WEISS, G. CHRISTENSEN, AND M. MILLER, *Mapping of Hyperelastic Deformable Templates Using the Finite Element Method*, in Proceedings SPIE, vol. 2573, SPIE, 1995, pp. 252–265.
- [23] A. RAOULT, *Non-polyconvexity of the stored energy function of a Saint Venant-Kirchhoff material*, Aplikace matematiky, 31 (1986), pp. 417–419.

In this chapter, we introduce a registration model based on the comparison of the gradients of the involved images. Indeed, in the case of multi-modal images, we would like to match the edges of the objects regardless of intensity levels.

The chapter is organized as follows. In a first section, we present the proposed model. Then we establish the existence of minimizers for this problem. Due to computational issues, we have to find an alternative method to minimize the functional. To do so, we propose two methods: the first one consists in introducing an auxiliary variable and in this case, we demonstrate the existence of solutions for this decoupled problem. The second one consists in approximating the term that raises issues using a sequence of integral operators involving a differential quotient and a suitable sequence of radial mollifiers, and we also demonstrate existence results as well as a result of Γ -convergence.

This chapter provides a complete theoretical study of the method, however, no satisfactory numerical result has been obtained for the moment. This study could constitute the beginning of future lines of research and perspectives.

Introduction

We plan to compare the gradients of the images instead of the gray levels, which would enable us to compare images with different modalities. Indeed, an important challenge is to compare multiple images obtained with different devices for example in medical imaging. In particular, this idea has been investigated by Haber and Modersitzki in [12] and by Droske and Rumpf in [10]. In [12], Haber *et al.* use derivatives to characterize similarity between two images. They base their work on the following observation: "Two images are considered similar, if intensity changes occur at the same location". To do so, they aim to match the normalized gradient vector fields of the two considered images. They define the normalized gradient vector field as follows:

$$n(I, x) = \begin{cases} \frac{\nabla I(x)}{\|\nabla I(x)\|} & \text{if } \nabla I(x) \neq 0, \\ 0 & \text{otherwise.} \end{cases}$$

The purpose is to align $n(T \circ \varphi, x)$ and $n(R, x)$. The angle between the two vectors is denoted by $\theta(x)$. The distance measure is then based on the angle $\theta(x)$: it is equivalent to minimizing

$\sin^2 \theta(x)$ or maximizing $\cos^2 \theta(x)$ to align the two vector fields. This observation comes from the definition of the inner product or the cross product. Therefore, they define the following distance measures:

$$\begin{aligned}\mathcal{D}^c(T, R) &= \frac{1}{2} \int_{\Omega} \|n(R, x) \times n(T \circ \varphi, x)\|^2 dx, \\ \mathcal{D}^d(T, R) &= -\frac{1}{2} \int_{\Omega} \langle n(R, x), n(T \circ \varphi, x) \rangle^2 dx.\end{aligned}$$

In [10], Droske *et al.* develop a similar idea but use the notion of morphologies. The morphology of an image I is the collection of the level sets of the image:

$$M[I] = \{\mathcal{M}_c^I | c \in \mathbb{R}\}, \quad \mathcal{M}_c^I = \{x \in \Omega \subset \mathbb{R}^d | I(x) = c\}.$$

They also use the normal field N_I on \mathcal{M}_c^I defined by:

$$N_I : \Omega \longrightarrow \mathbb{R}^d; x \longmapsto \frac{\nabla I}{\|\nabla I\|}.$$

They search for a deformation φ such that $M[T \circ \varphi] = M[R]$, that is to say that they try to align the normal fields. The energy functional to be minimized can be written as follows:

$$E_m[\varphi] = \int_{\Omega} g(N_T \circ \varphi, N_R, \text{Cof} \nabla \varphi) d\mu,$$

with $g(v, w, A) = \left(v - \frac{Aw}{\|Aw\|}\right)$, which corresponds to the energy

$$\int_{\Omega} \|N_T \circ \varphi - N_R^\varphi\|^2,$$

where N_R^φ is the transformed normal of the reference image on $\mathcal{T}_{\varphi(x)}\varphi(\mathcal{M}_{R(x)}^R)$ at position $\varphi(x)$.

In order to build our functional based on gradient vector field comparison of the images, we have been inspired by [4]. In [4], Ballester *et al.* are interested in an inpainting problem. They consider an image u_0 containing a hole of missing data, Ω , that they aim to fill-in. The energy functional they propose is minimized with respect to two variables: a vector field θ which represents the directions of the level lines of u , and the grey level u . Moreover, θ should satisfy $|\theta| \leq 1$ on Ω and should be related to u by trying to impose $\theta \cdot \nabla u = |\nabla u|$.

They thus propose to minimize a functional of the form

$$\begin{aligned}& \int_{\tilde{\Omega}} |\text{div } \theta|^p (a + b|\nabla k * u|) dx \\ & + \alpha \int_{\tilde{\Omega}} (|\nabla u| - \theta \cdot \nabla u) dx,\end{aligned}$$

where a, b and α are positive constants and k is a smoothing kernel.

Inspired by this model, we have tried to adapt the second term of this functional to our registration problem. We would like to match $\nabla(T \circ \varphi)$ and ∇R . Following [4], $T \circ \varphi$ is a substitute for u , the unknown corresponding to the grey level and $\frac{\nabla R}{|\nabla R|}$ a substitute for θ , normalized vector field. Then we propose the following distance measure:

$$\int_{\Omega} \left(|\nabla(T \circ \varphi)| - \left\langle \frac{\nabla R}{|\nabla R|}, \nabla(T \circ \varphi) \right\rangle \right).$$

7.1 Mathematical modelling

We make the same hypotheses as previously done. Let:

- Ω be a connected bounded open subset of \mathbb{R}^2 of class \mathcal{C}^1 ,
- $R : \bar{\Omega} \rightarrow \mathbb{R}$, be the Reference image,
- $T : \bar{\Omega} \rightarrow \mathbb{R}$, be a Lipschitz continuous function compactly supported, defining the Template image,
- $\varphi : \bar{\Omega} \rightarrow \mathbb{R}^2$ the sought deformation with $\varphi = \text{Id}$ on $\partial\Omega$.

As mentioned above, the data fidelity term will be written as follows:

$$\int_{\Omega} |\nabla(T \circ \varphi)| - \langle \nabla(T \circ \varphi), \frac{\nabla R}{|\nabla R|} \rangle.$$

As Ballester *et al.* in [4], we introduce θ a vector field with values in \mathbb{R}^2 satisfying

$$\theta(x) \cdot \nabla R(x) = |R(x)| \text{ and } |\theta(x)| \leq 1.$$

The vector field of normal θ can be defined as the Radon-Nikodym derivative of the measure ∇R with respect to $|\nabla R|$. We assume that $\theta \in L^\infty(\Omega, \mathbb{R}^2)$ and $\text{div } \theta \in L^2(\Omega)$ for theoretical purposes.

For the regularizer term, we can choose for instance: $\|\nabla\varphi\|_{L^2(\Omega, M_2)}^2$. Indeed, in this section, we focus primarily on the dissimilarity measure based on the gradient vector fields.

The problem is then phrased as follows:

$$\inf_{\varphi \in \text{Id} + W_0^{1,2}(\Omega, \mathbb{R}^2)} \left\{ E(\varphi) = \int_{\Omega} |\nabla(T \circ \varphi)| - \langle \nabla(T \circ \varphi), \theta \rangle + \frac{\alpha}{2} \int_{\Omega} \|\nabla\varphi\|^2 \right\}. \quad (7.1)$$

According to the following corollary:

Corollary 7.1.1 (*Ambrosio [1]*)

Let $\Omega \subset \mathbb{R}^n$. Let $p \in [1, +\infty]$, $u \in W^{1,p}(\Omega, \mathbb{R}^m)$, and let $f : \mathbb{R}^m \rightarrow \mathbb{R}^k$ be a Lipschitz continuous function such that $f(0) = 0$. Then $v = f(u)$ belongs to $W^{1,p}(\Omega, \mathbb{R}^k)$, for almost every $x \in \Omega$ the restriction of the function f to the affine space

$$T_x^u = \{y \in \mathbb{R}^m : y = u(x) + \langle \nabla u(x), z \rangle \text{ for some } z \in \mathbb{R}^n\}$$

is differentiable at $u(x)$, and

$$\nabla v = \nabla(f|_{T_x^u})(u) \nabla u \text{ a.e in } \Omega.$$

Then $T \circ \varphi \in W^{1,2}(\Omega)$ and so $T \circ \varphi \in BV(\Omega)$ since $W^{1,2}(\Omega) \subset BV(\Omega)$ and our functional is well defined.

We start by proving the existence of minimizers for the initial problem (7.1).

7.2 Existence minimizers for the initial problem

Theorem 7.2.1

Assuming that E is proper, the functional

$$E(\varphi) = \int_{\Omega} |\nabla(T \circ \varphi)| - \langle \nabla(T \circ \varphi), \theta \rangle + \frac{\alpha}{2} \int_{\Omega} \|\nabla\varphi\|^2$$

admits minimizers on $\text{Id} + W_0^{1,2}(\Omega, \mathbb{R}^2)$.

Proof:

Coercivity inequality

First,

$$\int_{\Omega} |\nabla(T \circ \varphi)| - \langle \nabla(T \circ \varphi), \theta \rangle \geq 0.$$

Using the generalized Poincaré inequality: $\|\varphi\|_{L^2(\Omega, \mathbb{R}^2)}^2 \leq c \left(\|\nabla\varphi\|_{L^2(\Omega, M_2)}^2 + \left| \int_{\partial\Omega} \varphi d\sigma \right|^2 \right)$,

so $\|\varphi\|_{W^{1,2}(\Omega, \mathbb{R}^2)}^2 \leq (c+1)\|\nabla\varphi\|_{L^2(\Omega, M_2)}^2 + k$, then we obtain:

$$E(\varphi) \geq c\|\varphi\|_{W^{1,2}(\Omega, \mathbb{R}^2)}^2 + k, \quad k \in \mathbb{R},$$

c denoting a constant depending on Ω that may change line to line.

Therefore, E being proper, the infimum denoted by d is finite.

Convergence of a minimizing sequence

Let (φ_n) be a minimizing sequence of E , that is a sequence such that

$$E(\varphi_n) \xrightarrow{n \rightarrow \infty} \inf_{\psi \in \text{Id} + W_0^{1,2}(\Omega, \mathbb{R}^2)} E(\psi).$$

Since E is assumed to be proper, there exists $\tilde{\varphi} \in \text{Id} + W^{1,2}(\Omega, \mathbb{R}^2)$ such that $E(\tilde{\varphi}) < +\infty$. From the previous coercivity inequality, we can deduce that, for n large enough,

$$c\|\varphi_n\|_{W^{1,2}(\Omega, \mathbb{R}^2)}^2 + k \leq E(\varphi_n) \leq E(\tilde{\varphi}) + 1,$$

which means that φ_n is uniformly bounded in $W^{1,2}(\Omega, \mathbb{R}^2)$.

Therefore, since $W^{1,2}(\Omega, \mathbb{R}^2)$ is a reflexive space, we can extract a subsequence of φ_n (still denoted by φ_n) such that:

$$\varphi_n \rightharpoonup \bar{\varphi} \text{ in } W^{1,2}(\Omega, \mathbb{R}^2).$$

It remains to prove that E is sequentially lower semi-continuous to conclude to the existence of minimizers.

Lower semicontinuity of E

The L^2 -norm is convex, lower semi-continuous for the weak topology in L^2 , since strongly sequentially continuous.

Since $\varphi_n \rightharpoonup \bar{\varphi}$ in $W^{1,2}(\Omega, \mathbb{R}^2)$, using Rellich-Kondrachov Theorem we obtain that $\varphi_n \rightarrow \bar{\varphi}$ in $L^2(\Omega, \mathbb{R}^2)$ and then

$$\varphi_n \rightarrow \bar{\varphi} \text{ in } L^1(\Omega, \mathbb{R}^2),$$

since Ω is a bounded subset.

Moreover, T is a Lipschitz continuous function (of Lipschitz constant k_T) so

$$\int_{\Omega} |T \circ \varphi_n - T \circ \bar{\varphi}| \leq \int_{\Omega} k_T |\varphi_n - \bar{\varphi}| \implies T \circ \varphi_n \rightarrow T \circ \bar{\varphi} \text{ in } L^1(\Omega).$$

According to Corollary 7.1.1, $T \circ \bar{\varphi} \in W^{1,2}(\Omega)$ and so it belongs to the space of bounded variation functions $BV(\Omega)$. The strong convergence of $T \circ \varphi_n$ to $T \circ \bar{\varphi}$ in $L^1(\Omega)$ enables us to conclude that

$$\int_{\Omega} |\nabla(T \circ \bar{\varphi})| \leq \liminf_{n \rightarrow +\infty} \int_{\Omega} |\nabla(T \circ \varphi_n)|. \quad (7.2)$$

The proof of (7.2) is rather classical.

Proof: Let $\phi \in \mathcal{C}_c^1(\Omega, \mathbb{R}^2)$ and $|\phi(x)| \leq 1$ everywhere, then

$$\int_{\Omega} T \circ \bar{\varphi}(x) \operatorname{div} \phi(x) dx = \lim_{k \rightarrow \infty} \int_{\Omega} T \circ \varphi_k(x) \operatorname{div} \phi(x) dx.$$

Consequently, $\forall \varepsilon > 0, \exists N(\varepsilon, \phi), \forall k \in \mathbb{N}$,

$$\begin{aligned} \left(k \geq N \implies \left| \int_{\Omega} T \circ \varphi_k(x) \operatorname{div} \phi(x) dx - \int_{\Omega} T \circ \bar{\varphi}(x) \operatorname{div} \phi(x) dx \right| \leq \varepsilon, \right. \\ \left. \implies \int_{\Omega} T \circ \bar{\varphi}(x) \operatorname{div} \phi(x) dx - \varepsilon \leq \int_{\Omega} T \circ \varphi_k(x) \operatorname{div} \phi(x) dx \leq \int_{\Omega} T \circ \bar{\varphi}(x) \operatorname{div} \phi(x) dx + \varepsilon \right). \end{aligned}$$

Since $\int_{\Omega} |\nabla u| = \sup \left\{ \int_{\Omega} u \operatorname{div} \phi, |\phi(x)| \leq 1 \text{ e.}, \phi \in \mathcal{C}_c^1(\Omega, \mathbb{R}^2) \right\}$, we have

$$\int_{\Omega} T \circ \varphi_k(x) \operatorname{div} \phi(x) dx \leq \int_{\Omega} |\nabla(T \circ \varphi_k)|.$$

Then $\forall k \geq N(\varepsilon, \phi)$,

$$\int_{\Omega} T \circ \bar{\varphi}(x) \operatorname{div} \phi(x) dx - \varepsilon \leq \int_{\Omega} |\nabla(T \circ \varphi_k)|,$$

which implies that

$$\int_{\Omega} T \circ \bar{\varphi}(x) \operatorname{div} \phi(x) dx \leq \liminf_{k \rightarrow \infty} \int_{\Omega} |\nabla(T \circ \varphi_k)|.$$

Taking the supremum over all $\phi \in \mathcal{C}_c^1(\Omega, \mathbb{R}^2)$, we conclude that

$$\int_{\Omega} |\nabla(T \circ \bar{\varphi})| \leq \liminf_{k \rightarrow \infty} \int_{\Omega} |\nabla(T \circ \varphi_k)|. \quad \blacksquare$$

Finally, we can apply the following theorem from [2]:

Theorem 7.2.2 (*Anzellotti [2, Theorem 1.9]*)

Let $\Omega \in \mathbb{R}^N$ with $N \geq 2$ be a bounded open set with Lipschitz boundary. Let us denote by ν the outward unit normal to $\partial\Omega$. If one of these conditions is satisfied :

1. $u \in \text{BV}(\Omega) \cap L^q(\Omega)$, $\psi \in \{\xi \in L^\infty(\Omega, \mathbb{R}^N), \text{div } \xi \in L^p(\Omega)\}$, $1 < p \leq N$, $\frac{1}{p} + \frac{1}{q} = 1$,
2. $u \in \text{BV}(\Omega) \cap L^\infty(\Omega)$, $\psi \in \{\xi \in L^\infty(\Omega, \mathbb{R}^N), \text{div } \xi \in L^1(\Omega)\}$,
3. $u \in \text{BV}(\Omega) \cap L^\infty(\Omega) \cap C^0(\Omega)$, $\psi \in \{\xi \in L^\infty(\Omega, \mathbb{R}^N), \text{div } \xi \text{ is a bounded measure in } \Omega\}$,

then one has

$$\int_{\Omega} u \text{div } \psi + \int_{\Omega} (\nabla u, \psi) = \int_{\partial\Omega} [\psi \cdot \nu] u d\mathcal{H}^{N-1}.$$

Therefore, we obtain:

$$\int_{\Omega} \langle \nabla(T \circ \varphi_n), \theta \rangle = - \int_{\Omega} T \circ \varphi_n \text{div } \theta + \underbrace{\int_{\partial\Omega} [\theta, \nu] T \circ \varphi_n d\mathcal{H}^1}_{\substack{\text{known on } \partial\Omega \text{ and} \\ \text{independent of } n \text{ since} \\ \varphi_n|_{\partial\Omega} = \text{Id}.}}$$

and we know that $\lim_{n \rightarrow \infty} \int_{\Omega} T \circ \varphi_n \text{div } \theta = \int_{\Omega} T \circ \bar{\varphi} \text{div } \theta$ since $T \circ \varphi_n$ strongly converges to $T \circ \bar{\varphi}$ in $L^2(\Omega)$ and $\text{div } \theta \in L^2(\Omega)$. Gathering all this results, we obtain that E is sequentially lower semi-continuous.

Moreover, $\text{Id} + W_0^{1,2}(\Omega, \mathbb{R}^2)$ is a closed convex subspace of $W^{1,2}(\Omega, \mathbb{R}^2)$ by continuity of the trace, thus it is a weakly closed convex space according to Theorem III.7 in [6]. We obtain that $\bar{\varphi} \in \text{Id} + W_0^{1,2}(\Omega, \mathbb{R}^2)$ and finally $\bar{\varphi} = \text{Id}$ on $\partial\Omega$. This completes the proof showing that E admits minimizers on $\text{Id} + W_0^{1,2}(\Omega, \mathbb{R}^2)$. ■

Numerically, the total variation of $T \circ \varphi$ may turn out to be complicated to compute, that is the reason why we have to find a suitable way to compute this term efficiently. To do so, we have investigated two methods.

7.3 Introduction of an auxiliary variable

Firstly, we propose to introduce an auxiliary variable to handle the term in $T \circ \varphi$.

$$\inf_{\mathcal{W} \times \mathcal{X}} \left\{ E_{\gamma}(\varphi, \tilde{T}) = \int_{\Omega} |\nabla \tilde{T}| - \langle \nabla \tilde{T}, \theta \rangle + \frac{\alpha}{2} \int_{\Omega} \|\nabla \varphi\|^2 dx + \gamma \|T \circ \varphi - \tilde{T}\|_{L^1(\Omega)} \right\} \quad (7.3)$$

with $\mathcal{W} = \{\varphi \in \text{Id} + W_0^{1,2}(\Omega, \mathbb{R}^2)\}$, $\mathcal{X} = \{\tilde{T} \in \text{BV}(\Omega) \text{ with } \tilde{T} = T \text{ on } \partial\Omega\}$.

However, the trace of BV functions is not continuous for the BV weak-* topology, which is an obstacle to prove that a minimizing sequence converges in $\mathcal{W} \times \mathcal{X}$. Indeed, as seen previously, the weak and strong topology are equivalent on a closed convex subspace but this property

does not hold for the weak-* topology.

That is the reason why, inspired by [9], we define two equivalent problems. Before, we use the formula introduced in Theorem 7.2.2, namely: $\int_{\Omega} \langle \nabla \tilde{T}, \theta \rangle = - \int_{\Omega} \tilde{T} \operatorname{div} \theta + \underbrace{\int_{\partial\Omega} [\theta, \nu] \tilde{T} \, d\mathcal{H}^1}_{\text{known on } \partial\Omega}$.

Therefore, problem (7.3) is equivalent to:

$$\inf_{\mathcal{W} \times BV_0(\Omega)} \left\{ E_{\gamma}(\varphi, \tilde{T}) = \int_{\Omega} |\nabla \tilde{T}| + \int_{\Omega} \tilde{T} \operatorname{div} \theta + \frac{\alpha}{2} \int_{\Omega} \|\nabla \varphi\|^2 \, dx + \gamma \|T \circ \varphi - \tilde{T}\|_{L^1(\Omega)} \right\} \quad (7.4)$$

(recalling the T is compactly supported and $\varphi|_{\partial\Omega} = \operatorname{Id}$), and we define an associated relaxed problem:

$$\inf_{\mathcal{W} \times BV(\Omega)} \left\{ \tilde{E}_{\gamma}(\varphi, \tilde{T}) = \int_{\Omega} |\nabla \tilde{T}| + \int_{\Omega} \tilde{T} \operatorname{div} \theta + \int_{\partial\Omega} |\tilde{T}| \, d\mathcal{H}^1 + \frac{\alpha}{2} \int_{\Omega} \|\nabla \varphi\|^2 \, dx + \gamma \|T \circ \varphi - \tilde{T}\|_{L^1(\Omega)} \right\}. \quad (7.5)$$

We aim to prove in a first step that

$$\inf_{\mathcal{W} \times BV_0(\Omega)} E_{\gamma}(\varphi, \tilde{T}) = \inf(7.4) = \inf_{\mathcal{W} \times BV(\Omega)} \tilde{E}_{\gamma}(\varphi, \tilde{T}) = \inf(7.5).$$

In this prospect, we need the following density result:

Theorem 7.3.1 (*Demengel [9, Theorem 6.70, Chapter 6, page 322]*)

Let Ω be an open subset of \mathbb{R}^N of class \mathcal{C}^1 and let $u \in BV(\Omega)$. Then there exists a sequence $\{u_n\}$ of functions in $\mathcal{C}_c^{\infty}(\Omega)$ such that

$$\|u_n - u\|_{L^1(\Omega)} \xrightarrow{n \rightarrow +\infty} 0 \quad \text{and} \quad \int_{\Omega} |\nabla u_n| \xrightarrow{n \rightarrow +\infty} \int_{\Omega} |\nabla u| + \int_{\partial\Omega} |u|.$$

First, as $\mathcal{W} \times BV_0(\Omega)$ is included in $\mathcal{W} \times BV(\Omega)$ it is clear that

$$\inf(7.5) \leq \inf(7.4).$$

Let us denote by $(\bar{\varphi}, \bar{\tilde{T}})$ a minimizing pair of problem (7.5) (we prove further that such a minimizing pair exists). According to Theorem 7.3.1, there exists a sequence $(\tilde{T}_n) \in \mathcal{C}_c^{\infty}(\Omega)$ such that:

$$\begin{cases} \tilde{T}_n \rightarrow \bar{\tilde{T}} \text{ in } L^1(\Omega), \\ \int_{\Omega} |\nabla \tilde{T}_n| \rightarrow \int_{\Omega} |\nabla \bar{\tilde{T}}| + \int_{\partial\Omega} |\bar{\tilde{T}}| \, d\mathcal{H}^1. \end{cases} \quad (7.6)$$

Also, there exists $(\varphi_n) \in W^{1,2}(\Omega, \mathbb{R}^2) \cap \mathcal{C}_c^{\infty}(\bar{\Omega}, \mathbb{R}^2)$ (as Ω is bounded, of class \mathcal{C}^1 , [6, Corollary IX.8]), such that

$$\varphi_n \xrightarrow{n \rightarrow +\infty} \bar{\varphi} \text{ in } W^{1,2}(\Omega, \mathbb{R}^2).$$

As \tilde{T}_n is uniformly bounded in $BV(\Omega)$ and thus in $L^2(\Omega)$ (due to the continuous embedding of $BV(\Omega)$ in $L^2(\Omega)$ - recall that $\Omega \subset \mathbb{R}^2$), we can extract a subsequence of \tilde{T}_n , still denoted by \tilde{T}_n , such that \tilde{T}_n converges to T^* in $L^2(\Omega)$. It is not difficult to prove that $T^* = \tilde{T}$. Consequently,

$$\begin{aligned} & \int_{\Omega} |\nabla \tilde{T}_n| + \int_{\Omega} \tilde{T}_n \operatorname{div} \theta + \frac{\alpha}{2} \int_{\Omega} \|\nabla \varphi_n\|^2 + \gamma \|T \circ \varphi_n - \tilde{T}_n\|_{L^1(\Omega)} \\ & \xrightarrow{n \rightarrow +\infty} \int_{\Omega} |\nabla \tilde{T}| + \int_{\partial\Omega} |\tilde{T}| d\mathcal{H}^1 + \int_{\Omega} \tilde{T} \operatorname{div} \theta + \frac{\alpha}{2} \int_{\Omega} \|\nabla \varphi\|^2 dx + \gamma \|T \circ \varphi - \tilde{T}\|_{L^1(\Omega)}. \end{aligned}$$

In conclusion,

$$\boxed{\inf (7.4) = \inf (7.5).}$$

7.3.1 Existence of minimizers for the decoupled problem

Theorem 7.3.2

Assuming that \tilde{E}_γ is proper. The decoupled problem

$$\begin{aligned} \inf_{\substack{\varphi \in \operatorname{Id} + W_0^{1,2}(\Omega, \mathbb{R}^2) \\ \tilde{T} \in BV(\Omega)}} \left\{ \tilde{E}_\gamma(\varphi, \tilde{T}) = \int_{\Omega} |\nabla \tilde{T}| + \int_{\Omega} \tilde{T} \operatorname{div} \theta + \int_{\partial\Omega} |\tilde{T}| d\mathcal{H}^1 \right. \\ \left. + \frac{\alpha}{2} \int_{\Omega} \|\nabla \varphi\|^2 dx + \gamma \|T \circ \varphi - \tilde{T}\|_{L^1(\Omega)} \right\}, \end{aligned}$$

admits at least one solution.

Remark 7.3.1

We can check that the problem is well defined since as $\Omega \subset \mathbb{R}^2$ is bounded with Lipschitz boundary, we have $BV(\Omega) \subset L^2(\Omega)$.

Proof:

Coercivity inequality

M is a positive constant that may change line to line and that may depend on γ (here, γ is fixed).

As $\left| \int_{\Omega} \tilde{T} \operatorname{div} \theta \right| \leq \|\tilde{T}\|_{L^2(\Omega)} \|\operatorname{div} \theta\|_{L^2(\Omega)}$, then

$$\int_{\Omega} \tilde{T} \operatorname{div} \theta \geq -\|\tilde{T}\|_{L^2(\Omega)} \|\operatorname{div} \theta\|_{L^2(\Omega)} \geq -\kappa \|\operatorname{div} \theta\|_{L^2(\Omega)} \|\tilde{T}\|_{BV(\Omega)},$$

$\kappa > 0$, still due to the continuous embedding $BV(\Omega) \subset L^2(\Omega)$. It follows that

$$\begin{aligned} \tilde{E}_\gamma(\varphi, \tilde{T}) & \geq \int_{\Omega} |\nabla \tilde{T}| - \kappa \|\tilde{T}\|_{BV(\Omega)} \|\operatorname{div} \theta\|_{L^2(\Omega)} + \gamma \|\tilde{T}\|_{L^1(\Omega)} - \gamma \|T \circ \varphi\|_{L^1(\Omega)} + \frac{\alpha}{2} \|\nabla \varphi\|_{L^2(\Omega, M_2)}^2, \\ & \geq (\min(1, \gamma) - \kappa \|\operatorname{div} \theta\|_{L^2(\Omega)}) \|\tilde{T}\|_{BV(\Omega)} - \gamma \|T \circ \varphi\|_{L^1(\Omega)} + \frac{\alpha}{2} \|\nabla \varphi\|_{L^2(\Omega, M_2)}^2. \end{aligned}$$

T is assumed to be Lipschitz continuous and compactly supported. For theoretical and numerical purposes, we may consider a linear extension operator ([6, Theorem IX.7, page 158]) $P : W^{1,\infty}(\Omega) \rightarrow W^{1,\infty}(\mathbb{R}^2)$ such that

- (i) $PT|_{\Omega} = T$,
- (ii) $\|PT\|_{L^{\infty}(\mathbb{R}^2)} \leq C\|T\|_{L^{\infty}(\Omega)}$ and
- (iii) $\|PT\|_{W^{1,\infty}(\mathbb{R}^2)} \leq C\|T\|_{W^{1,\infty}(\Omega)}$ with C depending only on Ω .

Thus

$$\tilde{E}_{\gamma}(\varphi, \tilde{T}) \geq (\min(1, \gamma) - \kappa\|\operatorname{div} \theta\|_{L^2(\Omega)}) \|\tilde{T}\|_{BV(\Omega)} - \gamma|\Omega|\|PT\|_{L^{\infty}(\mathbb{R}^2)} + \frac{\alpha}{2}\|\nabla\varphi\|_{L^2(\Omega, M_2)}^2.$$

Finally, using the generalized Poincaré inequality:

$$\boxed{\tilde{E}_{\gamma}(\varphi, \tilde{T}) \geq (\min(1, \gamma) - \kappa\|\operatorname{div} \theta\|_{L^2(\Omega)}) \|\tilde{T}\|_{BV(\Omega)} - \gamma|\Omega|\|PT\|_{L^{\infty}(\mathbb{R}^2)} + A\|\varphi\|_{W^{1,2}(\Omega, \mathbb{R}^2)}^2 - K}$$

with $A > 0, K \in \mathbb{R}$ and if $\|\operatorname{div} \theta\|_{L^2(\Omega)} < \frac{\min(1, \gamma)}{\kappa}$, the infimum is finite.

Convergence of a minimizing sequence

Let (φ_n, \tilde{T}_n) be a minimizing sequence of $\tilde{E}_{\gamma}(\varphi, \tilde{T})$. Since \tilde{E}_{γ} is proper, for n large enough,
 $(\min(1, \gamma) - \kappa\|\operatorname{div} \theta\|_{L^2(\Omega)}) \|\tilde{T}\|_{BV(\Omega)} + A\|\varphi\|_{W^{1,2}(\Omega, \mathbb{R}^2)}^2 - K \leq \tilde{E}_{\gamma}(\varphi_n, \tilde{T}_n) \leq M$, which implies that (φ_n) is uniformly bounded in $W^{1,2}(\Omega, \mathbb{R}^2)$. We can thus extract a subsequence, still denoted by φ_n , such that

$$\varphi_n \rightharpoonup \tilde{\varphi}_{\gamma} \text{ in } W^{1,2}(\Omega, \mathbb{R}^2).$$

Also, \tilde{T}_n is uniformly bounded in $BV(\Omega)$ (thus in $L^2(\Omega)$) and we can extract a subsequence, still denoted by \tilde{T}_n , of \tilde{T}_n such that:

$$\begin{cases} \tilde{T}_n \rightharpoonup \tilde{T}_{\gamma} \text{ in } L^2(\Omega) \\ \text{and} \\ \tilde{T}_n \overset{*}{\rightharpoonup} \tilde{T}_{\gamma} \text{ in } BV(\Omega), \end{cases}$$

which means, for the weak-* convergence in $BV(\Omega)$, that \tilde{T}_n converges strongly in $L^1(\Omega)$ to \tilde{T}_{γ} and for all ϕ in $(C^0(\Omega))^2$,

$$\int_{\Omega} \phi \nabla \tilde{T}_n \longrightarrow \int_{\Omega} \phi \nabla \tilde{T}_{\gamma}.$$

In summary, working with a common extraction mapping (we do not change the notations for the common extraction mappings),

$$\begin{cases} \varphi_n \rightharpoonup \tilde{\varphi}_{\gamma} \text{ in } W^{1,2}(\Omega, \mathbb{R}^2) \\ \tilde{T}_n \overset{*}{\rightharpoonup} \tilde{T}_{\gamma} \text{ in } BV(\Omega). \end{cases}$$

Rellich-Kondrachov embedding theorem gives that φ_n strongly converges to $\tilde{\varphi}_{\gamma}$ in $L^2(\Omega, \mathbb{R}^2)$ (and thus in $L^1(\Omega, \mathbb{R}^2)$).

Lower semicontinuity of \tilde{E}_γ

By lower semicontinuity of the total variation,

$$\int_{\Omega} |\nabla \tilde{T}_\gamma| \leq \liminf_{n \rightarrow \infty} \int_{\Omega} |\nabla \tilde{T}_n|.$$

The L^2 -norm being convex and strongly sequentially lower semi-continuous, it is lower semi-continuous and

$$\int_{\Omega} \|\nabla \tilde{\varphi}_\gamma\|^2 \leq \liminf_{n \rightarrow +\infty} \int_{\Omega} \|\nabla \varphi_n\|^2.$$

As $\operatorname{div} \theta$ is assumed to belong to $L^2(\Omega)$ and \tilde{T}_n weakly converges to \tilde{T}_γ in $L^2(\Omega)$,

$$\lim_{n \rightarrow +\infty} \int_{\Omega} \tilde{T}_n \operatorname{div} \theta = \int_{\Omega} \tilde{T}_\gamma \operatorname{div} \theta.$$

At last,

$$\begin{aligned} \|T \circ \varphi_n - \tilde{T}_n - (T \circ \tilde{\varphi}_\gamma - \tilde{T}_\gamma)\|_{L^1(\Omega)} &\leq \|T \circ \varphi_n - T \circ \tilde{\varphi}_\gamma\|_{L^1(\Omega)} + \|\tilde{T}_n - \tilde{T}_\gamma\|_{L^1(\Omega)}, \\ &\leq k_T \|\varphi_n - \tilde{\varphi}_\gamma\|_{L^1(\Omega)} + \|\tilde{T}_n - \tilde{T}_\gamma\|_{L^1(\Omega)}, \end{aligned}$$

which implies that $\lim_{n \rightarrow +\infty} \|T \circ \varphi_n - \tilde{T}_n\|_{L^1(\Omega)} = \|T \circ \tilde{\varphi}_\gamma - \tilde{T}_\gamma\|_{L^1(\Omega)}$.

Now, denoting by \hat{T}_n an extension of \tilde{T}_n by 0 outside of Ω , we have, according to the extension theorem ([11, Theorem 1, page 183]), that $\hat{T}_n \in BV(\mathbb{R}^2)$ and

$$\int_{\mathbb{R}^2} |\nabla \hat{T}_n| = \int_{\Omega} |\nabla \tilde{T}_n| + \int_{\partial\Omega} |\tilde{T}_n| d\mathcal{H}^1.$$

If \tilde{T}_n converges weakly-* to \tilde{T}_γ in $BV(\Omega)$, then \hat{T}_n converges weakly-* to an element u of $BV(\mathbb{R}^2)$. We must have $u = 0$ in the complement of $\bar{\Omega}$ and $u = \tilde{T}_\gamma$ in Ω . In particular,

$$\int_{\mathbb{R}^2} |\nabla u| = \int_{\Omega} |\nabla \tilde{T}_\gamma| + \int_{\partial\Omega} |\tilde{T}_\gamma| d\mathcal{H}^1.$$

By the weak lower semicontinuity property,

$$\int_{\mathbb{R}^2} |\nabla u| \leq \liminf_{n \rightarrow +\infty} \int_{\mathbb{R}^2} |\nabla \hat{T}_n|,$$

that is

$$\int_{\Omega} |\nabla \tilde{T}_\gamma| + \int_{\partial\Omega} |\tilde{T}_\gamma| d\mathcal{H}^1 \leq \liminf_{n \rightarrow +\infty} \int_{\mathbb{R}^2} \tilde{T}_n + \int_{\partial\Omega} |\tilde{T}_n| d\mathcal{H}^1.$$

In conclusion,

$$\begin{aligned} &\int_{\Omega} |\nabla \tilde{T}_\gamma| + \int_{\partial\Omega} |\tilde{T}_\gamma| d\mathcal{H}^1 + \int_{\Omega} \tilde{T}_\gamma \operatorname{div} \theta \\ &\quad + \frac{\alpha}{2} \int_{\Omega} \|\nabla \tilde{\varphi}_\gamma\|^2 + \gamma \|T \circ \tilde{\varphi}_\gamma - \tilde{T}_\gamma\|_{L^1(\Omega)} \\ &\leq \liminf_{n \rightarrow +\infty} \left(\int_{\Omega} |\nabla \tilde{T}_n| + \int_{\Omega} \tilde{T}_n \operatorname{div} \theta + \int_{\partial\Omega} |\tilde{T}_n| d\mathcal{H}^1 \right. \\ &\quad \left. + \frac{\alpha}{2} \int_{\Omega} \|\nabla \varphi_n\|^2 + \gamma \|T \circ \varphi_n - \tilde{T}_n\|_{L^1(\Omega)} \right), \end{aligned}$$

which implies that $(\tilde{\varphi}_\gamma, \tilde{T}_\gamma)$ is a minimizing pair of problem (7.5). ■

7.4 Approximation method of the total variation of $T \circ \varphi$

We now come to the second method to overcome the difficulties revealed by the total variation of $T \circ \varphi$.

As described in [3], Aubert and Kornprobst use an approximation of the semi-norm on $W^{1,p}(\Omega)$: $|u|_{W^{1,p}}^p = \int_{\Omega} |\nabla u|^p, \forall p$. They propose an alternative method based on a characterization of the Sobolev spaces by Bourgain *et al.* in [5] and extended by Ponce in [13]. Before providing approximation results, we introduce a sequence (ρ_n) of radial mollifiers, i.e.,

$$\begin{aligned} \rho_n(x) &= \rho_n(|x|), \\ \rho_n &\geq 0, \int_{\mathbb{R}^N} \rho_n(x) dx = 1, \end{aligned} \tag{7.7}$$

and for every $\delta > 0$, we assume that $\lim_{n \rightarrow \infty} \int_{\delta}^{\infty} \rho_n(r) r^{N-1} dr = 0$ ($\Omega \subset \mathbb{R}^N$).

In [5], the authors provide the following theorem:

Theorem 7.4.1 ([5, Theorem 2])

Assume $u \in L^p(\Omega), 1 < p < \infty$. Then

$$\lim_{n \rightarrow \infty} \int_{\Omega} \int_{\Omega} \frac{|u(x) - u(y)|^p}{|x - y|^p} \rho_n(x - y) dx dy = K_{p,N} \int_{\Omega} |\nabla u|^p dx = K_{p,N} |u|_{W^{1,p}}^p \tag{7.8}$$

with the convention that $|u|_{W^{1,p}} = \infty$ if $u \notin W^{1,p}(\Omega)$. Here $K_{p,N}$ depends only on p and N .

In [13], Ponce provides a follow-up to [5], replacing $|\cdot|^p$ with a continuous function w and using functions ρ_n that are no longer assumed to be radial. He also focuses on the *BV*-case and provides the following corollary:

Corollary 7.4.1 ([13, Corollary 1])

Suppose that ρ_n is radial for each $n > 0$. If $u \in W^{1,p}(\Omega), p > 1$ or if $u \in BV(\Omega)$ and $p = 1$, then

$$\lim_{n \rightarrow \infty} \int_{\Omega} \int_{\Omega} \frac{|u(x) - u(y)|^p}{|x - y|^p} \rho_n(x - y) dx dy = K_{p,N} \int_{\Omega} |Du|^p,$$

where $K_{p,N} = \int_{S^{N-1}} |e \cdot \sigma|^p d\mathcal{H}^{N-1}$.

In our work, we use this characterization to approximate the total variation. Then we propose minimizing the following functional:

$$\inf_{\varphi \in \mathcal{W}} \left\{ E_n(\varphi) = \frac{1}{K_{1,N}} \int_{\Omega} \int_{\Omega} \frac{|T \circ \varphi(x) - T \circ \varphi(y)|}{|x - y|} \rho_n(x - y) dx dy - \int_{\Omega} \langle \nabla(T \circ \varphi), \theta \rangle dx \tag{7.9} \right. \\ \left. + \frac{\alpha}{2} \int_{\Omega} \|\nabla \varphi\|^2 dx \right\},$$

with $\mathcal{W} = \left\{ \text{Id} + W_0^{1,2}(\Omega, \mathbb{R}^2) \right\}$.

Functional E_n is well defined for $\varphi \in W^{1,2}(\Omega)$, since T is Lipschitz continuous, $T \circ \varphi \in W^{1,2}(\Omega)$ according to Theorem 7.1.1, and then $T \circ \varphi \in BV(\Omega)$.

For the sake of clarity, we denote by $F_n(u)$ the approximation:

$$F_n(u) = \int_{\Omega} \int_{\Omega} \frac{|u(x) - u(y)|}{|x - y|} \rho_n(x - y) dx dy.$$

7.4.1 Existence of minimizers for the Problem with approximation of the total variation

Theorem 7.4.2

Assuming E_n is proper, for n large enough, Problem (7.9) admits at least one solution.

Proof:

Coercivity inequality

Let us fix $\varepsilon = 1$. According to Corollary 7.4.1,

$$\exists n_0 \in \mathbb{N}, \forall n \in \mathbb{N},$$

$$\left(n \geq n_0 \implies \left| F_n(T \circ \varphi) - K_{1,N} \int_{\Omega} |\nabla(T \circ \varphi)| \right| \leq 1 \right)$$

$$\text{so } \left(n \geq n_0 \implies \int_{\Omega} |\nabla(T \circ \varphi)| - \frac{1}{K_{1,N}} \leq \frac{1}{K_{1,N}} F_n(T \circ \varphi) \leq \int_{\Omega} |\nabla(T \circ \varphi)| + \frac{1}{K_{1,N}} \right).$$

Therefore, we obtain

$$\frac{1}{K_{1,N}} F_n(T \circ \varphi) - \int_{\Omega} \langle \nabla(T \circ \varphi), \theta \rangle dx \geq \int_{\Omega} |\nabla(T \circ \varphi)| - \int_{\Omega} \langle \nabla(T \circ \varphi), \theta \rangle dx - \frac{1}{K_{1,N}},$$

for n large enough.

Since $\int_{\Omega} |\nabla(T \circ \varphi)| - \int_{\Omega} \langle \nabla(T \circ \varphi), \theta \rangle dx \geq 0$, it yields to

$$E_n(\varphi) \geq \frac{\alpha}{2} \|\nabla \varphi\|_{L^2(\Omega, M_2)}^2 - \frac{1}{K_{1,N}}.$$

At last, using the generalized Poincaré inequality, we obtain:

$$E_n(\varphi) \geq c \|\varphi\|_{W^{1,2}(\Omega, \mathbb{R}^2)}^2 + \kappa, \quad \kappa \in \mathbb{R}. \quad (7.10)$$

Therefore, E_n being proper, the infimum of E_n is finite.

Convergence of a minimizing sequence

Let $(\varphi_n^k) \in \text{Id} + W_0^{1,2}(\Omega, \mathbb{R}^2)$ be a minimizing sequence of $E_n(\varphi)$.

$$E_n(\varphi_n^k) \xrightarrow{k \rightarrow \infty} \inf_{\Psi \in \text{Id} + W_0^{1,2}(\Omega, \mathbb{R}^2)} E_n(\Psi).$$

We have assumed that E_n is proper that is to say that there exists $\tilde{\varphi}_n$ such that $E_n(\tilde{\varphi}_n) < \infty$, then for k large enough we have $E_n(\varphi_n^k) \leq E_n(\tilde{\varphi}_n) + 1$. So, from the coercivity inequality, (φ_n^k) is bounded in $W^{1,2}(\Omega, \mathbb{R}^2)$, we can therefore extract a subsequence still denoted by (φ_n^k) such that:

$$(\varphi_n^k)_k \rightharpoonup \bar{\varphi}_n \text{ in } W^{1,2}(\Omega, \mathbb{R}^2).$$

And by continuity of the trace: $\bar{\varphi}_n = \text{Id}$ on $\partial\Omega$.

Lower semicontinuity

According to Rellich-Kondrachov theorem, we also have $\varphi_n^k \rightarrow \bar{\varphi}_n$ in $L^2(\Omega, \mathbb{R}^2)$ and so in $L^1(\Omega, \mathbb{R}^2)$.

T being a Lipschitz continuous function: $T \circ \varphi_n^k \rightarrow T \circ \bar{\varphi}_n$ in $L^2(\Omega)$. So $T \circ \varphi_n^k$ weakly converges to $T \circ \bar{\varphi}_n$ in $L^2(\Omega)$. Consequently, since it is assumed that $\text{div } \theta \in L^2(\Omega)$,

$$\int_{\Omega} (T \circ \varphi_n^k) \text{div } \theta \, dx \xrightarrow{k \rightarrow +\infty} \int_{\Omega} (T \circ \bar{\varphi}_n) \text{div } \theta \, dx.$$

Recalling that $\int_{\Omega} \langle \nabla (T \circ \varphi_n^k), \theta \rangle \, dx = - \int_{\Omega} T \circ \varphi_n^k \text{div } \theta \, dx + \int_{\partial\Omega} [\theta, n] T \circ \varphi_n^k \, d\mathcal{H}^1$, we obtain that

$$\int_{\Omega} \langle \nabla (T \circ \varphi_n^k), \theta \rangle \, dx \xrightarrow{k \rightarrow +\infty} \int_{\Omega} \langle \nabla (T \circ \bar{\varphi}_n), \theta \rangle \, dx,$$

since again $\varphi_n^k = \text{Id}$ on $\partial\Omega$ and T is assumed to be compactly supported.

Thanks to Theorem 2.1.11 ([6, Theorem IV.9]), we also have the convergence almost everywhere of a subsequence of $T \circ \varphi_n^k$ to $T \circ \bar{\varphi}_n$. Therefore $\frac{|T \circ \varphi_n^k(x) - T \circ \varphi_n^k(y)|}{|x - y|} \rho_n(x - y)$ converges to $\frac{|T \circ \bar{\varphi}_n(x) - T \circ \bar{\varphi}_n(y)|}{|x - y|} \rho_n(x - y)$ almost everywhere. Moreover, we use the following proposition:

Proposition 7.4.2 ([3, Proposition 2.1])

Assume $1 \leq p \leq \infty$ and $u \in W^{1,p}(\Omega)$ and let $\rho \in L^1(\mathbb{R}^N)$, $\rho > 0$. Then

$$\int_{\Omega} \int_{\Omega} \frac{|u(x) - u(y)|^p}{|x - y|^p} \rho(x - y) \, dx \, dy \leq C |u|_{W^{1,p}}^p \|\rho\|_{L^1(\mathbb{R}^N)},$$

where $|u|_{W^{1,p}}^p$ denote the semi-norm defined by $|u|_{W^{1,p}}^p = \int_{\Omega} |\nabla u|^p \, dx$ and C depends only on p and Ω .

Thus,

$$\begin{aligned}
& \int_{\Omega} \int_{\Omega} \frac{|T \circ \varphi_n^k(x) - T \circ \varphi_n^k(y)|}{|x - y|} \rho_n(x - y) dx dy \\
& \leq k_T \int_{\Omega} \int_{\Omega} \frac{|\varphi_n^k(x) - \varphi_n^k(y)|}{|x - y|} \rho_n(x - y) dx dy \\
& \leq k_T \int_{\Omega} \int_{\Omega} \frac{|(\varphi_n^k)^1(x) - (\varphi_n^k)^1(y)|}{|x - y|} \rho_n(x - y) dx dy \\
& \quad + k_T \int_{\Omega} \int_{\Omega} \frac{|(\varphi_n^k)^2(x) - (\varphi_n^k)^2(y)|}{|x - y|} \rho_n(x - y) dx dy, \\
& \leq k_T C \left(\|(\varphi_n^k)^1\|_{W^{1,2}(\Omega, \mathbb{R}^2)} + \|(\varphi_n^k)^2\|_{W^{1,2}(\Omega, \mathbb{R}^2)} \right),
\end{aligned}$$

which is bounded independently of k ($(\varphi_n^k)^1$ and $(\varphi_n^k)^2$ denoting the components of φ_n^k).

Then according to the dominated convergence theorem:

$$\begin{aligned}
& \int_{\Omega} \int_{\Omega} \frac{|T \circ \bar{\varphi}_n(x) - T \circ \bar{\varphi}_n(y)|}{|x - y|} \rho_n(x - y) dx dy \\
& = \lim_{k \rightarrow +\infty} \int_{\Omega} \int_{\Omega} \frac{|T \circ \varphi_n^k(x) - T \circ \varphi_n^k(y)|}{|x - y|} \rho_n(x - y) dx dy.
\end{aligned}$$

To conclude, the functional is weakly sequentially lower semicontinuous and

$$E_n(\bar{\varphi}_n) \leq \liminf_{k \rightarrow \infty} E_n(\varphi_n^k).$$

Therefore, there exists at least one minimizer of E_n on $\text{Id} + W_0^{1,2}(\Omega, \mathbb{R}^2)$. ■

7.4.2 Study of $\lim_{n \rightarrow \infty} \bar{\varphi}_n$ and Γ -convergence

According to Theorem 3 in [5]:

Theorem 7.4.3 ([5, Theorem 3])

Assume $f \in W^{1,1}(\Omega)$, $\Omega \subset \mathbb{R}^N$. Then

$$\lim_{j \rightarrow \infty} \int_{\Omega} \int_{\Omega} \frac{|f(x) - f(y)|}{|x - y|} \rho_{\varepsilon_j}(x - y) dx dy = K_{1,N} |f|_{W^{1,1}(\Omega)}.$$

$K_{1,N}$ only depends on N .

Proof (inspired of [5]): As $N = 2$ in practice, we restrict ourselves to this case in the proof.

For $f \in W^{1,1}(\Omega)$, let

$$F_n(x, y) = \frac{|f(x) - f(y)|}{|x - y|} \rho_n(x - y).$$

We have to prove that

$$\lim_{n \rightarrow \infty} \|F_n\|_{L^1(\Omega \times \Omega)} = K_{1,N} |f|_{W^{1,1}(\Omega)}.$$

Theorem 7.4.4 ([5, Theorem 1])

Assume $f \in W^{1,p}(\Omega)$, $1 \leq p < \infty$, and let $\rho \in L^1(\mathbb{R}^N)$, $\rho \geq 0$. Then

$$\int_{\Omega} \int_{\Omega} \frac{|f(x) - f(y)|^p}{|x - y|^p} \rho(x - y) dx dy \leq C |f|_{W^{1,p}}^p \|\rho\|_{L^1},$$

where C depends only on p and Ω .

The proof of Theorem 7.4.4 relies on Proposition IX.3 in [6].

By Theorem 7.4.4 and using the fact that ρ_n is radial, we have for any n and $f, g \in W^{1,1}(\Omega)$,

$$\left| \|F_n\|_{L^1(\Omega \times \Omega)} - \|G_n\|_{L^1(\Omega \times \Omega)} \right| \leq \|F_n - G_n\|_{L^1(\Omega \times \Omega)} \leq C |f - g|_{W^{1,1}(\Omega)},$$

with C being independent of f, g and n thanks to the properties of radial functions. Therefore, it suffices to establish the result for $f \in \mathcal{C}^2(\bar{\Omega})$ and by density, it will be satisfied for $f \in W^{1,1}(\Omega)$. Indeed, $\forall f \in W^{1,1}(\Omega)$, there exists a sequence $(f_k) \in \mathcal{C}^2(\bar{\Omega})$ such that

$$f_k \xrightarrow{k \rightarrow +\infty} f \text{ in } W^{1,1}(\Omega).$$

Then $|f - f_k|_{W^{1,1}(\Omega)} \xrightarrow{k \rightarrow +\infty} 0$ implies $\left| \|F_n\|_{L^1(\Omega \times \Omega)} - \|F_{k,n}\|_{L^1(\Omega \times \Omega)} \right| \xrightarrow{k \rightarrow +\infty} 0$, which yields to the validity of the result for $f \in W^{1,1}(\Omega)$ if the result holds for $f \in \mathcal{C}^2(\bar{\Omega})$.

Fix some $f \in \mathcal{C}^2(\bar{\Omega})$, then

$$\frac{|f(x) - f(y)|}{|x - y|} = \left| (\nabla f)(x) \cdot \frac{x - y}{|x - y|} \right| + O(|x - y|).$$

For each fixed $x \in \Omega$, let us set $R = \text{dist}(x, \partial\Omega)$. Denoting by $B(x, R)$ the open ball with center x and radius R ,

$$\begin{aligned} \int_{\Omega} \frac{|f(x) - f(y)|}{|x - y|} \rho_n(x - y) dy &= \int_{B(x,R)} \frac{|f(x) - f(y)|}{|x - y|} \rho_n(x - y) dy \\ &\quad + \int_{\Omega \setminus B(x,R)} \frac{|f(x) - f(y)|}{|x - y|} \rho_n(x - y) dy. \end{aligned}$$

$$\begin{aligned} \int_{\Omega \setminus B(x,R)} \frac{|f(x) - f(y)|}{|x - y|} \rho_n(x - y) dy &\leq \frac{2\|f\|_{\mathcal{C}^0(\bar{\Omega})}}{R} \int_{\Omega \setminus B(x,R)} \rho_n(x - y) dy, \\ &\leq \frac{2\|f\|_{\mathcal{C}^0(\bar{\Omega})}}{R} |\mathbb{S}^1| \int_R^{+\infty} r \rho_n(r) dr, \end{aligned}$$

which tends to 0 as $n \rightarrow \infty$, as a result of the properties of ρ_n . Let us now make the expression of $\int_{B(x,R)} \frac{|f(x) - f(y)|}{|x - y|} \rho_n(x - y) dy$ explicit. Denoting by $y = (y_1, y_2)$ and

$x = (x_1, x_2)$, we make the change of variables

$$\begin{cases} y_1 = x_1 + r \cos \theta \\ y_2 = x_2 + r \sin \theta, \end{cases} \quad \text{with } \theta \in [0, 2\pi] \text{ and } r \in [0, R].$$

Then

$$\begin{aligned} \int_{B(x,R)} \frac{|f(x) - f(y)|}{|x - y|} \rho_n(x - y) dy &= \int_{B(x,R)} \left(\left| (\nabla f)(x) \cdot \frac{x - y}{|x - y|} \right| \right. \\ &\quad \left. + O(|x - y|) \right) \rho_n(x - y) dy, \\ &= \int_0^R r \rho_n(r) \int_0^{2\pi} \left(\left| (\nabla f)(x) \cdot \begin{pmatrix} \cos \theta \\ \sin \theta \end{pmatrix} \right| \right) d\theta dr \\ &\quad + |S^1| O \left(\int_0^R r^2 \rho_n(r) dr \right). \end{aligned}$$

Then setting $\nabla f(x) = |\nabla f(x)|e$ with e a unit vector (here e depends on x), it yields to:

$$\begin{aligned} \int_{B(x,R)} \frac{|f(x) - f(y)|}{|x - y|} \rho_n(x - y) dy &= |\nabla f(x)| \int_0^R r \rho_n(r) \int_0^{2\pi} \left(\left| e \cdot \begin{pmatrix} \cos \theta \\ \sin \theta \end{pmatrix} \right| \right) d\theta dr, \\ &\quad + |S^1| O \left(\int_0^R r^2 \rho_n(r) dr \right), \end{aligned}$$

First of all, $\int_0^{2\pi} \left(\left| e \cdot \begin{pmatrix} \cos \theta \\ \sin \theta \end{pmatrix} \right| \right) d\theta$ is independent of the unit vector e .

Secondly,

$$\begin{aligned} |S^1| \int_0^R r \rho_n(r) dr &= |S^1| \underbrace{\int_0^{+\infty} r \rho_n(r) dr}_{= 1} - |S^1| \underbrace{\int_R^{+\infty} r \rho_n(r) dr}_{\downarrow_{n \rightarrow +\infty} 0}. \\ &\quad \text{according to the} \\ &\quad \text{hypotheses} \\ &\quad \text{on } \rho_n \end{aligned}$$

Thirdly, as proved by Spector in his PhD manuscript ([15, page 58]), if $E \subset \mathbb{R}^N$ is bounded and measurable, then

$$\lim_{n \rightarrow +\infty} \int_E |x| \rho_n(x) dx = 0.$$

In our case, taking $E = B(0, R)$ and making the change of variables $\begin{cases} x_1 = r \cos \theta \\ x_2 = r \sin \theta, \end{cases}$ we get

$$\int_{B(0,R)} |x| \rho_n(x) dx = |S^1| \int_0^R r^2 \rho_n(r) dr,$$

which tends to 0 when n tends to $+\infty$.

In conclusion,

$$\int_{B(x,R)} \frac{|f(x) - f(y)|}{|x - y|} \rho_n(x - y) dy = \frac{|\nabla f(x)|}{|S^1|} \left(\int_0^{2\pi} \left| e \cdot \begin{pmatrix} \cos \theta \\ \sin \theta \end{pmatrix} \right| d\theta \right) \int_0^R |S^1| r \rho_n(r) dr, \\ + |S^1| O \left(\int_0^R r^2 \rho_n(r) dr \right),$$

and with the material above,

$$\lim_{n \rightarrow +\infty} \int_{B(x,R)} \frac{|f(x) - f(y)|}{|x - y|} \rho_n(x - y) dy = K_{1,2} |\nabla f(x)|, \quad (7.11)$$

with $K_{1,2} = \frac{1}{|S^1|} \int_0^{2\pi} \left| e \cdot \begin{pmatrix} \cos \theta \\ \sin \theta \end{pmatrix} \right| d\theta$ and e any unit vector of \mathbb{R}^2 .

Since $f \in \mathcal{C}^2(\bar{\Omega})$, there exists L such that $|f(x) - f(y)| \leq L|x - y|$, $\forall x, y \in \Omega$, then

$$\int_{\Omega} \frac{|f(x) - f(y)|}{|x - y|} \rho_n(x - y) dy \leq L, \quad \forall x \in \Omega, \quad (7.12)$$

(one assume that Ω is connected, which is the case in practice).

Using the dominated convergence theorem, with (7.11) and (7.12), we conclude that for $f \in \mathcal{C}^2(\bar{\Omega})$, $\lim_{n \rightarrow \infty} \|F_n\|_{L^1(\Omega \times \Omega)} = K_{1,N} |f|_{W^{1,1}(\Omega)}$. That is to say

$$\boxed{\lim_{n \rightarrow \infty} \int_{\Omega} \int_{\Omega} \frac{|f(x) - f(y)|}{|x - y|} \rho_n(x - y) dx dy = K_{1,N} |f|_{W^{1,1}(\Omega)}}.$$

We complete the proof thanks to the density of $\mathcal{C}^2(\bar{\Omega})$ in $W^{1,1}(\Omega)$ (corollary IX.8 in [6]). ■

We have provided the proof in the case of $f \in W^{1,1}(\Omega)$, which is sufficient in our case since $T \circ \varphi \in W^{1,2}(\Omega)$ so $T \circ \varphi \in W^{1,1}(\Omega)$. However, in [8], Davila provides the proof for the BV case:

Theorem 7.4.5 ([8, Theorem 1])

Let $\Omega \subset \mathbb{R}^N$ be open bounded with a Lipschitz boundary and let $f \in BV(\Omega)$. Consider a sequence ρ_n satisfying (7.7). Then

$$\lim_{n \rightarrow \infty} \int_{\Omega} \int_{\Omega} \frac{|f(x) - f(y)|}{|x - y|} \rho_n(x - y) dx dy = K_{1,N} |f|_{BV(\Omega)}$$

with $|f|_{BV(\Omega)} = \left\{ \int_{\Omega} f \operatorname{div} \varphi \in \mathcal{C}_c^1(\Omega, \mathbb{R}^N), |\varphi| \leq 1 \text{ in } \Omega \right\}$.

For n fixed, we have proved the existence of a solution $\bar{\varphi}_n$ in $\operatorname{Id} + W^{1,2}(\Omega, \mathbb{R}^2)$ to problem (7.9) for n large enough.

$$\forall v \in \operatorname{Id} + W_0^{1,2}(\Omega), E_n(\bar{\varphi}_n) \leq E_n(v).$$

From this inequality and the coercivity inequality, $\bar{\varphi}_n$ is bounded independently of n then, up to a subsequence, $\bar{\varphi}_n$ weakly converges to $\bar{\varphi}$ in $W^{1,2}(\Omega, \mathbb{R}^2)$.

We would like to prove that $E_n(\bar{\varphi}_n)$ converges to $E(\bar{\varphi})$ when n tends to $+\infty$.

By definition of $\bar{\varphi}_n$, one has $E_n(\bar{\varphi}_n) \leq E_n(\bar{\varphi})$, thus by passing to the upper limit when n tends to $+\infty$,

$$\begin{aligned} \limsup_{n \rightarrow +\infty} E_n(\bar{\varphi}_n) &\leq \limsup_{n \rightarrow +\infty} E_n(\bar{\varphi}) \\ &= \lim_{n \rightarrow +\infty} \frac{1}{K_{1,2}} \int_{\Omega} \int_{\Omega} \frac{|T \circ \bar{\varphi}(x) - T \circ \bar{\varphi}(y)|}{|x - y|} \rho_n(x - y) dx dy \\ &\quad + \int_{\Omega} T \circ \bar{\varphi} \operatorname{div} \theta dx + \frac{\alpha}{2} \int_{\Omega} \|\nabla \bar{\varphi}\|^2 dx, \\ &= \int_{\Omega} |\nabla(T \circ \bar{\varphi})| + \int_{\Omega} T \circ \bar{\varphi} \operatorname{div} \theta dx + \frac{\alpha}{2} \int_{\Omega} \|\nabla \bar{\varphi}\|^2 dx, \\ &= E(\bar{\varphi}). \end{aligned}$$

Thus,

$$\boxed{\limsup_{n \rightarrow +\infty} E_n(\bar{\varphi}_n) \leq E(\bar{\varphi}).}$$

It remains to prove that

$$E(\bar{\varphi}) \leq \liminf_{n \rightarrow +\infty} E_n(\bar{\varphi}_n).$$

Due to compactness properties, it suffices to prove that

$$\int_{\Omega} |\nabla(T \circ \bar{\varphi})| \leq \liminf_{n \rightarrow +\infty} F_n(T \circ \bar{\varphi}_n).$$

In that purpose, let us introduce some notations.

For $r > 0$, we define the two following sets:

$$\Omega_r = \{x \in \Omega : \operatorname{dist}(x, \partial\Omega) > r\},$$

$$\Omega^r = \{x \in \mathbb{R}^2 : \operatorname{dist}(x, \Omega) < r\}.$$

Let $\eta \in C_0^\infty(\mathbb{R}^2)$ be a nonnegative radial function such that $\int_{\Omega} \eta = 1$, $\operatorname{Supp} \eta \subset B(0, 1)$, and let us define

$$f_\delta(x) = \frac{1}{\delta^2} \int_{\Omega} f(y) \eta\left(\frac{x - y}{\delta}\right) dy, \quad \forall x \in \Omega_\delta,$$

where f_δ is a regularization of f .

For the sake of clarity, we set $f = T \circ \bar{\varphi}$, and due to the properties of T , $f_n = T \circ \bar{\varphi}_n$ strongly converges to $f = T \circ \bar{\varphi}$ in $L^1(\Omega)$.

From Lemma 4 in [13], for each $r > 0$:

$$F_n(f_n) \geq \int_{\Omega_r} \int_{\Omega_r} \frac{|f_{n,\delta}(x) - f_{n,\delta}(y)|}{|x - y|} \rho_n(x - y) dx dy, \quad \forall \delta \in (0, r).$$

We first aim to prove that

$$\begin{aligned} \lim_{n \rightarrow +\infty} \int_{\Omega_r} \int_{\Omega_r} \frac{|f_{n,\delta}(x) - f_{n,\delta}(y)|}{|x - y|} \rho_n(x - y) dy dx &= \lim_{n \rightarrow +\infty} \int_{\Omega_r} \int_{\Omega_r} \left| \nabla f_\delta(x) \cdot \frac{x - y}{|x - y|} \right| \rho_n(x - y) dy dx \\ &= K_{1,2} \int_{\Omega_r} |\nabla f_\delta|. \end{aligned}$$

We start by proving that

$$\lim_{n \rightarrow +\infty} \left| \int_{\Omega_r} \int_{\Omega_r} \left(\frac{|f_{n,\delta}(x) - f_{n,\delta}(y)|}{|x-y|} - \nabla f_\delta(x) \cdot \frac{x-y}{|x-y|} \right) \rho_n(x-y) dy dx \right| = 0.$$

It is easily seen that

$$\begin{aligned} & \left| \int_{\Omega_r} \int_{\Omega_r} \left(\frac{|f_{n,\delta}(x) - f_{n,\delta}(y)|}{|x-y|} - \left| \nabla f_\delta(x) \cdot \frac{x-y}{|x-y|} \right| \right) \rho_n(x-y) dy dx \right| \\ & \leq \int_{\Omega_r} \int_{\Omega_r} \left| \frac{|f_{n,\delta}(x) - f_{n,\delta}(y)|}{|x-y|} - \left| \nabla f_\delta(x) \cdot \frac{x-y}{|x-y|} \right| \right| \rho_n(x-y) dy dx, \\ & \leq \int_{\Omega_r} \int_{\Omega_r} \frac{|f_{n,\delta}(x) - f_{n,\delta}(y) - \nabla f_\delta(x) \cdot (x-y)|}{|x-y|} \rho_n(x-y) dy dx. \end{aligned}$$

Let us take η such that $\eta \in (0, r - \delta)$. Then if $x \in \Omega_r$ and $y \in (\Omega_r)^\eta$, if $|x-y| < \eta$, the segment of endpoints x and y is contained in $(\Omega_r)^\eta$ so that, $f_{n,\delta}$ being sufficiently smooth, from Taylor's expansion:

$$f_{n,\delta}(y) - f_{n,\delta}(x) = \int_0^1 (y-x) \cdot \nabla f_{n,\delta}(x + s(y-x)) ds,$$

then,

$$f_{n,\delta}(x) - f_{n,\delta}(y) - \nabla f_\delta(x) \cdot (x-y) = \int_0^1 (x-y) \cdot (\nabla f_{n,\delta}(x + s(y-x)) - \nabla f_\delta(x)) ds,$$

and

$$\begin{aligned} |f_{n,\delta}(x) - f_{n,\delta}(y) - \nabla f_\delta(x) \cdot (x-y)| & \leq |x-y| \int_0^1 |\nabla f_{n,\delta}(x + s(y-x)) - \nabla f_\delta(x)| ds, \\ & \leq |x-y| \int_0^1 |\nabla f_{n,\delta}(x + s(y-x)) - \nabla f_\delta(x + s(y-x)) \\ & \quad + \nabla f_\delta(x + s(y-x)) - \nabla f_\delta(x)| ds. \end{aligned}$$

We know that $f_{n,\delta}$ converges to f_δ in $\mathcal{C}^2(\overline{\Omega_r})$, then

$$\begin{aligned} |f_{n,\delta}(x) - f_{n,\delta}(y) - \nabla f_\delta(x) \cdot (x-y)| & \leq |x-y| \|\nabla f_{n,\delta} - \nabla f_\delta\|_{L^\infty(\overline{(\Omega_n)^\eta})} \\ & \quad + |x-y| \int_0^1 |\nabla f_\delta(x + s(y-x)) - \nabla f_\delta(x)| ds, \\ & \leq |x-y| \|\nabla f_{n,\delta} - \nabla f_\delta\|_{L^\infty(\overline{(\Omega_n)^\eta})} + \frac{1}{2} |x-y|^2 \|\nabla^2 f_\delta\|_{L^\infty(\overline{(\Omega_n)^\eta})}. \end{aligned}$$

Thus,

$$\frac{|f_{n,\delta}(x) - f_{n,\delta}(y) - \nabla f_\delta(x) \cdot (x-y)|}{|x-y|} \leq \|\nabla f_{n,\delta} - \nabla f_\delta\|_{L^\infty(\overline{(\Omega_n)^\eta})} + \frac{1}{2} |x-y| \|\nabla^2 f_\delta\|_{L^\infty(\overline{(\Omega_n)^\eta})}.$$

Now,

$$\begin{aligned}
& \int_{\Omega_r} \int_{\Omega_r} \frac{|f_{n,\delta}(x) - f_{n,\delta}(y) - \nabla f_\delta(x) \cdot (x - y)|}{|x - y|} \rho_n(x - y) dy dx \\
& \leq \int_{\Omega_r} \int_{(\Omega_r)^\eta} \frac{|f_{n,\delta}(x) - f_{n,\delta}(y) - \nabla f_\delta(x) \cdot (x - y)|}{|x - y|} \rho_n(x - y) dy dx, \\
& \leq \int_{\Omega_r} \int_{(\Omega_r)^\eta \cap |x-y| < \eta} \frac{|f_{n,\delta}(x) - f_{n,\delta}(y) - \nabla f_\delta(x) \cdot (x - y)|}{|x - y|} \rho_n(x - y) dy dx \\
& + \int_{\Omega_r} \int_{(\Omega_r)^\eta \cap |x-y| \geq \eta} \frac{|f_{n,\delta}(x) - f_{n,\delta}(y) - \nabla f_\delta(x) \cdot (x - y)|}{|x - y|} \rho_n(x - y) dy dx.
\end{aligned}$$

We consider each component of the right-hand side of the inequality.

$$\begin{aligned}
& \int_{\Omega_r} \int_{(\Omega_r)^\eta \cap |x-y| < \eta} \frac{|f_{n,\delta}(x) - f_{n,\delta}(y) - \nabla f_\delta(x) \cdot (x - y)|}{|x - y|} \rho_n(x - y) dy dx \\
& \leq \int_{\Omega_r} \int_{(\Omega_r)^\eta \cap |x-y| < \eta} \left(\|\nabla f_{n,\delta} - \nabla f_\delta\|_{L^\infty(\overline{(\Omega_r)^\eta})} \right. \\
& \quad \left. + \frac{1}{2}|x - y| \|\nabla^2 f_\delta\|_{L^\infty(\overline{(\Omega_r)^\eta})} \right) \rho_n(x - y) dy dx, \\
& \leq |\Omega_r| \underbrace{\|\nabla f_{n,\delta} - \nabla f_\delta\|_{L^\infty(\overline{(\Omega_r)^\eta})}}_{\substack{\downarrow n \rightarrow +\infty \\ 0}} + \frac{|\Omega_r|}{2} \|\nabla^2 f_\delta\|_{L^\infty(\overline{(\Omega_r)^\eta})} \underbrace{\int_{|h| \leq \eta} |h| \rho_n(h) dh}_{\substack{\downarrow n \rightarrow +\infty \\ 0}}.
\end{aligned}$$

since $f_{n,\delta}$ converges to f_δ in $\mathcal{C}^2(\overline{(\Omega_r)^\eta})$
due to the result by D. Spector[15]

$$\begin{aligned}
& \int_{\Omega_r} \int_{(\Omega_r)^\eta \cap |x-y| \geq \eta} \frac{|f_{n,\delta}(x) - f_{n,\delta}(y) - \nabla f_\delta(x) \cdot (x-y)|}{|x-y|} \rho_n(x-y) dy dx \\
& \leq \frac{1}{\eta} \int_{\Omega_r} \int_{(\Omega_r)^\eta \cap |x-y| \geq \eta} |f_{n,\delta}(x) - f_{n,\delta}(y)| \rho_n(x-y) dy dx \\
& \quad + \int_{\Omega_r} \int_{(\Omega_r)^\eta \cap |x-y| \geq \eta} \left| \nabla f_\delta(x) \cdot \frac{(x-y)}{|x-y|} \right| \rho_n(x-y) dy dx, \\
& \leq \frac{1}{\eta} \int_{\Omega_r} \int_{(\Omega_r)^\eta \cap |x-y| \geq \eta} \left(|f_{n,\delta}(x) - f_\delta(x)| + |f_\delta(x) - f_\delta(y)| \right. \\
& \quad \left. + |f_\delta(y) - f_{n,\delta}(y)| \right) \rho_n(x-y) dy dx \\
& \quad + \|\nabla f_\delta\|_{L^\infty(\overline{(\Omega_r)^\eta})} \int_{\Omega_r} \int_{(\Omega_r)^\eta \cap |x-y| \geq \eta} \rho_n(x-y) dy dx, \\
& \leq \frac{2}{\eta} \|f_{n,\delta} - f_\delta\|_{L^\infty(\overline{(\Omega_r)^\eta})} |\Omega_r| \int_{|h| \geq \eta} \rho_n(h) dh \\
& \quad + \frac{2}{\eta} \|f_\delta\|_{L^\infty(\overline{(\Omega_r)^\eta})} |\Omega_r| \int_{|h| \geq \eta} \rho_n(h) dh \\
& \quad + \|\nabla f_\delta\|_{L^\infty(\overline{(\Omega_r)^\eta})} |\Omega_r| \int_{|h| \geq \eta} \rho_n(h) dh.
\end{aligned}$$

We thus have proved that

$$\begin{aligned}
& \lim_{n \rightarrow +\infty} \left| \int_{\Omega_r} \int_{\Omega_r} \frac{|f_{n,\delta}(x) - f_{n,\delta}(y)|}{|x-y|} \rho_n(x-y) dy dx \right. \\
& \quad \left. - \int_{\Omega_r} \int_{\Omega_r} \left| \nabla f_\delta(x) \cdot \frac{x-y}{|x-y|} \right| \rho_n(x-y) dy dx \right| = 0.
\end{aligned}$$

Now it suffices to prove that the limit of $\int_{\Omega_r} \int_{\Omega_r} \left| \nabla f_\delta(x) \cdot \frac{x-y}{|x-y|} \right| \rho_n(x-y) dy dx$ when n tends to $+\infty$ exists and compute it.

$$\begin{aligned}
\int_{\Omega_r} \int_{\mathbb{R}^2} \left| \nabla f_\delta(x) \cdot \frac{x-y}{|x-y|} \right| \rho_n(x-y) dy dx &= \int_{\Omega_r} \int_{\Omega_r} \left| \nabla f_\delta(x) \cdot \frac{x-y}{|x-y|} \right| \rho_n(x-y) dy dx \\
& \quad + \int_{\Omega_r} \int_{\mathbb{R}^2 \setminus \Omega_r} \left| \nabla f_\delta(x) \cdot \frac{x-y}{|x-y|} \right| \rho_n(x-y) dy dx.
\end{aligned}$$

Fixing $\lambda > 0$,

$$\begin{aligned}
& \int_{\Omega_r} \int_{\mathbb{R}^2 \setminus \Omega_r} \left| \nabla f_\delta(x) \cdot \frac{x-y}{|x-y|} \right| \rho_n(x-y) dy dx \\
& \leq |\Omega_r| \|\nabla f_\delta\|_{L^\infty(\overline{\Omega_r})} \int_{|h|>\lambda} \rho_n(h) dh \\
& \quad + \|\nabla f_\delta\|_{L^\infty(\overline{\Omega_r})} \int_{\Omega_r \setminus \Omega_{r+\lambda}} \int_{|x-y|\leq\lambda} \rho_n(x-y) dy dx, \\
& \leq |\Omega_r| \|\nabla f_\delta\|_{L^\infty(\overline{\Omega_r})} \int_{|h|>\lambda} \rho_n(h) dh \\
& \quad + |\Omega_r \setminus \Omega_{r+\lambda}| \|\nabla f_\delta\|_{L^\infty(\overline{\Omega_r})} \int_{|h|\leq\lambda} \rho_n(h) dh.
\end{aligned}$$

By letting n tend to $+\infty$, and then λ tend to 0, it follows that:

$$\lim_{n \rightarrow +\infty} \int_{\Omega_r} \int_{\mathbb{R}^2 \setminus \Omega_r} \left| \nabla f_\delta(x) \cdot \frac{x-y}{|x-y|} \right| \rho_n(x-y) dy dx = 0,$$

(using again the properties of ρ_n).

Now,

$$\int_{\Omega_r} \int_{\mathbb{R}^2} \left| \nabla f_\delta(x) \cdot \frac{x-y}{|x-y|} \right| \rho_n(x-y) dy dx = \int_{\Omega_r} \int_0^{2\pi} \int_0^{+\infty} \left| \nabla f_\delta(x) \cdot \begin{pmatrix} \cos \theta \\ \sin \theta \end{pmatrix} \right| \rho_n(r) r dr d\theta dx,$$

with the change of variables $\begin{cases} y_1 = x_1 + r \cos \theta \\ y_2 = x_2 + r \sin \theta, \end{cases} \theta \in [0, 2\pi]$ and $r \in [0, +\infty[$.

That is,

$$\int_{\Omega_r} |\nabla f_\delta(x)| \int_0^{+\infty} \left[\int_0^{2\pi} |e \cdot \begin{pmatrix} \cos \theta \\ \sin \theta \end{pmatrix}| d\theta \right] r \rho_n(r) dr dx,$$

with e any unit vector in \mathbb{R}^2 .

In the end,

$$\begin{aligned}
\lim_{n \rightarrow +\infty} \int_{\Omega_r} \int_{\mathbb{R}^2} \left| \nabla f_\delta(x) \cdot \frac{x-y}{|x-y|} \right| \rho_n(x-y) dy dx &= \frac{1}{|S^1|} \int_0^{2\pi} |e \cdot \begin{pmatrix} \cos \theta \\ \sin \theta \end{pmatrix}| d\theta \int_{\Omega_r} |\nabla f_\delta(x)| dx, \\
&= K_{1,2} \int_{\Omega_r} |\nabla f_\delta(x)| dx.
\end{aligned}$$

In particular,

$$K_{1,2} \int_{\Omega_r} |\nabla f_\delta| dx = \liminf_{n \rightarrow +\infty} \int_{\Omega_r} \int_{\Omega_r} \frac{|f_{n,\delta}(x) - f_{n,\delta}(y)|}{|x-y|} \rho_n(x-y) dx dy \leq \liminf_{n \rightarrow +\infty} F_n(f_n).$$

Using the fact that f_δ strongly converges to f in $L^1(\Omega_r)$ when $\delta \rightarrow 0^+$,

$$\begin{aligned}
K_{1,2} \int_{\Omega_r} |\nabla(T \circ \tilde{\varphi})| &\leq K_{1,2} \liminf_{\delta \rightarrow 0^+} \int_{\Omega_r} |\nabla f_\delta| \\
&\leq \liminf_{n \rightarrow +\infty} F_n(f_n).
\end{aligned}$$

Following Ponce [13], we obtain that $\sup_{ACC\Omega} \int_A |\nabla f| = \int_{\Omega} |\nabla f|$, then

$$\liminf_{n \rightarrow \infty} F_n(\varphi_n) \geq K_{1,2} \int_{\Omega} |\nabla(T \circ \bar{\varphi})|.$$

Combining the two previous results allows to conclude that

$$\lim_{n \rightarrow +\infty} E_n(\bar{\varphi}_n) = E(\bar{\varphi}).$$

7.4.3 Euler-Lagrange equation

Let us assume that φ_n minimizes F_n . Consequently, G_n defined below is minimum for $\varepsilon = 0$. We define the functional $G_n(\varepsilon)$ by

$$G_n(\varepsilon) = F_n(\varphi_n + \varepsilon\phi) = \int_{\Omega} \int_{\Omega} \frac{|T \circ (\varphi_n + \varepsilon\phi)(x) - T \circ (\varphi_n + \varepsilon\phi)(y)|}{|x - y|} \rho_n(x - y) dx dy,$$

$\forall \phi \in W^{1,2}(\Omega, \mathbb{R}^2)$. So necessarily,

$$\left. \frac{\partial G_n}{\partial \varepsilon} \right|_{\varepsilon=0} = 0.$$

To do so, we have to establish a chain rule for $T \circ \varphi_n$. We need further regularity on T than Lipschitz continuity.

Theorem 7.4.6

We assume that $T \in W^{2,\infty}(\Omega, \mathbb{R}^2)$, T is compactly supported and $T(0) = 0$. Let $\varphi \in W^{1,p}(\Omega, \mathbb{R}^2)$, then

$$T \circ \varphi \in W^{1,p} \text{ and } \begin{cases} \frac{\partial(T \circ \varphi)}{\partial x} = \frac{\partial T}{\partial x}(\varphi) \frac{\partial \varphi^1}{\partial x} + \frac{\partial T}{\partial y}(\varphi) \frac{\partial \varphi^2}{\partial x}, \\ \frac{\partial(T \circ \varphi)}{\partial y} = \frac{\partial T}{\partial x}(\varphi) \frac{\partial \varphi^1}{\partial y} + \frac{\partial T}{\partial y}(\varphi) \frac{\partial \varphi^2}{\partial y}. \end{cases}$$

Proof: For $\varphi \in W^{1,p}(\Omega, \mathbb{R}^2)$, $T \circ \varphi \in W^{1,p}(\Omega)$ and $\frac{\partial T}{\partial x_i} \frac{\partial \varphi^j}{\partial x_k} \in L^p(\Omega)$.

Let (φ_k) be a sequence of $C_c^\infty(\mathbb{R}^2, \mathbb{R}^2)$ such that

$$\begin{aligned} \varphi_k &\longrightarrow \varphi \text{ in } L^p(\Omega, \mathbb{R}^2), \\ \nabla \varphi_k &\longrightarrow \nabla \varphi \text{ in } L^p(\omega, \mathbb{R}^2), \forall \omega \subset\subset \Omega, \end{aligned}$$

according to Theorem IX.2 in [6]. (For a subsequence, φ_k and $\nabla \varphi_k$ converge almost everywhere to φ and $\nabla \varphi$).

We have $\forall \phi \in C_c^1(\Omega)$,

$$\int_{\Omega} T \circ \varphi_k \frac{\partial \phi}{\partial x} dx = - \int_{\Omega} \left[\frac{\partial T}{\partial x}(\varphi_k) \frac{\partial \varphi_k^1}{\partial x} + \frac{\partial T}{\partial y}(\varphi_k) \frac{\partial \varphi_k^2}{\partial x} \right] \phi dx.$$

But $T \circ \varphi_k \xrightarrow{k \rightarrow +\infty} T \circ \varphi$ in $L^p(\Omega)$ then $\int_{\Omega} T \circ \varphi_k \frac{\partial \phi}{\partial x} \xrightarrow{k \rightarrow +\infty} \int_{\Omega} T \circ \varphi \frac{\partial \phi}{\partial x}$, $\forall \phi \in \mathcal{C}_c^1(\Omega)$,
and $\frac{\partial T}{\partial x}(\varphi_k) \frac{\partial \varphi_k^1}{\partial x} \xrightarrow{k \rightarrow +\infty} \frac{\partial T}{\partial x}(\varphi) \frac{\partial \varphi^1}{\partial x}$ in $L^p(\omega)$ by dominated convergence.
Therefore,

$$\int_{\Omega} T \circ \varphi \frac{\partial \phi}{\partial x} dx = - \int_{\Omega} \left[\frac{\partial T}{\partial x}(\varphi) \frac{\partial \varphi^1}{\partial x} + \frac{\partial T}{\partial y}(\varphi) \frac{\partial \varphi^2}{\partial x} \right] \phi dx. \quad \blacksquare$$

Now we can compute the Euler-Lagrange equation:

$$\begin{aligned} \left. \frac{\partial G_n}{\partial \varepsilon} \right|_{\varepsilon=0} &= \lim_{\varepsilon \rightarrow 0} \frac{F_n(\varphi_n + \varepsilon \phi) - F_n(\varphi_n)}{\varepsilon}, \\ \left. \frac{\partial G_n}{\partial \varepsilon} \right|_{\varepsilon=0} &= \int_{\Omega} \int_{\Omega} \frac{T \circ \varphi_n(x) - T \circ \varphi_n(y)}{|T \circ \varphi_n(x) - T \circ \varphi_n(y)|} \left(\nabla T(\varphi_n(x)) \phi(x) - \nabla T(\varphi_n(y)) \phi(y) \right) \frac{\rho_n(x-y)}{|x-y|} dx dy, \\ &= \int_{\Omega} \int_{\Omega} \frac{T \circ \varphi_n(x) - T \circ \varphi_n(y)}{|T \circ \varphi_n(x) - T \circ \varphi_n(y)|} \nabla T(\varphi_n(x)) \phi(x) \frac{\rho_n(x-y)}{|x-y|} dx dy \\ &\quad - \int_{\Omega} \int_{\Omega} \frac{T \circ \varphi_n(x) - T \circ \varphi_n(y)}{|T \circ \varphi_n(x) - T \circ \varphi_n(y)|} \nabla T(\varphi_n(y)) \phi(y) \frac{\rho_n(x-y)}{|x-y|} dx dy. \end{aligned}$$

We exchange x and y in the second integral, and assuming that the order of integration does not matter,

$$\begin{aligned} \left. \frac{\partial G_n}{\partial \varepsilon} \right|_{\varepsilon=0} &= \int_{\Omega} \int_{\Omega} \frac{T \circ \varphi_n(x) - T \circ \varphi_n(y)}{|T \circ \varphi_n(x) - T \circ \varphi_n(y)|} \nabla T(\varphi_n(x)) \phi(x) \frac{\rho_n(x-y)}{|x-y|} dx dy \\ &\quad - \int_{\Omega} \int_{\Omega} \frac{T \circ \varphi_n(y) - T \circ \varphi_n(x)}{|T \circ \varphi_n(y) - T \circ \varphi_n(x)|} \nabla T(\varphi_n(x)) \phi(x) \frac{\rho_n(y-x)}{|y-x|} dy dx \\ &= 2 \int_{\Omega} \int_{\Omega} \frac{T \circ \varphi_n(x) - T \circ \varphi_n(y)}{|T \circ \varphi_n(x) - T \circ \varphi_n(y)|} \nabla T(\varphi_n(x)) \phi(x) \frac{\rho_n(x-y)}{|x-y|} dx dy. \end{aligned}$$

If φ_n is a minimizer, necessarily:

$$\boxed{\frac{2}{K_{1,2}} \nabla T(\varphi_n(x)) \int_{\Omega} \text{sign}(T \circ \varphi_n(x) - T \circ \varphi_n(y)) \frac{\rho_n(x-y)}{|x-y|} dy + \nabla T(\varphi_n) \text{div}(\theta) - \alpha \Delta \varphi = 0.}$$

7.5 Implementation details

In this section, implementation details are provided to compute numerically the Euler-Lagrange equation obtained in the previous section. Indeed, a nonlocal term whose discretization requires special care appears in the Euler-Lagrange equation, making the implementation difficult.

To do so, we take a simple example stemming from a restoration problem and then, we apply the method to our problem.

7.5.1 Experiments on a restoration problem

Problem

As Aubert and Kornprobst in [3], we have implemented a classical model for image restoration problem to understand the approximation method and its performances.

Let $u : \Omega \subset \mathbb{R}^2 \rightarrow \mathbb{R}$ be an original image describing a real scene, and let u_0 be the observed image of the same scene. We assume that the degradation model reads as

$$u_0 = Ru + \eta,$$

where η stands for a white additive Gaussian noise and where R is a linear operator representing the blur. Given u_0 , the problem is then to reconstruct u . The following minimization problem is proposed :

$$\inf_u \int_{\Omega} |u_0 - Ru|^2 dx + \lambda \int_{\Omega} |\nabla u|^p dx. \quad (7.13)$$

The idea developed by Aubert and Kornprobst is to replace the smoothing term $\int_{\Omega} |\nabla u|^p dx$ by the considered sequence of integral operators. Without loss of generality, the operator R is supposed to be the identity operator.

We have implemented the model introduced by Rudin, Osher and Fatemi in [14] for $p = 1$.

Implementation

The Euler-Lagrange equation of (7.13) is defined by:

$$2p\lambda \int_{\Omega} \frac{|u(x) - u(y)|^{p-2}}{|x - y|^p} (u(x) - u(y)) \rho_n(x - y) dy - 2(u_0 - u) = 0. \quad (7.14)$$

Using a gradient descent method, we obtain:

$$\begin{cases} \frac{u^{k+1}(x) - u^k(x)}{dt} = -2p\lambda I_{u^k}(x) + 2(u_0(x) - u^k(x)), \\ u^0(x) = u_0(x). \end{cases} \quad (7.15)$$

with

$$I_{u^k}(x) = \int_{\Omega} \frac{|u^k(x) - u^k(y)|^{p-2}}{|x - y|^p} (u^k(x) - u^k(y)) \rho_n(x - y) dy,$$

and dt is the discrete time step.

The problem is to discretize in space the integral I_{u^k} which has a singular kernel, not defined when $x = y$. The authors introduce the function $J_{u^k}(x, y)$ such that:

$$I_{u^k}(x) = \int_{\Omega} \frac{J_{u^k}(x, y)}{|x - y|} dy, \quad (7.16)$$

with

$$J_{u^k}(x, y) = \frac{|u^k(x) - u^k(y)|^{p-2} (u^k(x) - u^k(y)) \rho_n(x - y)}{|x - y|^{p-1}}.$$

Because of the singularity, the schemes using finite differences and integral approximations will not lead to a suitable numerical solution. That is the reason why, the method proposed by the authors in [3] is the following:

- The discretization in space is performed using a triangulation. The family of triangles covering Ω is denoted by \mathcal{T} .
- For x fixed, the function $J_{u^k}(x, y)$ is linearly interpolated on each triangle.
- On each triangle $T_i \in \mathcal{T}$, explicit expressions for $\int_{T_i} \frac{J_{u^k}(x, y)}{|x - y|} dy$ are provided.

Then, the integral $I_{u^k}(x)$ becomes

$$I_{u^k}(x) = \sum_{T_i \in \mathcal{T}} \int_{T_i} \frac{J_{u^k}(x, y)}{|x - y|} dy.$$

Given a triangle $T \in \mathcal{T}$, let us denote the three nodes of T by $\{y_i = (y_i^1, y_i^2)^T\}_{i=1\dots 3}$ where the superscript indicates the components.

Then the authors define the 3-D points $\left\{A_i = \left((y_i)^T, J_{u^k}(x, y_i)\right)^T\right\}$.

To make things clear, we provide a scheme of the triangulation. The pixels are represented as plain squares. We represent in red dotted line the two kinds of triangle. For a point $x = (i_0, j_0)$, the integral $I_{u^k}(x)$ is computed on each triangle included in a window of size $2m \times 2m$, with $y_i = (i_0 + n, j_0 + l)$, $n = -m \dots m - 1$, $l = -m + 1 \dots m$.

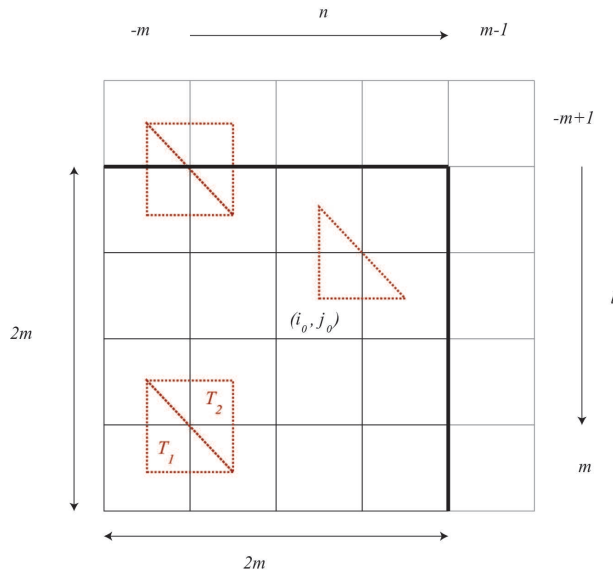


Figure 7.1: Scheme of the mesh definition.

In the case where $x \neq y_i$, $J_{u^k}(x, y_i)$ is well defined, otherwise (it means that x is in fact a node of \mathcal{T}), we use a linear interpolation algorithm: using a point $M \in T$ close to $x = y_i$, the value of $J_{u^k}(M, y_i)$ is estimated and the value of $J(x, y_i)$ is deduced by interpolation.

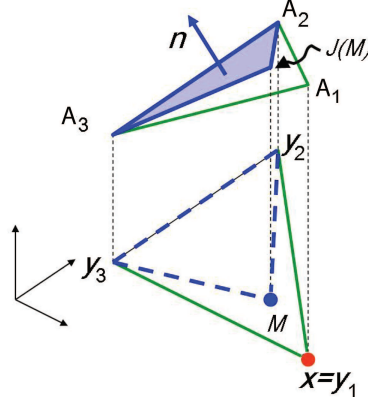


Figure 7.2: Scheme of the interpolation (from [3]).

Given $\{A_j\}_{j=1\dots 3}$ and any node y_i , we have

$$J(x, y) = J(x, y_i) - \frac{1}{n^3} \begin{pmatrix} n^1 \\ n^2 \end{pmatrix} (y - y_i),$$

where $n = (n^1, n^2, n^3)$ is the normal to the triangle $A_1A_2A_3$ as displayed on Fig 7.2. Then

$$\begin{aligned} \int_T \frac{J(x, y)}{|x - y|} dy &= J(x, y_i) \int_T \frac{1}{|x - y|} - \frac{1}{n^3} \begin{pmatrix} n^1 \\ n^2 \end{pmatrix} \int_T \frac{(y - y_i)}{|x - y|} dy, \\ &= J(x, y_i) \int_T \frac{1}{|x - y|} dy - \frac{1}{n^3} \begin{pmatrix} n^1 \\ n^2 \end{pmatrix} \left[\int_T \frac{(y - x)}{|x - y|} + (x - y_i) \int_T \frac{1}{|x - y|} dy \right]. \end{aligned}$$

Therefore, the computation of the integral over the triangle T only requires the computation of the two following integrals:

$$\int_T \frac{1}{|x - y|} dy \quad \text{and} \quad \int_T \frac{(y - x)}{|x - y|} dy.$$

The authors introduce the distance function:

$$\text{Dist}(x, y) = |x - y| = \sqrt{(x^1 - y^1)^2 + (x^2 - y^2)^2},$$

and

$$\begin{aligned} \nabla_y \text{Dist}(x, y) &= \frac{y - x}{|x - y|}, \\ \Delta_y \text{Dist}(x, y) &= \frac{1}{\text{Dist}(x, y)}. \end{aligned}$$

Hence

$$\begin{aligned} \int_T \frac{1}{|x - y|} dy &= \int_T \Delta_y \text{Dist}(x, y) dy = \sum_{i=1,2} \int_{\partial T} \frac{\partial \text{Dist}(x, y)}{\partial y^i} N^i ds, \\ \int_T \frac{y - x}{|x - y|} dy &= \int_T \nabla_y \text{Dist}(x, y) dy = \int_{\partial T} \text{Dist}(x, y) N ds, \end{aligned}$$

when N is outer the normal to the edges of the triangle T .

Lemma 7.5.1

Let us consider a segment $S = (\alpha, \beta)$ of extremities $\alpha = (\alpha_1, \alpha_2), \beta = (\beta_1, \beta_2)$, N the normal to this segment, and x a given point. Let us define:

$$\begin{aligned} a &= |\alpha\beta|, & \delta &= a^2b^2 - c^2, & l_1 &= c/\sqrt{\delta}, \\ b &= |x\alpha|, & d &= x\vec{\alpha}.N, & l_2 &= (a^2 + c)/\sqrt{\delta}, \\ c &= x\vec{\alpha}.\vec{\alpha}\beta. \end{aligned}$$

We have

$$I_1 = \sum_{i=1,2} \int_S \frac{\partial \text{Dist}(x, y)}{\partial y^i} N^i ds = \begin{cases} 0 & \text{if } x \text{ is aligned with } S, \\ d(\text{asinh}(l_2) - \text{asinh}(l_1)) & \text{otherwise,} \end{cases} \quad (7.17)$$

and

$$I_2 = \int_S \text{Dist}(x, y) ds = \begin{cases} a^2/2 & \text{if } x = \alpha \text{ or } x = \beta, \\ a^2/2 + c & \text{if } c = ab \text{ (} x \text{ aligned with } \vec{\alpha}\beta \text{ and } c > 0), \\ -a^2/2 - c & \text{if } c = -ab \text{ (} x \text{ aligned with } \vec{\alpha}\beta \text{ and } c < 0), \\ \frac{\delta}{2a^2}(l_2\sqrt{1+l_2^2} + \text{asinh}(l_2) - l_1\sqrt{1+l_1^2} - \text{asinh}(l_1)) & \text{otherwise,} \end{cases} \quad (7.18)$$

Proof: First, let us parametrize the segment S so that:

$$S = \left\{ y(t) = t \begin{pmatrix} \beta^1 \\ \beta^2 \end{pmatrix} + (1-t) \begin{pmatrix} \alpha^1 \\ \alpha^2 \end{pmatrix} : t \in [0, 1] \right\}.$$

The unit normal to the segment S can be written as follows: $N = \frac{1}{a} \begin{pmatrix} \beta^2 - \alpha^2 \\ -(\beta^1 - \alpha^1) \end{pmatrix}$ and the distance function can be expressed with respect to t :

$$\begin{aligned} \text{Dist}(x, y(t)) &= \sqrt{(t\beta^1 + (1-t)\alpha^1 - x^1)^2 + (t\beta^2 + (1-t)\alpha^2 - x^2)^2}, \\ &= \sqrt{a^2t^2 + 2ct + b^2}, \\ &= \sqrt{a^2\left(t + \frac{c}{a^2}\right)^2 - \frac{c^2}{a^2} + b^2}, \\ &= \frac{\sqrt{\delta}}{a} \sqrt{\frac{a^4}{\delta}\left(t + \frac{c}{a^2}\right)^2 + 1}, \text{ if } \delta \neq 0. \end{aligned}$$

- To start with, let us prove the result for I_1 .

– In the case where x is not aligned with S .

$$\begin{aligned}
I_1 &= \frac{1}{a} \int_0^1 \left(\frac{(t\beta^1 + (1-t)\alpha^1 - x^1)(\beta^2 - \alpha^2) - (t\beta^2 + (1-t)\alpha^2 - x^2)(\beta^1 - \alpha^1)}{\text{Dist}(x, y(t))} \right) a dt, \\
&= \frac{1}{a} \int_0^1 \left(\frac{(\beta^2 - \alpha^2)(\alpha^1 - x^1) - (\beta^1 - \alpha^1)(\alpha^2 - x^2)}{\text{Dist}(x, y(t))} \right) a dt, \\
&= \vec{\alpha}\beta \cdot x\vec{\alpha}^\perp \int_0^1 \frac{1}{\text{Dist}(x, y(t))} dt, \\
&= \vec{\alpha}\beta \cdot x\vec{\alpha}^\perp \int_0^1 \frac{1}{\frac{\sqrt{\delta}}{a} \sqrt{\frac{a^4}{\delta} (t + \frac{c}{a^2})^2 + 1}} dt,
\end{aligned}$$

and using the change of variable $z = \frac{a^2}{\sqrt{\delta}}(t + \frac{c}{a^2})$ it yields to:

$$\begin{aligned}
I_1 &= \frac{\vec{\alpha}\beta x\vec{\alpha}^\perp}{a} \int_{l_1}^{l_2} \frac{dz}{\sqrt{z^2 + 1}}, \\
&= \frac{x\vec{\alpha}N}{a} \int_{l_1}^{l_2} \frac{dz}{\sqrt{z^2 + 1}}, \\
&= d(\text{asinh}(l_2) - \text{asinh}(l_1)).
\end{aligned}$$

– In the case where x is aligned with S , then $x\vec{\alpha}$ and N are orthogonal and $x\vec{\alpha} \cdot N = 0 \implies I_1 = 0$.

- We now prove the result for I_2 .

$$I_2 = \int_S \text{Dist}(x, y) ds = \int_0^1 a \text{Dist}(x, y(t)) dt.$$

– If $x = \alpha$,

$$\left. \begin{array}{l} b = 0 \\ c = 0 \\ \delta = 0 \end{array} \right\} \implies \text{Dist}(x, y(t)) = at.$$

Then

$$I_2 = \int_0^1 a^2 t dt = \frac{a^2}{2}.$$

– If $x = \beta$

$$\left. \begin{array}{l} b = a \\ c = -a^2 = -b^2 \\ \delta = 0 \end{array} \right\} \implies \text{Dist}(x, y(t)) = -a(t - 1).$$

Then

$$I_2 = \int_0^1 -a(t - 1) dt = \frac{a^2}{2}.$$

- If $c = -ab$ (it means that x is aligned with S but $x\vec{\alpha}$ and $\vec{\alpha}\beta$ have opposite direction)

$$\text{So } b \geq a \text{ and } \text{Dist}(x, y(t)) = -at + b.$$

Then

$$I_2 = \int_0^1 a(-at + b)dt = -\frac{a^2}{2} - c.$$

- If $c = ab$ (it means that x is aligned with S but $x\vec{\alpha}$ and $\vec{\alpha}\beta$ have the same direction)

$$\text{Dist}(x, y(t)) = at + b.$$

Then

$$I_2 = \int_0^1 a(at + b)dt = \frac{a^2}{2} + c.$$

- Otherwise,

$$\begin{aligned} I_2 &= \int_0^1 \sqrt{\delta} \sqrt{\frac{a^4}{\delta} \left(t + \frac{c}{a^2}\right)^2 + 1} dt, \text{ using the change of variable } z = \frac{a^2}{\sqrt{\delta}} \left(t + \frac{c}{a^2}\right), \\ &= \int_{l_1}^{l_2} \sqrt{\delta} \frac{\sqrt{\delta}}{a^2} \sqrt{z^2 + 1} dz \\ &= \int_{l_1}^{l_2} \frac{\delta}{a^2} \sqrt{z^2 + 1} dz, \text{ using the change of variable } z = \sinh(u), \\ &= \frac{\delta}{a^2} \int_{\text{asinh}(l_1)}^{\text{asinh}(l_2)} \cosh(u)^2 du = \frac{\delta}{a^2} \int_{\text{asinh}(l_1)}^{\text{asinh}(l_2)} \frac{1}{2} (1 + \cosh(2u)) du \\ &= \frac{\delta}{2a^2} \left[u + \frac{1}{2} \sinh(2u) \right]_{\text{asinh}(l_1)}^{\text{asinh}(l_2)}, \\ &= \frac{\delta}{2a^2} (l_2 \sqrt{1 + l_2^2} + \text{asinh}(l_2) - l_1 \sqrt{1 + l_1^2} - \text{asinh}(l_1)). \quad \blacksquare \end{aligned}$$

To summarize, we recall that

$$I_{u^k}(x) = \sum_{T_i \in \mathcal{T}} \int_{T_i} \frac{J_{u^k}(x, y)}{|x - y|} dy,$$

with \mathcal{T} is a family of triangles, and

$$J_{u^k}(x, y) = \frac{|u^k(x) - u^k(y)|^{p-2} (u^k(x) - u^k(y)) \rho_n(x - y)}{|x - y|^{p-1}}.$$

We can simplify the previous expression as follows:

$$\int_T \frac{J(x, y)}{|x - y|} dy = J(x, y_i) I_1 - \frac{1}{n^3} \binom{n^1}{n^2} [I_2 + I_1(x - y_i)],$$

with $T \in \mathcal{T}$, and I_1 and I_2 explicitly given in the previous proposition.

Numerical results

In this section, we compare two implementations of the total variation: the approximation proposed by Aubert *et al.* in [3] and the classical Chambolle's projection algorithm [7].

We can say that the approximation method performs very well the restoration, however this method tends to smooth more than the projection algorithm.

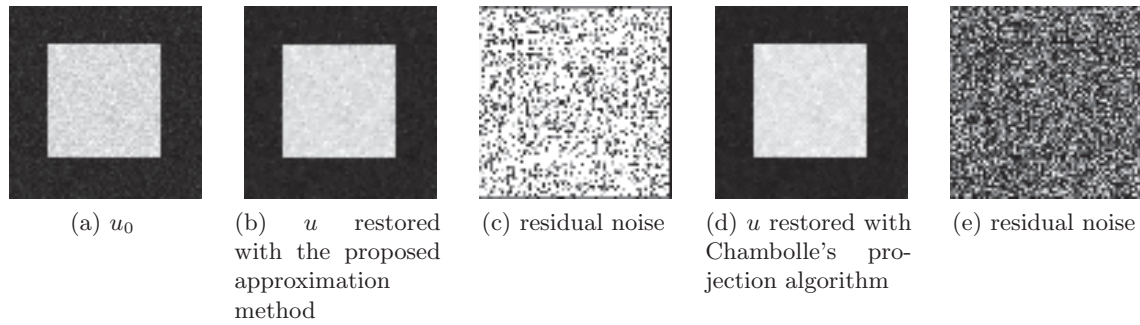


Figure 7.3: Restoration results with the proposed approximation method and Chambolle projection algorithm on a toy example.

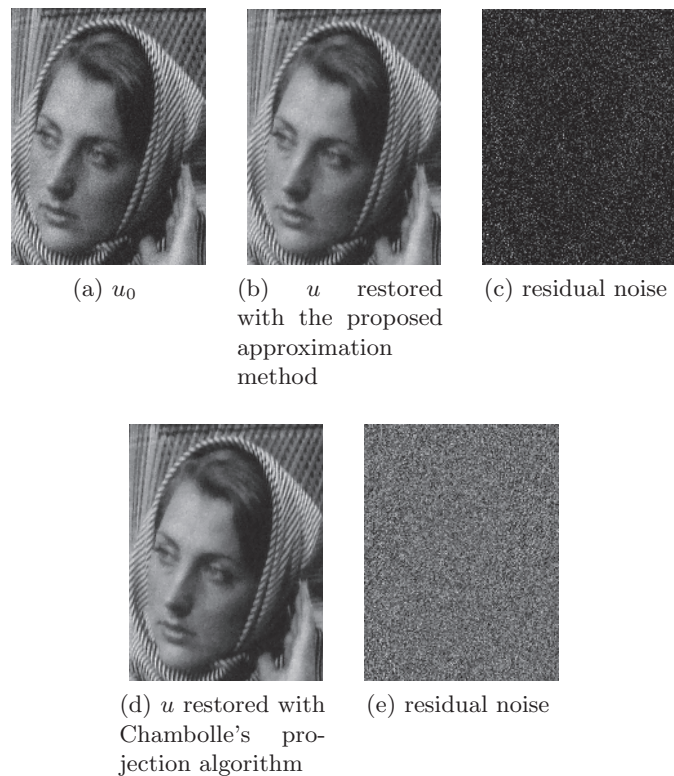


Figure 7.4: Restoration results with the proposed approximation method and Chambolle's projection algorithm on Barbara example.

7.6 Implementation of the registration problem

7.6.1 Scheme for the auxiliary variable method

We recall that the problem is the following

$$\inf_{\hat{W} \times BV_0(\Omega)} \left\{ E_\varepsilon(\varphi, \tilde{T}) = \int_\Omega |\nabla \tilde{T}| + \int_\Omega \tilde{T} \operatorname{div} \theta + \frac{\alpha}{2} \int_\Omega \|\nabla \varphi\|^2 + \gamma \|T \circ \varphi - \tilde{T}\|_{L^1(\Omega)} \right\} \quad (7.19)$$

In practice, we use the non linear elastic regularization used in the previous chapter: the quasiconvex envelope of the stored energy function of a Saint Venant-Kirchhoff material supplemented with the penalty term on the Jacobian. Moreover, we decouple the problem with an auxiliary variable V to eliminate the non linearity in $\nabla \varphi$:

$$\inf_{\hat{W} \times BV_0(\Omega)} \left\{ \int_\Omega |\nabla \tilde{T}| + \int_\Omega \tilde{T} \operatorname{div} \theta + \int_\Omega QW(V) dx + \frac{\alpha}{2} \int_\Omega \|V - \nabla \varphi\|^2 dx + \gamma \|T \circ \varphi - \tilde{T}\|_{L^1(\Omega)} \right\} \quad (7.20)$$

$$\text{with } QW(V) = \begin{cases} W(V) & \text{if } \|V\|^2 \geq 2 \frac{\lambda + \mu}{\lambda + 2\mu}, \\ \Psi(\det V) & \text{if } \|V\|^2 < 2 \frac{\lambda + \mu}{\lambda + 2\mu}. \end{cases}$$

Similar numerical tools to those implemented in Chapter 4 are used to design the associated algorithm. To avoid redundancy, we do not go into details.

7.6.2 Scheme for the approximation method

In practice, we would like to minimize

$$E_n(\varphi) = \frac{1}{K_{1,2}} \int_\Omega \int_\Omega \frac{|T \circ \varphi(x) - T \circ \varphi(y)|}{|x - y|} \rho_n(x - y) dx dy \quad (7.21)$$

$$+ \int_\Omega T \circ \varphi \operatorname{div} \theta dx + \int_\Omega QW(\nabla \varphi) dx,$$

with $\varphi \in \operatorname{Id} + W_0^{1,4}(\Omega, \mathbb{R}^2)$.

As already mentioned, we decouple the problem by introducing the auxiliary variable V simulating $\nabla \varphi$ and we solve:

$$E_n(\varphi, V) = \frac{1}{K_{1,2}} \int_\Omega \int_\Omega \frac{|T \circ \varphi(x) - T \circ \varphi(y)|}{|x - y|} \rho_n(x - y) dx dy \quad (7.22)$$

$$+ \int_\Omega T \circ \varphi \operatorname{div} \theta dx + \int_\Omega QW(V) dx + \frac{\alpha}{2} \int_\Omega \|V - \nabla \varphi\|^2 dx,$$

with $\varphi \in \operatorname{Id} + W_0^{1,2}(\Omega, \mathbb{R}^2)$, $V \in L^4(\Omega, M_2)$. The corresponding Euler-Lagrange equation for φ is the following:

$$0 = \frac{2}{K_{1,2}} \nabla T(\varphi_n(x)) \int_\Omega \operatorname{sign}(T \circ \varphi_n(x) - T \circ \varphi_n(y)) \frac{\rho_n(x - y)}{|x - y|} dy$$

$$+ \nabla T(\varphi_n) \operatorname{div}(\theta) - \alpha \Delta \varphi + \alpha \begin{pmatrix} \operatorname{div} V_1 \\ \operatorname{div} V_2 \end{pmatrix}.$$

The system of equations satisfied by V remains unchanged.

7.6.3 Numerical results

We have implemented both methods for our problem, that is to say, the decoupled problem with an auxiliary variable and the approximation method of the total variation by the sequence of integral operators.

Unfortunately, we have not been able to obtain satisfactory results. This could partly be explained by the fact that the gradient information is meaningful in texture regions and close to 0 in homogeneous areas, then there is not enough information to match.

Conclusion

To conclude this chapter, we have designed a theoretically well-motivated method, and proved several interesting theoretical results. This model is inspired by other works which are not registration models but inpainting ones and we have tried to apply these methods to our problem. We have also proposed two alternative solutions which have been theoretically justified. However, we have been unable to obtain satisfactory numerical results although the computing codes are consistent with the theory.

- [1] L. AMBROSIO AND G. DAL MASO, *A general chain rule for distributional derivatives*, Proceedings of the American Mathematical Society, 108 (1990), pp. 691–702.
- [2] G. ANZELLOTTI, *Pairings between measures and bounded functions and compensated compactness*, Annali di Matematica Pura ed Applicata, 135 (1983), pp. 293–318.
- [3] G. AUBERT AND P. KORNPORST, *Can the nonlocal characterization of Sobolev spaces by Bourgain et al. be useful for solving variational problems?*, SIAM Journal on Numerical Analysis, 47 (2009), pp. 844–860.
- [4] C. BALLESTER, M. BERTALMIO, V. CASELLES, G. SAPIRO, AND J. VERDERA, *Filling-in by joint interpolation of vector fields and gray levels*, Image Processing, IEEE Transactions on, 10 (2001), pp. 1200–1211.
- [5] J. BOURGAIN, H. BREZIS, AND P. MIRONESCU, *Another look at sobolev spaces*, IOS Press, (2001), pp. 439–455.
- [6] H. BRÉZIS, *Analyse Fonctionnelle, Théorie et Applications. 1999*, Dunod, Paris, 1999.
- [7] A. CHAMBOLLE, *An algorithm for total variation minimization and applications*, J. Math. Imaging Vis., 20 (2004), pp. 89–97.
- [8] J. DÁVILA, *On an open question about functions of bounded variation*, Calculus of Variations and Partial Differential Equations, 15 (2002), pp. 519–527.
- [9] F. DEMENGEL, G. DEMENGEL, AND R. ERNÉ, *Functional spaces for the theory of elliptic partial differential equations*, Springer, 2012.
- [10] M. DROSKE AND M. RUMPF, *A variational approach to nonrigid morphological image registration*, SIAM Journal on Applied Mathematics, 64 (2004), pp. 668–687.
- [11] L. C. EVANS AND R. F. GARIEPY, *Measure theory and fine properties of functions*, vol. 5, CRC press, 1991.
- [12] E. HABER AND J. MODERSITZKI, *Intensity gradient based registration and fusion of multi-modal images*, in Medical Image Computing and Computer-Assisted Intervention—MICCAI 2006, Springer, 2006, pp. 726–733.

- [13] A. C. PONCE, *A new approach to Sobolev spaces and connections to Gamma-convergence*, Calculus of Variations and Partial Differential Equations, 19 (2004), pp. 229–255.
- [14] L. I. RUDIN, S. OSHER, AND E. FATEMI, *Nonlinear total variation based noise removal algorithms*, Physica D: Nonlinear Phenomena, 60 (1992), pp. 259–268.
- [15] D. SPECTOR, *Characterization of Sobolev and BV Spaces*, PhD thesis, Carnegie Mellon University, 2011.